INTRACELLULAR DELIVERY OF REACTIVE OXYGEN SPECIES GENERATING POLYPEPTIDE-DRUG CONJUGATES FOR CANCER THERAPY

Saurabh Wadhwa

A dissertation submitted to the faculty of the University of North Carolina at Chapel Hill in partial fulfillment of the requirements for the degree of Doctor of Philosophy in the UNC Eshelman School of Pharmacy.

Chapel Hill
2011

Approved by:

Russell J. Mumper, Ph.D., Advisor

Michael Jay, Ph.D., Chairperson

Moo J. Cho, Ph.D., Reader

Rihe Liu, Ph.D., Reader

Nancy DeMore, M.D., Ph.D., Reader

ABSTRACT

SAURABH WADHWA: Intracellular Delivery of Reactive Oxygen Species Generating Polypeptide-Drug Conjugates for Cancer Therapy
(Under the direction of Russell J. Mumper, Ph.D.)

Auto-oxidation of D-penicillamine (D-pen), FDA registered for the treatment of Wilson's disease and rheumatoid arthritis, generates reactive oxygen species (ROS), a reaction catalyzed by transition metal ions (TMIs). D-pen has anti-proliferative and anti-angiogenic effects and is known to modulate several signaling pathways. However, an exact mechanism of action is not known. A reactive thiol group, strong plasma protein binding, rapid clearance, higher effective concentrations and cell impermeability challenge the development of D-pen as an anticancer agent. This dissertation work investigates poly(α)-L-glutamic acid (PGA) conjugates of D-pen for enhanced delivery to cancer cells and overcome the challenges mentioned above. Complete biodegradability, ability to carry large payloads of D-pen, reversible conjugation, biocompatibility, longer circulation and passive tumor accumulation make PGA an ideal drug carrier.

Evidence is presented that PGA-D-pen conjugates enhance the intracellular uptake of D-pen. Upon release from the conjugate, D-pen causes significant elevation in ROS levels leading to apoptotic cell death in murine and human leukemia, and breast cancer cells. Treatment with PGA-D-pen improves the survival of CD2F1 mice bearing intra-peritoneal (i.p.) leukemia with no apparent adverse events.

Idarubicin (Ida), an anthracycline chemotherapeutic, has shown efficacy as first-line treatment in acute leukemia and other cancers. ROS elevation that plays a major role in mediating its cytotoxicity is dependent on and augmented in the presence of low molecular weight thiols (LMWTs) like D-pen. We hypothesized that a combination of Ida and D-pen formulated as dual drug conjugates (DDCs) will provide co-delivery leading to enhanced anticancer effects while increasing the therapeutic index of Ida. Targeting to sigma-1 receptors, known to be over-expressed in many different cancers, to further enhance the efficacy and specificity was also examined.

It was shown that stable DDCs could be synthesized with programmed drug release properties. The conjugates were successfully targeted *in-vitro* to sigma-1 receptor over-expressing non-small cell lung cancer (NSCLC) cells with a novel benzamide derivative, trivalent anisamide, as the ligand. DDCs showed prolonged circulation, enhanced tumor accumulation, reduced cardiac exposure of Ida, and improved tumor efficacy and survival in athymic nu/nu mice bearing NSCLC tumor xenografts.

ACKNOWLEDGMENTS

I am profoundly grateful to my advisor, Dr. Russell J. Mumper for his mentorship, encouragement, optimism, and support throughout my graduate training. He inspired me to become an independent thinker and challenging me to explore new ideas. I am deeply thankful to all my doctoral dissertation committee members, Drs. Michael Jay, Moo J. Cho, Rihe Liu, and Nancy DeMore for their time, suggestions and support.

I would also like to acknowledge all the faculty, staff and students at the UNC Eshelman School of Pharmacy for making my "Tarheel" experience richer and more fruitful. I would particularly like to thank Dr. Leaf Huang for providing me access to his laboratory and for advice while working on sigma-1 targeted conjugates. My sincere thanks are due to all the current and past members of Dr. Mumper's laboratory for their support.

This dissertation was partly possible by the financial support of Amgen through Amgen Graduate Fellowship 2009-2010.

Finally, I am deeply indebted to my family; my parents for their constant support and encouragement, my wife, Rashmi, for her incredible sacrifices and support during this challenging time and to our daughter Aaliya for bringing tremendous joy to our lives. My life is incomplete without you.

TABLE OF CONTENTS

List of Tables

List of Figures

List of Abbreviations

ACE	Angiotensin converting enzyme
ADR	Adriamycin
AGM	Aminoglutethimide
ALN	Alendronate
AP-1	Activator protein-1
APC	Antigen presenting cell
ASGP	Asialoglycoprotein receptor
AUC	Area under the curve
BME	β-mercaptoethanolamine
CAM	Chorioallantoic membrane
CD	Circular dichroism
CDDP	Cis-dichlorodiammine platinum (II)
CMC	Critical micellar concentration
CPP	Cell penetrating peptides
CPT	Camptothecin
DC	Dendritic cells
DDC	Dual drug conjugates
DMARD	Disease modifying anti-rheumatic drug
DMSP	N,N-Dimethyl sphingosine
Dox	Doxorubicin
D-pen	D-penicillamine
DTC	Dithiocarbamates

DTT	Dithiothreitol
ECGF	Endothelial cell growth factor
ECM	Extracellular matrix
EGFR	Epidermal growth factor receptor
EPR	Enhanced permeability and retention
FGF	Fibroblast growth factor
FI	Fluorescence intensity
FITC	Fluorescein isothiocyanate
FRET	Fluorescence resonance energy transfer
FU	Fluorouracil
FUD	Fluoro-2-deoxyuridine
GFP	Green fluorescent protein
GSH	Glutathione
GSSG	Glutathione disulfide
HA	Hyaluronic acid
HLB	Hydrophilic lipophilic balance
HP	Haloperidol
HPMA	N-(2-hydroxypropyl) methacrylamide
HRPC	Hormone refractory prostate cancer
Ida	Idarubicin
IFP	Interstitial fluid pressure
Ig	Immunoglobulin
ILS	Increase in life span

i.p.	Intraperitoneal
LMWT	Low molecular weight thiols
Mce_6	Mesochlorine e_6
MDR	Multi-drug resistance
MHC	Major histocompatibility complex
MMP	Matrix metalloproteinase
MTD	Maximum tolerated dose
MTX	Methotrexate
NAC	N-acetyl cysteine
NC	Nanocapsule
NP	Nanoparticle
NSCLC	Non-small cell lung cancer
OAS	Octa (3-aminopropyl) silsesquioxane
PAA	Poly-aspartic acid
PAMA	Poly-α-malic acid
PAMAM	Polyamidoamine
PBMA	Poly-β-malic acid
PDC	Polymer-drug conjugate
PDL	Poly-D-lysine
PDM	*p*-Phenylenediamine mustard
PDTC	Pyrrolidine dithiocarbamate
PEG	Polyethylene glycol
PEI	Polyethylenimine

PGA	Poly(α)-L-glutamic acid
PHEA	α,β-poly(N-2-hydroxyethyl)-DL-aspartamide
PHEG	Poly-(N-(2-hydroxyethyl)-L-glutamine)
PI	Propidium iodide
PI3	Phosphatidylinositol 3
PK	Pharmacokinetic
PLL	Poly-L-lysine
PTD	Protein transduction domain
PTX	Paclitaxel
RA	Rheumatoid arthritis
RCS	Reactive carbonyl scavenging
RES	Reticuloendothelial system
RNS	Reactive nitrogen species
ROS	Reactive oxygen species
RT	Room temperature
SOD	Superoxide dismutase
TA	Trivalent anisamide
TGD	Tumor growth delay
TGF	Tumor growth factor
TM	Tetrathiomolybdate
TMI	Transition metal ion
tPA	Tissue plasminogen activators
VEGF	Vascular endothelial growth factor

Chapter 1

Introduction

1.1. Introduction and Statement of the Problem

1.1.1. Background and Rationale of the Proposed Research

D-penicillamine (D-pen) is a low molecular weight thiol (LMWT) used in the treatment of Wilson's disease and as a disease modifying anti-rheumatic drug (DMARD) in rheumatoid arthritis (RA). The presence of a free thiol or sulfhydryl group ($pk_a \sim 7.9$) plays a significant role in its pharmacological activities (Netter et al., 1987). D-pen is a strong metal chelator. Redox cycling or auto-oxidation of D-pen generates reactive oxygen species (ROS). This reaction is catalyzed in the presence of metal ions like copper and iron (Starkebaum and Root, 1985). D-pen also undergoes thiol-disulfide exchange reactions with proteins that contain cysteine domains (Joyce et al., 1991). It can also interact with proteins having transition metal ions in their catalytic domains. Therefore, D-pen can potentially affect several signaling pathways. Its interactions with the components of redox buffer e.g. glutathione (GSH) depletion and GSH peroxidase inhibition can modulate the redox homeostasis (Chaudiere et al., 1984).

Early investigations focused heavily on investigating the mechanism of beneficial effects of D-pen in RA and its interactions with the immune system (Gerber, 1978). D-pen was later discovered to have strong anti-angiogenic and anti-proliferative activity against epithelial and cancer cells respectively (Baier-Bitterlich et al., 1993; Matsubara et al., 1989). Moreover, the cytotoxicity was shown to be specific to transformed cells and normal cells were comparatively resistant (Havre et al., 2002). The underlying mechanism is not yet completely understood. However, ROS generation and effect on signaling proteins such as vascular endothelial growth factor (VEGF), tumor suppressor protein (p53), and matrix

metalloproteinases (MMPs) has been shown to play a significant role (Havre et al., 2002; Volpert et al., 1996).

The major challenges that must be overcome to develop D-pen as an anticancer agent are; 1) highly reactive thiol group that is prone to irreversible serum protein conjugation and auto-oxidation before reaching the target site of action (Joyce et al., 1991; Joyce et al., 1989), 2) poor cell permeability due to high hydrophilicity and unfavorable stereochemistry (Lodemann, 1981), 3) rapid clearance from plasma due to low molecular weight, and 4) need for higher effective concentrations (Gupte and Mumper, 2007a; Gupte et al., 2008).

Natural and synthetic hydrophilic aqueous soluble polymers have been successfully used as drug carriers in the form of polymer-drug conjugates (PDCs), also referred to as polymeric prodrugs (Duncan, 2003). They have enhanced the efficacy, therapeutic index and reduced adverse events associated with chemotherapeutic drugs such as paclitaxel (PTX) and doxorubicin (dox). The presence of multiple functional groups and availability of numerous biochemically sensitive linkers makes PDCs versatile drug delivery systems. The cellular uptake of PDCs can be further enhanced by incorporating cell-specific targeting residues.

The present work investigated high molecular weight, aqueous-soluble PDCs as delivery systems for D-pen. Such a delivery system would enable development of D-pen as a potential anticancer agent by overcoming the limitations summarized above.

Cancer cells are characterized by multiple genetic and metabolic aberrations that vary widely among different types, and a tumor is composed of a heterogeneous population of cells (Bae, 2009; Jain and Stylianopoulos, 2010). Therefore, a combination therapy approach is widely used and has proven to be more effective than treatments with single agents. Ideally, a combination therapy should deliver two or more drugs to the tumor such that

maximum benefit can be achieved. In case of a combination drug therapy, where one drug augments the potential of the second, simultaneous delivery is desired. This has been successfully shown with PDCs (Vicent et al., 2005). The present work further investigated the potential of combination drug therapy with D-pen and idarubicin (ida), which is also known to mediate its toxicity by elevation of intracellular ROS levels among other actions, by developing dual drug conjugates (DDCs) with a polymeric macromolecule.

1.1.2. Plan of Research

The overall goal of this research was to investigate PDCs as drug delivery platforms for the anticancer delivery of ROS generating agent, D-pen, that would stabilize its thiol group, allow larger payload of drug to be delivered to the cancer cells, prolong the blood circulation time and release the drug through biochemically sensitive linkers upon uptake by cancer cells leading to strong anticancer effect. The research further aimed to investigate the potential of co-delivery of D-pen with Ida, conjugated to the same polymer chain, to enhance the anticancer effect while reducing the adverse events associated with the administration of Ida.

The studies described in this dissertation investigated the following hypotheses:

1. Conjugation of D-pen to a biodegradable and biocompatible polymer through its thiol group using a reducible disulfide linker will provide a stable delivery system with enhanced intracellular delivery of D-pen.
2. The polymer-D-pen conjugate will lead to ROS mediated cytotoxicity in human cancer cells and will have potent anticancer effects.

3. Co-delivery of D-pen and Ida with DDCs targeted to sigma-1 receptor will result in enhanced cell uptake and cytotoxicity in human cancer cells over-expressing sigma-1 receptor.
4. *In-vivo* administration of DDCs in mice bearing sigma-1 over-expressing cancer cells will result in strong anticancer effect that will lead to tumor regression and enhanced survival.

To evaluate the hypotheses outlined above, a research plan that included specific aims and major objectives to achieve these aims was designed.

Specific Aim 1. Synthesize poly(α)-L-glutamic acid (PGA) conjugates of D-pen and investigate the intracellular delivery of the conjugates.

a. Synthesize PGA-D-pen conjugate with a reproducible chemical conjugation pathway using a hetero-bifunctional disulfide linker.
b. Develop sensitive analytical methods to quantitatively characterize the extent of drug conjugation and assess the *in-vitro* release of D-pen from PGA-D-pen conjugate.
c. Develop microscopic methods to analyze the cellular uptake of PGA-D-pen in human leukemia cells.

Specific Aim 2. Investigate the intracellular ROS generation, the resulting *in-vitro* cytotoxicity and anticancer efficacy of PGA-D-pen.

a. Determine the kinetics of intracellular ROS generation as a function of the dose of PGA-D-pen employing a ROS marker, carboxy-H_2DCFDA (5-(and-6)-carboxy-2',7'-dichlorodihydrofluorescein diacetate).

b. Determine the *in-vitro* cytotoxicity of PGA-D-pen in human leukemia and breast cancer cells, and determine the extent of apoptotic cell death in the cytotoxicity by utilizing the annexin V/propidium iodide dual label method.

c. Evaluate the maximum tolerated dose (MTD) of PGA-D-pen by dose escalation studies and an increase in life span (ILS) upon treatment with PGA-D-pen in intra-peritoneal (i.p.) leukemia bearing mice.

Specific Aim 3. Develop DDCs containing both D-pen and Ida conjugated to PGA as a co-delivery system further targeted to sigma-1 receptor over-expressing cancer cells.

a. Develop a reproducible synthetic pathway for DDCs and quantitative analytical methods to analyze the extent of conjugation and *in-vitro* release of Ida from the DDC.

b. Synthesize DDCs targeted to sigma-1 receptors using anisamide and trivalent anisamide as ligands, and develop spectroscopic methods to estimate the number of ligands per polymer chain.

c. Optimize the number of ligands per polymer chain by assessing the differential cell uptake and cytotoxicity of targeted vs. untargeted DDCs in cancer cells over-expressing sigma-1 receptors.

Specific Aim 4. Evaluate the anticancer efficacy of DDCs in mice bearing human cancer cells over-expressing sigma-1 receptors.

a. Develop a mouse (athymic *nu/nu*) model of human NSCLC (NCI-H460) and optimize for growth properties.
b. Perform dose escalation studies to determine the MTD and dose-related toxicity of DDCs.
c. Determine the plasma, tumor and organ disposition of targeted and untargeted DDCs.
d. Assess the tumor regression or tumor growth delay (TGD) and survival enhancement upon treatment with targeted and untargeted DDCs.

1.2. Low Molecular Weight Thiols (LMWTs) as Anticancer Agents

1.2.1. Introduction

In anticancer therapy, LMWTs have been widely used as chemopreventive agents to reduce the risk of cancer by primarily scavenging the harmful reactive oxygen (ROS) and nitrogen (RNS) species and as adjuvants to chemotherapy thereby reducing the associated toxicity to normal tissue while increasing the therapeutic index. Interestingly, several investigators have shown that LMWTs are also capable of elevating intracellular oxidative stress and causing cytotoxicity to cancer cells. The generation of ROS occurs through one-electron oxidation of LMWTs and is catalyzed by transition metals such as copper and iron (Munday, 1989). We have highlighted the significance of elevated serum and tissue copper levels in cancer patients and utilizing this as a potential strategy for anticancer therapy (Gupte and Mumper, 2009). The presence of free thiol group makes LMWTs unique among other antioxidants or chemopreventive agent in their interaction with cancer cells and so it is important to understand the redox chemistry of thiols. In particular, the variation in acidity and the oxidation potential of the thiol group results in differences in biological activity.

Glutathione, which is a tripeptide composed of glycine, glutamic acid and cysteine, is the predominant endogenous LMWT besides cysteine which is a precursor of GSH. GSH has a very important role in detoxification of xenobiotics mediated by GSH-S-transferase as well as maintenance of the intracellular redox balance by balancing the ratio of the reduced and oxidized form of GSH (GSH/GSSG). Selective perturbation of this balance in cancer cells by increasing the levels of GSSG (NOV-002®) or decreasing the levels of GSH (buthionine sulfoximine and phoron) has been successfully investigated as a therapeutic strategy (Trapp et al., 2009; van Doorn et al., 1978). On the other hand, elevated GSH levels have been

shown to sensitize cancer cells to chemotherapy by complex redox pathways that involve interaction with copper (Chen et al., 2008a). The ratio of GSH/GSSG and the redox buffer capacity of cancer cells are significantly lower than normal cells due to increased metabolic stress (Fruehauf and Meyskens, 2007; Lopez-Lazaro, 2007; Nicco et al., 2005). Such persistent oxidative stress makes cancer cells susceptible to killing upon further elevation of ROS to levels that the normal cells will be able to buffer.

The anticancer effects of LMWTs can be described in four distinct categories that include; i) generation of ROS causing direct cellular damage, ii) inhibition of enzyme activity by chelation of metal co-factors like copper and zinc leading to anti-angiogenesis and extracellular matrix perturbation, iii) modulation of cellular and membrane proteins by thiol disulfide exchange or disulfide formation at cysteine sites, and iv) effect on signaling pathways. LMWTs *viz.*, D-pen, tetrathiomolybdate (TM), NOV-002 and others are currently under clinical investigation for anticancer therapy (**Figure 1.1**).

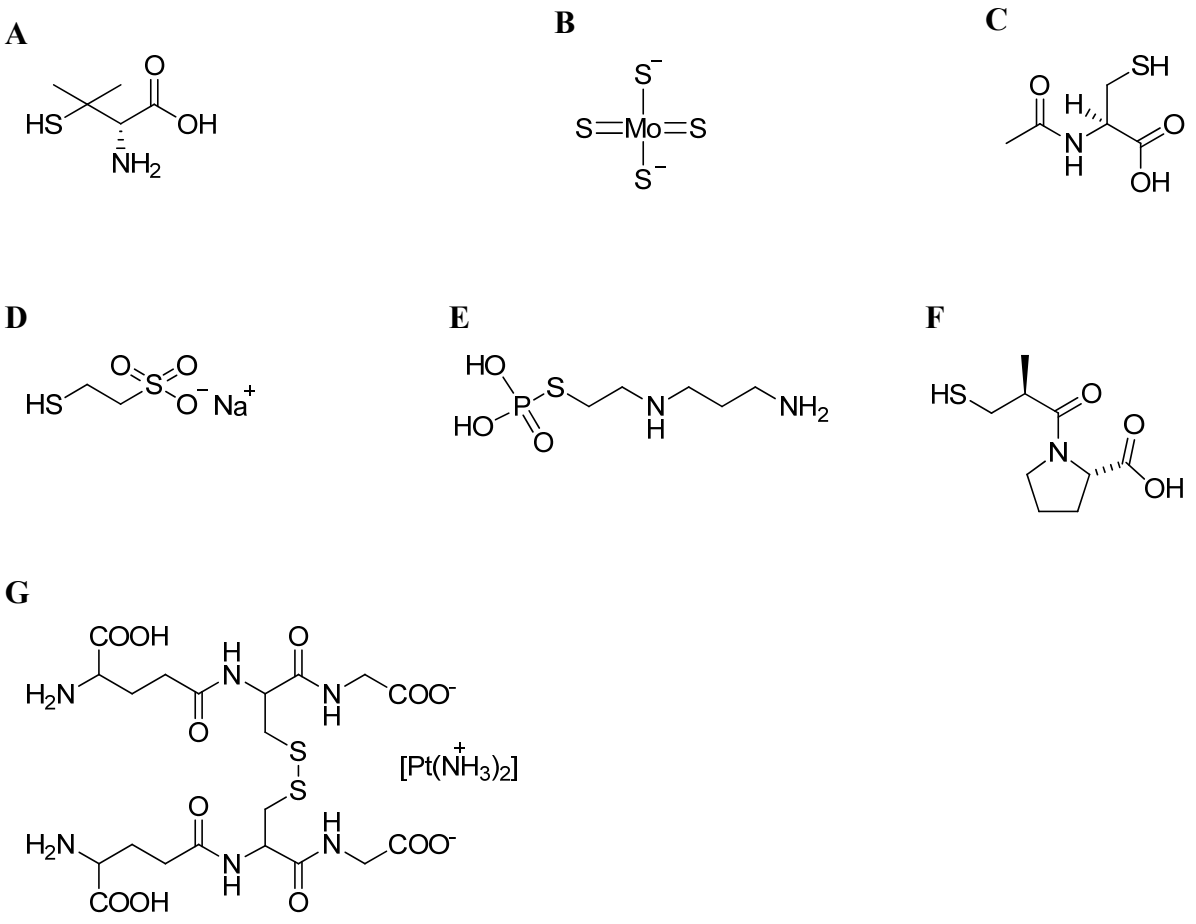

Figure 1.1 Chemical structures of some low molecular weight thiols (LMWTs) investigated for their anticancer properties.
A) D-penicillamine (D-pen), B) Tetrathiomolybdate (TM), C) N-acetyl cysteine (NAC), D) Mesna, E) Amifostine, F) Captopril and G) NOV-002.

1.2.2. Redox Status of Normal vs. Cancer Cells

Intracellular ROS are by-products of mitochondrial respiration and oxidative enzyme activity in the cytosol and other organelles (Murphy, 2009). They have diverse roles in cell signaling when present at optimum concentrations. However, elevated levels of ROS have the potential to cause cellular damage by oxidizing cellular components (e.g. lipid peroxidation), direct damage to DNA (e.g., strand breaks) or by triggering stress responses leading to apoptotic cell death (Martin and Barrett, 2002). The cellular redox buffer system that is composed of small molecule antioxidants like GSH and enzymatic components including GSH peroxidase, catalase, superoxide dismutase, and thioredoxin helps maintain a low level of ROS by converting them to inert chemicals. GSH is utilized as a single electron donor in most of the scavenging reactions resulting in its oxidation to GSSG (**Figure 1.2**). The ratio of GSH to GSSG (GSH/GSSG) is often used as a measure of the redox buffer capacity of a cell, a higher value indicating an improved ability to counter an oxidative insult.

Elevated levels of intracellular ROS otherwise termed as “oxidative stress” has been associated with several pathological conditions including cancer, neurodegenerative diseases and cardiovascular diseases. It is known that cancer cells are under persistent oxidative stress making them more susceptible to killing by further elevation of intracellular ROS levels (Pelicano et al., 2004).

Serum thiol levels, a marker for overall oxidative stress, in patients with several different types of cancer have been found to be significantly lower than normal patients (Nayak and Pinto, 2007; Ozkan et al., 2007; Rao et al., 1999). An increase in serum thiols is correlated with enhanced survival. In addition, the GSH/GSSG ratio is significantly lowered in tumor cells of different types (Lusini et al., 2001; Navarro et al., 1999) indicating reduced

ability to neutralize ROS. Comparatively, the redox buffer capacity of normal cells is much greater and they are able to neutralize ROS and prevent any associated damage at similar concentrations (Gupte et al., 2009). Therefore, agents that act predominantly by ROS elevation such as LMWTs, have an inherent selectivity towards killing cancer cells. This is supported by several studies that showed cancer cells to be more sensitive to treatment with LMWTs as compared to normal cells.

N-acetyl cysteine was shown to selectively induce apoptosis in several transformed cell lines with no effect on normal cells (Liu et al., 1998b). Havre et al. showed that D-pen selectively induced a p53 mediated apoptosis in transformed cells compared to human fibroblasts (Havre et al., 2002). Wondrak et al. (Wondrak et al., 2004; Wondrak et al., 2006) showed that more than 60% of the murine (B16) and human (A-375, G-361 and LOX) melanoma cells were apoptotic within 24 hr of treatment with D-pen whereas no apoptosis induction was seen in primary human skin fibroblasts and epidermal keratinocytes.

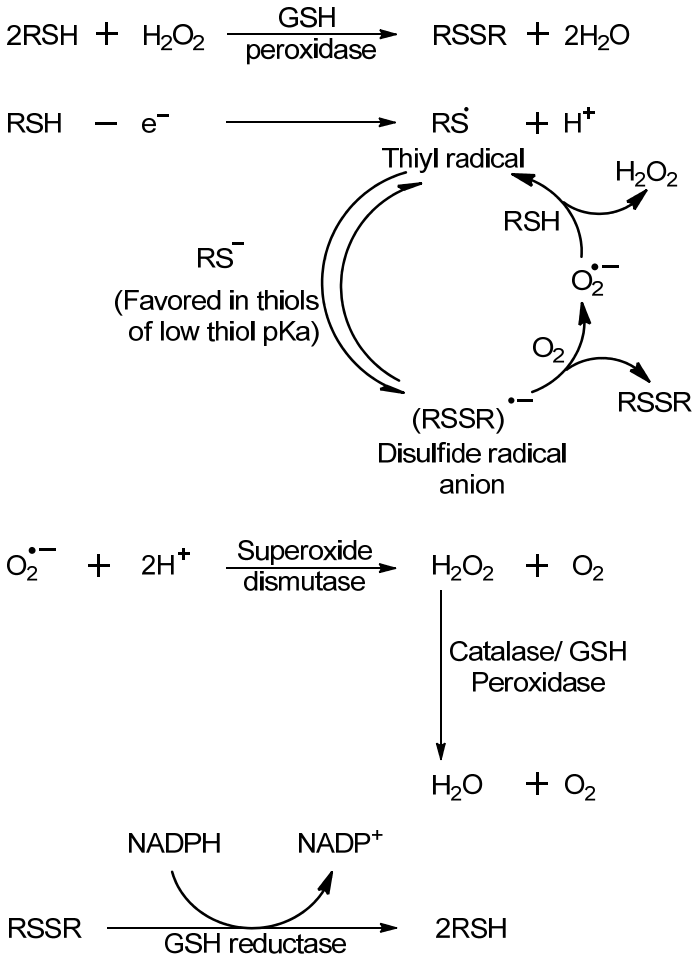

Figure 1.2 Pathways of neutralization of reactive oxygen species (ROS) by the cellular redox buffer components.

RSH = Low molecular weight thiol (LMWT) containing compound. Glutathione (GSH) is the predominant intracellular LMWT. RSSR = Symmetrical disulfide of the corresponding LMWT, H_2O_2 = Hydrogen peroxide, $O_2^{\cdot -}$ = Superoxide radical anion, NADP = Nicotinamide adenine dinucleotide phosphate.

1.2.3. The Oxidant-Antioxidant Paradigm

LMWTs have been historically used as antioxidants due to their radical scavenging properties. The antioxidant property of LMWTs can be attributed to the presence of free thiol group(s) that can act as an electron donor and cause radical scavenging in a way similar to GSH. In addition, metal complexes of LMWTs have also shown superoxide dismutase (SOD) mimicking properties (Jay et al., 1995; Roberts and Robinson, 1985) which may further enhance their antioxidant activity.

However, cytotoxic responses with LMWTs involving free radical species have been observed indicating an oxidant nature (Munday, 1989). The presence of free thiol group makes LMWTs susceptible to oxidation by other compounds or autoxidation resulting in the formation of symmetrical/mixed disulfides if another thiol containing compound is present. Although LMWTs may generate ROS during normal redox cycling (Searcy, 1996) as shown in **Figure 1.2**, oxidation of LMWTs may be catalyzed by several transition metals. Metal catalyzed oxidation of LMWT involves a series of single-electron steps that have been experimentally elucidated (Munday, 1989; Munday, 1994; Starkebaum and Root, 1985) (**Figure 1.3**). Reduction of the metal by thiol generates thiyl radical (step 1). The reduced metal further reacts with molecular oxygen to generate superoxide anion (step 2) followed by sequential reduction to hydrogen peroxide (step 3). The two thiyl radicals come together to form a symmetrical disulfide (step 4). The utilization of 1 mole of oxygen for every 2 moles of thiols has been experimentally shown (Starkebaum and Root, 1985). Gupte and Mumper have also observed the formation of one mole of hydrogen peroxide for every 2 moles of D-pen oxidized (Gupte and Mumper, 2007a; Gupte and Mumper, 2007b). Hydrogen peroxide generated during metal catalysis of LMWTs can further undergo Fenton reaction to generate

the highly potent hydroxyl radical (step 5) (Kehrer, 2000). This has been confirmed in several reports (Held et al., 1996; Rowley and Halliwell, 1982). It has also been shown that thiol may be directly involved in Fenton reaction and may not depend on the generation of hydrogen peroxide (Issels et al., 1984).

The generation of ROS by LMWTs is dependent on the generation of thiolate anion which in turn depends on the acidity of the thiol group and the pH of the medium. Moreover, it has been suggested that the thiolate anion is the active species that binds DNA and causes single strand DNA breaks (Sawada and Okada, 1970). The acidity of thiol group in LMWTs has been correlated with the efficiency to generate ROS whereby the lower the pk_a of the thiol group, the higher is the concentration-dependent increase in ROS generation. Winterbourne and Metodiewa compared seven different LMWTs. D-pen caused the highest increase in hydrogen peroxide generation by the xanthine oxidase/hypoxanthine system (Winterbourn and Metodiewa, 1999). The acidity of the thiol group may be affected by the type of substituent on neighboring carbon and the steric hindrance around the sulfur atom. Electron withdrawing substituents would increase the acidity of the thiol group. Aromatic and unsaturated aliphatic thiols are expected to be more toxic while sterically hindered thiols will be less toxic (Munday, 1989). Therefore, if the therapeutic benefit of LMWTs depends on ROS generation *in-vivo*, only those LMWT with thiol pk_a values closer to or lower than the physiological pH of 7.4 should be investigated for further development.

Another important factor that may determine the oxidative potential of LMWTs is the type of metal ion and the concentrations needed to achieve a catalytic enhancement in the rate of oxidation. D-pen, in the presence of copper (II), was shown to inhibit the proliferation of lymphocytes, fibroblasts, endothelial cells and cause apoptosis mediated cytotoxicity in

several cancer cell lines. The effect of varying the metal salt in combination with D-pen upon inhibition of lymphocyte proliferation has been studied (Lipsky and Ziff, 1978). It was found that copper (II) salts (sulfate, acetate and chloride) were similar in their synergistic effects in combination with D-pen while addition of zinc chloride ($ZnCl_2$), ferrous sulfate ($FeSO_4$) or other divalent cations did not have any significant effect on mitogen induced lymphocyte proliferation by D-pen. It was further reported that the copper ions could be completely replaced with ceruloplasmin bound copper without any loss of synergism (Lipsky, 1984). This is significant as endogenous copper is almost entirely bound to ceruloplasmin. As a result, several investigations have focused on using pre-chelated compounds as anticancer agents (Daniel et al., 2004). Moreover, a number of reports have found significant elevation in serum as well as tumor copper levels in several different types of cancers (Carpentieri et al., 1986; Gupta et al., 1991; Rizk and Sky-Peck, 1984; Sharma et al., 1994). Therefore, metal catalysis of ROS generated during thiol autooxidation may be significantly higher in cancer patients and has been proposed as a potential anticancer strategy (Gupte and Mumper, 2009).

Some LMWTs show a biphasic cytotoxic response with intermediate doses being toxic while being minimally toxic at low or high concentrations (Held and Biaglow, 1994; Held and Melder, 1987; Morse et al., 1995). It has been postulated that LMWTs may act as oxidants or antioxidants based on the biochemical conditions and the chemical nature of the thiol containing compound whereby the two opposing roles may be connected through redox pathways as discussed above. This paradox was first observed with cysteamine (Takagi et al., 1974; Vos et al., 1962). The toxicity of cysteamine to cervical cancer (HeLa) cells was greatest at 2 mM and pH 7.4 while decreasing at lower pH values and higher concentrations.

The decrease in toxicity correlated with reduction in the concentration of hydrogen peroxide generated (Takagi et al., 1974). Low concentrations of cysteamine (0.5 mM) were more effective than higher concentrations (>2 mM) in inducing single-strand breaks in DNA, depressing DNA synthesis and inhibiting the rejoining of breaks (Sawada and Okada, 1970). At similar concentrations of cysteamine, while no toxicity was observed at low temperatures (5^{o}C), there was a synergistic enhancement in toxicity to chinese hamster ovary (CHO) cells at higher temperatures (44^{o}C). The increase in cytotoxicity correlated with oxygen uptake by the cells indicating an involvement of redox reactions (Issels et al., 1984). It was hypothesized that at higher concentrations, the generation of ROS by cysteamine may be overcome by its reaction with the generated hydrogen peroxide leading to neutralization of toxicity with concomitant formation of disulfide (**Figure 1.2**). Further investigations confirmed that LMWTs that reacted the slowest with hydrogen peroxide, were more cytotoxic than those that reacted at a faster rate. It was also reported that the biphasic cytotoxicity is not a universal property among LMWT and they differ in their relative cytotoxicity. However, the cytotoxicity was independent of the rate of thiol oxidation (Held and Biaglow, 1994). The rate of reaction between hydrogen peroxide and LMWTs may be slowed by indirect effects e.g. potent glutathione peroxidase inhibition by D-pen and mercaptosuccinate (Chaudiere et al., 1984).

In another study by Betts et al., D-pen affected the degradation of hyaluronic acid (HA) in a biphasic manner where concentrations of 1 mM or lower enhanced the degradation of HA while higher concentrations had a protecting effect. The effect was determined in the presence of an enzymatic system (xanthine oxidase-hypoxanthine) to generate oxidative radicals. The degradation of HA by D-pen was more pronounced in the presence of Fe (III)

ions (Betts et al., 1984). This is possibly due to the generation of hydroxyl radical in Fenton reaction as shown in **Figure 1.2**. Other thiols like GSH, cysteine and NAC had similar effects on HA degradation. However, the corresponding disulfides were ineffective. Staite et al. reported hydrogen peroxide generation by D-pen that was dependent on the concentration of both Cu and D-pen. These authors also reported a dual redox property of D-pen whereby D-pen, when present in excess of Cu (>500 μg/mL), acts as a scavenger of hydrogen peroxide and not as an oxidant (Staite et al., 1985).

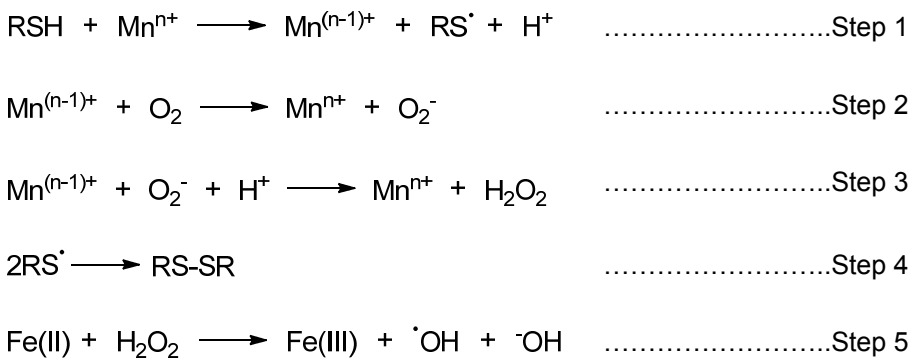

Figure 1.3 Generation of ROS during one electron oxidation of LMWT and subsequent generation of hydroxyl radical by Fenton reaction.

1.2.4. Mechanisms Underlying Anticancer Effects of LMWTs

Several early reports suggested systemic toxicity accompanied with significant redox disturbance upon administration of LMWTs such as bucillamine, captopril and dithiothreitol (DTT) (Helliwell et al., 1985; Munday, 1989; Yeung, 1991). High doses of captopril resulted in hepatic necrosis in mice through GSH depletion (Helliwell et al., 1985). In a study in rats, NAC acted as a protectant against LPS (lipopolysaccharide) induced oxidative stress in lungs at low doses but higher doses led to rapid lung GSH depletion and increased mortality (Sprong et al., 1998). Further evidence of ROS generation during redox cycling of LMWTs and DNA binding activity led the investigators to drop the notion that LMWTs only had a chemoprotective effect with no therapeutic benefit of their own. In addition, this also highlighted the need to direct the delivery of LMWTs to organs of interest.

Many LMWTs have now been reported to show potent antiangiogenesis and cytotoxic effect in cell lines and animal models of cancer. It has been suggested that most of the observed effects of LMWTs can be attributed to either generation of oxidative species, modulation of essential proteins by thiol-disulfide exchange or perturbation of the redox balance. On a cellular level, the effects range from DNA damage, activation of apoptotic transcriptional factors that act as signaling molecules and GSH depletion. Many of these effects are thought to be mediated by intracellular ROS generation. However, direct involvement of the thiyl radical in binding to metal or cysteine containing active sites of enzymes, transcriptional factors as well as DNA has also been shown (**Figure 1.4**).

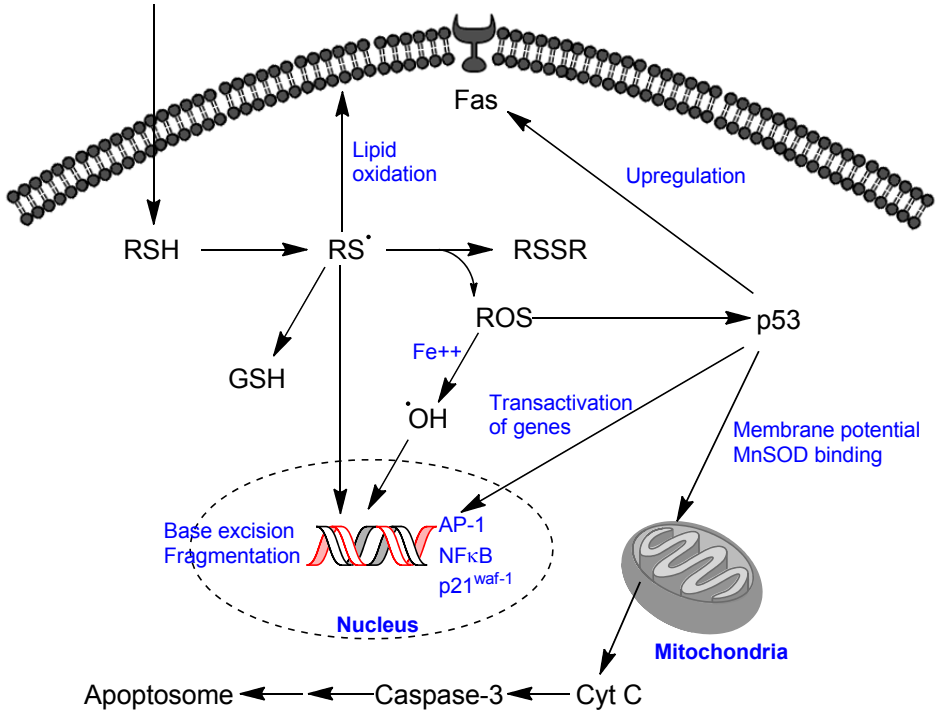

Figure 1.4 A model for cellular interactions induced by LMWTs.

1.2.4.a. Direct Cellular Damage by Free Radical Generation

As outlined above, LMWTs are capable of generating free radicals intracellularly which can cause direct as well as indirect damage leading to cell death. Reactive oxygen species can cause extensive DNA damage through histone oxidation, base excision and strand breaks leading to generation of low molecular weight DNA fragments (Park and Floyd, 1994; Wallace, 1987). This can subsequently result in inhibition of DNA replication and mitotic arrest. Hydroxyl radicals generated as a consequence of Fenton reaction are especially potent at causing DNA damage. They can cause single strand breaks by abstracting hydrogen atoms from the deoxyribose sugars causing the sugar-phosphate backbone to cleave, and can form adducts with both purine and pyrimidine bases (Breen and Murphy, 1995). A system containing thiol, ferric ion and oxygen induced strand breaks in calf thymus DNA associated with the formation of 8-hydroxy-2'-deoxyguanosine. Dihydrolipoic acid was the most potent among those tested (Park and Floyd, 1994). Metal ion complexes of LMWTs are also very potent in binding and cleaving DNA (Dulger et al., 2000).

Although cells have the capability to repair DNA damage, extensive fragmentation can lead to activation of apoptotic triggers (Bertram and Hass, 2008; Breen and Murphy, 1995). Both D-pen and bucillamine, in the presence of copper sulfate, induced extensive double stranded DNA strand breaks in human peripheral blood lymphocytes and completely suppressed the repair at higher concentrations. In this study, most of the effect could be attributed to damage by free radicals generated upon interaction with copper as no effect was observed with the drugs alone (Yamanaka et al., 1993). Cysteamine also induced single strand DNA breaks and almost complete inhibition of DNA synthesis at concentrations of 0.5

mM in mouse leukemia cells. The number of breaks synergistically enhanced when the cells were irradiated with X-rays (Sawada and Okada, 1970). Amifostine treatment resulted in an exposure dependent DNA fragmentation in hematopoietic stem cells (Ribizzi et al., 2000). Four different LMWT, NAC, cysteine, 2-mercaptoethanol and GSH induced DNA fragmentation in CEM cells at a dose of 1 mM that resolved as 180 bp DNA ladder on gel electrophoresis which is characteristic of apoptotic cell death (Morse et al., 1995). The position of the thiol group also affects DNA fragmentation. Vicinal LMWT increased the number of DNA breaks in human leukemia cells in the presence of nickel chloride whereas monothiols partially protected the DNA from nickel induced damage (Lynn et al., 1999).

Lipid peroxidation mediated by free radical generation by LMWT can destabilize cell membrane by oxidizing the lipids to hydroperoxides that further lead to the accumulation of aldehydes capable of forming stable toxic adducts with cellular proteins, DNA and lipids. The presence of metal ions such as iron and copper is known to potentiate the conversion of hydroperoxides to aldehydes. Two of the common aldehydic products are malondialdehyde and 4-hydroxy-2E-nonenal (Cejas et al., 2004). A combination of cysteine and iron synergistically stimulated lipid peroxidation in liver microsomes mediated by ROS generation (Searle and Willson, 1983). Fenton chemistry and generation of hydroxyl radical during oxidation of LMWTs has an important role as the latter can initiate lipid peroxidation. Peroxidation of microsomal phospholipids was observed with LMWTs in combination with ADP-chelated iron (III). The nature of peroxidation was biphasic for cysteine and DTT with higher concentrations being less active, analogous to the cytotoxic property of some LMWTs (Tien et al., 1982).

Thiyl radical formed during the redox recycling of LMWT (**Figure 1.1** and **Figure 1.2**) can mediate oxidation of polyunsaturated fatty acids such as linoleic acid. Reaction of captopril with hydroxyl radical generates captopril thiyl radicals. The thiyl radicals attack polyunsaturated fatty acids leading to the formation of pentadienyl type radical which upon reaction with molecular oxygen forms conjugated dienes (Schoneich et al., 1992). Thiyl radicals can also attack unsaturated phospholipids and cause reversible isomerization of *cis*-fatty acids to *trans*-fatty acids leading to membrane destabilization (Ferreri et al., 1999). Oxidation of phospholipids by glutathionyl radicals, generated by myeloperoxidase stimulated phenol oxidation system, has been shown in human leukemia cells leading to cell death (Borisenko et al., 2004).

Studies using DTT showed that free radical damage by LMWT may be partly mediated by stimulation of the pentose phosphate pathway as higher cytotoxicity was observed in the presence of medium containing glucose and cells deficient in glucose-6-phosphate dehydrogenase were more sensitive to DTT in the presence of glucose (Held et al., 1993).

1.2.4.b. Apoptosis and Cell Signaling Interactions

Hydrogen peroxide and ROS generating agents can lead to apoptotic or necrotic cell death depending on the concentrations of ROS generated and severity of cellular damage with apoptosis being the preferred pathway at lower concentrations (Chandra et al., 2000). Apoptosis or programmed cell death is comprised of a series of intracellular events triggered by different pathways. Although apoptosis induction may occur through different pathways, one of the modes of ROS mediated induction involves loss of mitochondrial membrane

potential accompanied by the release of cytochrome c (Stridh et al., 1998). Subsequently, cytochrome c forms a part of the apoptosome in the cytosol leading to activation of a series of downstream signaling molecules including the caspase family of proteases. A combination of DTT with Vitamin B_{12b} caused 50% decrease in mitochondrial potential and release of cytochrome c in human epidermoid larynx carcinoma cells. Other indicators of apoptosis including caspase-3 activation and DNA ladder formation were also observed (Solovieva et al., 2008). Another LMWT, PDTC (pyrrolidine dithiocarbamate), showed similar effects human leukemia cells in the presence of copper chloride (Chen et al., 2008b).

Apoptotic cell death can be mediated by the reactive carbonyl species (RCS) scavenging activity of LMWTs. This has been observed in both human and murine melanoma cells. Reactive carbonyl species such as methylglyoxal, glyoxal and malondialdehyde play an active role in proliferation and metastasis. For example, they inhibit cytochrome c release from mitochondria and inhibit pro-apoptotic signals by interacting with proteins such as heat shock protein (Hsp 27) and mitochondrial permeability transition pore protein (Johans et al., 2005; Sakamoto et al., 2002). A structure activity relationship study by Wondrak et al. showed that a thiol and amino functional group was required for carbonyl scavenging via thiazolidine ring formation and apoptotic activity in melanoma cells. The loss of thiol by disulfide formation or S-methylation resulted in a complete loss of activity. NAC also did not show strong carbonyl scavenging due to the acetylation of the amino group. However, stereochemical configuration did not have any significant effect on the apoptogenicity as D-pen and L-pen were reported to be equally effective (Wondrak et al., 2006).

LMWTs may also cause apoptosis by interaction with several transcription factors. Such interaction may involve induction or suppression of the transcription factors that is independent of the redox properties of LMWTs or may be mediated by ROS generation. Tumor suppressor protein, p53, has an important role in redox regulation and maintaining a physiological balance between oxidant and antioxidant status of cells (Liu et al., 2008). It does so by regulating the expression of both pro- and anti-oxidant genes. Upregulation of p53 leads to increased transcription of genes coding for pro-oxidant enzymes. Agents that promote nuclear translocation of p53 have similar effect. This may be accompanied by mitochondrial translocation and inhibition of manganese superoxide dismutase (MnSOD) (Liu et al., 2008; Zhao et al., 2005). Interestingly, downregulation of p53 leads to suppression of genes coding for antioxidant enzymes (Liu et al., 2008; Sablina et al., 2005). Therefore, any changes in the physiological concentrations of p53 result in increased oxidative stress and apoptosis with further attack on mitochondrial enzymes (Polyak et al., 1997). On the other hand, any changes in the redox status of the cell may also act as a trigger for p53 induction (ROS generators) or suppression (ROS scavengers). Due to the presence of several cysteines and zinc in the DNA binding domain of p53 (Hainaut and Mann, 2001), LMWTs have the potential to directly interact with p53 by virtue of their thiol group and metal chelating properties. Alternately, modulation of the redox status via ROS generation or DNA damage by LMWTs may also induce p53 expression. Induction of p53 can further lead to increased expression of $p21^{waf-1}$, which is a known cyclin dependent kinase inhibitor. It can cause p53 dependent growth arrest at different phases of cell division (Abbas and Dutta, 2009). However, $p21^{waf-1}$ can also act independent of p53. This was reported with PDTC and

other antioxidants. PDTC induced G1 arrest and apoptotic death in human colorectal cells. The levels of $p21^{waf-1}$ were elevated whereas p53 was unchanged (Chinery et al., 1997).

Apoptosis induced by p53 upregulation may also be mediated via Fas signaling as p53 is a known inducer of Fas (Bennett et al., 1998). Fas-signaling involves binding of the trimeric Fas ligand simultaneously to three Fas receptors on the cell surface to trigger caspase activation followed by apoptosis. Harada et al. reported an elevated surface expression of *Fas* receptor on rheumatoid synovial fibroblasts upon treatment with D-pen and copper sulfate leading to apoptotic death (Harada et al., 2002).

NAC and 2,3-dimercapto propanol elevated p53 levels in both transformed ($p53^{+/+}$) and normal ($p53^{-/-}$) mouse embryo fibroblasts. However, apoptosis was caused only in the transformed cells. Elevation of p53 and apoptosis induction was independent of the redox status of the cells but dependent on the presence of thiol group indicating a separate mechanism for the specificity towards transformed cells (Liu et al., 1998b). In an extended study, the transformed human cells, the cells became 480-fold more sensitive to D-pen at the immortalization stage. The sensitivity was found to be predominantly occurring through p53 induction leading to caspase-3 activation and apoptosis (Havre et al., 2002).

It was recently shown that apoptosis induced by D-pen and NAC in cervical cancer (HeLa) cells is also mediated through an ER stress response (Guan et al., 2010). Treatment with either D-pen or NAC resulted in an increase in expression of glucose-regulated protein (GRP78), caspase-3 and C/EBP homologous protein (CHOP), all being important mediators of apoptosis. Tartier et al. observed significant caspase-3 activity upon treatment of human leukemia (HL-60) cells with DTT while absence of caspase-9 activity showed that the

apoptosis induced by some LMWTs may be non-mitochondrial in origin (Tartier et al., 2000).

LMWTs affect different phases of cell cycle based on which downstream processes are involved in mediating their cytostatic actions. Friteau et al. studied the effect of D-pen on the cell cycle progression and observed that the type of effect varies in different cell lines. While D-pen arrested the articular chondrocytes (normal cells) in G0/1 phase, the HeLa and L929 (transformed cells) cells were arrested in the G2+M phase (Friteau et al., 1988). Similarly, β-mercaptoethanolamine (BME) was shown to effect different phases in lymphocytes and leukemia cells (Jeitner et al., 1998). BME arrested the leukemia cells in the S phase whereas lymphocytes in G0/1 phase similar to D-pen. The authors proposed that these differences can be attributed to lower redox buffer capacity of cancer cells that makes the cells in S phase preferentially sensitive to oxidative stress.

1.2.4.c Anti-angiogenic Effects of LMWT

Angiogenesis is essential for tumors to vascularize, grow and metastasize to other sites. The theory of tumor inhibition by arresting angiogenesis was first proposed by Folkman (Folkman, 1971). LMWTs have been shown to cause anti-angiogenic effects *in-vitro* and *in-vivo*. Attempts to understand the mechanism of anti-angiogenic effect of LMWT have also shown differences within these compounds in their ability to inhibit angiogenesis.

Copper is an established cofactor in angiogenesis. LMWTs have been investigated as anti-angiogenic compounds due to their strong copper chelation property. Copper depletion and generation of hydrogen peroxide by a combination of D-pen and copper synergistically inhibited DNA synthesis and the proliferation of endothelial cell growth factor (ECGF)

stimulated as well as unstimulated endothelial cells (EC) (Matsubara et al., 1989). D-pen also inhibited ECGF induced neo-vascularization in rabbit cornea. A combination of diet and D-pen resulted in copper depletion in rabbits and the VX2 carcinomas formed were smaller and avascular while rabbits with normal serum copper levels had large vascularized VX2 carcinomas (Brem et al., 1990).

Angiostatin is a 38 kDa endogenous protein fragment that has potent anti-angiogenesis activity. First isolated by O'Reilly, angiostatin inhibited endothelial cell proliferation and strong reduction in the growth of metastases subsequent to the removal of primary tumors in Lewis lung carcinoma (O'Reilly et al., 1994). Angiostatin may be generated from plasminogen via its conversion to plasmin by tissue plasminogen activators (tPA). LMWTs acting as free sulfhydryl donors, facilitate the conversion of plasmin to angiostatin and therefore a combination of LMWTs and tPA can produce antiangiogenic effects by *in-situ* generation of angiostatin (Gately et al., 1997). L-cysteine, captopril, GSH, NAC and D-pen were investigated for their efficiency in supporting the conversion of plasminogen to angiostatin. D-pen was found to be the most potent *in-vitro* and *in-vivo*, the combination resulting in 58% inhibition of tumor growth in BLM melanoma model (de Groot-Besseling et al., 2006).

Matrix metalloproteinases play a significant role in the metastatic growth and invasive ability of cancer cells. Secreted by either the cancer cells or the stromal cells in response to signaling molecules including growth factors and cytokines, MMPs act by degrading extracellular matrix (ECM) components to aid in the mobilization and escape of cancer cells. For example, MMP-2 (72 kDa) and MMP-9 (92 kDa), categorized as collagenases or gelatinases, act on collagen type IV which is the major protein in the

basement membrane (Duffy, 1992). These collagenases have been overexpressed in metastatic tumors and the levels correlate with the metastatic potential (Liotta et al., 1980). Some of the other MMPs of significance in promoting cancer metastasis (angiogenesis and migration) and progression (proliferation and survival) are MMP-1, -3, -7 and -14 (Egeblad and Werb, 2002; Noe et al., 2001; Pavlaki and Zucker, 2003; Rundhaug, 2003). Zinc is present in the active site of MMPs and has strong affinity for thiol group (Tu et al., 2008). It is no surprise that many LMWTs such as D-pen and captopril are potent inhibitors of both MMP-2 and MMP-9 (Volpert et al., 1996). This inhibition has been shown to reduce the metastatic potential and antitumor effect in several studies. In spite of promising preclinical data, most of the clinical trials with MMP inhibitors have suffered from lack of efficacy and/or unexpected side effects owing to a lack of specificity towards the desired type of MMP enzymes (Pavlaki and Zucker, 2003). Utilizing the structure-activity relationship, several LMWTs with high specificity towards selective MMPs have been identified which could pave the way for further development (**Figure 1.5**).

Low molecular weight thiols such as D-pen have also been reported to inhibit denovo collagen cross-linking and destabilize cross-linked collagen in the ECM. However, several mechanisms of collagen inhibition have been proposed. One of the mechanisms involves inhibition of lysyl oxidase. Lysyl oxidase catalyzes conversion of amino groups in lysine to aldehydes thus promoting cross-linking. Nimni and co-workers have proposed a mechanism whereby LMWT such as D-pen inhibit cross-linking by formation of thiazolidine ring complexes with these aldehydes (Nimni, 1968; Nimni et al., 1972). LMWT may also cause direct inhibition of lysyl oxidase via depletion of copper which is a co-factor of lysyl oxidase. The inhibition of lysyl oxidase in tumors may result in delayed tumor growth, anti-

angiogenesis and decreased metastatic potential as observed in several studies (Chvapil, 2005; Chvapil and Dorr, 2005; Chvapil et al., 2005). In another study, Siegel (Siegel, 1977) reported that D-pen acts by blocking the synthesis of polyfunctional cross-link products from Schiff base crosslink intermediates thus causing accumulation of the Schiff base precursors during collagen cross-linking.

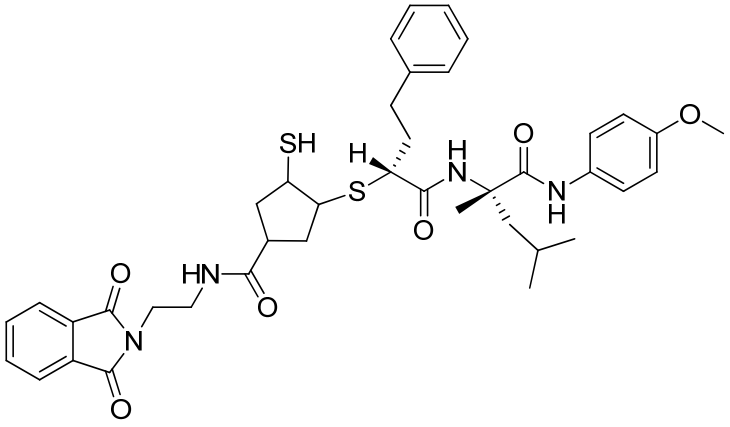

MMP-1 (K_i > 3000 nM)
MMP-2 (K_i = 31 nM)
MMP-3 (K_i = 1.5 nM)
MMP-7 (K_i = 76 nM)
MMP-9 (K_i = 4.6 nM)
(Hurst et al., 2005)

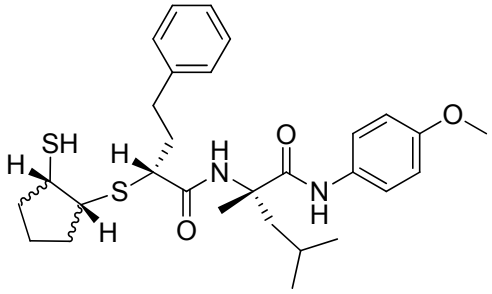

MMP-1 (K_i > 12000 nM)
MMP-2 (K_i = 20 nM)
MMP-3 (K_i = 100 nM)
MMP-7 (K_i = 1000 nM)
MMP-9 (K_i = 8.6 nM)
(Park et al., 2003)

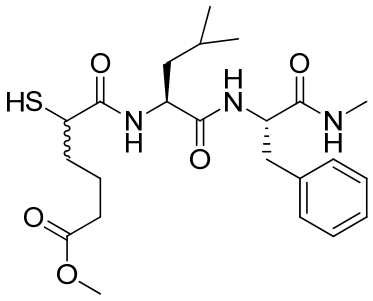

MMP-3 (IC_{50} = 0.49 μM)
MMP-8 (IC_{50} = 0.014 μM)
MMP-9 (IC_{50} = 0.001 μM)
(Baxter et al., 1997)

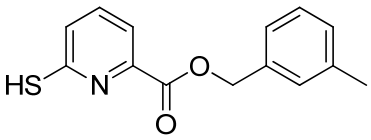

MMP-1 (IC_{50} > 150 μM)
MMP-2 (IC_{50} = 7 μM)
MMP-9 (IC_{50} = 7 μM)
Mmp-12 (IC_{50} = 70 μM)
(Hayashi et al., 2007)

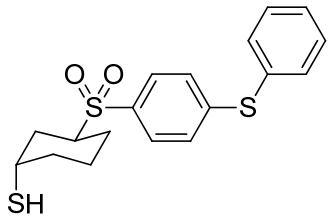

MMP-1 (IC_{50} > 10 μM)
MMP-8 (IC_{50} = 0.05 μM)
MMP-13 (IC_{50} = 0.0004 μM)
(Freskos et al., 1999)

Figure 1.5 Examples of synthetically designed matrix metalloproteinase (MMP) enzyme inhibitors.
The inhibitors contain free thiol groups and show differential activity or binding affinity to different MMP enzyme subtypes.

1.2.5. LMWTs Investigated for Anticancer Properties

1.2.5.a. D-penicillamine

D-pen (**Fig. 1.1**) is FDA approved for the treatment of rheumatoid arthritis and is classified as a disease modifying anti-rheumatic drug (DMARD). However, the exact mechanism of therapeutic action is not known. Some of the proposed mechanisms include inhibition of collagen cross-linking (Nimni et al., 1972; Siegel, 1977) and immunomodulation (Gerber, 1978). D-pen is a very strong metal chelator and its interaction with endogenous metals has been widely investigated to study the mechanism of its pharmacological effects. Several investigations have focused on the generation of ROS by D-pen in the presence of copper. A direct evidence of H_2O_2 generation upon incubation of D-pen with catalytic amounts of copper sulfate was shown and this combination of D-pen and copper sulfate was cytotoxic to breast cancer and leukemia cells (Gupte and Mumper, 2007a; Gupte and Mumper, 2007b).

In a previous study, treatment of cells from 25 different human tumors with D-pen plus copper sulfate significantly decreased the percentage of viable cells. Leukemia cells were found to be more sensitive than other type of cancer cells while DTT failed to show effectiveness. The authors concluded that the cytotoxicity of D-pen cannot be solely attributed to the thiol group. However, the inhibition of murine plasmacytoma xenograft was not significant when treated with a combination of D-pen and copper (Samoszuk and Nguyen, 1996).

The effect of D-pen on various cell lines has also been studied in the absence of externally added copper. Baier-Bitterlich et al. studied the effect of D-pen in various human cell lines without addition of copper and found that the sensitivity to D-pen was different for

each cell type. The promyelocytic (HL-60) and lymphoblastoid (H9 and NC37) cells showed a bimodal dose-response curve where the inhibition was partly restored at higher concentrations of D-pen (Baier-Bitterlich et al., 1993). D-pen has also been shown to inhibit endothelial cell proliferation *in-vitro* and neovascularization in rabbit cornea *in-vivo* as discussed above.

D-pen has distinct advantages over other LMWTs in that; 1) the pKa of its thiol group (7.9) makes it more reactive than other endogenous LMWTs at physiological pH of 7.4 and, 2) being a D-isoform, it is resistant to degradation by endogenous enzymes such as L-amino acid oxidase, and L-cysteine desulfhydrase. Additionally, D-pen is much less sensitive to degradation by D-amino acid oxidase as well (Aposhian and Bradham, 1959).

In spite of a clear potential for further development as an anticancer agent, the delivery of D-pen to cancer cells remains a challenge. D-pen is essentially cell impermeable. Lodemann (Lodemann, 1981) reported that the uptake of D-pen was >100-fold less than L-pen in mouse fibroblasts and D-pen did not utilize the amino acid transport system to gain cellular entry. Schumacher et al. also proposed that D-pen possibly acts at the membrane level to inhibit lymphocyte stimulation (Schumacher et al., 1975).

The second challenge to the delivery of D-pen is the reactive thiol group. The thiol group of D-pen is reported to conjugate with plasma proteins through disulfide linkages especially albumin. The protein binding in plasma is so rapid that essentially no free D-pen can be detected after 4 hours of oral administration (Planas-Bohne, 1981). Protein conjugation modifies the plasma disposition of D-pen whereby the albumin conjugate of the drug can circulate in the plasma for longer periods leading to slower elimination of the metabolites. In a study comprised of 5 human volunteers, the half-life of D-pen was found to

be 59 ± 8.4 min while the albumin conjugate formed *in*-situ circulates with a half-life of 1.65 ± 0.29 days (Joyce et al., 1991). Additionally, D-pen may also form conjugates with tissue proteins. The albumin conjugate of D-pen is very stable to reduction. This is possibly due to steric hindrance from the β, β-dimethyl groups. Therefore, the D-pen-albumin conjugate is not expected to contribute to the amount of free drug available in the body (Joyce et al., 1989). However, rapid disposition of the free form and essentially non-reducible protein conjugates is a challenge to the delivery of D-pen and there is a need to stabilize the thiol group until D-pen reaches the therapeutic target site.

Long-chain alkyl esters of D-pen have been synthesized and investigated for their anticancer potential (Chvapil, 2005; Chvapil and Dorr, 2005; Chvapil et al., 2005). Methyl, hexyl and benzyl esters of D-pen were synthesized and tested for antitumor effectiveness in breast adenocarcinoma and melanoma. An intratumoral injection of the hexyl ester of D-pen significantly decreased the tumor growth rate and delayed the detection of metastatic sites in rats bearing mammary adenocarcinoma. The alkyl chain may help in improving the cellular permeability of D-pen. However, the challenges to the anticancer delivery of D-pen including rapid oxidation in plasma and faster clearance still remain with this strategy.

Conjugates of D-pen with gelatin (Gupte et al., 2008) were investigated to overcome some of the challenges to the delivery of D-pen. The polymer conjugate successfully delivered D-pen to cancer cells and showed a dose dependent cell uptake. The conjugate resulted in cytotoxicity in human leukemia cells.

A phase II trial evaluated the antiangiogenic effect of a hypocupremia induced by a combination of copper deficient diet and D-pen in 40 patients with glioblastoma multiforme. D-pen showed a median survival of 11.3 months and progression free survival of 7.1 months.

The treatment was able to reduce the serum copper levels significantly to the desired level of <50 μg/dL after 2 months of therapy. The survival enhancement was not significant when compared to the reference group treated with concurrent radiation therapy and either an angiogenesis inhibitor (suramin or carboxyamidotriazole) or a radiosensitizer (RSR 13) (Brem et al., 2005). However, it is not clear if the patients in this trial had significantly elevated serum or tumor copper levels as generation of ROS and apoptosis induction is dependent on the availability of copper as shown by other reports (Staite et al., 1985). Additionally, we and others have shown that D-pen is essentially impermeable to the cell membrane and most of the therapeutic effects are possibly due to extracellular ROS generation or other unknown mechanisms.

1.2.5.b. N-acetyl cysteine

NAC is a cysteine precursor which in turn is a precursor of GSH. The role of NAC as an antioxidant and a chemopreventive in cancer has been studied and reviewed in detail. However, several recent studies indicate a greater role of NAC in cancer therapy and involvement of additional mechanisms that may lead to protective effects in cancer progression and metastasis. Oral treatment with NAC decreased the tumor weight and number of lung metastases (Albini et al., 1995). Similar reduction in tumor growth and increased survival in mice bearing Kaposi sarcoma was observed in a separate study. The levels of VEGF were decreased and NAC caused a dose dependent inhibition of type IV collagenases, MMP-2 and MMP-9 (Albini et al., 1995; Albini et al., 2001). The inhibition of MMPs may be mediated by chelation of zinc, a co-factor, by the free thiol group of NAC. This was evident as ascorbic acid, which lacks a free thiol group, did not affect MMP-2

levels (Albini et al., 2001). Inhibition of VEGF by NAC has been previously reported and could be responsible for its antiangiogenic effect. NAC also reduced chemotaxis and invasion ability of endothelial cells at much lower concentrations than the concentrations at which it reduced the viability of these cells (Cai et al., 1999). NAC showed a biphasic effect on sciatic nerve fiber action potential where concentrations above 1 mM were inhibitory and below 1 mM were neuroprotective (Moschou et al., 2008). This is analogous to the oxidant-antioxidant paradigm discussed for some other LMWTs above.

When used in combination with dox, NAC had a synergistic effect on the tumor growth and lung metastasis in a murine model (De Flora et al., 1996). The addition of NAC to therapy did not result in the loss of efficacy of dox, which is known to generate radical species in cancer cells. Some of the possible reasons for the synergy may be a reduction in MMP-2 and MMP-9 activity leading to enhanced penetration of dox in the tumor (Albini et al., 2001) and a synergistic elevation of oxidative stress (Zheng et al., 2010).

1.2.5.c. Tetrathiomolybdate

Tetrathiomolybdate is available as an ammonium (TM) or choline (ATN-224®) salt and is FDA approved for the treatment of Wilson's disease. **Figure 1.1** shows the structure of the ammonium salt of TM. It has been widely used in the treatment of Wilson's disease due to its strong copper chelating property. It is well absorbed orally when administered prior to food intake and forms a tripartite complex with the non-ceruloplasmin bound copper in the systemic circulation. TM is also a potent inhibitor of Cu-Zn SOD and was found to be cytotoxic to melanoma cells via increased oxidative stress as a result of decreased cellular ROS scavenging (Trapp et al., 2009).

In several preclinical studies, TM has shown potent anti-angiogenic activity. In a study, TM decreased the microvessel density and the number of secondary branching in the mammary glands of nulliparous Her2/neu transgenic mice (Pan et al., 2009). In another mouse model of neovascularization, TM treatment significantly reduced neovascular cell nuclei and VEGF expression compared to control mice (Elner et al., 2005). Other effects such as a reduction in NFκB expression and basic fibroblast growth factor (bFGF) by TM also contribute to the anti-angiogenic effect (Pan et al., 2002). Systemic treatment with TM inhibited tumor growth and angiogenesis in SUM149 breast cancer xenografts. The levels of several angiogenic precursors including VEGF, FGF-2, IL-1α, IL-6 and IL-8 were significantly decreased in TM treated mice (Pan et al., 2002). Similar tumor suppression was shown in mice bearing squamous cell carcinoma (Cox et al., 2003; Cox et al., 2001).

A phase I study in patients with metastatic solid tumors investigated the effect of copper depletion by TM on disease progression. Ceruloplasmin was used as a surrogate marker for serum copper and a reduction to 20% of the baseline value was considered as a target level to begin therapy with TM. Five of the six patients that achieved the target levels in the highest dose group showed a stable disease for >3 months (Brewer et al., 2000). Phase II trials have been conducted in patients with advanced kidney cancer (Redman et al., 2003) and hormone refractory prostate cancer (HRPC) (Henry et al., 2006), respectively. These trials also aimed to establish a correlation between the angiogenic precursors (VEGF, bFGF, IL-6 and IL-8), serum copper levels and disease progression.TM treatment did not improve disease progression in HRPC patients and there was no correlation between the levels of angiogenic precursors and prostate specific antigen. However, patients with advanced kidney cancer treated with TM that reached target levels of copper depletion, showed stabilization of

disease and there was a correlation between serum copper levels and angiogenic precursors. In another phase II trial in 30 patients with malignant pleural mesothelioma, efficacy of TM in stage I or II patients terms of time to progression was comparable to patients previously treated with standard chemotherapy regimen while the efficacy in stage III patients was not improved (Pass et al., 2008).

TM has also been investigated in combination chemotherapy regimens in both pre-clinical and clinical studies. Mice receiving a combination of TM and radiation therapy showed a significant decrease in tumor growth compared to either of the treatments alone (Khan et al., 2006).

1.2.5.d. NOV-002

NOV-002 is a glutathione disulfide (GSSG) mimetic composed of a complex between GSSG and cisplatinum in a ratio of 1000:1. As the amount of cisplatin is very low, GSSG is considered the active component (Townsend and Tew, 2009). It is believed to act primarily by perturbation of redox homeostasis but multiple effects have been seen in cancer cells. As NOV-002 has been shown not to enter cells passively (Brennan et al., 2006), most of its effects may be extracellular or mediated through membrane interactions on the cell surface. Treatment of human leukemia (HL-60) cells with NOV-002 resulted in decreased GSH/GSSG ratio, oxidation of cell surface protein thiols and increased S-glutathionylation of intracellular proteins.

It is interesting to note that NOV-002, that itself has small amounts of complexed cisplatin, when administered in combination with other chemotherapeutic drugs, increased the anticancer effects and improved tolerance (Townsend et al., 2008a). Concomitant therapy

with NOV-002 in mice resulted in a decrease in cisplatin associated nephrotoxicity (Jenderny et al., 2010). Treatment in mice showed a transient oxidative signal in plasma and a sustained decrease in total plasma free thiol. Other strategies based on modulating the GSH/GSSG balance have also shown synergistic enhancement in the sensitivity of cancer cells as adjuvant therapy (Zhao et al., 2009).

NOV-002, that already contains a small amount of cisplatin, showed a significant improvement in 1 year survival and decreased tumor progression rates in non-small cell lung cancer (NSCLC) and ovarian cancer patients when administered in combination with standard dose of cisplatin (Pazoles and Gernstein, 2006; Townsend et al., 2008b). In spite of promising Phase 1/2 results in NSCLC patients, a recent Phase III trial failed to show an improved survival with NOV-002 in combination with chemotherapy (PTX + Carboplatin) when compared to chemotherapy alone (Fidias et al., 2010). NOV-002 is currently being investigated in breast cancer patients.

1.2.5.e. Mesna

Mesna (2-mercaptoethanesulfonate) was approved as uroprotector to be used with oxazaphosphorines such as cyclophosphamide and ifosphamide which have severe urotoxicity associated with them. Since then, mesna has been investigated with other chemotherapeutic drugs in a number of combination trials in several different types of cancers including bladder cancer, metastatic breast cancer, uterine sarcoma and ovarian cancer (Aksoy et al., 2008; Baur et al., 2006; Walters et al., 1998). It has been suggested that mesna acts by neutralizing the free radical species associated with chemotherapy thus reducing the overall toxicity and increasing the tolerance. A disulfide compound, BNP7787

(2,2-dithio-bis-ethanesulfonate sodium), which is a precursor of mesna is also currently being investigated as chemopreventive against ciplatin associated toxicity (Verschraagen et al., 2003). However, like other LMWTs, mesna has also been shown to affect cancer cell viability when used alone. Mesna inhibited several human malignant cell lines and caused sensitization of some resistant cell lines (Blomgren et al., 1991). Interestingly, the cytotoxicity of mesna was also biphasic in nature, whereby the cell inhibition was reversed at higher doses (Blomgren et al., 1990). Interaction of mesna with transition metal ions especially copper has been shown to change the accumulation site from kidney to liver when administered simultaneously (Shaw and Weeks, 1986). Mesna when used in combination with tPA in patients with advanced solid tumors, generated two different isoforms of angiostatin *in-situ* and the treatment led to a decrease in tumor markers in two of the fifteen patients although no clinical response was observed (Soff et al., 2005). Antitumor activity of mesna in patients with metastatic or relapsed tumors previously treated with chemotherapy has also been studied (Yurkow and Mermelstein, 2006) (**Table 1.1**). It may also act as a redox clamping agent whereby treatment with mesna following a brief exposure to chemotherapeutic agent significantly sensitizes cancer cells. The redox clamping action is mediated by promotion of apoptotic signals and suppression of antioxidant response following exposure to the chemotherapeutic agent.

1.2.5.f. Amifostine

Amifostine (WR-2721, S-2-(3-aminopropylamino) ethyl phosphorothioic acid) has been widely investigated for its radioprotective and chemoprotective properties that were specific to normal tissue but did not affect radiation induced damage to malignant tissue

allowing for higher doses to be administered (Treskes et al., 1992; Yuhas, 1972; Yuhas, 1979; Yuhas and Storer, 1969). This effect was found to be dependent on the tumor type, size and radiation dose (Milas et al., 1984; Milas et al., 1983). Hydrophilicity is considered as a major barrier to cell entry of amifostine (Yuhas et al., 1982). *In-vivo* dephosphorylation of WR-2721 in the presence of alkaline phosphatases leads to the formation of its thiol metabolite, WR-1065. This decreases the hydrophilicity resulting in an increase in tumor cell uptake (Issels and Nagele, 1989; Treskes et al., 1992). Although most of the clinical trials have focused on the chemoprotective effects of amifostine and WR-1065 when used in combination with cytotoxic agents, some of the trials indicated that amifostine may have anticancer properties of its own are summarized in **Table 1.1**. In addition, recent *in-vitro* studies show that novel mechanisms may be involved in anticancer effects of amifostine.

The first report of anticancer properties of amifostine when administered alone showed suppression of the growth of Ehrlich's ascites tumors (Ikebuchi et al., 1981). A synergistic enhancement in toxicity was observed when amifostine was used in combination with a free radical generator, 6-hydroxydopamine, due to hepatic GSH depletion (Schor, 1987). However, GSH depletion is probably mediated by mechanisms other that simple disulfide formation as the effect plateaus at smaller doses. Comparative studies showed that both WR-1065 and amifostine, activate and induce the expression of p53 resulting in a delayed G1/S transition, mediated by $p21^{waf-1}$, in breast cancer cells which is p53 dependent (North et al., 2000). Similar studies in lung cancer cells showed that p53 upregulation by amifostine resulted in sensitization of resistant cells (Swisher et al., 2000). Amifostine alone caused dose dependent apoptosis and G2/M arrest in lung cancer cells, and the effect was synergistic in combination with adenoviral vector containing wild type p53. Further

investigations indicated involvement of dephosphorylation of Cdc2 kinase leading to p53 mediated DNA damage and apoptosis (Pataer et al., 2006). However, apoptosis and cell growth inhibition independent of p53 expression was induced in myelodysplastic syndrome cells by amifostine (Ribizzi et al., 2000). Other LMWT especially aminothiols seem to have some effect on the activity of p53 as discussed above and this mechanism seems to play an important role in their anticancer effects.

Amifostine has also shown antiangiogenic effects in chorioallantoic membrane (CAM) model where it reduced the number of vessels, decreased the VEGF mRNA levels and decreased laminin and collagen deposition (Giannopoulou et al., 2003). In a murine sarcoma model, amifostine inhibited spontaneous metastases formation, increased serum levels of angiostatin and inhibited MMP enzymes (MMP-2 and MMP-9) (Grdina et al., 2002).

1.2.5.g. Captopril

Captopril (D-3-mercapto-2-methylpropanoyl-L-proline) is an angiotensin converting enzyme (ACE) inhibitor with a free thiol group approved for the treatment of hypertension. In addition to the FDA approved indication, ACE inhibitors have been shown to arrest the growth of several different types of cancer cells and to inhibit angiogenesis. In a clinical study of 287 patients with advanced NSCLC, adding an ACE inhibitor to cisplatin regimen increased the median survival by 3.1 months (Wilop et al., 2009).

The ACE inhibitors with a free thiol group were found to be the most potent in this category and research has been conducted to further investigate the mechanism of cytotoxicity (Molteni et al., 2003). Captopril completely inhibited corneal neovascularization

and specifically prevented chemotaxis of endothelial cells, both stimulated in the presence of bFGF (Volpert et al., 1996). The antiangiogenic effect could not be explained by ACE inhibition as other ACE inhibitors lacking a free thiol group failed to show any effect although this enzyme has been shown to induce new vessel formation (Fernandez et al., 1985; Le Noble et al., 1993). Captopril, like some other LMWTs, was shown to inhibit the activity of MMP-2 and MMP-9 mediated through its zinc chelating ability which is an important cofactor for these enzymes (Sorbi et al., 1993). This could partly explain the stronger antiangiogenic effect of captopril among other ACE inhibitors. MMP inhibition directly correlated with a decrease in the tumor volume and number of metastases in Lewis-lung carcinoma model in mice (Prontera et al., 1999). Captopril has also shown a decrease in the invasiveness of glioma cells. The effects could be overcome by excess zinc (Nakagawa et al., 1995).

Interaction of captopril with metal ions and associated cell death has also been studied. A dose dependent generation of hydrogen peroxide in the presence of copper (sulfate or chloride salt or ceruloplasmin bound) but not with iron (ferric or ferrous chloride salt or transferrin bound) was observed which led to loss of viability in human mammary ductal carcinoma cells (Small et al., 1999).

Captopril showed anticancer effects in renal cancer cells which was mediated by upregulation of type II receptors for transforming growth factor (TGF)-β thus causing growth inhibition (Miyajima et al., 2001). Similar decrease in cell viability was observed in human parotid gland adenocarcinoma cells, the mechanism being independent of ACE inhibition (Nittler et al., 1998). Its effect on neuroblastoma was cytostatic and could be attributed to ACE inhibition (Chen et al., 1991).

Antineoplastic effects of captopril have been investigated in several animal models. Oral administration of 50 mg/kg captopril to rats reduced the number of radiation induced squamous cell carcinomas and fibrosarcomas. The tumors were smaller and less vascularized compared to controls (Ward et al., 1990). Captopril also caused a significant tumor growth delay in mammary ductal carcinoma in mice (Molteni et al., 2003). In a patient suffering from Kaposi sarcoma, captopril treatment resulted in complete regression of 50% and partial regression of 25% of the lesions (Vogt and Frey, 1997). Captopril is currently being investigated in clinical trials for treating patients with metastatic cancer due to its ability to generate angiostatin in combination with a tissue plasminogen factor (ClinicalTrials.gov Identifier: NCT00086723).

Table 1.1 Anticancer clinical trials investigating the potential of Low Molecular Weight Thiols (LMWTs).

LMWT	Study Composition	Comments	Reference
D-penicillamine	40 patients with glioblastoma multiforme	Median survival of 11.3 months and progression free survival of 7.1 months; No significant enhancement in survival over reference group.	(Brem et al., 2005)
Tetrathiomolybdate	18 patients with metastatic solid tumors; Evaluated 14 with target copper deficiency	8/14 progressed within 30 days or had stable disease for <90 days; 5/14 had stable disease; 1 with progression at one site and stable elsewhere	(Brewer et al., 2000)
Tetrathiomolybdate	15 patients with advanced kidney cancer; Evaluated 8/15 evaluable with target copper deficiency	4/8 had progressive disease and 4/8 had stable disease at 3 months	(Redman et al., 2003)
Tetrathiomolybdate	19 patients with hormone refractory prostate cancer; 16/19 evaluable with target copper deficiency	14/16 had progressive disease and 2 discontinued therapy	(Henry et al., 2006)
NOV-002	68 chemotherapy-naïve patients with Stage IIIb/IV NSCLC	One year survival of 63% with NOV-002 + cisplatin (38 patients) compared to 17% with cisplatin alone (30 patients)	(Townsend et al., 2008b)
NOV-002	44 chemotherapy-naïve patients with Stage IIIb/IV NSCLC	>50% tumor shrinkage in 69% (11/16) patients treated with NOV-002+PTX+carboplatin while only in 33% (5/15) with PTX+carboplatin alone.	(Pazoles and Gernstein,
Mesna	14 patients with metastatic tumors refractory to chemotherapy	50% tumor reduction in colorectal and gastric cancer patients (2/14). No objective response in other types.	(Yurkow et al. 2006)

NOV-002	903 patients with advanced NSCLC	NOV-002+PTX+Carboplatin and PTX+ Carboplatin alone showed a median overall survival of 10.2 and 10.8 months and median progression free survival of 5.3 and 5.6 months respectively.	(Fidias et al., 2010)
Amifostine	25 chemotherapy naïve patients with metastatic NSCLC	Amifostine + cisplatin + weekly vinblastine. 16/25 showed objective response (64%) and median survival of	(Schiller et al., 1996)
Amifostine	36 patients with metastatic melanoma	Amifostine + cisplatin showed objective response (53%) in 19/36 patients and 3 others showed minor response.	(Glover et al., 1987)

1.B.6.8. Others

Several other LMWT have been investigated and have shown promising anti-cancer potential. Further investigations are needed before they can be evaluated clinically. Some of them are discussed below.

Bucillamine or [N-(2-mercaptopropionyl)-Lcystiene] with two free thiol groups was shown to be redox active by mechanisms similar to D-pen whereby generation of hydrogen peroxide catalyzed by transition metals was observed. The presence of two thiol groups results in the formation of intramolecular disulfide bond. Administration of bucillamine resulted in a significant impact on the *in-vivo* redox status of mice marked by hepatic GSH depletion, 2-7-fold increase in serum GSSG and a 2-13-fold increase in serum GST (Yeung, 1991). This may significantly limit its clinical usage unless redox activation in non-target organs is avoided.

Dithiocarbamates (DTCs) and their corresponding disulfides can efficiently transfer external copper inside the cells and their treatment is associated with rapid GSH oxidation and DNA fragmentation leading to apoptotic cell death. However, DTCs were found to suppress hydroxyl radical formation *in-vitro* by stabilization of Cu(I) state thus inhibiting further redox recycling of the metal (Burkitt et al., 1998). In addition, PDTC (pyrrolidine dithiocarbamate) was shown to cause apoptosis and DNA fragmentation in rat aortic smooth muscle cells which was not affected in the presence of iron and copper chelators indicating mechanisms separate and independent of ROS generation in spite of the presence of a thiol group (Tsai et al., 1996). This is also evident by the higher cytotoxicity of disulfiram, which is a disulfide, than PDTC (Burkitt et al., 1998). Molecular investigations of DTCs indicate a p53 dependent apoptosis and cell cycle arrest mediated by modulation of effectors such as $p21^{waf-1}$, NF-κB, AP-1 and Bcl-2 in the presence or absence of copper (Chen et al., 2008b;

Liu et al., 1998a). DTCs also affect the oxidation state of p53 by increasing intracellular copper transport (Furuta et al., 2002). Recently, spontaneously formed copper complexes of PDTC showed inhibition of proteasome chymotrypsin-like activity and apoptotic death of breast cancer cells (Daniel et al., 2005; Daniel et al., 2004). When used in combination with other chemotherapeutics drugs 5-fluorouracil (5-FU) and dox, PDTC decreased their IC_{50} (viability) in human colon carcinoma cells by 10-13-fold while *in-vivo* the combination of PDTC and 5-FU showed complete regression of tumors (Chinery et al., 1997).

1.3. Polymer-Drug Conjugates (PDCs) in Anticancer Drug Delivery

1.3.1. Introduction

Polymer-drug conjugates (PDCs), for the purpose of this discussion, may be defined as polymeric prodrugs whereby a small molecule therapeutic agent(s) is covalently linked, directly or through a spacer, to the end or pendant functional group(s) of a linear polymer chain composed of one or different types of monomers. PDCs have been widely investigated for anticancer drug delivery in the past two decades due to their distinct advantages including a) enhanced drug stability in plasma due to covalent conjugation, b) altered pharmacokinetics in terms of prolonged plasma circulation time, decreased clearance and altered biodistribution, c) enhanced aqueous solubility of hydrophobic drugs, d) improved therapeutic index of chemotherapy due to reduction in non-specific organ uptake leading to a lower incidence of adverse events, e) improved tumor accumulation due to the "enhanced permeability and retention" (EPR) effect and/or inclusion of targeting ligands; and f) tumor specific drug release due to biochemically sensitive linkages or spacer molecules.

Almost all the PDCs that are currently being investigated partially fit the model of a pharmacologically active polymer first proposed by Ringsdorf (Ringsdorf, 1975). This model consisted of a polymer backbone that may contain; a) "solubilizer" arm to enhance solubility of hydrophilic or hydrophobic drugs, b) covalently linked drug with or without a spacer and, c) a "transport system" that may function as a homing device or non-specific enhancer and is similar in concept to the targeting ligands widely used in current research. The first report of a system containing all three components was published in 1975 where PGA-p-phenylenediamine mustard (PDM) conjugate was further covalently linked to immunoglobulin (Ig) against mouse lymphoma cells. The PDC showed decreased *in-vitro*

cytotoxicity compared to free PDM but resulted in longer median survival time (>100 days) compared to PGA-PDM (25 days) or Ig alone (19 days) in mice bearing i.p. EL4 lymphoma (Rowland et al., 1975).

Polymers that have been investigated as multi-functional PDCs may be categorized into poly-amino acid derivatives such as poly-L-lysine (PLL), PGA, gelatin, poly-(N-(2-hydroxyethyl)-L-glutamine (PHEG), poly-aspartic acid (PAA), polyacids such as poly-α malic acid (PAMA) and poly-β-malic acid (PBMA), polysaccharides such as dextran, pullulan, HA, chitosan, and others such as N-(2-hydroxypropyl) methacrylamide (HPMA) copolymer and polyethylene glycol (PEG). Many have focused on conjugating well established small molecular weight chemotherapeutic drugs such as anthracyclines, platinates and taxanes for conjugation to polymers. The functional groups that have been most widely utilized to conjugate drugs directly or through a spacer to the polymer chain are amino, carboxyl, hydroxyl and thiol.

Drugs conjugated to a polymer backbone face multiple barriers to successful delivery at the target site some of which are commonly shared with other macromolecular drug delivery systems for anticancer therapy such as nanoparticles, liposomes etc. and are summarized below (**Figure 1.6**). These barriers are discussed with regards to parenteral (intravenous) administration. During blood circulation, PDCs may undergo clearance by renal and/or reticulo-endothelial system (RES), protein binding, drug release and organ sequestration all of which are barriers to successful delivery to the target site i.e. the tumor. Solid tumors have shown preferential accumulation of macromolecular drugs due to poor lymphatic drainage and leaky vasculature collectively termed as the "EPR effect" (Matsumura and Maeda, 1986) and several PDCs do exhibit significant improvement in

therapeutic efficacy over unconjugated drug. However, delivery to solid tumors is hindered by elevated interstitial fluid pressure (IFP) and diffusional resistance (Jain and Stylianopoulos, 2010) limiting the depth of drug permeation within the tumor.

Passive or receptor-mediated endocytosis remains the major route of intracellular entry of PDCs. Mechanisms of endosomal release or escape, and further transport of the drug to its subcellular target have been widely investigated. Due to additional steps involved in the uptake and release of a polymer-conjugated drug, many have reported decreased or comparable *in-vitro* cytotoxicity compared to unconjugated drug (Guan et al., 2008; Ye et al., 2006). However, *in-vivo* this may result in an increase in the therapeutic window allowing for higher dosing of the conjugates resulting in improved anticancer efficacy. This has been observed in many cases (Chau et al., 2006; Huang et al., 2010; Ye et al., 2006). For example, *cis*-dichlorodiammine platinum (II) (CDDP) conjugated to PGA via ester linkage had 7-8-fold higher IC_{50} values than the unconjugated drug when tested *in-vitro*. However, the conjugate resulted in no weight loss at an equivalent dose of CDDP that caused 20-30% loss in body weight of the mice when administered as unconjugated. The conjugate could be dosed at a 3-fold higher dose than unconjugated CDDP without significant weight loss. The conjugate also showed better antitumor efficacy than CDDP at equivalent dose (Ye et al., 2006). Methotrexate (MTX) conjugated to dextran via peptide spacer sensitive to cleavage by MMPs was 100-fold less active than free drug *in-vitro* but showed tumor inhibition *in-vivo* while the free drug was inactive at a similar dose (Chau et al., 2006).

Significant improvements have been made in terms of the design of PDCs, availability of biochemically sensitive spacers and novel highly specific tumor targeting ligands to enhance the delivery of drug to the target site. As a result, several PDCs have

shown improved efficacy and are being currently investigated in clinical trials. **Figure 1.7** represents a model of PDCs with different components and their variations that have been investigated. Variations in any component may affect the *in-vitro* and *in-vivo* performance of the PDCs. However, the choice of the polymer carrier itself is paramount and dictates the overall effectiveness. An ideal polymer carrier must be biocompatible, readily biodegradable, non-immunogenic, sufficiently large to allow long circulation as well as passive tumor accumulation and able to avoid uptake by the RES (Christie and Grainger, 2003; Ofek et al., 2010). Factors such as the molecular weight, charge on the polymer chain, hydrodynamic radius, hydrophilic-lipophilic balance and formation of secondary structures such as micelles or hydrophobic aggregates affect the organ biodistribution, pharmacokinetics and the toxicological properties of PDCs (Takakura et al., 1989).

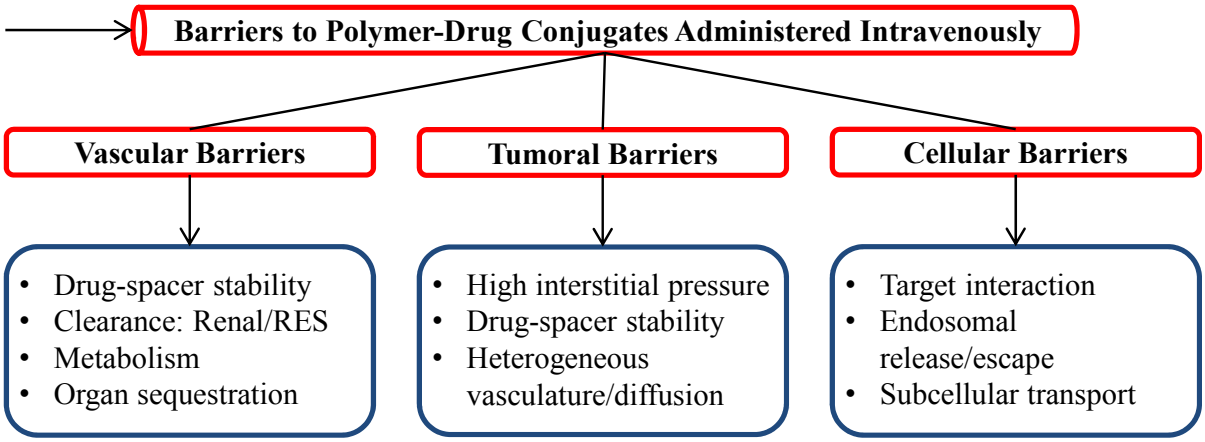

Figure 1.6 Barriers in drug delivery to solid tumors using polymer-drug conjugates (PDCs).

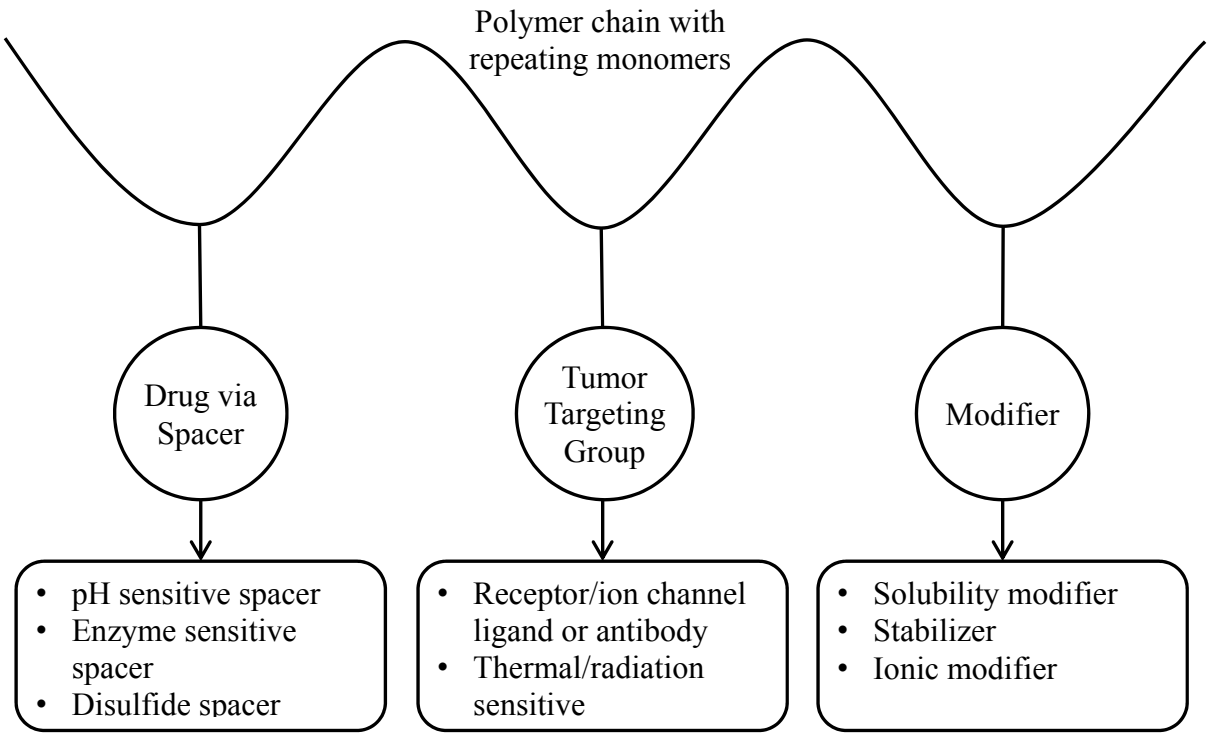

Figure 1.7 An inclusive model of PDC and different components for drug delivery to solid tumors.
(modified from Ringdorf, 1975)

1.3.2. Critical Aspects in the Design of PDCs

1.3.2.a. Molecular Weight and Functionalization of the Polymer

An increase in the molecular weight of PDCs above the threshold of renal filtration is shown to prolong the circulation half-life. Pullulan (M_w 136 kDa) conjugates of dox administered i.v. showed 10-fold higher area under the plasma-drug concentration-time curve (AUC) when compared to free dox in BALB/c mice (Scomparin et al., 2011). Longer circulation provides an increased opportunity for passive accumulation at the tumor site which is further facilitated by the leaky tumor vasculature or the EPR effect. However, very large molecular weight significantly hinders the permeability and mobility within the tumor microenvironment. Fluorescein labeled dextran of 40-70 kDa molecular weights showed maximal tumor vascular permeability and highest tumor accumulation when compared to dextran of 3.3 kDa, 10 kDa and 2 MDa (Dreher et al., 2006). Similar results have been reported by several other studies with dextrans (Harada et al., 2001; Mehvar et al., 1995). When copolymer of HPMA and N-methacryoyltyrosinamide was tested in the range of 12 to 778 kDa, 45 ± 2.5 kDa was found to be the threshold molecular weight that limited glomerular filtration of the polymer. An increase in molecular weight above that correlated with accumulation in the RES organs (Seymour et al., 1987). The tumor accumulation and plasma circulation time correlated with an increase in molecular weight of HPMA copolymers from 23 kDa to 65 kDa in mice bearing Dunning AT xenografts (Lammers et al., 2005). Sodium alginate showed a threshold molecular weight of 48 kDa in similar studies (Alshamkhani and Duncan, 1995a; Alshamkhani and Duncan, 1995b).

Availability and number of suitable functional groups for drug conjugation is also an important aspect to consider when designing PDCs. For homopolymers such as PGA, the

number of functional groups increases with increasing molecular weight. Percent of functional group that can be conjugated depends on factors such as steric crowding, desired physicochemical properties of the PDC and chemical nature of the drug. Spacers have been routinely used to avoid steric hindrance. Polymerization of drug-conjugated monomers or attaching the spacer to the drug followed by polymer conjugation (Khandare et al., 2005) has also been attempted to increase the extent of conjugation.

Polymer chains may also be derivatized with spacers to provide for desired functional groups. However, this may affect the *in-vivo* disposition. HPMA copolymers functionalized to have either free carboxyl groups or hydrazide groups were compared for their accumulation in tissues and plasma pharmacokinetics (Lammers et al., 2005). While both functionalities reduced the plasma circulation time and tumor accumulation of the polymers which was proportional to the extent of functionalization, the HPMA-hydrazide showed greater increase in rate and extent of renal elimination and reduced tumor accumulation compared to the HPMA-carboxyl. The presence of non-polar functional groups on the polymer chain or contributed by the conjugated drug may cause aggregation mediated by hydrophobic interactions. This is discussed in more detail below.

Hydrophobization of the polymer may also occur due to drug conjugation. An increase in the extent of dox conjugated to carboxymethylpullulan led to an increase in the uptake by RES organs and a decrease in plasma circulation half-life (Nogusa et al., 2000a). Therefore, it is important to optimize the PDCs for hydrophilic-lipophilic balance to achieve maximal activity.

1.3.2.b. Charges on the Polymer Chain

Polymer drug conjugates may bear a net positive charge, negative charge or stay electroneutral at physiological pH depending on the ionization properties of the drug and the unconjugated functional groups on the backbone. The net charge may affect the membrane interaction of PDCs thus affecting the cell uptake and enzyme accessibility leading to differences in *in-vivo* degradation. PDCs with a net positive charge at physiological pH show greater interaction with the negatively charged cell membranes which may enhance their endocytic uptake. On the other hand, a net negative charge will reduce membrane interaction. This can have a significant impact on the biodistribution and toxicity of the PDCs.

The effect of charge on the pharmacokinetics and biodistribution of dextrans has been studied in detail by derivatization with charged substituents. In general, it was reported that neutral dextrans are cleared very rapidly. Positively charged dextrans were taken up very efficiently by macrophages. Dextrans optimally negatively charged were shown to increase the plasma circulation half-life as well as tumor uptake. For example, carboxymethylation at the pendant hydroxyl groups of dextran led to an increase in the plasma half-life until a degree of substitution of 0.4 beyond which there was rapid uptake in liver (Harada et al., 2001). This was also observed with carboxymethylated pullulan with a degree of substitution of 0.6 (Nogusa et al., 1995). Negatively charged dextran derivative had longer plasma circulation and lesser accumulation in liver and spleen in mice bearing fibrosarcoma than positively charged dextran derivative (Tabata et al., 1997).

Polycationic conjugates of poly-D-lysine (PDL) with daunomycin showed preferential accumulation in the organs of the RES system. Anionic or amphoteric modification of PDL by branching with poly-amino acids of different charge (glutamic acid)

or polarity (alanine, leucine) resulted in altered biodistribution and cytotoxicity of the conjuagtes. The PDL-daunomycin conjugate modified amphoterically using glutamic acid and alanine side chains were the most cytotoxic and showed prolonged circulation with lesser accumulation in liver and spleen (Hudecz et al., 1992).

The net **c**harge on PDCs can also affect their interaction with the cell surface receptors in case of targeted systems or spacer sensitivity in case of enzyme cleavable spacers affecting overall drug release. The residual negative charges on dextran-MTX conjugate with a peptide spacer sensitive to cleavage by MMP-2 and MMP-9 were variably masked with ethanolamine to study the effect on drug release. A decrease in the charge resulted in improved sensitivity towards cleavage of the peptide spacer by the MMPs (Chau et al., 2004). Conjugates of 5-fluorouracil (5-FU) with PAMA where the residual carboxyl groups of the polymer were masked by methyl groups had superior antitumor activity compared to the negatively charged conjugates (Ouchi et al., 1990).

1.3.2.c. Cell Uptake and Drug Release

1.3.2.c.i. Endosomal Uptake and Escape

The molecular size of PDCs inhibits them from passively diffusing across cell membranes. Like other macromolecules, they are dependent on non-specific passive transport by endocytosis. In the presence of targeting ligands, endocytosis can become an active transport pathway mediated by receptor or ion-channel interaction. Fluid phase endocytosis or macropinocytosis has been shown to be the major route of cell entry for PDCs that do not possess a molecular recognition component (Abdellaoui et al., 1998b). While this may present as an additional barrier to drug delivery, the benefit appears to be a reduction in

systemic adverse events associated with chemotherapy. For example, mice treated with TNP-470 showed decreased neurological function while this effect was not seen with HPMA-TNP-470 conjugate. This may be due to a decreased brain uptake of the conjugated drug. The conjugate also did not show skin irritation and weight loss associated with administration of free TNP-470 (Satchi-Fainaro et al., 2004).

In addition, endocytosis provides a mechanism of cell uptake that is less affected by the efflux transporters and may help in overcoming multi-drug resistance (MDR) that is commonly associated with chemotherapy. The dose of HPMA copolymer-adriamycin (ADR) conjugate that caused a 50% reduction in viability in resistant cells was only 20% higher than a corresponding dose of the conjugate in sensitive cells which indicates a relative insensitivity towards resistance mechanisms. However, there was a 40-fold decrease in sensitivity of resistant cells to unconjugated ADR (Minko et al., 1998). The authors also showed that chronic treatment of cancer cells with HPMA copolymer-ADR conjugate did not induce the expression of either *MDR1* or MDR associated protein (*MRP)* gene, both of which are associated with the development of resistance to chemotherapy (Minko et al., 1999). Higher intracellular concentrations of HPMA copolymer-ADR conjugate were observed in ADR resistant cells than free ADR (Omelyanenko et al., 1998).

The cell uptake kinetics and subcellular distribution of HPMA copolymers has been studied in detail. The mechanism of endocytosis of HPMA copolymer drug conjugates has been studied in breast cancer cells. The uptake was confirmed to be vesicular and partly cholesterol-dependent in nature indicating a clathrin or caveolin mediated pathway (Greco et al., 2007). Jensen et al. provided qualitative evidence that HPMA copolymers with galactose as targeting ligand were endocytosed and remained in membrane bound vesicles even after

24 hr treatment. Only at 96 hr, the polymer began transferring to cytosol and nucleus. The conjugate rapidly transferred to nucleus upon microinjection into the cytosol indicating a preferential nuclear accumulation of the polymer (Jensen et al., 2001).

In spite of reducing non-specific uptake and playing a role in overcoming resistance, endocytosis is a significant barrier to drug action. For drugs that are known to passively diffuse through the membrane, this barrier function can be minimized by designing conjugates that efficiently release the drug in endosomal/lysosomal conditions. Such release could be achieved by using spacers that are hydrolytically cleaved at endosomal pH or are sensitive to enzyme catalyzed degradation (Omelyanenko et al., 1998).

On the other hand, drugs that do not freely diffuse across the plasma membrane, have stability concerns at lysosomal pH and for PDCs where cytosol is the ideal drug release environment, additional components must be incorporated in PDCs to enable endosomal escape of the conjugate or enable cytosolic delivery.

Endosomal membrane disruption by Polyethylenimine (PEI) that contains ionizable amino groups has been explained by the proton sponge effect. The endosomal uptake of the polymer triggers ATPases to pump protons inside the vesicle followed by chloride counter ion diffusing in the vesicle to maintain equilibrium. This leads to osmotic swelling and burst of the membrane releasing the entrapped contents (Boussif et al., 1995). Other polymers such as polyamidoamine (PAMAM), polylipoamines and carboxymethyl poly-L-histidine have shown similar effects (Asayama et al., 2007; Lavignac et al., 2009). Lysosomotropic agents such as chloroquine that act decreasing the pH gradient between endosomes and cytosol leading to osmotic swelling have also been used to disrupt this barrier (Erbacher et al., 1996). Sucrose and polyvinylpyrolidone (PVP) are also taken up by the cells through fluid-phase

endocytosis and act by osmotic swelling (Ciftci and Levy, 2001). However, their application with PDCs has not been studied yet.

A mechanism to avoid endosomal pathway and direct cellular delivery is by using cell penetrating peptides (CPP), also known as protein transduction domains (PTDs) (Lindgren et al., 2000). Intracellular transport of CPPs in unsaturable, occurs even at low temperatures in a protein independent and in some cases energy independent manner through a non-endosomal route at a much faster rate than normal endocytotic uptake (Lindgren et al., 2000; Schwarze et al., 2000). This has resulted in tremendous interest in investigating their applications in the cellular delivery of drugs, genes, peptides, oligonucleotides and other hydrophilic therapeutics by conjugating CPPs to the desired cargo including PDCs (Allinquant et al., 1995; Calvet et al., 1998; Fawell et al., 1994; Schwarze et al., 1999). Fluorescein isothiocyanate (FITC) labeled HPMA-dox conjugates containing a single TAT peptide per polymer chain showed diffuse fluorescence in the cytosolic and nuclear regions while the conjugate with no TAT showed a punctate pattern of fluorescence typical of endocytic vesicular uptake (Nori et al., 2003).

1.3.2.c.ii. Drug Release Mechanism

The covalently conjugated drug must be released from the PDCs to perform its pharmacological function. For anticancer therapy, it is desirable that PDCs release the drug only upon tumor uptake or upon entry in the tumor cells. However, in some cases the intact conjugates have been found to have some activity. Irreversible conjugation of ADR to glutaraldehyde bound to membrane impermeable solid support (microspheres) by Schiff base formation was performed. While the conjugate was equally cytostatic in sensitive cell lines,

the activity increased by 15-20-fold in resistant cell lines (Rogers et al., 1983; Tokes et al., 1982).

By considering the factors that control drug release, it is possible to design PDCs that are highly sensitive to the biochemical environment at the target site and release the conjugated drug in a predictable way at a desired rate. This may be achieved by linking the drug to the polymer backbone with cleavable linkage or through suitable spacers (**Figure 1.8**). The spacer allows for the incorporation of mechanisms of release of the conjugated drug under desired conditions. Additionally, spacers have been sometimes used to reduce the steric or "crowding" effect to achieve higher drug conjugation or to improve the binding of the targeting ligand to its target by having it further away from the polymer backbone (Erez et al., 2009). For example, the half-life of hydrolytic release of mitomycin C conjugated to dextran through alkyl spacers increased with increasing chain length from C4 to C8. A similar trend was observed in the antitumor activity of the PDCs while the therapeutic index of the C8 substituted conjugated was highest (Takakura et al., 1989). Conjugation of a trivalent dendrimeric spacer to HPMA copolymer increased the payload of PTX by 3-fold (Erez et al., 2009). The activity of PDCs has been shown to be greatly affected by the type, length and sensitivity of the spacer used as it determines the rate and extent of drug release at the site of action. Enzyme sensitive and pH sensitive spacers and linkages have been investigated.

Drugs can have multiple sites and functional groups that may be used to conjugate with the polymer chain. Differences in drug release due to the site of drug conjugation are primarily due to steric factors. PTX conjugated to through the 2'- hydroxyl to a B sensitive

spacer showed a hydrolysis half-life of 9 hr compared to half-life of 40 min when conjugated through 7-hydroxyl position (Dubowchik et al., 1998).

a) Enzyme Cleavable Spacers/Linkages

Polymer drug conjugates where the drug is conjugated through a spacer sensitive to cleavage by a specific enzyme is a strategy to sustain or prolong the release of the drug at a specific site where high concentrations of the enzyme are available while increasing the stability of the conjugate in plasma circulation and reduced drug release in non-target organs. The stability of the conjugation before it reaches the target site is highly dependent on the specificity of the spacer. Many enzymes, especially proteases with different functions, have been reported to be elevated in solid tumors.

Matrix metalloproteinases are secreted in the tumor microenvironment and have an important role in promoting tumor growth and metastasis. The overexpression of MMPs has been seen in many human cancers and is associated with poor prognosis (Davidson et al., 1999; Liu et al., 2010; Passlick et al., 2000). PDCs targeting MMP-2 and MMP-9 were synthesized by incorporating peptide spacer sensitive to cleavage by these enzymes. MTX was conjugated to dextran through Pro-Val-Gly-Leu-Ile-Gly (PVGLIG) as spacer and was found to be specifically cleaved in the presence of MMP-2 and MMP-9. However, upon cleavage, the conjugate released MTX-PVG instead of free drug and was less active (Chau et al., 2004).

Cathepsins or lysosomal cysteine proteases are papain-like enzymes present in the lysosomal vesicles that have optimal activity at lysosomal pH conditions and have also been shown to over-express in the tumor microenvironment (Campo et al., 1994; Turk et al.,

2001). PDCs have been synthesized with spacers sensitive to cleavage by these enzymes for drug release upon endosomal uptake. The length and the amino acid composition of the spacer are known to influence the rate and extent of drug cleavage, and the type of enzyme that plays a major role in drug release. Dox-carboxymethylpullulan conjugates through Gly-Gly-Phe-Gly (GGFG) and Gly-Phe-Gly-Gly (GFGG) spacers had higher antitumor effect than free dox (Nogusa et al., 1995). A systematic study with PHEG conjugated mitomycin C showed that tripeptide spacers are less effective in releasing the polymer-bound drug than tetrapeptides when tested in the presence of lysosomal enzymes as well as at pH 5.5. This study identified Gly-Phe-Leu-Gly (GFLG), Gly-Phe-Ala-Leu (GFAL) and Ala-Leu-Ala-Leu (ALAL) as spacers with efficient drug release properties (Demarre et al., 1994). The presence of hydrophobic amino acids Phe or Leu at the C-terminal end decreased the rate of enzymatic hydrolysis of the spacer, an effect reported with carboxymethylpullulan conjugates as well (Nogusa et al., 1995).

Cathepsin B, a carboxydipeptidase, specifically recognizes the tetrapeptide sequence GFLG (Duncan et al., 1989). Another tetrapeptide sequence, Gly-Gly-Pro-Nle is specific substrate for cathepsin K (Segal et al., 2009). A dipeptide spacer composed of a basic or hydrogen bonding amino acid at P1 and a hydrophobic amino acid at P2 e.g. Phe-Lys-(p-aminobenzylcarbonyl) (PK-PABC) spacer was shown to be cleaved specifically by cathepsin B and L (Dubowchik et al., 1998). Nogusa showed that the specificity is maintained even if the basic or hydrogen bonding amino acid is substituted with a hydrophilic amino acid e.g. a Gly-Phe spacer (Nogusa et al., 2000a; Nogusa et al., 2000b). ADR conjugates of PGA with or without a peptide spacer were investigated for their cytotoxicity in leukemia cells and release of conjugated drug in the presence of peptidases such as papain. The peptide spacers

were GGL or GGGL. The conjugates with the spacers had lower IC_{50} values and released most of the conjugated drug in the presence of papain compared to no drug release with PGA-ADR direct conjugates through amide bonds (Hoes et al., 1985).

A tripeptide spacer, D-Val-Leu-Lys, was used to conjugate cytarabine to α,β-poly(N-2-hydroxyethyl)-DL-aspartamide (PHEA) targeting specific cleavage by elevated plasmin levels in tumors. Complete drug release was seen in the presence of plasmin compared to minimal release in plasma indicating the specificity of the conjugation (Cavallaro et al., 2001).

PDCs sensitive to cleavage by esterases have been investigated. N,N-Dimethyl sphingosine (DMSP) was conjugated to PGA via ester linkages at two different sites on the drug. The drug release was transient and the conjugate showed similar *in-vitro* toxicity to cancer cells as the free drug. The authors suggested that enzymatic hydrolysis (esterases) of the ester linkages and the extent of drug loading is the rate-limiting step determining the overall toxicity of the conjugate. The solubility was enhanced several fold and the maximum tolerated dose of the conjugate was almost 2-fold higher than the effective antitumor dose of the drug in mice (Ghosh et al., 2009).

b) Hydrolytically Cleavable Spacer/Linkages

The actions of 'vacuolar H^+-ATPases' in the endosomal membrane result in a gradual decrease in the vesicle pH as they progress towards lysosomes. The pH of the endosomes was observed to vary between 4.7 and 5.8 with 5.0 being the most frequent value measured using folate conjugated dextran (Lee et al., 1996). While low pH aids in proteolytic degradation of the contents in lysosomes, it may cause the release of receptor bound ligands

and enhancement in the activity of several pathogens among other things (Mellman et al., 1986). Conjugating drugs to the polymer chain with covalent linkages that are prone to acid-catalyzed hydrolysis, results in selective drug release following cellular uptake. *Cis*-aconityl and hydrazone linkages or spacers containing these linkages have been widely investigated in polymer-drug conjugation for their pH sensitive cleavage. Other linkages sensitive to pH mediated cleavage include amide, ester and carbamate bonds. The rate of hydrolysis and sensitivity may be different with different linkages.

The half-life of daunomycin release from a poly-D-lysine conjugate was 6 hr at pH 5.0 while there was no release at pH 7.0 after 96 hr when conjugated via a *cis*-aconityl bond. This conjugate showed significant growth inhibition in lymphoma cells. Similar conjugate with polyacrylamide gel beads and PDL conjugated to daunomycin via maleyl linkage were inactive indicating a lysosomal release of the drug upon cellular uptake (Shen and Ryser, 1981). Similar pH dependent drug release was seen with sodium alginate derivatized to have amino groups conjugated to *cis*-aconityl-daunomycin (Alshamkhani and Duncan, 1995b).

PGA based dendrimer with octa(3-aminopropyl) silsesquioxane (OAS) cores were conjugated to dox via acid-cleavable hydrazone bonds (Yuan et al., 2010). PGA bound to the OAS core was derivatized to contain hydrazine end groups that readily react with the carbonyl group of dox to form hydrazone via a Schiff base reaction. The dendrimer conjugate released 90% of the bound dox after 20 hr incubation at pH 5.0 whereas only 12% release occurred at pH 7.4 after 24 hr incubation (Yuan et al., 2010). Pullulan conjugated to dox via hydrazone bonds also showed a pH dependent release profile whereby complete release was observed at pH 5.5 within 40 hr compared to only 20% release at pH 7.4 in 72 hr (Scomparin et al., 2011).

A comparison of hydrazone and *cis*-aconityl spacers (HPMA-dox conjugate) showed a slower release of drug and consequently decreased bioactivity with the *cis*-aconityl spacer (Ulbrich et al., 2003). Another comparison of dox bound to HPMA copolymer via acid (hydrazone) or enzyme cleavable (GFLG) spacers showed that the cell uptake and corresponding cytotoxicity of the former was greater. This could be partially due to differences in the rate, extent and site of intracellular uptake of the two conjugates (Kovar et al., 2004). Similar studies showed a *cis*-aconityl spacer containing HPMA- ADR conjugate to be more cytotoxic compared to GLFG spacer containing conjugate (Choi et al., 1999). A rapid release of the pH sensitive spacers combined with their non-dependence on the location and level of enzyme expression make them more suitable for clinical development than enzyme-cleavable spacers.

PGA-gemcitabine conjugate linked via an ester bond without any spacer were shown to release the drug in a pH dependent manner while increasing the plasma stability of gemcitabine (Kiew et al., 2010). Effect of spacer was studied by conjugating gemcitabine to PHEA via succinyl or diglycolyl spacer with folic acid as the targeting ligand. The drug release was slower with the diglycol spacer, presence of folate reduced it even further and this conjugate showed diminished cytotoxic activity (Cavallaro et al., 2006).

5-FU was conjugated to PAMA via ester, amide or carbamoyl bonds with or without a polymethylene spacer to study the effect of type and hydrophobicity of the spacer on drug release from the PDC. The carbamoyl linkages showed the highest rate of drug release and maximal susceptibility to cleavage in all solutions of pH ranging from acidic to alkaline. The PDCs with tri- and hexamethylene spacers showed a superior antitumor activity than free 5-FU (Ouchi et al., 1990). It has also been shown that the amide bonds in the side chain are

more sensitive to hydrolysis as compared to the polymeric amide bonds in poly-amino acid type polymers (Abdellaoui et al., 1998a; Abdellaoui et al., 1998b).

c) Reducible Spacers

Drugs have been conjugated to polymers through intracellularly cleavable disulfide bonds. The benefit of using disulfide spacers has previously been seen in several antibody-drug conjugates, also referred to as immunoconjugates (Liu et al., 1996; Ross et al., 2002). Mesochlorin e_6 (Mce_6) was conjugated to HPMA copolymer via a disulfide spacer or GFLG (discussed above) spacer for photodynamic therapy of cancer. The disulfide linked conjugate showed greater intracellular drug release and higher cytotoxicity compared to the GLFG linked conjugate. An increase in quantum yield upon cellular entry with disulfide conjugate indicated drug cleavage as the conjugated drug has lower quantum yield (Cuchelkar et al., 2008b).

For drug release to occur, the disulfide bond containing PDCs must escape from the endocytic vesicle and enter the highly reducing environment of cytosol (Yang et al., 2006) or undergo disulfide reduction within the endocytic vesicles. Thioredoxin family of enzymes in conjunction with glutathione reductase and GSH/GSSG equilibrium play a major role in cytosolic disulfide reduction. However, there is a lack of consensus on the efficiency of disulfide reduction within the endocytic vesicles. Disulfide reduction was previously proposed to be a prelysosomal event, independent of endosomal pH and glutathione concentrations based on studies with MTX-S-S-PDL conjugate that showed comparable cytotoxicity to free MTX while a direct amide-linked MTX-PDL conjugate was inactive (Shen and Ryser, 1979; Shen et al., 1985). However, using [^{125}I] tyramine-S-S-PDL these

authors later proposed that cell surface thiols and elements of golgi apparatus play a major role in disulfide reduction of endocytosed molecules with no significant reduction occurring in endosomes (Feener et al., 1990). Further, the endosomal and lysosomal environment was found to be oxidizing as indicated by reduction potential (-240 mV) measurements (Austin et al., 2005). Therefore disulfide reduction mediated by thiol-disulfide exchange reactions, that requires the generation of thiolate anion is not expected to be very efficient in endosomes (Shen et al., 1985; Yang et al., 2006).

On the other hand, γ-interferon inducible lysosomal thiol reductase (GILT) is a disulfide reducing enzyme that has optimal activity between pH 4-5 and therefore, is expected to be active at endosomal conditions. GILT transfected melanoma cells showed enhanced reduction of $F(ab')_2$ to Fab' (Arunachalam et al., 2000). Protein disulfide isomerase has also been detected in endosomes (Noiva, 1999). Fluorescence resonance energy transfer (FRET) based imaging showed that disulfide reduction in folate-BODIPY-S-S-rhodamine conjugate had a half-time of 6 hr and was independent of redox components as well as recycling (Yang et al., 2006) indicating that enzymatic reduction may be involved. Disulfide reduction is an important step in the activation of certain toxins as well as during antigen processing and a strong evidence of disulfide reduction in lysosomes was shown using subcellular fractionation technique (Collins et al., 1991). Recently, Langer and co-workers developed a PEG containing FRET pair, where the FRET donor was bound to PEG through a disulfide linker. They were further able to show that PEG shedding occurs from nanoparticles containing this (FRET)-PEG during early endocytosis (Gao et al., 2010).

Table 1.2 Polymer-drug conjugates (PDCs) with different mechanisms for the release of covalently conjugated drugs.

Conjugate	Release Mechanism	Comments	Reference
PGA-ADR	Papain mediated cleavage of peptide spacer (GGL or GGGL) between ADR and PGA	GGL spacer led to 5-fold increase in activity over GGGL. All conjugates were less toxic *in-vitro* than free ADR.	(Hoes et al., 1985)
HPMA Copolymer-Mesochlorin e_6	Enzymatic or GSH mediated reduction of disulfide bond between drug and the polymer.	Conjugate with disulfide spacer were more cytotoxic than the peptide (GFLG) spacer	(Cuchelkar et al., 2008b)
Dextran-MTX	MMP-2 and MMP-9 mediated cleavage of peptide spacer PVGLIG.	Released product was MTX-PVG instead of free MTX and the conjugate was less toxic than free MTX.	(Chau et al., 2004)
HPMA Copolymer-Dox	Acid sensitive cleavage of *cis*-aconityl or hydrazone linkage containing spacers in endosomes.	Hydrazone bound conjugates were more toxic *in-vitro* and more potent *in-vivo* than *cis*-aconityl and free dox.	(Ulbrich et al., 2003)
PGA-DMSP	Acid or enzyme mediated hydrolysis of ester bond between drug and the polymer.	*In-vitro* cytotoxicity of conjugate was similar to free DMSP at 7% drug loading.	(Ghosh et al., 2009)
PMA-5-FU	5-FU bound to PMA through an acid/enzyme cleavable amide, ester or carbamoyl bonds.	Carbamoyl bound conjugates released the drug fastest but ester bound conjugates with partially masked carboxyl groups were more active *in-vivo* than 5-FU and other conjugates	(Ouchi et al., 1990)

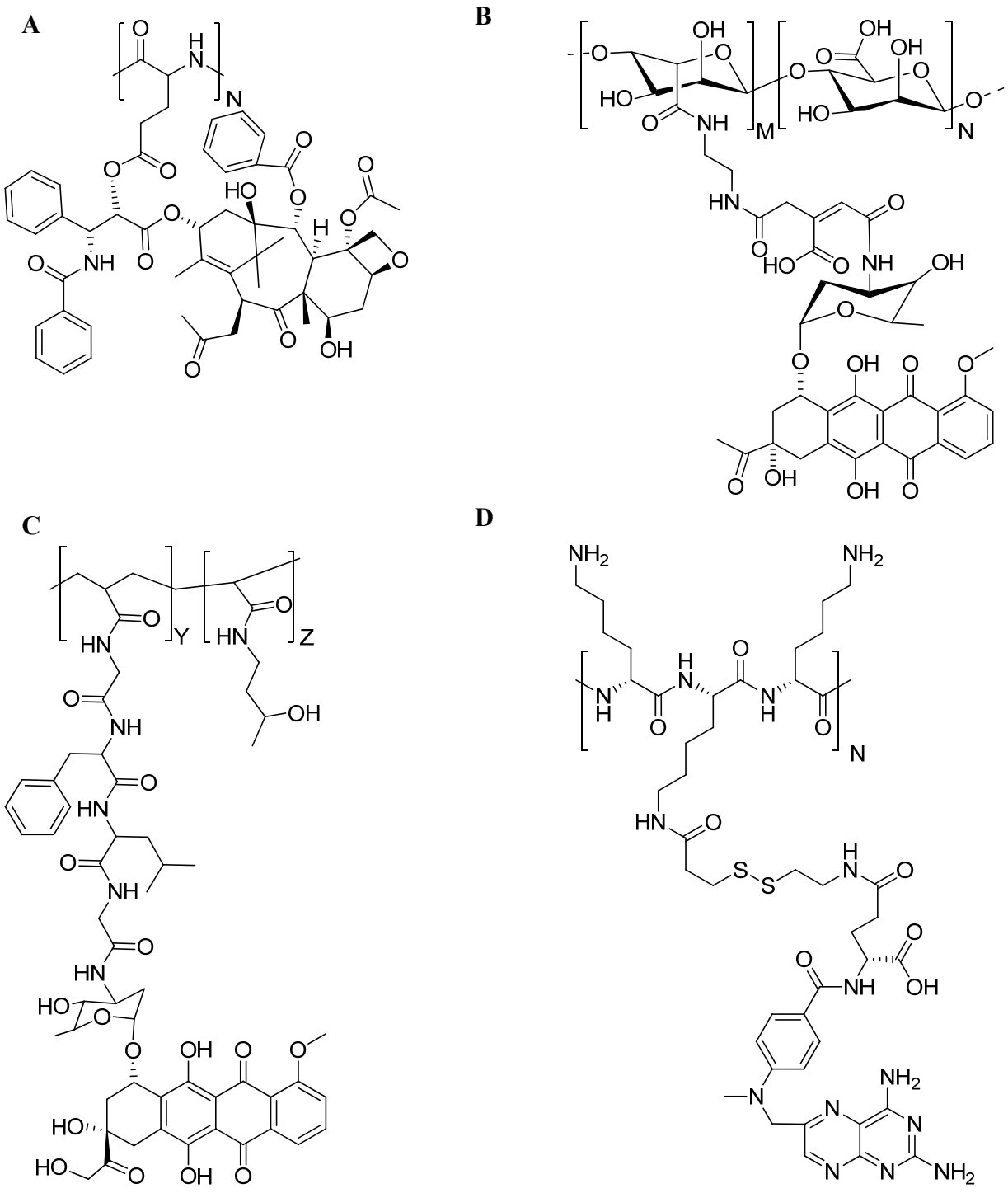

Figure 1.8 Designer drug release from PDCs using spacers bound via cleavable bonds
A. Paclitaxel bound to PGA through an ester bond (Li et al., 1998), B.*Cis*-aconityl linked alginate-daunomycin conjugate (Alshamkhani and Duncan, 1995b), C. Cathepsin B sensitive GFLG-linked HPMA copolymer-doxorubicin conjugate (Ulbrich et al., 2000), and D. Poly-D-lysine-methotrexate conjugate linked with a reducible disulfide linker (Shen et al., 1985).

1.3.2.d. *In-vivo* Disposition

Although prolonged circulation is a desirable feature in the design of PDCs, the residual polymer chain should not contribute to adverse events, be pharmacologically inert, non-immunogenic, and undergo predictable degradation followed by rapid clearance of the degradation products from the body. Factors like drug conjugation, presence of a linker, amount of cross-linking during reaction and final molecular weight of the conjugate can significantly alter the *in-vivo* degradation of the polymer. Polymers that have been used to construct PDCs have been investigated for their *in-vivo* fate.

As an example, PGA, which is composed of endogenous amino acid monomer, is susceptible to lysosomal degradation by cathepsin B (Kishore et al., 1990). At a molecular weight of 42 kDa PGA rapidly degraded in the presence of cathepsin B within 6-8 hr of incubation (Wen et al., 2004). However, only 30% degradation of PGA-DTPA conjugate with a 6-amino hexyl linker was observed after 48 hr in the presence of cathepsin B. Conjugation of hydrophobic amino acids like tyrosine and phenylalanine to the carboxyl groups of PGA resulted in faster degradation in the presence of lysosomal enzymes while conjugation via a peptide cleavable linker such as Gly-Leu-Gly decreased the rate of polymer degradation (Chiu et al., 1997). Degradation of PGA was studied *in-vivo* with a PGA-NIR813 conjugate in orthotopic human U87 glioma in mouse. Liver was the major site of degradation and cathepsin B and L were efficient in degrading PGA. PGA was insensitive to cathepsins E and D, and MMP-2 (Melancon et al., 2007). PGA was dosed as a single i.v. injection in mice at 800 mg/kg with no adverse events reported (Li et al., 1998). PGA conjugates of melphalan were shown to have a sustained release property that was dependent

on the exopeptidases when injected i.v. and were absorbed through the lymphatic route when injected s.c. (Morimoto et al., 1984).

The overall degradation *in-vivo* of PDCs is also complicated by rate of drug release. If the rate of drug release is different than the rate of polymer degradation, a modified pharmacological effect may be observed depending on the activity of the drug attached to the polymer remnants or the rate of final conversion to the drug. In the case of PGA-PTX conjugate, formation of mono- and di-glutamyl-PTX metabolites in the tumors and cells was observed, the ester bond between the drug and the polymer being resistant to hydrolysis while the polymer backbone is susceptible to enzymatic cleavage upon cellular uptake (Shaffer et al., 2007).

The estimation of true degradation rate of PDCs can be complicated by the formation of smaller fragments of the polymer with the drug still attached to them. Elastin like polypeptides (ELPs) are recombinant polypeptides expressed in *Escherichia coli* with repeat units of a pentapeptide sequence which can be varied in the amino acid composition. Due to their thermally reversible phase transition behavior, ELPs have been investigated for the delivery of chemotherapy in combination with hyperthermia whereby an increase in temperature is associated with enhanced accumulation in the tumor (McDaniel et al., 2010). The *in-vivo* disposition shows a rapid distribution phase followed by a prolonged elimination phase. ELPs degrade in serum with an apparent rate of 2.49 wt %/day which only accounts for detectable fragments in the serum (Liu et al., 2006). ELPs have been shown to lack systemic toxicity, are non-mutagenic at very high doses and are thus biocompatible (Urry et al., 1991).

1.3.2.e. Tumor accumulation

Tumor accumulation is typically presented as the percent of administered dose that reaches the tumor. However, it is also important to consider the depth of penetration or tumor permeability especially in the case of macromolecules. Macromolecular drugs show higher accumulation and slower clearance from solid tumors compared to small molecules. This has been partly attributed to the EPR effect (Matsumura and Maeda, 1986). Hypervascularization in solid tumors characterized by distorted vascular architecture and poor lymphatic drainage lead to the EPR effect whereby macromolecular entities smaller than the pores within the tumor vasculature, extravasate into the tumor microenvironment and are retained for a longer time due to impaired clearance. A number of investigations have shown preferential accumulation of macromolecular carriers in solid tumors including PDCs (Duncan, 2009), polymeric micelles (Iyer et al., 2007), nanoparticles (Zalipsky et al., 2007) and immunoglobulins (Matsumura and Maeda, 1986).

On the other side, it has also been shown that EPR effect is heterogenous in nature and the extent of leakiness in tumor vasculature depends on the type, size and location of the tumor among other factors (Bae, 2009; Jain and Stylianopoulos, 2010). Further, the depth of penetration is determined by the resistance posed by the extracellular matrix (ECM) components to diffusive transport and by the IFP to the convective transport. Within the interstitial space, the pore size and connectedness also plays a significant role in the transport of macromolecules (Yuan et al., 2001). Some of the other factors affecting drug penetration and release from PDCs include the low pH and hypoxic conditions in the core of solid tumors (Jain and Stylianopoulos, 2010).

In a human squamous cell carcinoma xenograft mouse model, Dreher et al. showed that the apparent permeability of the tumor blood vessels and the depth of penetration within the tumor decreased with increasing molecular weight of dextran. However, if the molecular size allows for prolonged circulation, the decrease in permeability may have a comparatively smaller effect on the cumulative tumor accumulation (Dreher et al., 2006).

1.3.2.f. Formation of Multi-molecular Assemblies

Conjugation of a hydrophobic drug to a hydrophilic polymer has an impact on the physicochemical properties of the conjugate. The extent of the impact is determined by the hydrophilicity of the polymer before conjugation and the degree of hydrophobization upon conjugation which is dictated by the number of drug molecules or substituents per polymer chain. Hydrophobic substitution can result in a decrease in the aqueous solubility, spontaneous aggregation due to hydrophobic interactions and precipitation of the product at higher substitutions. However, if the conjugation results in the formation of an amphiphile with a hydrophilic-lipophilic balance (HLB) that allows for formation of stable assemblies or micelles, a higher degree of drug solubilization as well as stabilization in the hydrophobic core could be achieved (Gautier et al., 1997). Dox conjugated (6.2 wt %) to pullulan resulted in formation of two different populations with mean diameters of 145 nm and 24 nm respectively (Scomparin et al., 2011). PGA conjugates of PTX with or without a RGD peptide had hydrodynamic diameters of 6-7 nm (Eldar-Boock et al., 2011).

The pendant carboxyl groups of PLL-citramide upon alkyl substitution formed multi-molecular aggregates with C7 and C12 derivatives but not with C2 derivatives (Abdellaoui et al., 1998a). The aggregate size increased with an increasing amount of heptyl or lauryl

substitution on PLL-citramide. The presence of ions may enhance aggregation by shielding of charges thus promoting hydrophobic interactions and aggregation. A variation in the pH may have a similar effect on weak acid or weak base behavior of polymer functional groups (Gautier et al., 1997). A PGA-poly-L-phenylalanine block copolypeptide spontaneously formed vesicles with a critical micellar concentration (CMC) of 0.11 mg/mL and the size of the aggregates was pH dependent (Kim et al., 2009). Branched or block copolymers are other types of modifications that lead to the micellization of the conjugated drug carrier e.g. PEG-PAA-ADR conjugate (Yokoyama et al., 1990).

Incorporation of amphiphilic properties causing micellar aggregation to enhance the drug solubility, serum stability and take advantage of the EPR effect has been the intent in several PDCs. PAMAM conjugated to camptothecin (CPT) and PEG formed micelles of 88 nm with a CMC value of 0.003 mg/mL. Formation of micelles resulted in improving the stability of the lactone form of CPT (Fan et al., 2010).

The stability of the micellar assemblies *in-vivo* is dictated by their CMC or the HLB, interaction with plasma components and the ionic behavior. Their formation can have significant effect of the biodistribution, cell uptake and antitumor efficacy. ELPs have been characterized for the formation of stable multi-molecular assemblies following dox conjugation to these soluble polypeptides modified at the C-terminus with a cysteine containing peptide sequence to limit the site and number of drug attachment (MacKay et al., 2009). The CMC, in dox equivalents (14.4 μM), were 40-fold lower than the plasma concentrations of dox at the time of injection (600 μM) and therefore the assemblies are expected to be stable to dilution in plasma (Dreher et al., 2003; MacKay et al., 2009). This further highlights the significance of the location and number of hydrophobic substituents in

PDCs in the formation of reversible yet stable and predictable aggregates. Interestingly, in case of cysteine derivatized ELPs, only anionic and neutral polymers self-assembled when substituted with dox and the size increased with increasing molecular weight of the polymer (MacKay et al., 2009).

1.3.3. PDCs as Delivery Systems for Hydrophobic Drugs

Many first line chemotherapy drugs like PTX suffer from low aqueous solubility (Trissel, 1997). This creates the need for delivery systems that are able to solubilize them to make it possible to administer therapeutic doses. Chemical conjugation to hydrophilic polymers to generate a polymeric prodrug is one of the ways to enhance the solubility. Micellization as discussed above may lead to further enhancement in solubility by creating hydrophobic pockets that minimize interaction with surrounding water molecules. Solubility enhancement in this manner also avoids the need to add additional modifiers that can be associated with adverse hypersensitivity reactions e.g. cremophor and ethanol in Taxol® (Weiss et al., 1990).

PEG has been widely used as a hydrophilic polymeric substituent to provide enhanced aqueous solubility in addition to other advantages of PDCs as outlined above. Conjugation of PEG to PTX at 7-position via a urethane or a carbonate linkage led to a 30,000-fold enhancement (>650 mg/mL) in the aqueous solubility (Greenwald et al., 1995). However, the biological activity of these conjugates was highly reduced compared to PTX (Greenwald, 2001). Moreover, unmodified PEG only provides a maximum of two sites for conjugation and is therefore, limited if a higher drug payload per polymer or multi-functionality is desired (Khandare and Minko, 2006).

In this respect, hydrophilic polymers with multiple pendant groups have the potential to overcome this limitation while providing the solubility enhancement. PGA has been used to enhance the aqueous solubility of several hydrophobic drugs such as PTX, dox and CPT (Singer et al., 2000) by covalently conjugating them to the carboxyl groups of PGA. PGA-PTX conjugate had aqueous solubility of 20 mg/mL of PTX equivalent which is 80,000-fold greater than the solubility of unconjugated PTX and has been shown to have improved anti-tumor efficacy and increased therapeutic index *in-vivo* (Li et al., 1999).

PGA-CPT conjugates prepared with different amounts of drug loading and varying length of the glycine linker were analyzed for their aqueous solubility. The conjugate with the triglycine linker and 30 wt % CPT had an aqueous solubility of 5 mg/mL while the conjugate with monoglycine linker and 29 wt % CPT had an aqueous solubility of 30 mg/mL (Bhatt et al., 2003). This is a 10,000-fold enhancement over the solubility of CPT (2-3 μg/mL).

1.3.4. Targeting PDCs for Enhanced Effectiveness

Endocytosis is a non-specific process of cell uptake and presents as a rate-limiting step in the cellular entry of many PDCs. Covalent attachment of residues that have specific cell uptake activity by virtue of their affinity towards a cell surface receptor or alternate molecular pathway of cellular entry have been investigated to transport PDCs inside the cells. Receptor-mediated targeting of PDCs is based on the over-expression of certain receptors in cancer cells leading to preferential binding and active uptake of receptor-bound PDCs. This is expected to enhance the overall rate and extent of cellular entry resulting in improved activity. Successful targeting depends on the affinity of the targeting ligand after conjugation

to PDC, number of ligands necessary to provide desired accumulation, rate of receptor internalization and the subcellular fate of receptor-bound cargo.

Epidermal growth factor receptor (EGFR)-overexpressing A431 cells were targeted using C225 antibody attached through a polyethylene glycol (PEG) spacer to PGA-dox conjugate (C225-PEG-PGA-Dox). The conjugate showed comparable binding to the receptors as free antibody and was internalized very rapidly compared to unconjugated dox or conjugates without C225. Pre-incubation with C225 prevented the uptake of the C225-PEG-PGA-Dox (Vega et al., 2003). Targeting of the PGA-PTX conjugates discussed above to epithelial cells with cyclic RGD peptides showed selective tumor accumulation of the conjugate with anti-proliferative effect on the orthotopic tumors in mice over-expressing $\alpha_v\beta_3$ integrin receptors (Eldar-Boock et al., 2011). Similar preferential accumulation and higher cytotoxicity was reported with PGA-dox-H2009.1 conjugate where H2009.1 peptide targeted cells over-expressing $\alpha_v\beta_6$ integrin receptors (Guan et al., 2008). Pulluan conjugates of dox (6.2 wt %) containing folate (4.3 wt %) as the targeting ligand showed higher uptake and cytotoxicity in cells over-expressing folate receptor compared to the conjugate with no folate (Scomparin et al., 2011). Asialoglycoprotein (ASGP) receptors expressed on hepatocytes were targeted using dox-linear PAMAM dendrimer-PEG-galactose conjugate where galactose was the ligand for ASGP receptors. The targeted conjugate showed improved hepatocyte uptake and antitumor effect in hepatoma xenografts in mice (Huang et al., 2010). A trivalent galactose ligand on HPMA copolymer recently showed 8-10-fold higher cell uptake compared to galactose in hepatocarcinoma cells (David et al., 2001).

HPMA copolymer-drug conjugates have been investigated with a wide range of targeting residues. RGD peptides have been used to target HPMA copolymer drug conjugates

to $\alpha_v\beta_3$ integrin receptors on epithelial cells in angiogenic blood vessels of tumors (Line et al., 2005; Mitra et al., 2006). A copolymer conjugate of HPMA-geldanamycin with RGDfK peptide showed competitive binding to receptors on human umbilical vein endothelial cells (HUVEC) in the presence of free peptide and enhanced cytotoxicity compared to conjugate without the peptide (Borgman et al., 2009). Targeting HPMA copolymer-drug conjugates using Fab' fragment of a monoclonal antibody against the OA-3 (ovarian carcinoma) antigen was reported where the Fab' was covalently conjugated to a monomer unit and copolymerized with another monomer covalently conjugated to the drug via an enzyme cleavable spacer. This approach allowed precise control of the number of targeting molecules and the size of the final conjugate (Lu et al., 1999). HPMA copolymer-triphenylphosphonium conjugate localized in mitochondria upon microinjection into the cytosol indicating organelle specific targeting (Cuchelkar et al., 2008a). Alendronate (ALN) shows high affinity for hydroxyapatite and has been used to target PDCs to bone to treat metastatic growth or primary bone tumors. A multifunctional HPMA copolymer conjugate containing both ALN and TNP-470 had greater antitumor effect than a combination of the two drugs administered simultaneously (Segal et al., 2009).

Drug conjugation to the polymer can sometimes lead to decreased cytotoxicity when determined *in-vitro* due to additional steps involved in the uptake of the conjugate and eventual drug release (Kovar et al., 2002; Nogusa et al., 1997). In such cases, incorporation of efficient targeting ligands in combination with suitable spacers, once again, can attenuate this decrease in activity both *in-vitro* and *in-vivo*. For example, the HPMA-GLFG-Dox conjugate was almost 1000-fold less cytotoxic in lymphoma cells than free dox. Transferrin receptor targeting using an antibody for CD71 receptor (HPMA copolymer-dox-CD71

antibody) increased the cell uptake by almost 10-fold and had significantly high antitumor efficacy compared to free dox (Kovar et al., 2002).

1.3.5. Combination Therapy with Multi-functional PDCs

Combination therapy is routinely used in cancer patients to enhance the effectiveness and reduce drug associated adverse events. PDCs provide a unique opportunity in combination therapy of cancer. A combination of two drugs bound to the same polymer backbone, a PDC co-administered with another PDC or a PDC co-administered with standard treatment regimens (radiation or chemotherapeutic) have been investigated. The drugs used in combination may be similar or different in their mechanism of action based on the rationale and desired clinical outcome.

In the first case, where two or more drugs are covalently linked to the same polymer chain, the resulting pharmacokinetics of the conjugated drugs is expected to be similar unlike the drugs administered separately. Simultaneous, selectively enhanced accumulation of two or more drugs to the solid tumor may result in lowering of the effective dose of each of the drugs leading to fewer associated adverse events. Additionally, it is possible to take advantage of pharmacological synergy among two different drugs based on the mechanism of action or physicochemical properties. For example, phosphatidylinositol-3 (PI3) kinase inhibitors like wortamannin have been shown to sensitize cells to dox. Combination therapy using dox and wortmannin covalently conjugated to amphiphilic block copolymer of PEG-poly(aspartate hydrazide) via hydrazine bonds was investigated. The combination conjugate was equally effective at 50 mol% of dox compared to treatment with free drug indicating a possible synergy between the two drugs (Bae et al., 2007). HPMA copolymer simultaneously

linked to dox and aminoglutethimide (AGM) using GFLG as a cleavable linker was investigated for combination therapy. The single drug HPMA conjugates of dox or AGM used alone or in physical mixtures were less active than free dox *in-vitro* whereas the HPMA-GFLG-AGM-Dox conjugate showed synergistic enhancement in cytotoxicity (Vicent et al., 2005). HPMA copolymer conjugated simultaneously to gemcitabine and dox using separate GFLG spacers and to tyrosinamide through an amide bond (P-Gem-Dox) was reported. The P-Gem-Dox conjugate showed stronger tumor growth inhibitory effect than HPMA-Dox and HPMA-Gem conjugate administered together or the two free drugs administered in combination (Lammers et al., 2009). Similarly, dox and dexamethasone ester derivatives have been conjugated to the same HPMA copolymer chain via hydrazone linkage and the conjugate showed simultaneous pH dependent release of the two drugs (Krakovicova et al., 2009). ALN and PTX were conjugated to HPMA to combine the anti-angiogenic effects of ALN with anticancer effects of PTX. While ALN was conjugated through GFLG peptide spacer, an additional self-cleaving PABC spacer was included between PTX and the polymer chain (Miller et al., 2009).

Two different polymer-drug conjugates if co-administered would provide co-delivery while still incorporating the merits of long circulation, enhanced passive tumor accumulation, improved tolerance and such. Such a co-administration if comparable in efficacy to two drugs linked to the same polymer backbone would be simpler and easier to characterize than multi-drug conjugate approaches discussed above. HPMA copolymer-Mce_6 was co-administered with HPMA copolymer-ADR conjugate in mice bearing ovarian carcinoma to investigate a combination of chemotherapy with photodynamic therapy of cancer. The two

conjugates were administered separately followed by light dose at 18 and 24 hr and showed significant antitumor effect compared to single conjugates alone (Shiah et al., 2000).

In the third case, the concomitant delivery of polymer-drug conjugates with radiation therapy or other standard chemotherapeutic regimens has been explored. A PGA-feretinide conjugate sensitized cancer cells to radiation treatment leading to synergistic improvement in tumor (A549 lung cancer xenografts) growth control (Zhu et al., 2007).

A combination of drug and gene delivery has recently shown promising anticancer properties. PEI-β-cyclodextrin conjugates further covalently linked to 5-fluoro-2-deoxyuridine (FUD) showed a higher cell uptake and increased cytotoxic potential compared to unconjugated FUD. This drug conjugate was further complexed with plasmid DNA (pDNA) and showed enhanced gene transfer efficiency at N/P of 25 compared to a 25 kDa PEI at N/P of 10 (Lu et al., 2010).

1.3.6. Preclinical and Clinical Investigations

The success of chemical conjugation of drugs to polymers is evident by several recent FDA approvals of products based on this approach including Neulasta™, PEGasys®, PEG-Intron™ and Oncaspar® (Soo et al., 2009). The polymeric component in all of these is PEG. However, products based on other hydrophilic polymers e.g. PGA, HPMA copolymer and dextran, that are multivalent and multifunctional are still in various phases of clinical trials.

Two different types of dox conjugates with HPMA copolymer are currently in clinical trials. PK1 contains dox conjugated to HPMA copolymer through a cathepsin B sensitive tetrapeptide (GFLG) linker (Vasey et al., 1999). PK2 is similar to PK1 but contains galactosamine bound to the polymer chain for additional targeting to the ASGP receptors on

hepatocarcinoma cells (David et al., 2001). In a Phase I study, PK1 was found to be longer circulating and less cardiotoxic than free dox in patients with refractory or resistant cancers administered at mean cumulative dose 508 mg/m^2. The elimination half-life of PK1 was 93 hr (Vasey et al., 1999). A dose, based on the Phase I studies, of 280 mg/m^2 every 3 weeks was used in subsequent Phase II trials in patients with breast cancer (17/62), non-small cell lung cancer (NSCLC) (16/62) and colorectal cancer (29/62). Partial responses were observed in 6/62 patients (Seymour et al., 2009). PK1 is currently under Phase II trials in women with advanced breast cancer (ClinicalTrials.gov Identifier: NCT00003165). In a Phase I study with PK2 in patients with solid tumors, 3.3% of total dose could be detected in areas of tumor in the liver and the conjugate showed increased uptake in the metastatic sites. The antitumor effects observed in this study are summarized in **Table 1.3** (Seymour et al., 2002).

PGA-PTX (Opaxio^{TM}, formerly known as Xyotax^{TM}) has been widely investigated for its antitumor efficacy. A single i.v. dose of the conjugate completely eliminated the mammary adenocarcinoma in mice (Li et al., 1998). The conjugate showed a 2-fold increase in the maximum tolerated dose in PTX equivalents. The conjugate enhanced the exposure by 12-fold compared to unconjugated PTX. Multiple injections of the conjugate had similar efficacy compared to a single i.v. dose suggesting that administration of the highest possible single dose is a better strategy than multiple dosing for long circulating drug conjugates such as PGA-PTX (Li et al., 1999; Li et al., 1998).In a Phase II study in ovarian cancer patients, the conjugate was found to be active with a response rate of 10% (10/99) and median time to progression of 2 months. In three separate Phase III clinical trials in NSCLC patients with poor performance status, the conjugate had comparable survival compared to the control

treatments (Chipman et al., 2006; Langer et al., 2008) (**Table 1.3**). However, the female patients showed a longer survival compared to male patients.

PGA conjugates of CPT, 9-amino-CPT, SN-38 and 10-hydroxy-CPT have been reported where the drugs were linked to the polymer via ester bonds. The conjugates with a glycine linker between the drug and the polymer were also evaluated. The glycine linker allowed for higher drug loading (37% w/w) and >2-fold increase in solubility (25 mg/mL) compared to the PGA-CPT conjugate with 14% w/w drug loading and aqueous solubility of 11 mg/mL. However, there was no difference in the efficacy of the conjugates with or without the glycine linker in terms of tumor growth delay in a human lung cancer xenograft in mice. The maximum tolerated dose (MTD) of the PGA conjugates was approximately 2-fold higher than unconjugated CPT (Bhatt et al., 2006). The conjugate with glycine linker (39 mg/kg CPT equivalent dose) resulted in TGD of 26 days compared to 17 days with unconjugated CPT (20 mg/kg dose) in HT-29 colon carcinoma model. In the same model, the conjugate with glycine linker (18 mg/kg CPT equivalent dose) increased the tumor exposure (AUC) by >7-fold compared to unconjugated CPT (15 mg/kg dose) (Bhatt et al., 2003). A 50 kDa conjugate showed better efficacy than a 33 kDa conjugate. This is probably due to slower clearance of the higher molecular weight conjugate resulting in longer circulation and thus allowing higher tumor accumulation (Singer et al., 2001; Singer et al., 2000).

Recently, dextran conjugates of CPT and dox have been shown to be effective. DX-8951 (exatecan mesylate) conjugated to carboxymethyldextran polyalcohol via a cathepsin sensitive GGFG linker, the product named DE-310, showed antitumor activity in mouse models. In a Phase I study with DE-310, the conjugate showed a 600-fold increase in the drug exposure and an apparent terminal half-life of 13 days (Soepenberg et al., 2005).

Table 1.3 Anticancer clinical trials with PDCs.

Conjugate	Study Composition	Comments	Reference
PGA-PTX	99 platinum sensitive (42/99) or resistant (57/99) ovarian cancer patients with prior chemotherapy.	Overall response rate (RR) of 10% (14% in sensitive and 7% in resistant) and time to progression of 2 months	(Sabbatini et al., 2004)
PGA-PTX	Chemotherapy naïve NSCLC patients; 199/400 received PGA-PTX and carboplatin; 201/400 received PTX and carboplatin.	Median survival in PGA-PTX group was 7.8 months compared to 7.9 months in PTX group.	(Langer et al., 2008)
HPMA-GFLG-Dox (PK1)	Patients with breast (14 evaluated), NSCLC (26 evaluated) and colorectal cancer (16 evaluated)	6 showed partial response (PR) (3 breast and 3 NSCLC patients)	(Seymour et al., 2009)
Galactosamine-HPMA-GFLG-Dox (PK2)	Liver cancer patients with primary (25/31) or metastatic (6/31) cancer with or without (11/31) prior chemotherapy.	PR in 3/25 patients with primary cancers. 2/31 patients had reduced levels of α-FP marker; median survival was 11 months.	(Seymour et al., 2002)
HPMA-GFLG-Platinate (AP5280)	Patients (19/29 evaluable) with solid tumors with prior chemotherapy	5/19 patients had stable disease (9 to 24 weeks). 14/19 showed disease progression; No PR or complete responses (CR)	(Rademaker-Lakhai et al., 2004)
Carboxymethyldextran polyalcohol-GGFG-DX-8951	Patients (27) with solid tumors (25/27 evaluated).	1/25 showed complete remission for >2 years; 15/25 had stable disease that ranged from 6 weeks to 32 weeks.	(Soepenberg et al., 2005)

1.3.7. Future of PDCs Cancer Therapy

With several different PDCs currently being evaluated in clinical trials, future investigations are expected to focus on designing systems that are more efficient in overcoming some of the delivery barriers discussed above. Some of the approaches currently being investigated include conjugates targeting specific molecular pathways, designing highly specific yet biologically sensitive spacers, incorporating components that allow efficient endosomal escape, conformationally favorable conjugates (Deacon et al., 2011) and polymer-directed enzyme prodrug therapy (PDEPT) (Satchi-Fainaro et al., 2003). Additionally, inclusion of multi-functionality in linear polymers allows for a combination of therapeutic functions as discussed above or a theranostic property. A recent report investigated formation of 50 nm particles upon formation of electrostatic complex between a positively charged fluorescent polymer (quenched when in complex) and negatively charged PGA-dox conjugate. The drug release caused fluorescence signal to "turn-on" thus enabling the monitoring of drug release and the cellular localization of the complex (Feng et al., 2010).

Coiled-coil conjugates that contain a 1:1 heterodimer of polymer-peptide conjugates with a target protein have been developed as cellular delivery systems. PEG conjugate of a FOSWc (cysteine derivatized synthetic peptide) was shown to form a coiled-coil heterodimer with c-Jun peptide. The coiled-coil conjugate was investigated as a molecular target for the activator protein 1 (AP-1) and was shown to be dependent on the presence of transfection reagent (Tfx-50) for cell uptake and cytotoxicity (Deacon et al., 2011).

PDCs linked via an enzyme cleavable spacer are limited by the availability of the cleaving enzyme at the desired site of drug release. To overcome this limitation, an approach

involving the administration of a polymer-enzyme sensitive spacer-drug conjugate followed by polymer-enzyme conjugate was explored. HPMA copolymer-β-lactamase conjugate was administered 5 hr after administration of HPMA copolymer-cephalosporin-dox conjugate. The enzyme conjugate is expected to release dox by hydrolysis of the cephalosporin linker within the tumor microenvironment. This combination resulted in improved survival and reduced tumor growth in mice (Satchi-Fainaro et al., 2003). A similar combination of HPMA-GFLG-dox conjugate and HPMA-Cathepsin B conjugate showed increase in dox concentration in the tumors following administration of the enzyme conjugate (Satchi et al., 2001).

1.3.8. Poly(α)-L-glutamic Acid as the Polymer of Choice for Drug Conjugation

PGA is a synthetic homopolypeptide composed of L-glutamic acid monomers linked by amide bonds between α-carbon and nitrogen attached to the α-carbon of adjacent L-glutamic acid monomer. The γ-carboxyl groups are available for covalent conjugation as shown below (**Figure 1.9**). The figure also shows structural differences between PGA and the naturally occurring Poly (γ)-L-glutamic acid (γPGA), usually isolated from *Bacillus subtilis* cultures, that has also been used as therapeutic delivery system (Manocha and Margaritis, 2010; Matsusaki et al., 2002; Schneerson et al., 2003).

PGA undergoes reversible helix-coil transition that is critically dependent on the degree of ionization of PGA and therefore pH changes induce corresponding conformational changes as shown in **Figure 1.10** (Krejtschi and Hauser, 2011; Lumry et al., 1964). The random coil is the predominant conformation at physiological pH of 7.4, the mid-point of transition being at pH 5.0 (Morcellet and Loucheux, 1976). The polymer solution begins to

become turbid as the pH is dropped to 4.5 with visible precipitation below pH 3.0. Circular dichroism (CD), optical rotatory dispersion (ORD) and potentiometry have been used to investigate the helix-coil transition and the effect of degree of polymerization, extent of ionization, type of counterion and ionic strength of the solvent on the optical behavior of PGA (Nagasawa and Holtzer, 1964; Rinaudo and Domard, 1976). The random coil conformation is favorable for chemical conjugation reactions and was also reported to be more stable at higher temperatures than the helix form (Krejtschi and Hauser, 2011). Therefore, formulations containing PGA-drug conjugates should be carefully adjusted for pH and ionic strength for maximum stability and desired conformation.

The molecular weight of PGA has been determined using Size Exclusion Chromatography (SEC), viscosity measurements using Mark-Houwink equation and concentration based determinations by multi-angle laser light scattering (MALLS) analysis (Morcellet and Loucheux, 1976; Tansey et al., 2004). PGA has been investigated as a drug delivery system in the form of direct drug conjugates, cross-linked nanoparticles, hydrogels etc.

Drug conjugates of PGA have been formulated as lyophilized products for extended shelf stability. In such cases the formulation may contain other inactive components intended to stabilize the formulation (buffers, salts etc.) or reduce the reconstitution time (sugars, polyols, amino acids etc.) (Besman et al., 2009). PGA is relatively stable to lyophilization due to good anti-freeze activity (Shih et al., 2003), and thus formulations containing PGA-drug conjugates may not need any cryoprotectants during freeze-drying.

PGA is completely biodegradable, biocompatible and has high aqueous solubility (>50 mg/mL) at physiological pH. Further, the presence of easily modifiable pendant carboxyl groups makes it a versatile drug carrier.

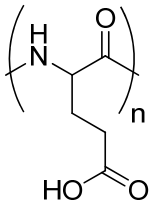

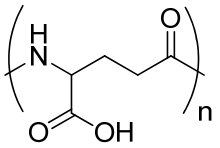

Poly(α)-L-glutamic acid **Poly(γ)-L-glutamic acid**

Figure 1.9 Structure of synthetic poly(α)-L-glutamic acid (PGA) and the naturally occurring poly(γ)-L-glutamic acid.

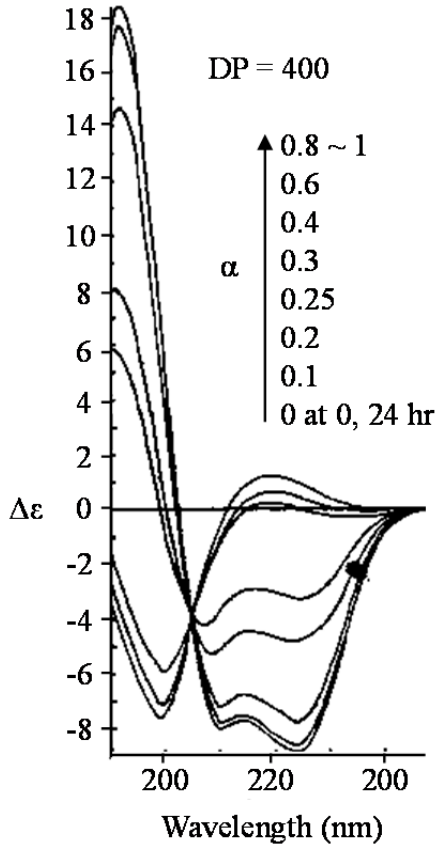

Figure 1.10 Helix-coil transition of PGA
Degree of neutralization (α; from 0 to 1) and pH-dependent helix-coil transition of poly-α-L-glutamic acid (PGA) with a degree of polymerization (DP) = 400 by circular dichroism spectra. PGA transitions from a random coil conformation to an α-helix as the degree of neutralization of the carboxyl pendant groups increases (reproduced with permission from the *Journal of American Chemical Society* (Rinaudo and Domard, 1976)

1.4. References

Abbas, T., and A. Dutta. 2009. p21 in cancer: intricate networks and multiple activities. Nat Rev Cancer. 9:400-414.

Abdellaoui, K., M. Boustta, H. Morjani, M. Manfait, and M. Vert. 1998a. Uptake and intracellular distribution of 4-aminofluorescein-labelled poly(L-lysine citramide imide) in K562 cells. J Drug Target. 5:193-206.

Abdellaoui, K., M. Boustta, M. Vert, H. Morjani, and M. Manfait. 1998b. Metabolite-derived artificial polymers designed for drug targeting, cell penetration and bioresorption. Eur J Pharm Sci. 6:61-73.

Aksoy, S., D. Hizli, S. Sarici, R. Ocalan, M.F. Kose, and N. Guler. 2008. A retrospective review of metastatic or recurrent uterine sarcomas treated with ifosfamide and doxorubicin (IMA). Uluslararasi Hematol Onkol Derg. 18:129-134.

Albini, A., F. D'Agostini, D. Giunciuglio, I. Paglieri, R. Balansky, and S. De Flora. 1995. Inhibition of invasion, gelatinase activity, tumor take and metastasis of malignant cells by N-acetylcysteine. Int J Cancer. 61:121-129.

Albini, A., M. Morini, F. D'Agostini, N. Ferrari, F. Campelli, G. Arena, D.M. Noonan, C. Pesce, and S. De Flora. 2001. Inhibition of angiogenesis-driven Kaposi's sarcoma tumor growth in nude mice by oral N-acetylcysteine. Cancer Res. 61:8171-8178.

Allinquant, B., P. Hantraye, P. Mailleux, K. Moya, C. Bouillot, and A. Prochiantz. 1995. Downregulation of amyloid precursor protein inhibits neurite outgrowth in vitro. J Cell Biol. 128:919-927.

Alshamkhani, A., and R. Duncan. 1995a. Radioiodination of alginate via covalently bound tyrosinamide allows monitoring of its fate *in-vivo*. J Bioact Compat Polym. 10:4-13.

Alshamkhani, A., and R. Duncan. 1995b. Synthesis, controlled release properties and antitumor activity of alginate-cis-aconityl-daunomycin conjugates. Int J Pharm. 122:107-119.

Aposhian, H.V., and L.S. Bradham. 1959. Metabolism in vitro of the sulphydryl amino acids, L- and D-penicillamine. Biochem Pharmacol. 3:38-41.

Arunachalam, B., U.T. Phan, H.J. Geuze, and P. Cresswell. 2000. Enzymatic reduction of disulfide bonds in lysosomes: characterization of a gamma-interferon-inducible lysosomal thiol reductase (GILT). Proc Natl Acad Sci U S A. 97:745-750.

Asayama, S., H. Kato, H. Kawakami, and S. Nagaoka. 2007. Carboxymethyl poly(L-histidine) as a new pH-sensitive polypeptide at endosomal/lysosomal pH. Polym Advan Technol. 18:329-333.

Austin, C.D., X. Wen, L. Gazzard, C. Nelson, R.H. Scheller, and S.J. Scales. 2005. Oxidizing potential of endosomes and lysosomes limits intracellular cleavage of disulfide-based antibody-drug conjugates. Proc Natl Acad Sci U S A. 102:17987-17992.

Bae, Y., T.A. Diezi, A. Zhao, and G.S. Kwon. 2007. Mixed polymeric micelles for combination cancer chemotherapy through the concurrent delivery of multiple chemotherapeutic agents. J Control Release. 122:324-330.

Bae, Y.H. 2009. Drug targeting and tumor heterogeneity. J Control Release. 133:2-3.

Baier-Bitterlich, G., W. Schumacher, T.F. Schulz, H. Wachter, and M.P. Dierich. 1993. Effects of D-penicillamine on human cell lines. Arzneimittelforschung. 43:395-398.

Baur, M., B. Fazeny-Doerner, M. Hudec, P. Sevelda, H. Salzer, and C. Dittrich. 2006. Ifosfamide/Mesna as Salvage Therapy in Platinum Pretreated Ovarian Cancer Patients-Long-Term Results of a Phase II Study. Cancer Invest. 24:22-27.

Baxter, A.D., R. Bhogal, J.B. Bird, G.M. Buckley, D.S. Gregory, P.C. Hedger, D.T. Manallack, T. Massil, K.J. Minton, J.G. Montana, S. Neidle, D.A. Owen, and R.J. Watson. 1997. Mercaptoacyl matrix metalloproteinase inhibitors: The effect of substitution at the mercaptoacyl moiety. Bioorg Med Chem Lett. 7:2765-2770.

Bennett, M., K. Macdonald, S.W. Chan, J.P. Luzio, R. Simari, and P. Weissberg. 1998. Cell surface trafficking of Fas: a rapid mechanism of p53-mediated apoptosis. Science. 282:290-293.

Bertram, C., and R. Hass. 2008. Cellular responses to reactive oxygen species-induced DNA damage and aging. Biol Chem. 389:211-220.

Besman, M., J. Carpenter, M. Manning, L. McNamara, and R. Nayar. 2009. Hydrophobic compositions containing reconstitution enhancer, US Patent Publication 2009/0298743.

Betts, W.H., L.G. Cleland, D.J. Gee, and M.W. Whitehouse. 1984. Effects of D-penicillamine on a model of oxygen-derived free radical mediated tissue damage. Agents and Actions. 14:283-290.

Bhatt, R., P. de Vries, J. Tulinsky, G. Bellamy, B. Baker, J.W. Singer, and P. Klein. 2003. Synthesis and in vivo antitumor activity of poly(l-glutamic acid) conjugates of 20S-camptothecin. J Med Chem. 46:190-193.

Bhatt, R., P.D. Vries, P.J. Klein, J. Tulinsky, R.A. Lewis, and J.W. Singer. 2006. Polyglutamic acid-camptothecin conjugates and methods of preparation, US Patent 7153864.

Blomgren, H., M. Hallstroem, and H. Hillgren. 1990. Antitumor activity of 2-mercaptoethanesulfonate (mesna) in vitro. Methods Find. Exp. Clin. Pharmacol. 12:691-697.

Blomgren, H., M. Hallstroem, and H. Hillgren. 1991. Antitumor activity of 2-mercaptoethanesulfonate (mesna) in vitro. Its potential use in the treatment of superficial bladder cancer. Anticancer Res. 11:773-776.

Borgman, M.P., A. Ray, R.B. Kolhatkar, E.A. Sausville, A.M. Burger, and H. Ghandehari. 2009. Targetable HPMA copolymer-aminohexylgeldanamycin conjugates for prostate cancer therapy. Pharm Res. 26:1407-1418.

Borisenko, G.G., I. Martin, Q. Zhao, A.A. Amoscato, Y.Y. Tyurina, and V.E. Kagan. 2004. Glutathione propagates oxidative stress triggered by myeloperoxidase in HL-60 cells. Evidence for glutathionyl radical-induced peroxidation of phospholipids and cytotoxicity. J Biol Chem. 279:23453-23462.

Boussif, O., F. Lezoualc'h, M.A. Zanta, M.D. Mergny, D. Scherman, B. Demeneix, and J.P. Behr. 1995. A versatile vector for gene and oligonucleotide transfer into cells in culture and in vivo: polyethylenimine. Proc Natl Acad Sci U S A. 92:7297-7301.

Breen, A.P., and J.A. Murphy. 1995. Reactions of oxyl radicals with DNA. Free Radic Biol Med. 18:1033-1077.

Brem, S., S.A. Grossman, K.A. Carson, P. New, S. Phuphanich, J.B. Alavi, T. Mikkelsen, J.D. Fisher, and T. New Approaches Brain Tumor. 2005. Phase 2 trial of copper depletion and penicillamine as antiangiogenesis therapy of glioblastoma. Neuro Oncol. 7:246-253.

Brem, S.S., D. Zagzag, A.M. Tsanaclis, S. Gately, M.P. Elkouby, and S.E. Brien. 1990. Inhibition of angiogenesis and tumor growth in the brain. Suppression of endothelial cell turnover by penicillamine and the depletion of copper, an angiogenic cofactor. Am J Pathol. 137:1121-1142.

Brennan, J.P., J.I. Miller, W. Fuller, R. Wait, S. Begum, M.J. Dunn, and P. Eaton. 2006. The utility of N,N-biotinyl glutathione disulfide in the study of protein S-glutathiolation. Mol Cell Proteomics. 5:215-225.

Brewer, G.J., R.D. Dick, D.K. Grover, V. LeClaire, M. Tseng, M. Wicha, K. Pienta, B.G. Redman, T. Jahan, V.K. Sondak, M. Strawderman, G. LeCarpentier, and S.D. Merajver. 2000. Treatment of metastatic cancer with tetrathiomolybdate, an anticopper, antiangiogenic agent: Phase I study. Clin Cancer Res. 6:1-10.

Burkitt, M.J., H.S. Bishop, L. Milne, S.Y. Tsang, G.J. Provan, C.S. Nobel, S. Orrenius, and A.F. Slater. 1998. Dithiocarbamate toxicity toward thymocytes involves their copper-catalyzed conversion to thiuram disulfides, which oxidize glutathione in a redox cycle without the release of reactive oxygen species. Arch Biochem Biophys. 353:73-84.

Cai, T., G. Fassina, M. Morini, M.G. Aluigi, L. Masiello, G. Fontanini, F. D'Agostini, S. De Flora, D.M. Noonan, and A. Albini. 1999. N-acetylcysteine inhibits endothelial cell invasion and angiogenesis. Lab Invest. 79:1151-1159.

Calvet, S., P. Doherty, and A. Prochiantz. 1998. Identification of a signaling pathway activated specifically in the somatodendritic compartment by a heparan sulfate that regulates dendrite growth. J Neurosci. 18:9751-9765.

Campo, E., J. Munoz, R. Miquel, A. Palacin, A. Cardesa, B.F. Sloane, and M.R. Emmert-Buck. 1994. Cathepsin B expression in colorectal carcinomas correlates with tumor progression and shortened patient survival. Am J Pathol. 145:301-309.

Carpentieri, U., J. Myers, L. Thorpe, C.W. Daeschner, 3rd, and M.E. Haggard. 1986. Copper, zinc, and iron in normal and leukemic lymphocytes from children. Cancer Res. 46:981-984.

Cavallaro, G., L. Mariano, S. Salmaso, P. Caliceti, and G. Gaetano. 2006. Folate-mediated targeting of polymeric conjugates of gemcitabine. Int J Pharm. 307:258-269.

Cavallaro, G., G. Pitarresi, M. Licciardi, and G. Giammona. 2001. Polymeric prodrug for release of an antitumoral agent by specific enzymes. Bioconjug Chem. 12:143-151.

Cejas, P., E. Casado, C. Belda-Iniesta, J. De Castro, E. Espinosa, A. Redondo, M. Sereno, M.A. Garcia-Cabezas, J.A. Vara, A. Dominguez-Caceres, R. Perona, and M. Gonzalez-Baron. 2004. Implications of oxidative stress and cell membrane lipid peroxidation in human cancer (Spain). Cancer Causes Control. 15:707-719.

Chandra, J., A. Samali, and S. Orrenius. 2000. Triggering and modulation of apoptosis by oxidative stress. Free Radic Biol Med. 29:323-333.

Chau, Y., R.F. Padera, N.M. Dang, and R. Langer. 2006. Antitumor efficacy of a novel polymer-peptide-drug conjugate in human tumor xenograft models. Int J Cancer. 118:1519-1526.

Chau, Y., F.E. Tan, and R. Langer. 2004. Synthesis and characterization of dextran-peptide-methotrexate conjugates for tumor targeting via mediation by matrix metalloproteinase II and matrix metalloproteinase IX. *Bioconjug Chem*. 15:931-941.

Chaudiere, J., E.C. Wilhelmsen, and A.L. Tappel. 1984. Mechanism of selenium-glutathione peroxidase and its inhibition by mercaptocarboxylic acids and other mercaptans. J Biol Chem. 259:1043-1050.

Chen, H.H., I.S. Song, A. Hossain, M.K. Choi, Y. Yamane, Z.D. Liang, J. Lu, L.Y. Wu, Z.H. Siddik, L.W. Klomp, N. Savaraj, and M.T. Kuo. 2008a. Elevated glutathione levels confer cellular sensitization to cisplatin toxicity by up-regulation of copper transporter hCtr1. Mol Pharmacol. 74:697-704.

Chen, L., R.N. Re, O. Prakash, and D. Mondal. 1991. Angiotensin-converting enzyme inhibition reduces neuroblastoma cell growth rate. Proc Soc Exp Biol Med. 196:280-283.

Chen, S.H., J.K. Lin, Y.C. Liang, M.H. Pan, S.H. Liu, and S.Y. Lin-Shiau. 2008b. Involvement of activating transcription factors JNK, NF-kappaB, and AP-1 in apoptosis induced by pyrrolidine dithiocarbamate/Cu complex. Eur J Pharmacol. 594:9-17.

Chinery, R., J.A. Brockman, M.O. Peeler, Y. Shyr, R.D. Beauchamp, and R.J. Coffey. 1997. Antioxidants enhance the cytotoxicity of chemotherapeutic agents in colorectal cancer: a p53-independent induction of p21WAF1/CIP1 via C/EBPbeta. Nat Med. 3:1233-1241.

Chipman, S.D., F.B. Oldham, G. Pezzoni, and J.W. Singer. 2006. Biological and clinical characterization of paclitaxel poliglumex (PPX, CT-2103), a macromolecular polymer-drug conjugate. Int J Nanomedicine. 1:375-383.

Chiu, H.C., P. Kopeckova, S.S. Deshmane, and J. Kopecek. 1997. Lysosomal degradability of poly(alpha-amino acids). J Biomed Mater Res. 34:381-392.

Choi, W.M., P. Kopeckova, T. Minko, and J. Kopecek. 1999. Synthesis of HPMA copolymer containing adriamycin bound via an acid-labile spacer and its activity toward human ovarian carcinoma cells. J Bioact Compat Polym. 14:447-456.

Christie, R.J., and D.W. Grainger. 2003. Design strategies to improve soluble macromolecular delivery constructs. Adv Drug Deliv Rev. 55:421-437.

Chvapil, M. 2005. Inhibition of breast adenocarcinoma growth by intratumoral injection of lipophilic long-acting lathyrogens. Anti-Cancer Drugs. 16:201-210.

Chvapil, M., and R. Dorr. 2005. Single intratumoral injection of long-acting benzyl ester of D-penicillamine inhibits the growth of melanoma tumor in mice. Anti-Cancer Drugs. 16:757-762.

Chvapil, M., F. Kielar, F. Liska, A. Silhankova, and K. Brendel. 2005. Synthesis and evaluation of long-acting D-penicillamine derivatives. Connect Tissue Res. 46:242-250.

Ciftci, K., and R.J. Levy. 2001. Enhanced plasmid DNA transfection with lysosomotropic agents in cultured fibroblasts. Int J Pharm. 218:81-92.

Collins, D.S., E.R. Unanue, and C.V. Harding. 1991. Reduction of disulfide bonds within lysosomes is a key step in antigen processing. J Immunol. 147:4054-4059.

Cox, C., S.D. Merajver, S. Yoo, R.D. Dick, G.J. Brewer, J.S. Lee, and T.N. Teknos. 2003. Inhibition of the growth of squamous cell carcinoma by tetrathiomolybdate-induced copper suppression in a murine model. Arch Otolaryngol Head Neck Surg. 129:781-785.

Cox, C., T.N. Teknos, M. Barrios, G.J. Brewer, R.D. Dick, and S.D. Merajver. 2001. The role of copper suppression as an antiangiogenic strategy in head and neck squamous cell carcinoma. Laryngoscope. 111:696-701.

Cuchelkar, V., P. Kopeckova, and J. Kopecek. 2008a. Novel HPMA copolymer-bound constructs for combined tumor and mitochondrial targeting. Mol Pharm. 5:776-786.

Cuchelkar, V., P. Kopeckova, and J. Kopecek. 2008b. Synthesis and biological evaluation of disulfide-linked HPMA copolymer-mesochlorin e6 conjugates. Macromol Biosci. 8:375-383.

Daniel, K.G., D. Chen, S. Orlu, Q.C. Cui, F.R. Miller, and Q.P. Dou. 2005. Clioquinol and pyrrolidine dithiocarbamate complex with copper to form proteasome inhibitors and apoptosis inducers in human breast cancer cells. Breast Cancer Res. 7:R897-908.

Daniel, K.G., P. Gupta, R.H. Harbach, W.C. Guida, and Q.P. Dou. 2004. Organic copper complexes as a new class of proteasome inhibitors and apoptosis inducers in human cancer cells. Biochem Pharmacol. 67:1139-1151.

David, A., P. Kopeckova, A. Rubinstein, and J. Kopecek. 2001. Enhanced biorecognition and internalization of HPMA copolymers containing multiple or multivalent carbohydrate side-chains by human hepatocarcinoma cells. Bioconjug Chem. 12:890-899.

Davidson, B., I. Goldberg, J. Kopolovic, L. Lerner-Geva, W.H. Gotlieb, G. Ben-Baruch, and R. Reich. 1999. MMP-2 and TIMP-2 expression correlates with poor prognosis in cervical carcinoma--a clinicopathologic study using immunohistochemistry and mRNA in situ hybridization. Gynecol Oncol. 73:372-382.

De Flora, S., F. D'Agostini, L. Masiello, D. Giunciuglio, and A. Albini. 1996. Synergism between N-acetylcysteine and doxorubicin in the prevention of tumorigenicity and metastasis in murine models. Int J Cancer. 67:842-848.

de Groot-Besseling, R.R.J., T.J.M. Ruers, I.L. Lamers-Elemans, C.N. Maass, R.M.W. de Waal, and J.R. Westphal. 2006. Angiostatin generating capacity and anti-tumour effects of D-penicillamine and plasminogen activators. BMC Cancer. 6.

Deacon, S.P., B. Apostolovic, R.J. Carbajo, A.K. Schott, K. Beck, M.J. Vicent, A. Pineda-Lucena, H.A. Klok, and R. Duncan. 2011. Polymer coiled-coil conjugates: potential for development as a new class of therapeutic "molecular switch". Biomacromolecules. 12:19-27.

Demarre, A., L.W. Seymour, and E. Schacht. 1994. Evaluation of the hydrolytic and enzymatic stability of macromolecular mitomycin C derivatives. J Control Release. 31:89-97.

Dreher, M.R., W. Liu, C.R. Michelich, M.W. Dewhirst, F. Yuan, and A. Chilkoti. 2006. Tumor vascular permeability, accumulation, and penetration of macromolecular drug carriers. J Natl Cancer Inst. 98:335-344.

Dreher, M.R., D. Raucher, N. Balu, O. Michael Colvin, S.M. Ludeman, and A. Chilkoti. 2003. Evaluation of an elastin-like polypeptide-doxorubicin conjugate for cancer therapy. J Control Release. 91:31-43.

Dubowchik, G.M., K. Mosure, J.O. Knipe, and R.A. Firestone. 1998. Cathepsin B-sensitive dipeptide prodrugs. 2. Models of anticancer drugs paclitaxel (Taxol), mitomycin C and doxorubicin. Bioorg Med Chem Lett. 8:3347-3352.

Duffy, M.J. 1992. The role of proteolytic enzymes in cancer invasion and metastasis. Clin Exp Metastasis. 10:145-155.

Dulger, S., N. Saglam, A.O. Belduz, S. Guner, and S. Karabocek. 2000. DNA cleavage by homo- and heterotetranuclear Cu(II) and Mn(II) complexes with tetrathioether-tetrathiol moiety. Biometals. 13:261-265.

Duncan, R. 2003. The dawning era of polymer therapeutics. Nat Rev Drug Discov. 2:347-360.

Duncan, R. 2009. Development of HPMA copolymer-anticancer conjugates: clinical experience and lessons learnt. Adv Drug Deliv Rev. 61:1131-1148.

Duncan, R., I.C. Hume, P. Kopeckova, K. Ulbrich, J. Strohalm, and J. Kopecek. 1989. Anticancer agents coupled to N-(2-hydroxypropyl) methacrylamide copolymers 3. Evaluation of adriamycin conjugates against mouse leukemia L1210 *in-vivo*. J Control Release. 10:51-63.

Egeblad, M., and Z. Werb. 2002. New functions for the matrix metalloproteinases in cancer progression. Nat Rev Cancer. 2:161-174.

Eldar-Boock, A., K. Miller, J. Sanchis, R. Lupu, M.J. Vicent, and R. Satchi-Fainaro. 2011. Integrin-assisted drug delivery of nano-scaled polymer therapeutics bearing paclitaxel. Biomaterials.

Elner, S.G., V.M. Elner, A. Yoshida, R.D. Dick, and G.J. Brewer. 2005. Effects of tetrathiomolybdate in a mouse model of retinal neovascularization. Invest Ophthalmol Vis Sci. 46:299-303.

Erbacher, P., A.C. Roche, M. Monsigny, and P. Midoux. 1996. Putative role of chloroquine in gene transfer into a human hepatoma cell line by DNA/lactosylated polylysine complexes. Exp Cell Res. 225:186-194.

Erez, R., E. Segal, K. Miller, R. Satchi-Fainaro, and D. Shabat. 2009. Enhanced cytotoxicity of a polymer-drug conjugate with triple payload of paclitaxel. Bioorg Med Chem. 17:4327-4335.

Fan, H.L., J. Huang, Y.P. Li, J.H. Yu, and J.H. Chen. 2010. Fabrication of reduction-degradable micelle based on disulfide-linked graft copolymer-camptothecin conjugate for enhancing solubility and stability of camptothecin. Polymer. 51:5107-5114.

Fawell, S., J. Seery, Y. Daikh, C. Moore, L.L. Chen, B. Pepinsky, and J. Barsoum. 1994. Tat-mediated delivery of heterologous proteins into cells. Proc Natl Acad Sci U S A. 91:664-668.

Feener, E.P., W.C. Shen, and H.J. Ryser. 1990. Cleavage of disulfide bonds in endocytosed macromolecules. A processing not associated with lysosomes or endosomes. J Biol Chem. 265:18780-18785.

Feng, X., F. Lv, L. Liu, H. Tang, C. Xing, Q. Yang, and S. Wang. 2010. Conjugated polymer nanoparticles for drug delivery and imaging. ACS Appl Mater Interfaces. 2:2429-2435.

Fernandez, L.A., J. Twickler, and A. Mead. 1985. Neovascularization produced by angiotensin II. J Lab Clin Med. 105:141-145.

Ferreri, C., C. Costantino, L. Landi, Q.G. Mulazzani, and C. Chatgilialoglu. 1999. The thiyl radical-mediated isomerization of cis-monounsaturated fatty acid residues in phospholipids: a novel path of membrane damage? Chem Commun:407-408.

Fidias, P., T.A. Ciuleanu, O. Gladkov, G.M. Manikhas, I.N. Bondarenko, A. Pluzanska, R. Ramlau, and T.J. Lynch. 2010. A randomized, open-label, phase III trial of NOV-002 in combination with paclitaxel (P) and carboplatin (C) versus paclitaxel and carboplatin alone for the treatment of advanced non-small cell lung cancer (NSCLC). In 2010 ASCO Annual Meeting Proceedings. Vol. 28. LBA7007.

Folkman, J. 1971. Tumor angiogenesis: therapeutic implications. N Engl J Med. 285:1182-1186.

Freskos, J.N., J.J. McDonald, B.V. Mischke, P.B. Mullins, H.S. Shieh, R.A. Stegeman, and A.M. Stevens. 1999. Synthesis and identification of conformationally constrained selective MMP inhibitors. Bioorg Med Chem Lett. 9:1757-1760.

Friteau, L., P. Jaffray, X. Ronot, and M. Adolphe. 1988. Differential effect of D-penicillamine on the cell kinetic parameters of various normal and transformed cellular types. J Cell Physiol. 136:514-518.

Fruehauf, J.P., and F.L. Meyskens, Jr. 2007. Reactive oxygen species: a breath of life or death? Clin Cancer Res. 13:789-794.

Furuta, S., F. Ortiz, X. Zhu Sun, H.H. Wu, A. Mason, and J. Momand. 2002. Copper uptake is required for pyrrolidine dithiocarbamate-mediated oxidation and protein level increase of p53 in cells. Biochem J. 365:639-648.

Gao, W., R. Langer, and O.C. Farokhzad. 2010. Poly(ethylene glycol) with observable shedding. Angew Chem Int Ed Engl. 49:6567-6571.

Gately, S., P. Twardowski, M.S. Stack, D.L. Cundiff, D. Grella, F.J. Castellino, J. Enghild, H.C. Kwaan, F. Lee, R.A. Kramer, O. Volpert, N. Bouck, and G.A. Soff. 1997. The

mechanism of cancer-mediated conversion of plasminogen to the angiogenesis inhibitor angiostatin. Proc Natl Acad Sci U S A. 94:10868-10872.

Gautier, S., M. Boustta, and M. Vert. 1997. Poly (L-lysine citramide), a water-soluble bioresorbable carrier for drug delivery: Aqueous solution properties of hydrophobized derivatives. J Bioact Compat Polym. 12:77-98.

Gerber, D.A. 1978. Inhibition of the denaturation of human gamma globulin by a mixture of D-penicillamine disulfide and copper. A possible mechanism of action of D-penicillamine in rheumatoid arthritis. Biochem Pharmacol. 27:469-472.

Ghosh, S.C., E. Auzenne, M. Khodadadian, D. Farquhar, and J. Klostergaard. 2009. N,N-Dimethylsphingosine conjugates of poly-L-glutamic acid: synthesis, characterization, and initial biological evaluation. Bioorg Med Chem Lett. 19:1012-1017.

Giannopoulou, E., P. Katsoris, D. Kardamakis, and E. Papadimitriou. 2003. Amifostine inhibits angiogenesis in vivo. J Pharmacol Exp Ther. 304:729-737.

Glover, D., J.H. Glick, C. Weiler, K. Fox, and D. Guerry. 1987. WR-2721 and high-dose cisplatin: an active combination in the treatment of metastatic melanoma. J Clin Oncol. 5:574-578.

Grdina, D.J., Y. Kataoka, J.S. Murley, N. Hunter, R.R. Weichselbaum, and L. Milas. 2002. Inhibition of spontaneous metastases formation by amifostine. Int J Cancer. 97:135-141.

Greco, F., M.J. Vicent, S. Gee, A.T. Jones, J. Gee, R.I. Nicholson, and R. Duncan. 2007. Investigating the mechanism of enhanced cytotoxicity of HPMA copolymer-Dox-AGM in breast cancer cells. J Control Release. 117:28-39.

Greenwald, R.B. 2001. PEG drugs: an overview. J Control Release. 74:159-171.

Greenwald, R.B., A. Pendri, and D. Bolikal. 1995. Highly Water-Soluble Taxol Derivatives - 7-Polyethylene Glycol Carbamates and Carbonates. J Org Chem. 60:331-336.

Guan, D., Y. Xu, M. Yang, H. Wang, X. Wang, and Z. Shen. 2010. N-acetyl cysteine and penicillamine induce apoptosis via the ER stress response-signaling pathway. Mol Carcinog. 49:68-74.

Guan, H., M.J. McGuire, S. Li, and K.C. Brown. 2008. Peptide-targeted polyglutamic acid doxorubicin conjugates for the treatment of alpha(v)beta(6)-positive cancers. Bioconjug Chem. 19:1813-1821.

Gupta, S.K., V.K. Shukla, M.P. Vaidya, S.K. Roy, and S. Gupta. 1991. Serum trace elements and Cu/Zn ratio in breast cancer patients. J Surg Oncol. 46:178-181.

Gupte, A., and R.J. Mumper. 2007a. Copper chelation by D-penicillamine generates reactive oxygen species that are cytotoxic to human leukemia and breast cancer cells. Free Radic Biol Med. 43:1271-1278.

Gupte, A., and R.J. Mumper. 2007b. An investigation into copper catalyzed D-penicillamine oxidation and subsequent hydrogen peroxide generation. J Inorg Biochem. 101:594-602.

Gupte, A., and R.J. Mumper. 2009. Elevated copper and oxidative stress in cancer cells as a target for cancer treatment. Cancer Treat Rev. 35:32-46.

Hainaut, P., and K. Mann. 2001. Zinc binding and redox control of p53 structure and function. Antioxid Redox Signal. 3:611-623.

Harada, M., J. Murata, Y. Sakamura, H. Sakakibara, S. Okuno, and T. Suzuki. 2001. Carrier and dose effects on the pharmacokinetics of T-0128, a camptothecin analogue-carboxymethyl dextran conjugate, in non-tumor- and tumor-bearing rats. J Control Release. 71:71-86.

Harada, S., E. Sugiyama, H. Taki, K. Shinoda, T. Fujita, M. Maruyama, and M. Kobayashi. 2002. D-penicillamine cooperates with copper sulfate to enhance the surface expression of functional Fas antigen in rheumatoid synovial fibroblasts via the generation of hydrogen peroxide. Clin Exp Rheumatol. 20:469-476.

Havre, P.A., S. O'Reilly, J.J. McCormick, and D.E. Brash. 2002. Transformed and tumor-derived human cells exhibit preferential sensitivity to the thiol antioxidants, N-acetyl cysteine and penicillamine. Cancer Res. 62:1443-1449.

Hayashi, R., X. Jin, and G.R. Cook. 2007. Synthesis and evaluation of novel heterocyclic MMP inhibitors. Bioorg Med Chem Lett. 17:6864-6870.

Held, K.D., and J.E. Biaglow. 1994. Mechanisms for the oxygen radical-mediated toxicity of various thiol-containing compounds in cultured mammalian cells. Radiat Res. 139:15-23.

Held, K.D., and D.C. Melder. 1987. Toxicity of the sulfhydryl-containing radioprotector dithiothreitol. Radiat Res. 112:544-554.

Held, K.D., F.C. Sylvester, K.L. Hopcia, and J.E. Biaglow. 1996. Role of Fenton chemistry in thiol-induced toxicity and apoptosis. Radiat Res. 145:542-553.

Held, K.D., S.W. Tuttle, and J.E. Biaglow. 1993. Role of the pentose cycle in oxygen radical-mediated toxicity of the thiol-containing radioprotector dithiothreitol in mammalian cells. Radiat Res. 134:383-389.

Helliwell, T.R., J.H. Yeung, and B.K. Park. 1985. Hepatic necrosis and glutathione depletion in captopril-treated mice. Br J Exp Pathol. 66:67-78.

Henry, N.L., R. Dunn, S. Merjaver, Q. Pan, K.J. Pienta, G. Brewer, and D.C. Smith. 2006. Phase II trial of copper depletion with tetrathiomolybdate as an antiangiogenesis strategy in patients with hormone-refractory prostate cancer. Oncology. 71:168-175.

Hoes, C.J.T., W. Potman, W.A.R. Van Heeswijk, J. Mud, B.G. De Grooth, J. Greve, and J. Feijen. 1985. Optimization of macromolecular prodrugs of the antitumor antibiotic adriamycin. J Control Release. 2:205-214.

Huang, J., F. Gao, X.X. Tang, J.H. Yu, D.X. Wang, S.Y. Liu, and Y.P. Li. 2010. Liver-targeting doxorubicin-conjugated polymeric prodrug with pH-triggered drug release profile. Polym Int. 59:1390-1396.

Hudecz, F., J.A. Clegg, J. Kajtar, M.J. Embleton, M. Szekerke, and R.W. Baldwin. 1992. Synthesis, conformation, biodistribution, and in vitro cytotoxicity of daunomycin-branched polypeptide conjugates. Bioconjug Chem. 3:49-57.

Hurst, D.R., M.A. Schwartz, Y. Jin, M.A. Ghaffari, P. Kozarekar, J. Cao, and Q.X. Sang. 2005. Inhibition of enzyme activity of and cell-mediated substrate cleavage by membrane type 1 matrix metalloproteinase by newly developed mercaptosulphide inhibitors. Biochem J. 392:527-536.

Ikebuchi, M., S. Shinohara, H. Kimura, K. Morimoto, A. Shima, and T. Aoyama. 1981. Effects of daily treatment with a radioprotector WR-2721 on Ehrlich's ascites tumors in mice: suppression of tumor cell growth and earlier death of tumor-bearing mice. J. Radiat. Res. 22:258-264.

Issels, R.D., J.E. Biaglow, L. Epstein, and L.E. Gerweck. 1984. Enhancement of cysteamine cytotoxicity by hyperthermia and its modification by catalase and superoxide dismutase in Chinese hamster ovary cells. Cancer Res. 44:3911-3915.

Issels, R.D., and A. Nagele. 1989. Promotion of cystine uptake, increase of glutathione biosynthesis, and modulation of glutathione status by S-2-(3-aminopropylamino)ethyl phosphorothioic acid (WR-2721) in Chinese hamster cells. Cancer Res. 49:2082-2086.

Iyer, A.K., K. Greish, T. Seki, S. Okazaki, J. Fang, K. Takeshita, and H. Maeda. 2007. Polymeric micelles of zinc protoporphyrin for tumor targeted delivery based on EPR effect and singlet oxygen generation. J Drug Target. 15:496-506.

Jain, R.K., and T. Stylianopoulos. 2010. Delivering nanomedicine to solid tumors. Nat Rev Clin Oncol. 7:653-664.

Jay, D., A. Cuella, and E. Jay. 1995. Superoxide dismutase activity of the captopril-iron complex. Mol Cell Biochem. 146:45-47.

Jeitner, T.M., E.J. Delikatny, W.A. Bartier, H.R. Capper, and N.H. Hunt. 1998. Inhibition of drug-naive and -resistant leukemia cell proliferation by low molecular weight thiols. Biochem Pharmacol. 55:793-802.

Jenderny, S., H. Lin, T. Garrett, K.D. Tew, and D.M. Townsend. 2010. Protective effects of a glutathione disulfide mimetic (NOV-002) against cisplatin induced kidney toxicity. Biomed Pharmacother. 64:73-76.

Jensen, K.D., P. Kopeckova, J.H. Bridge, and J. Kopecek. 2001. The cytoplasmic escape and nuclear accumulation of endocytosed and microinjected HPMA copolymers and a basic kinetic study in Hep G2 cells. AAPS PharmSci. 3:E32.

Johans, M., E. Milanesi, M. Franck, C. Johans, J. Liobikas, M. Panagiotaki, L. Greci, G. Principato, P.K. Kinnunen, P. Bernardi, P. Costantini, and O. Eriksson. 2005. Modification of permeability transition pore arginine(s) by phenylglyoxal derivatives in isolated mitochondria and mammalian cells. Structure-function relationship of arginine ligands. J Biol Chem. 280:12130-12136.

Joyce, D.A., R.O. Day, and B.R. Murphy. 1991. The pharmacokinetics of albumin conjugates of D-penicillamine in humans. Drug Metab Disp. 19:309-311.

Joyce, D.A., D.N. Wade, and B.R. Swanson. 1989. The pharmacokinetics of albumin conjugates of D-penicillamine in rats. Drug Metab Disp. 17:208-211.

Kehrer, J.P. 2000. The Haber-Weiss reaction and mechanisms of toxicity. Toxicology. 149:43-50.

Khan, M.K., F. Mamou, M.J. Schipper, K.S. May, A. Kwitny, A. Warnat, B. Bolton, B.M. Nair, M.S. Kariapper, M. Miller, G. Brewer, D. Normolle, S.D. Merajver, and T.N. Teknos. 2006. Combination tetrathiomolybdate and radiation therapy in a mouse model of head and neck squamous cell carcinoma. Arch Otolaryngol Head Neck Surg. 132:333-338.

Khandare, J., P. Kolhe, O. Pillai, S. Kannan, M. Lieh-Lai, and R.M. Kannan. 2005. Synthesis, cellular transport, and activity of polyamidoamine dendrimer-methylprednisolone conjugates. Bioconjug Chem. 16:330-337.

Khandare, J., and T. Minko. 2006. Polymer-drug conjugates: Progress in polymeric prodrugs. Prog Polym Sci. 31:359-397.

Kiew, L.V., S.K. Cheong, K. Sidik, and L.Y. Chung. 2010. Improved plasma stability and sustained release profile of gemcitabine via polypeptide conjugation. Int J Pharm. 391:212-220.

Kim, M.S., K. Dayananda, E.Y. Choi, H.J. Park, J.S. Kim, and D.S. Lee. 2009. Synthesis and characterization of poly(L-glutamic acid)-block-poly(L-phenylalanine). Polymer. 50:2252-2257.

Kishore, B.K., P. Lambricht, G. Laurent, P. Maldague, R. Wagner, and P.M. Tulkens. 1990. Mechanism of protection afforded by polyaspartic acid against gentamicin-induced phospholipidosis. II. Comparative in vitro and in vivo studies with poly-L-aspartic, poly-L-glutamic and poly-D-glutamic acids. J Pharmacol Exp Ther. 255:875-885.

Kovar, M., L. Kovar, V. Subr, T. Etrych, K. Ulbrich, T. Mrkvan, J. Loucka, and B. Rihova. 2004. HPMA copolymers containing doxorubicin bound by a proteolytically or hydrolytically cleavable bond: comparison of biological properties in vitro. J Control Release. 99:301-314.

Kovar, M., J. Strohalm, K. Ulbrich, and B. Rihova. 2002. In vitro and in vivo effect of HPMA copolymer-bound doxorubicin targeted to transferrin receptor of B-cell lymphoma 38C13. J Drug Target. 10:23-30.

Krakovicova, H., T. Etrych, and K. Ulbrich. 2009. HPMA-based polymer conjugates with drug combination. Eur J Pharm Sci. 37:405-412.

Krejtschi, C., and K. Hauser. 2011. Stability and folding dynamics of polyglutamic acid. Eur Biophys J. 40:673-685.

Lammers, T., R. Kuhnlein, M. Kissel, V. Subr, T. Etrych, R. Pola, M. Pechar, K. Ulbrich, G. Storm, P. Huber, and P. Peschke. 2005. Effect of physicochemical modification on the biodistribution and tumor accumulation of HPMA copolymers. J Control Release. 110:103-118.

Lammers, T., V. Subr, K. Ulbrich, P. Peschke, P.E. Huber, W.E. Hennink, and G. Storm. 2009. Simultaneous delivery of doxorubicin and gemcitabine to tumors in vivo using prototypic polymeric drug carriers. Biomaterials. 30:3466-3475.

Langer, C.J., K.J. O'Byrne, M.A. Socinski, S.M. Mikhailov, K. Lesniewski-Kmak, M. Smakal, T.E. Ciuleanu, S.V. Orlov, M. Dediu, D. Heigener, A.J. Eisenfeld, L. Sandalic, F.B. Oldham, J.W. Singer, and H.J. Ross. 2008. Phase III trial comparing paclitaxel poliglumex (CT-2103, PPX) in combination with carboplatin versus standard paclitaxel and carboplatin in the treatment of PS 2 patients with chemotherapy-naive advanced non-small cell lung cancer. J Thorac Oncol. 3:623-630.

Lavignac, N., J.L. Nicholls, P. Ferruti, and R. Duncan. 2009. Poly(amidoamine) conjugates containing doxorubicin bound via an acid-sensitive linker. Macromol Biosci. 9:480-487.

Le Noble, F.A., N.H. Schreurs, H.W. van Straaten, D.W. Slaaf, J.F. Smits, H. Rogg, and H.A. Struijker-Boudier. 1993. Evidence for a novel angiotensin II receptor involved in angiogenesis in chick embryo chorioallantoic membrane. Am J Physiol. 264:R460-465.

Lee, R.J., S. Wang, and P.S. Low. 1996. Measurement of endosome pH following folate receptor-mediated endocytosis. Biochim Biophys Acta. 1312:237-242.

Li, C., J.E. Price, L. Milas, N.R. Hunter, S. Ke, D.F. Yu, C. Charnsangavej, and S. Wallace. 1999. Antitumor activity of poly(L-glutamic acid)-paclitaxel on syngeneic and xenografted tumors. Clin Cancer Res. 5:891-897.

Li, C., D.F. Yu, R.A. Newman, F. Cabral, L.C. Stephens, N. Hunter, L. Milas, and S. Wallace. 1998. Complete regression of well-established tumors using a novel water-soluble poly(L-glutamic acid)-paclitaxel conjugate. Cancer Res. 58:2404-2409.

Lindgren, M., M. Hallbrink, A. Prochiantz, and U. Langel. 2000. Cell-penetrating peptides. Trends Pharmacol Sci. 21:99-103.

Line, B.R., A. Mitra, A. Nan, and H. Ghandehari. 2005. Targeting tumor angiogenesis: comparison of peptide and polymer-peptide conjugates. J Nucl Med. 46:1552-1560.

Liotta, L.A., K. Tryggvason, S. Garbisa, I. Hart, C.M. Foltz, and S. Shafie. 1980. Metastatic potential correlates with enzymatic degradation of basement membrane collagen. Nature. 284:67-68.

Lipsky, P.E. 1984. Immunosuppression by D-penicillamine in vitro. Inhibition of human T lymphocyte proliferation by copper- or ceruloplasmin-dependent generation of hydrogen peroxide and protection by monocytes. J Clin Invest. 73:53-65.

Lipsky, P.E., and M. Ziff. 1978. The effect of D-penicillamine on mitogen-induced human lymphocyte proliferation: synergistic inhibition by D-penicillamine and copper salts. J Immunol. 120:1006-1013.

Liu, B., Y. Chen, and D.K. St Clair. 2008. ROS and p53: a versatile partnership. Free Radic Biol Med. 44:1529-1535.

Liu, C., B.M. Tadayoni, L.A. Bourret, K.M. Mattocks, S.M. Derr, W.C. Widdison, N.L. Kedersha, P.D. Ariniello, V.S. Goldmacher, J.M. Lambert, W.A. Blattler, and R.V. Chari. 1996. Eradication of large colon tumor xenografts by targeted delivery of maytansinoids. Proc Natl Acad Sci U S A. 93:8618-8623.

Liu, G.Y., N. Frank, H. Bartsch, and J.K. Lin. 1998a. Induction of apoptosis by thiuramdisulfides, the reactive metabolites of dithiocarbamates, through coordinative modulation of NFkappaB, c-fos/c-jun, and p53 proteins. Mol Carcinog. 22:235-246.

Liu, M., J.C. Pelling, J. Ju, E. Chu, and D.E. Brash. 1998b. Antioxidant action via p53-mediated apoptosis. Cancer Res. 58:1723-1729.

Liu, W., M.R. Dreher, D.Y. Furgeson, K.V. Peixoto, H. Yuan, M.R. Zalutsky, and A. Chilkoti. 2006. Tumor accumulation, degradation and pharmacokinetics of elastin-like polypeptides in nude mice. J Control Release. 116:170-178.

Liu, Z., L. Li, Z. Yang, W. Luo, X. Li, H. Yang, K. Yao, B. Wu, and W. Fang. 2010. Increased expression of MMP9 is correlated with poor prognosis of nasopharyngeal carcinoma. BMC Cancer. 10:270.

Lodemann, E. 1981. Transport of D- and L-penicillamine by mammalian cells. Biochem Biophys Res Commun. 102:775-783.

Lopez-Lazaro, M. 2007. Dual role of hydrogen peroxide in cancer: possible relevance to cancer chemoprevention and therapy. Cancer Lett. 252:1-8.

Lu, X., Y. Ping, F.J. Xu, Z.H. Li, Q.Q. Wang, J.H. Chen, W.T. Yang, and G.P. Tang. 2010. Bifunctional conjugates comprising beta-cyclodextrin, polyethylenimine, and 5-fluoro-2'- deoxyuridine for drug delivery and gene transfer. Bioconjug Chem. 21:1855-1863.

Lu, Z.R., P. Kopeckova, and J. Kopecek. 1999. Polymerizable Fab' antibody fragments for targeting of anticancer drugs. Nat Biotechnol. 17:1101-1104.

Lumry, R., R. Legare, and W.G. Miller. 1964. The dynamics of the helix-coil transition in poly-α, L-glutamic acid. Biopolymers. 2:489-500.

Lusini, L., S.A. Tripodi, R. Rossi, F. Giannerini, D. Giustarini, M.T. del Vecchio, G. Barbanti, M. Cintorino, P. Tosi, and P. Di Simplicio. 2001. Altered glutathione anti-oxidant metabolism during tumor progression in human renal-cell carcinoma. Int J Cancer. 91:55-59.

Lynn, S., G.L. Yu, and K. Yan. 1999. Vicinal-thiol-containing molecules enhance but mono-thiol-containing molecules reduce nickel-induced DNA strand breaks. Toxicol Appl Pharmacol. 160:198-205.

MacKay, J.A., M. Chen, J.R. McDaniel, W. Liu, A.J. Simnick, and A. Chilkoti. 2009. Self-assembling chimeric polypeptide-doxorubicin conjugate nanoparticles that abolish tumours after a single injection. Nat Mater. 8:993-999.

Manocha, B., and A. Margaritis. 2010. A novel Method for the selective recovery and purification of gamma-polyglutamic acid from Bacillus licheniformis fermentation broth. Biotechnol Prog. 26:734-742.

Martin, K.R., and J.C. Barrett. 2002. Reactive oxygen species as double-edged swords in cellular processes: low-dose cell signaling versus high-dose toxicity. Hum Exp Toxicol. 21:71-75.

Matsubara, T., R. Saura, K. Hirohata, and M. Ziff. 1989. Inhibition of human endothelial cell proliferation in vitro and neovascularization in vivo by D-penicillamine. J Clin Invest. 83:158-167.

Matsumura, Y., and H. Maeda. 1986. A new concept for macromolecular therapeutics in cancer chemotherapy: mechanism of tumoritropic accumulation of proteins and the antitumor agent smancs. Cancer Res. 46:6387-6392.

Matsusaki, M., T. Serizawa, A. Kishida, T. Endo, and M. Akashi. 2002. Novel functional biodegradable polymer: synthesis and anticoagulant activity of poly(gamma-glutamic acid)sulfonate (gamma-PGA-sulfonate). Bioconjug Chem. 13:23-28.

McDaniel, J.R., D.J. Callahan, and A. Chilkoti. 2010. Drug delivery to solid tumors by elastin-like polypeptides. Adv Drug Deliv Rev. 62:1456-1467.

Mehvar, R., M.A. Robinson, and J.M. Reynolds. 1995. Dose dependency of the kinetics of dextrans in rats: effects of molecular weight. J Pharm Sci. 84:815-818.

Melancon, M.P., W. Wang, Y. Wang, R. Shao, X. Ji, J.G. Gelovani, and C. Li. 2007. A novel method for imaging in vivo degradation of poly(L-glutamic acid), a biodegradable drug carrier. Pharm Res. 24:1217-1224.

Mellman, I., R. Fuchs, and A. Helenius. 1986. Acidification of the endocytic and exocytic pathways. Annu Rev Biochem. 55:663-700.

Milas, L., N. Hunter, H. Ito, and L.J. Peters. 1984. Effect of tumor type, size, and endpoint on tumor radioprotection by WR-2721. Int. J. Radiat. Oncol., Biol., Phys. 10:41-48.

Milas, L., N. Hunter, H. Ito, E.L. Travis, and L.J. Peters. 1983. Factors influencing radioprotection of tumors by WR-2721. Proceedings of First Conference on Radioprotectors and Anticarcinogens. Academic Press, New York. 695-718.

Miller, K., R. Erez, E. Segal, D. Shabat, and R. Satchi-Fainaro. 2009. Targeting bone metastases with a bispecific anticancer and antiangiogenic polymer-alendronate-taxane conjugate. Angew Chem Int Ed Engl. 48:2949-2954.

Minko, T., P. Kopeckova, and J. Kopecek. 1999. Chronic exposure to HPMA copolymer-bound adriamycin does not induce multidrug resistance in a human ovarian carcinoma cell line. J Control Release. 59:133-148.

Minko, T., P. Kopeckova, V. Pozharov, and J. Kopecek. 1998. HPMA copolymer bound adriamycin overcomes MDR1 gene encoded resistance in a human ovarian carcinoma cell line. J Control Release. 54:223-233.

Mitra, A., T. Coleman, M. Borgman, A. Nan, H. Ghandehari, and B.R. Line. 2006. Polymeric conjugates of mono- and bi-cyclic alphaVbeta3 binding peptides for tumor targeting. J Control Release. 114:175-183.

Miyajima, A., T. Asano, and M. Hayakawa. 2001. Captopril restores transforming growth factor-beta type II receptor and sensitivity to transforming growth factor-beta in murine renal cell cancer cells. J Urol. 165:616-620.

Molteni, A., W.F. Ward, C.H. Ts'ao, J. Taylor, W. Small, Jr., L. Brizio-Molteni, and P.A. Veno. 2003. Cytostatic properties of some angiotensin I converting enzyme inhibitors and of angiotensin II type I receptor antagonists. Curr Pharm Des. 9:751-761.

Morcellet, M., and C. Loucheux. 1976. Viscosity/molecular-weight relationship of poly(alpha-L-glutamic acid) in water and in water/dioxane mixtures. Biopolymers. 15:1857-1862.

Morimoto, Y., K. Sugibayashi, S. Sugihara, K. Hosoya, S. Nozaki, and Y. Ogawa. 1984. Antitumor agent poly (amino acid) conjugates as a drug carrier in cancer chemotherapy. J Pharmacobiodyn. 7:688-698.

Morse, N.R., P.W. Tebbey, P.A. Sandstrom, and T.M. Buttke. 1995. Induction of Apoptosis in Lymphoid-Cells by Thiol-Mediated Oxidative Stress. Protoplasma. 184:181-187.

Moschou, M., E.K. Kosmidis, M. Kaloyianni, A. Geronikaki, N. Dabarakis, and G. Theophilidis. 2008. In vitro assessment of the neurotoxic and neuroprotective effects of N-acetyl-L-cysteine (NAC) on the rat sciatic nerve fibers. Toxicol In Vitro. 22:267-274.

Munday, R. 1989. Toxicity of thiols and disulphides: involvement of free-radical species. Free Radic Biol Med. 7:659-673.

Munday, R. 1994. Bioactivation of thiols by one-electron oxidation. Adv Pharmacol. 27:237-270.

Murphy, M.P. 2009. How mitochondria produce reactive oxygen species. Biochem J. 417:1-13.

Nagasawa, M., and A. Holtzer. 1964. Helix-coil transition in solutions of polyglutamic acid. J Am Chem Soc. 86:538-&.

Nakagawa, T., T. Kubota, M. Kabuto, and T. Kodera. 1995. Captopril inhibits glioma cell invasion in vitro: involvement of matrix metalloproteinases. Anticancer Res. 15:1985-1989.

Navarro, J., E. Obrador, J. Carretero, I. Petschen, J. Avino, P. Perez, and J.M. Estrela. 1999. Changes in glutathione status and the antioxidant system in blood and in cancer cells associate with tumour growth in vivo. Free Radic Biol Med. 26:410-418.

Nayak, B.S., and S. Pinto. 2007. Protein thiols and thiobarbituric acid reactive substance status in colon cancer patients. Scand J Gastroenterol. 42:848-851.

Netter, P., B. Bannwarth, P. Pere, and A. Nicolas. 1987. Clinical pharmacokinetics of D-penicillamine. Clin Pharmacokinet. 13:317-333.

Nicco, C., A. Laurent, C. Chereau, B. Weill, and F. Batteux. 2005. Differential modulation of normal and tumor cell proliferation by reactive oxygen species. Biomed Pharmacother. 59:169-174.

Nimni, M.E. 1968. A defect in the intramolecular and intermolecular cross-linking of collagen caused by penicillamine. I. Metabolic and functional abnormalities in soft tissues. J Biol Chem. 243:1457-1466.

Nimni, M.E., K. Deshmukh, and N. Gerth. 1972. Collagen defect induced by penicillamine. Nat New Biol. 240:220-221.

Nittler, T., M. Stone, D. Shroff, C. McArthur, P. Veno, L. Dobbs, L. Brizio-Molteni, and A. Molteni. 1998. Inhibitory effect of captopril on proliferation of a human salivary gland adenocarcinoma cell line. Faseb Journal. 12:4702.

Noe, V., B. Fingleton, K. Jacobs, H.C. Crawford, S. Vermeulen, W. Steelant, E. Bruyneel, L.M. Matrisian, and M. Mareel. 2001. Release of an invasion promoter E-cadherin fragment by matrilysin and stromelysin-1. J Cell Sci. 114:111-118.

Nogusa, H., K. Yamamoto, T. Yano, M. Kajiki, H. Hamana, and S. Okuno. 2000a. Distribution characteristics of carboxymethylpullulan-peptide-doxorubicin conjugates in tumor-bearing rats: different sequence of peptide spacers and doxorubicin contents. Biol Pharm Bull. 23:621-626.

Nogusa, H., T. Yano, M. Kajiki, A. Gonsho, H. Hamana, and S. Okuno. 1997. Antitumor effects and toxicities of carboxymethylpullulan-peptide-doxorubicin conjugates. Biol Pharm Bull. 20:1061-1065.

Nogusa, H., T. Yano, N. Kashima, K. Yamamoto, S. Okuno, and H. Hamana. 2000b. Structure-activity relationships of carboxymethylpullulan-peptide-doxorubicin conjugates--systematic modification of peptide spacers. Bioorg Med Chem Lett. 10:227-230.

Nogusa, H., T. Yano, S. Okuno, H. Hamana, and K. Inoue. 1995. Synthesis of carboxymethylpullulan-peptide-doxorubicin conjugates and their properties. Chem Pharm Bull (Tokyo). 43:1931-1936.

Noiva, R. 1999. Protein disulfide isomerase: the multifunctional redox chaperone of the endoplasmic reticulum. Semin Cell Dev Biol. 10:481-493.

Nori, A., K.D. Jensen, M. Tijerina, P. Kopeckova, and J. Kopecek. 2003. Tat-conjugated synthetic macromolecules facilitate cytoplasmic drug delivery to human ovarian carcinoma cells. Bioconjug Chem. 14:44-50.

North, S., F. El-Ghissassi, O. Pluquet, G. Verhaegh, and P. Hainaut. 2000. The cytoprotective aminothiol WR1065 activates p21waf-1 and down regulates cell cycle progression through a p53-dependent pathway. Oncogene. 19:1206-1214.

O'Reilly, M.S., L. Holmgren, Y. Shing, C. Chen, R.A. Rosenthal, M. Moses, W.S. Lane, Y. Cao, E.H. Sage, and J. Folkman. 1994. Angiostatin: a novel angiogenesis inhibitor that mediates the suppression of metastases by a Lewis lung carcinoma. Cell. 79:315-328.

Ofek, P., K. Miller, A. Eldar-Boock, D. Polyak, E. Segal, and R. Satchi-Fainaro. 2010. Rational Design of Multifunctional Polymer Therapeutics for Cancer Theranostics. Israel Journal of Chemistry. 50:185-203.

Omelyanenko, V., P. Kopeckova, C. Gentry, and J. Kopecek. 1998. Targetable HPMA copolymer-adriamycin conjugates. Recognition, internalization, and subcellular fate. J Control Release. 53:25-37.

Ouchi, T., T. Banba, T. Matsumoto, S. Suzuki, and M. Suzuki. 1990. Synthesis and antitumor activity of conjugates of 5-fluorouracil and chito-oligosaccharides involving a hexamethylene spacer group and carbamoyl bonds. Drug Des Deliv. 6:281-287.

Ozkan, Y., S. Yardim-Akaydin, H. Firat, E. Caliskan-Can, S. Ardic, and B. Simsek. 2007. Usefulness of homocysteine as a cancer marker: total thiol compounds and folate levels in untreated lung cancer patients. Anticancer Res. 27:1185-1189.

Pan, Q., C.G. Kleer, K.L. van Golen, J. Irani, K.M. Bottema, C. Bias, M. De Carvalho, E.A. Mesri, D.M. Robins, R.D. Dick, G.J. Brewer, and S.D. Merajver. 2002. Copper deficiency induced by tetrathiomolybdate suppresses tumor growth and angiogenesis. Cancer Res. 62:4854-4859.

Pan, Q., D.T. Rosenthal, L. Bao, C.G. Kleer, and S.D. Merajver. 2009. Antiangiogenic tetrathiomolybdate protects against Her2/neu-induced breast carcinoma by hypoplastic remodeling of the mammary gland. Clin Cancer Res. 15:7441-7446.

Park, H.I., Y. Jin, D.R. Hurst, C.A. Monroe, S. Lee, M.A. Schwartz, and Q.X. Sang. 2003. The intermediate S1' pocket of the endometase/matrilysin-2 active site revealed by enzyme inhibition kinetic studies, protein sequence analyses, and homology modeling. J Biol Chem. 278:51646-51653.

Park, J.W., and R.A. Floyd. 1994. Generation of strand breaks and formation of 8-hydroxy-2'-deoxyguanosine in DNA by a Thiol/Fe3+/O2-catalyzed oxidation system. Arch Biochem Biophys. 312:285-291.

Pass, H.I., G.J. Brewer, R. Dick, M. Carbone, and S. Merajver. 2008. A phase II trial of tetrathiomolybdate after surgery for malignant mesothelioma: final results. Ann Thorac Surg. 86:383-389.

Passlick, B., W. Sienel, R. Seen-Hibler, W. Wockel, O. Thetter, W. Mutschler, and K. Pantel. 2000. Overexpression of matrix metalloproteinase 2 predicts unfavorable outcome in early-stage non-small cell lung cancer. Clin Cancer Res. 6:3944-3948.

Pataer, A., M.A. Fanale, J.A. Roth, S.G. Swisher, and K.K. Hunt. 2006. Induction of apoptosis in human lung cancer cells following treatment with amifostine and an adenoviral vector containing wild-type p53. Cancer Gene Ther. 13:806-814.

Pavlaki, M., and S. Zucker. 2003. Matrix metalloproteinase inhibitors (MMPIs): the beginning of phase I or the termination of phase III clinical trials. Cancer Metastasis Rev. 22:177-203.

Pazoles, C.J., and H. Gernstein. 2006. NOV-002, a chemoprotectant/immunomodulator, added to first-ine carboplatin/paclitaxel in advanced non-small cell lung cancer

(NSCLC): A randomized phase 1/2, open-label, controlled study In 2006 ASCO Annual Meeting Proceedings Part I. Vol. 24. 17021.

Pelicano, H., D. Carney, and P. Huang. 2004. ROS stress in cancer cells and therapeutic implications. Drug Resist Updat. 7:97-110.

Planas-Bohne, F. 1981. Metabolism and pharmacokinetics of penicillamine in rats -- an overview. J Rheumatol Suppl. 7:35-40.

Polyak, K., Y. Xia, J.L. Zweier, K.W. Kinzler, and B. Vogelstein. 1997. A model for p53-induced apoptosis. Nature. 389:300-305.

Prontera, C., B. Mariani, C. Rossi, A. Poggi, and D. Rotilio. 1999. Inhibition of gelatinase A (MMP-2) by batimastat and captopril reduces tumor growth and lung metastases in mice bearing Lewis lung carcinoma. Int J Cancer. 81:761-766.

Rademaker-Lakhai, J.M., C. Terret, S.B. Howell, C.M. Baud, R.F. De Boer, D. Pluim, J.H. Beijnen, J.H. Schellens, and J.P. Droz. 2004. A Phase I and pharmacological study of the platinum polymer AP5280 given as an intravenous infusion once every 3 weeks in patients with solid tumors. Clin Cancer Res. 10:3386-3395.

Rao, A.V., N. Fleshner, and S. Agarwal. 1999. Serum and tissue lycopene and biomarkers of oxidation in prostate cancer patients: a case-control study. Nutr Cancer. 33:159-164.

Redman, B.G., P. Esper, Q. Pan, R.L. Dunn, H.K. Hussain, T. Chenevert, G.J. Brewer, and S.D. Merajver. 2003. Phase II trial of tetrathiomolybdate in patients with advanced kidney cancer. Clin Cancer Res. 9:1666-1672.

Ribizzi, I., J.W. Darnowski, F.A. Goulette, M.R. Sertoli, and P. Calabresi. 2000. Amifostine cytotoxicity and induction of apoptosis in a human myelodysplastic cell line. Leuk Res. 24:519-525.

Rinaudo, M., and A. Domard. 1976. Circular dichroism studies on alpha-L-glutamic acid oligomers in solution. J Am Chem Soc. 98:6360-6364.

Ringsdorf, H. 1975. Structure and properties of pharmacologically active polymers. J Polym Sci Symp. 51:135-153.

Rizk, S.L., and H.H. Sky-Peck. 1984. Comparison between concentrations of trace elements in normal and neoplastic human breast tissue. Cancer Res. 44:5390-5394.

Roberts, N.A., and P.A. Robinson. 1985. Copper chelates of antirheumatic and anti-inflammatory agents: their superoxide dismutase-like activity and stability. Br J Rheumatol. 24:128-136.

Rogers, K.E., B.I. Carr, and Z.A. Tokes. 1983. Cell surface-mediated cytotoxicity of polymer-bound Adriamycin against drug-resistant hepatocytes. Cancer Res. 43:2741-2748.

Ross, S., S.D. Spencer, I. Holcomb, C. Tan, J. Hongo, B. Devaux, L. Rangell, G.A. Keller, P. Schow, R.M. Steeves, R.J. Lutz, G. Frantz, K. Hillan, F. Peale, P. Tobin, D. Eberhard, M.A. Rubin, L.A. Lasky, and H. Koeppen. 2002. Prostate stem cell antigen as therapy target: tissue expression and in vivo efficacy of an immunoconjugate. Cancer Res. 62:2546-2553.

Rowland, G.F., G.J. O'Neill, and D.A. Davies. 1975. Suppression of tumour growth in mice by a drug-antibody conjugate using a novel approach to linkage. Nature. 255:487-488.

Rowley, D.A., and B. Halliwell. 1982. Superoxide-dependent formation of hydroxyl radicals in the presence of thiol compounds. FEBS Lett. 138:33-36.

Rundhaug, J.E. 2003. Matrix metalloproteinases, angiogenesis, and cancer: commentary re: A. C. Lockhart et al., Reduction of wound angiogenesis in patients treated with BMS-275291, a broad spectrum matrix metalloproteinase inhibitor. Clin Cancer Res. 9:551-554.

Sabbatini, P., C. Aghajanian, D. Dizon, S. Anderson, J. Dupont, J.V. Brown, W.A. Peters, A. Jacobs, A. Mehdi, S. Rivkin, A.J. Eisenfeld, and D. Spriggs. 2004. Phase II study of CT-2103 in patients with recurrent epithelial ovarian, fallopian tube, or primary peritoneal carcinoma. J Clin Oncol. 22:4523-4531.

Sablina, A.A., A.V. Budanov, G.V. Ilyinskaya, L.S. Agapova, J.E. Kravchenko, and P.M. Chumakov. 2005. The antioxidant function of the p53 tumor suppressor. Nat Med. 11:1306-1313.

Sakamoto, H., T. Mashima, K. Yamamoto, and T. Tsuruo. 2002. Modulation of heat-shock protein 27 (Hsp27) anti-apoptotic activity by methylglyoxal modification. J Biol Chem. 277:45770-45775.

Samoszuk, M., and V. Nguyen. 1996. In vitro and in vivo interactions of D-penicillamine with tumors. Anticancer Res. 16:1219-1223.

Satchi-Fainaro, R., H. Hailu, J.W. Davies, C. Summerford, and R. Duncan. 2003. PDEPT: polymer-directed enzyme prodrug therapy. 2. HPMA copolymer-beta-lactamase and HPMA copolymer-C-Dox as a model combination. Bioconjug Chem. 14:797-804.

Satchi-Fainaro, R., M. Puder, J.W. Davies, H.T. Tran, D.A. Sampson, A.K. Greene, G. Corfas, and J. Folkman. 2004. Targeting angiogenesis with a conjugate of HPMA copolymer and TNP-470. Nat Med. 10:255-261.

Satchi, R., T.A. Connors, and R. Duncan. 2001. PDEPT: polymer-directed enzyme prodrug therapy. I. HPMA copolymer-cathepsin B and PK1 as a model combination. Br J Cancer. 85:1070-1076.

Sawada, S., and S. Okada. 1970. Cysteamine, cystamine, and single-strand breaks of DNA in cultured mammalian cells. Radiat Res. 44:116-132.

Schiller, J.H., B. Storer, J. Berlin, J. Wittenkeller, M. Larson, L. Pharo, and W. Berry. 1996. Amifostine, cisplatin, and vinblastine in metastatic non-small-cell lung cancer: a report of high response rates and prolonged survival. J Clin Oncol. 14:1913-1921.

Schneerson, R., J. Kubler-Kielb, T.Y. Liu, Z.D. Dai, S.H. Leppla, A. Yergey, P. Backlund, J. Shiloach, F. Majadly, and J.B. Robbins. 2003. Poly(gamma-D-glutamic acid) protein conjugates induce IgG antibodies in mice to the capsule of Bacillus anthracis: a potential addition to the anthrax vaccine. Proc Natl Acad Sci U S A. 100:8945-8950.

Schoneich, C., U. Dillinger, F. von Bruchhausen, and K.D. Asmus. 1992. Oxidation of polyunsaturated fatty acids and lipids through thiyl and sulfonyl radicals: reaction kinetics, and influence of oxygen and structure of thiyl radicals. Arch Biochem Biophys. 292:456-467.

Schor, N.F.T. 1987. Adjunctive use of ethiofos (WR-2721) with free radical-generating chemotherapeutic agents in mice: new caveats for therapy. Cancer Res. 47:5411-5414.

Schumacher, K., G. Maerker-Alzer, and R. Preuss. 1975. Effect of D-penicillamine on lymphocyte function. Arzneimittelforschung. 25:603-606.

Schwarze, S.R., A. Ho, A. Vocero-Akbani, and S.F. Dowdy. 1999. In vivo protein transduction: delivery of a biologically active protein into the mouse. Science. 285:1569-1572.

Schwarze, S.R., K.A. Hruska, and S.F. Dowdy. 2000. Protein transduction: unrestricted delivery into all cells? Trends Cell Biol. 10:290-295.

Scomparin, A., S. Salmaso, S. Bersani, R. Saatchi-Fainaro, and P. Calceti. 2011. Novel folated and non-folated pullulan bioconjugates for anticancer drug delivery. Eur J Pharm Sci.

Searcy, D.G. 1996. HS-:O2 oxidoreductase activity of Cu,Zn superoxide dismutase. Arch Biochem Biophys. 334:50-58.

Searle, A.J., and R.L. Willson. 1983. Stimulation of microsomal lipid peroxidation by iron and cysteine. Characterization and the role of free radicals. Biochem J. 212:549-554.

Segal, E., H. Pan, P. Ofek, T. Udagawa, P. Kopeckova, J. Kopecek, and R. Satchi-Fainaro. 2009. Targeting angiogenesis-dependent calcified neoplasms using combined polymer therapeutics. PLoS One. 4:e5233.

Seymour, L.W., R. Duncan, J. Strohalm, and J. Kopecek. 1987. Effect of molecular weight (Mw) of N-(2-hydroxypropyl)methacrylamide copolymers on body distribution and rate of excretion after subcutaneous, intraperitoneal, and intravenous administration to rats. J Biomed Mater Res. 21:1341-1358.

Seymour, L.W., D.R. Ferry, D. Anderson, S. Hesslewood, P.J. Julyan, R. Poyner, J. Doran, A.M. Young, S. Burtles, and D.J. Kerr. 2002. Hepatic drug targeting: phase I evaluation of polymer-bound doxorubicin. J Clin Oncol. 20:1668-1676.

Seymour, L.W., D.R. Ferry, D.J. Kerr, D. Rea, M. Whitlock, R. Poyner, C. Boivin, S. Hesslewood, C. Twelves, R. Blackie, A. Schatzlein, D. Jodrell, D. Bissett, H. Calvert, M. Lind, A. Robbins, S. Burtles, R. Duncan, and J. Cassidy. 2009. Phase II studies of polymer-doxorubicin (PK1, FCE28068) in the treatment of breast, lung and colorectal cancer. Int J Oncol. 34:1629-1636.

Shaffer, S.A., C. Baker-Lee, J. Kennedy, M.S. Lai, P. de Vries, K. Buhler, and J.W. Singer. 2007. In vitro and in vivo metabolism of paclitaxel poliglumex: identification of metabolites and active proteases. Cancer chemotherapy and pharmacology. 59:537-548.

Sharma, K., D.K. Mittal, R.C. Kesarwani, V.P. Kamboj, and Chowdhery. 1994. Diagnostic and prognostic significance of serum and tissue trace elements in breast malignancy. Indian J Med Sci. 48:227-232.

Shaw, I.C., and M.S. Weeks. 1986. Interaction between mesna and selected transition metals in vitro and in vivo. Arzneim.-Forsch. 36:997-1000.

Shen, W.C., and H.J. Ryser. 1979. Poly (L-lysine) and poly (D-lysine) conjugates of methotrexate: different inhibitory effect on drug resistant cells. Mol Pharmacol. 16:614-622.

Shen, W.C., and H.J. Ryser. 1981. cis-Aconityl spacer between daunomycin and macromolecular carriers: a model of pH-sensitive linkage releasing drug from a lysosomotropic conjugate. Biochem Biophys Res Commun. 102:1048-1054.

Shen, W.C., H.J. Ryser, and L. LaManna. 1985. Disulfide spacer between methotrexate and poly(D-lysine). A probe for exploring the reductive process in endocytosis. J Biol Chem. 260:10905-10908.

Shiah, J.G., Y. Sun, C.M. Peterson, R.C. Straight, and J. Kopecek. 2000. Antitumor activity of N-(2-hydroxypropyl) methacrylamide copolymer-Mesochlorine e6 and adriamycin conjugates in combination treatments. Clin Cancer Res. 6:1008-1015.

Shih, I.L., Y.T. Van, and Y.Y. Sau. 2003. Antifreeze activities of poly(gamma-glutamic acid) produced by Bacillus licheniformis. Biotechnol Lett. 25:1709-1712.

Siegel, R.C. 1977. Collagen cross-linking. Effect of D-penicillamine on cross-linking in vitro. J Biol Chem. 252:254-259.

Singer, J.W., R. Bhatt, J. Tulinsky, K.R. Buhler, E. Heasley, P. Klein, and P. de Vries. 2001. Water-soluble poly-(L-glutamic acid)-Gly-camptothecin conjugates enhance camptothecin stability and efficacy in vivo. J Control Release. 74:243-247.

Singer, J.W., P. De Vries, R. Bhatt, J. Tulinsky, P. Klein, C. Li, L. Milas, R.A. Lewis, and S. Wallace. 2000. Conjugation of camptothecins to poly-(L-glutamic acid). Ann N Y Acad Sci. 922:136-150.

Small, W., Jr., A. Molteni, Y.T. Kim, J.M. Taylor, C.H. Ts'ao, and W.F. Ward. 1999. Mechanism of captopril toxicity to a human mammary ductal carcinoma cell line in the presence of copper. Breast Cancer Res Treat. 55:223-229.

Soepenberg, O., M.J. de Jonge, A. Sparreboom, P. de Bruin, F.A. Eskens, G. de Heus, J. Wanders, P. Cheverton, M.P. Ducharme, and J. Verweij. 2005. Phase I and pharmacokinetic study of DE-310 in patients with advanced solid tumors. Clin Cancer Res. 11:703-711.

Soff, G.A., H. Wang, D.L. Cundiff, K. Jiang, B. Martone, A.W. Rademaker, J.A. Doll, and T.M. Kuzel. 2005. In vivo Generation of Angiostatin Isoforms by Administration of a Plasminogen Activator and a Free Sulfhydryl Donor: A Phase I Study of an Angiostatic Cocktail of Tissue Plasminogen Activator and Mesna. Clin. Cancer Res. 11:6218-6225.

Solovieva, M.E., V.V. Solovyev, A.A. Kudryavtsev, Y.A. Trizna, and V.S. Akatov. 2008. Vitamin B12b enhances the cytotoxicity of dithiothreitol. Free Radic Biol Med. 44:1846-1856.

Soo, P.L., M. Dunne, J. Liu, and C. Allen. 2009. Nano-sized Advanced Delivery Systems as Parenteral Formulation Strategies for Hydrophobic Anti-cancer Drugs. In Nanotechnology in Drug Delivery. Vol. X. M.M. Villiers, P. Aramwit, and G.S. Kwon, editors. Springer New York. 349-383.

Sorbi, D., M. Fadly, R. Hicks, S. Alexander, and L. Arbeit. 1993. Captopril inhibits the 72 kDa and 92 kDa matrix metalloproteinases. Kidney Int. 44:1266-1272.

Sprong, R.C., A.M. Winkelhuyzen-Janssen, C.J. Aarsman, J.F. van Oirschot, T. van der Bruggen, and B.S. van Asbeck. 1998. Low-dose N-acetylcysteine protects rats against endotoxin-mediated oxidative stress, but high-dose increases mortality. Am J Respir Crit Care Med. 157:1283-1293.

Staite, N.D., R.P. Messner, and D.C. Zoschke. 1985. In vitro production and scavenging of hydrogen peroxide by D-penicillamine. Relationship to copper availability. Arthritis Rheum. 28:914-921.

Starkebaum, G., and R.K. Root. 1985. D-Penicillamine: analysis of the mechanism of copper-catalyzed hydrogen peroxide generation. J Immunol. 134:3371-3378.

Stridh, H., M. Kimland, D.P. Jones, S. Orrenius, and M.B. Hampton. 1998. Cytochrome c release and caspase activation in hydrogen peroxide- and tributyltin-induced apoptosis. FEBS Lett. 429:351-355.

Swisher, S.G., A. Pataer, R. Yu, M. Nishizaki, B. Fang, K.K. Hunt, and J.A. Roth. 2000. Enhancement of adenoviral-mediated p53 tumor killing with amifostine-induced CDC2 kinase activation. Surg. Forum. 51:312-313.

Tabata, Y., T. Kawai, Y. Murakami, and Y. Ikada. 1997. Electric charge influence of dextran derivatives on their tumor accumulation after intravenous injection. Drug Delivery. 4:213-221.

Takagi, Y., M. Shikita, T. Terasima, and S. Akaboshi. 1974. Specificity of radioprotective and cytotoxic effects of cysteamine in HeLa S3 cells: generation of peroxide as the mechanism of paradoxical toxicity. Radiat Res. 60:292-301.

Takakura, Y., S. Matsumoto, M. Hashida, and H. Sezaki. 1989. Physicochemical properties and antitumor activities of polymeric prodrugs of mitomycin-C with different regeneration rates. Journal of Controlled Release. 10:97-105.

Tansey, W., S. Ke, X.Y. Cao, M.J. Pasuelo, S. Wallace, and C. Li. 2004. Synthesis and characterization of branched poly(L-glutamic acid) as a biodegradable drug carrier. J Control Release. 94:39-51.

Tartier, L., Y.L. McCarey, J.E. Biaglow, I.E. Kochevar, and K.D. Held. 2000. Apoptosis induced by dithiothreitol in HL-60 cells shows early activation of caspase 3 and is independent of mitochondria. Cell Death Differ. 7:1002-1010.

Tien, M., J.R. Bucher, and S.D. Aust. 1982. Thiol-dependent lipid peroxidation. Biochem Biophys Res Commun. 107:279-285.

Tokes, Z.A., K.E. Rogers, and A. Rembaum. 1982. Synthesis of adriamycin-coupled polyglutaraldehyde microspheres and evaluation of their cytostatic activity. Proc Natl Acad Sci U S A. 79:2026-2030.

Townsend, D.M., L. He, S. Hutchens, T.E. Garrett, C.J. Pazoles, and K.D. Tew. 2008a. NOV-002, a glutathione disulfide mimetic, as a modulator of cellular redox balance. Cancer Res. 68:2870-2877.

Townsend, D.M., C.J. Pazoles, and K.D. Tew. 2008b. NOV-002, a mimetic of glutathione disulfide. Expert Opin Invest Drugs. 17:1075-1083.

Townsend, D.M., and K.D. Tew. 2009. Pharmacology of a mimetic of glutathione disulfide, NOV-002. Biomed Pharmacother. 63:75-78.

Trapp, V., K. Lee, F. Doñate, A.P. Mazar, and J.P. Fruehauf. 2009. Redox-related antimelanoma activity of ATN-224. Melanoma Res. 19:350-360.

Treskes, M., L. Nijtmans, A.M.J. Fichtinger-Schepman, and d.V.W.J.F. Van. 1992. Cytostatic activity of cisplatin in the presence of WR2721 and its thiol metabolite WR1065 in OVCAR-3 human ovarian cancer cells as compared to V79 fibroblasts. Anticancer Res. 12:2261-2265.

Trissel, L.A. 1997. Pharmaceutical properties of paclitaxel and their effects on preparation and administration. Pharmacotherapy. 17:133S-139S.

Tsai, J.C., M. Jain, C.M. Hsieh, W.S. Lee, M. Yoshizumi, C. Patterson, M.A. Perrella, C. Cooke, H. Wang, E. Haber, R. Schlegel, and M.E. Lee. 1996. Induction of apoptosis by pyrrolidinedithiocarbamate and N-acetylcysteine in vascular smooth muscle cells. J Biol Chem. 271:3667-3670.

Tu, G., W. Xu, H. Huang, and S. Li. 2008. Progress in the development of matrix metalloproteinase inhibitors. Curr Med Chem. 15:1388-1395.

Turk, V., B. Turk, and D. Turk. 2001. Lysosomal cysteine proteases: facts and opportunities. Embo J. 20:4629-4633.

Ulbrich, K., T. Etrych, P. Chytil, M. Jelinkova, and B. Rihova. 2003. HPMA copolymers with pH-controlled release of doxorubicin: in vitro cytotoxicity and in vivo antitumor activity. J Control Release. 87:33-47.

Ulbrich, K., V. Subr, J. Strohalm, D. Plocova, M. Jelinkova, and B. Rihova. 2000. Polymeric drugs based on conjugates of synthetic and natural macromolecules. I. Synthesis and physico-chemical characterisation. J Control Release. 64:63-79.

Urry, D.W., T.M. Parker, M.C. Reid, and D.C. Gowda. 1991. Biocompatibility of the Bioelastic Materials, Poly(Gvgvp) and Its Gamma-Irradiation Cross-Linked Matrix - Summary of Generic Biological Test-Results. J Bioact Compat Polym. 6:263-282.

van Doorn, R., C.M. Leijdekkers, and P.T. Henderson. 1978. Synergistic effects of phorone on the hepatotoxicity of bromobenzene and paracetamol in mice. Toxicology. 11:225-233.

Vasey, P.A., S.B. Kaye, R. Morrison, C. Twelves, P. Wilson, R. Duncan, A.H. Thomson, L.S. Murray, T.E. Hilditch, T. Murray, S. Burtles, D. Fraier, E. Frigerio, and J. Cassidy. 1999. Phase I clinical and pharmacokinetic study of PK1 [N-(2-hydroxypropyl)methacrylamide copolymer doxorubicin]: first member of a new class of chemotherapeutic agents-drug-polymer conjugates. Cancer Research Campaign Phase I/II Committee. Clin Cancer Res. 5:83-94.

Vega, J., S. Ke, Z. Fan, S. Wallace, C. Charsangavej, and C. Li. 2003. Targeting doxorubicin to epidermal growth factor receptors by site-specific conjugation of C225 to poly(L-glutamic acid) through a polyethylene glycol spacer. Pharm Res. 20:826-832.

Verschraagen, M., E. Boven, I. Zegers, F.H. Hausheer, and d.V.W.J.F. Van. 2003. Pharmacokinetics of BNP7787 and its metabolite mesna in plasma and ascites: a case report. Cancer Chemother Pharmacol. 51:525-529.

Vicent, M.J., F. Greco, R.I. Nicholson, A. Paul, P.C. Griffiths, and R. Duncan. 2005. Polymer therapeutics designed for a combination therapy of hormone-dependent cancer. Angew Chem Int Ed Engl. 44:4061-4066.

Vogt, B., and F.J. Frey. 1997. Inhibition of angiogenesis in Kaposi's sarcoma by captopril. Lancet. 349:1148.

Volpert, O.V., W.F. Ward, M.W. Lingen, L. Chesler, D.B. Solt, M.D. Johnson, A. Molteni, P.J. Polverini, and N.P. Bouck. 1996. Captopril inhibits angiogenesis and slows the growth of experimental tumors in rats. J Clin Invest. 98:671-679.

Vos, O., L. Budke, and A.J. Vergroesen. 1962. Protection of tissueculture cells against ionizing radiation. I. The effect of biological amines, disulphide compounds and thiols. Int J Radiat Biol. 5:543-557.

Wallace, S.S. 1987. The biological consequences of oxidized DNA bases. Br J Cancer Suppl. 8:118-128.

Walters, R.S., F.A. Holmes, V. Valero, L. Esparza-Guerra, and G.N. Hortobagyi. 1998. Phase II study of ifosfamide and mesna in patients with metastatic breast cancer. Am J Clin Oncol. 21:413-415.

Ward, W.F., A. Molteni, C. Ts'ao, and J.M. Hinz. 1990. The effect of Captopril on benign and malignant reactions in irradiated rat skin. Br J Radiol. 63:349-354.

Weiss, R.B., R.C. Donehower, P.H. Wiernik, T. Ohnuma, R.J. Gralla, D.L. Trump, J.R. Baker, Jr., D.A. Van Echo, D.D. Von Hoff, and B. Leyland-Jones. 1990. Hypersensitivity reactions from taxol. J Clin Oncol. 8:1263-1268.

Wen, X., E.F. Jackson, R.E. Price, E.E. Kim, Q. Wu, S. Wallace, C. Charnsangavej, J.G. Gelovani, and C. Li. 2004. Synthesis and characterization of poly(L-glutamic acid) gadolinium chelate: a new biodegradable MRI contrast agent. Bioconjug Chem. 15:1408-1415.

Wilop, S., S. von Hobe, M. Crysandt, A. Esser, R. Osieka, and E. Jost. 2009. Impact of angiotensin I converting enzyme inhibitors and angiotensin II type 1 receptor blockers on survival in patients with advanced non-small-cell lung cancer undergoing first-line platinum-based chemotherapy. J Cancer Res Clin Oncol. 135:1429-1435.

Winterbourn, C.C., and D. Metodiewa. 1999. Reactivity of biologically important thiol compounds with superoxide and hydrogen peroxide. Free Radic Biol Med. 27:322-328.

Wondrak, G.T., M.K. Jacobson, and E.L. Jacobson. 2004. Anti-melanoma activity of D-pencillamine and other carbonyl scavengers In Proc Amer Assoc Cancer Res. Vol. 45, Orlando, FL. 472-473.

Wondrak, G.T., M.K. Jacobson, and E.L. Jacobson. 2006. Antimelanoma activity of apoptogenic carbonyl scavengers. J Pharmacol Exp Ther. 316:805-814.

Yamanaka, H., M. Hakoda, N. Kamatani, S. Kashiwazaki, and D.A. Carson. 1993. Formation of DNA strand breaks by D-penicillamine and bucillamine in human lymphocytes. Immunopharmacology. 26:113-118.

Yang, J., H. Chen, I.R. Vlahov, J.X. Cheng, and P.S. Low. 2006. Evaluation of disulfide reduction during receptor-mediated endocytosis by using FRET imaging. Proc Natl Acad Sci U S A. 103:13872-13877.

Ye, H., L. Jin, R. Hu, Z. Yi, J. Li, Y. Wu, X. Xi, and Z. Wu. 2006. Poly(gamma,L-glutamic acid)-cisplatin conjugate effectively inhibits human breast tumor xenografted in nude mice. Biomaterials. 27:5958-5965.

Yeung, J.H. 1991. The effects of bucillamine on glutathione and glutathione-related enzymes in the mouse. Biochem Pharmacol. 42:847-852.

Yokoyama, M., M. Miyauchi, N. Yamada, T. Okano, Y. Sakurai, K. Kataoka, and S. Inoue. 1990. Polymer Micelles as Novel Drug Carrier - Adriamycin-Conjugated Poly(Ethylene Glycol) Poly(Aspartic Acid) Block Copolymer. J Control Release. 11:269-278.

Yuan, F., A. Krol, and S. Tong. 2001. Available space and extracellular transport of macromolecules: effects of pore size and connectedness. Ann Biomed Eng. 29:1150-1158.

Yuan, H., K. Luo, Y. Lai, Y. Pu, B. He, G. Wang, Y. Wu, and Z. Gu. 2010. A novel poly(l-glutamic acid) dendrimer based drug delivery system with both pH-sensitive and targeting functions. Mol Pharm. 7:953-962.

Yuhas, J.M. 1972. Improvement of lung tumor radiotherapy through differential chemoprotection of normal and tumor tissue. J. Nat. Cancer Inst. 48:1255-1257.

Yuhas, J.M. 1979. Differential protection of normal and malignant tissues against the cytotoxic effects of mechlorethamine. Cancer Treat. Rep. 63:971-976.

Yuhas, J.M., M.E. Davis, D. Glover, D.Q. Brown, and M. Ritter. 1982. Circumvention of the tumor membrane barrier to WR-2721 absorption by reduction of drug hydrophilicity. Int. J. Radiat. Oncol. Biol. Phys. 8:519-522.

Yuhas, J.M., and J.B. Storer. 1969. Differential chemoprotection of normal and malignant tissues. J. Nat. Cancer Inst. 42:331-335.

Yurkow, E.J., and F.H. Mermelstein. 2006. Method for treating cancer, US Patent Publication 2006/0111284.

Zalipsky, S., M. Saad, R. Kiwan, E. Ber, N. Yu, and T. Minko. 2007. Antitumor activity of new liposomal prodrug of mitomycin C in multidrug resistant solid tumor: insights of the mechanism of action. J Drug Target. 15:518-530.

Zhao, Y., L. Chaiswing, J.M. Velez, I. Batinic-Haberle, N.H. Colburn, T.D. Oberley, and D.K. St Clair. 2005. p53 translocation to mitochondria precedes its nuclear translocation and targets mitochondrial oxidative defense protein-manganese superoxide dismutase. Cancer Res. 65:3745-3750.

Zhao, Y., T. Seefeldt, W. Chen, L. Carlson, A. Stoebner, S. Hanson, R. Foll, D.P. Matthees, S. Palakurthi, and X. Guan. 2009. Increase in thiol oxidative stress via glutathione reductase inhibition as a novel approach to enhance cancer sensitivity to X-ray irradiation. Free Radic Biol Med. 47:176-183.

Zheng, J., J.R. Lou, X.X. Zhang, D.M. Benbrook, M.H. Hanigan, S.E. Lind, and W.Q. Ding. 2010. N-Acetylcysteine interacts with copper to generate hydrogen peroxide and selectively induce cancer cell death. Cancer Lett. 298:186-194.

Zhu, G., X. Cao, J.Y. Chang, L. Milas, S. Wallace, and C. Li. 2007. Polymeric retinoid prodrug PG-4HPR enhances the radiation response of lung cancer. Oncol Rep. 18:645-651.

Chapter 2

Intracellular Delivery of the Reactive Oxygen Species Generating Agent D-Penicillamine upon Conjugation to Poly-L-glutamic Acid

Reproduced with permission from Wadhwa, S., and R.J. Mumper. 2010. Intracellular delivery of the reactive oxygen species generating agent D-penicillamine upon conjugation to poly-L-glutamic acid. *Molecular Pharmaceutics*. 7:854-862.

2.1. Abstract

D-Pen is an aminothiol that is cytotoxic to cancer cells and generates dose dependent ROS via copper catalyzed oxidation. However, the delivery of D-pen to cancer cells remains a challenge due to its high hydrophilicity, highly reactive thiol group and impermeability to the cell membrane. To overcome this challenge, we investigated a novel PGA conjugate of D-pen (PGA-D-pen) where D-pen was conjugated to PGA modified with 2-(2-pyridyldithio)-ethylamine (PDE) via disulfide bonds. Confocal microscopy and cell uptake studies showed that the fluorescently labeled PGA-D-pen was taken up by human leukemia cells (HL-60) in a time dependent manner. Treatment of HL-60, murine leukemia cells (P388) and human breast cancer cells (MDA-MB-468) with PGA-D-pen resulted in dose dependent cytotoxicity and elevation of intracellular ROS levels. PGA-D-pen induced apoptosis in HL-60 cells which was verified by Annexin V binding. The *in-vivo* evaluation of the conjugate in the P388 murine leukemia model (i.p.) resulted in significant enhancement in the survival of CD2F1 mice over vehicle control.

2.2. Introduction

Cancer cells are under persistent increased reactive oxygen species (ROS) stress due to oncogenic stimulation, increased metabolic activity and mitochondrial malfunction (Pelicano et al., 2004). Such a sustained oxidative stress and thus exhausted redox buffering capacity makes cancer cells more susceptible to killing by oxidative insult compared to normal cells.(Gupte and Mumper, 2009) Therefore, agents that elevate intracellular ROS levels can lead to cytotoxic effects in cancer cells.

D-Pen is an aminothiol and a strong copper chelator. It has been registered by the FDA for the treatment of Wilson's disease. We recently showed that D-pen is cytotoxic to leukemia (HL-60, HL-60/VCR) and breast cancer cells (MCF-7 and BT-474) when externally supplied with copper via concentration dependent generation of hydrogen peroxide (H_2O_2) (Gupte and Mumper, 2007a; Gupte and Mumper, 2007b).The mechanism of H_2O_2 generation in the presence of copper was first proposed by Starkebaum and Root (Starkebaum and Root, 1985). In a recent study, D-pen was found to produce maximum amount of ROS among different amino thiols due to favorable pK_a (7.9) of its thiol group (Winterbourn and Metodiewa, 1999). The H_2O_2 generated by D-pen oxidation may result in a ROS cascade involving hydroxyl radical via Fenton type reactions (Held et al., 1996).

Copper has been established as a key cofactor required by a number of proangiogenic molecules including FGF, VEGF and interleukin-1 (Mamou et al., 2006; Pan et al., 2002). Several *in-vitro* studies have shown that high copper concentrations facilitate proliferation of cancer cells (Hu, 1998; Lowndes and Harris, 2004; Raju et al., 1982). Significantly elevated levels of copper have been found in the serum and tumors of patients compared to healthy individuals (Gupta et al., 1991; Santoliquido et al., 1976; Siddiqui et al., 2006; Yucel et al.,

1994; Zuo et al., 2006). Therefore, the delivery of D-pen to the cancer cells may result in a dual anticancer effect involving metal catalyzed elevation of cellular ROS levels leading to cytotoxicity (mechanism 1) as well as an antiangiogenic effect (mechanism 2). In fact, D-pen has been explored in the clinic as an antiangiogenic agent. For example, Matsubara et al. reported that D-pen inhibited human endothelial cell proliferation and endothelial cell growth factor induced neovascularization in rabbit cornea (Matsubara et al., 1989).

Although a few previous studies have shown D-pen to cause cytotoxicity in the presence of copper in *in-vitro* studies, these effects were almost certainly due to the extracellular production of cytotoxic H_2O_2 (Duncan et al., 2006; Gupte et al., 2008; Joyce et al., 1991; Joyce et al., 1989) since our recent studies confirmed that D-pen is impermeable to cancer cells (Gupte et al., 2008). Thus, the cell membrane presents a significant barrier to the therapeutic delivery of D-pen as a ROS-producing cytotoxic agent. Moreover, D-pen has been shown to rapidly oxidize to D-pen disulfide *in-vivo* and bind strongly to the plasma proteins, mainly albumin, via thiol disulfide exchange (Joyce et al., 1991; Joyce et al., 1989). This further limits the availability of D-pen for uptake by the cancer cells. Thus, there is a need to devise a delivery system for D-pen that could (i) protect the thiol group; (ii) enhance the intracellular delivery; and (iii) deliver high concentration of D-pen to cancer cells. It is hypothesized that conjugation of D-pen to the pendant groups of a polymer via disulfide bonds could lead to the delivery of higher concentrations of D-pen resulting in enhanced intracellular accumulation of D-pen by uptake via endocytosis. It is further hypothesized that release of D-pen from its polymeric conjugate in the intracellular reducing environment will result in time and concentration dependent cytotoxicity in cancer cells via the generation of cytotoxic ROS.

Polymer-drug conjugates or "polymer therapeutics" (Duncan et al., 2006) provide distinct advantages for the delivery of small drug molecules by acting as passive targeting carriers via enhanced uptake and longer retention in the tumors. This ability has been attributed to the characteristic leaky vasculature of tumors termed as the EPR effect by Maeda (Maeda et al., 2009; Maeda et al., 1992). Several polymer-drug conjugates are being investigated for their potential to enhance the anticancer efficacy of drugs bound to them (Duncan, 2006).

Our previous studies using a gelatin-D-pen conjugate showed cellular uptake and cytotoxicity in leukemia cells (Gupte et al., 2008). However, the conjugation efficiency was low and the conjugate only showed long-term cytotoxicity possibly due to slower uptake and release of D-pen from the conjugate. PGA is a biodegradable and biocompatible polymer composed of L-glutamic acid monomer units linked together with amide bonds. The pendant carboxyl groups of PGA provide excellent sites for drug conjugation. Several anticancer drugs have been conjugated to PGA via ester (Li, 2002; Li et al., 1999; Zou et al., 2001), hydrazone (Hurwitz et al., 1980) or amide bonds (Kato et al., 1984), with or without spacers (Singer et al., 2001; Singer et al., 2000) between the drug and the polymer.

In the present studies, we describe the synthesis, characterization and *in-vivo* anticancer activity of a novel water-soluble PGA-D-pen conjugate where D-pen is covalently bound to PGA via a disulfide bond. The conjugate was also investigated for its ability to enhance the intracellular delivery of D-pen and subsequent cytotoxicity through a ROS-mediated mechanism in leukemia cells.

2.3. Experimental Section

2.3.1. Materials

Poly-L-glutamic acid (MW 50−70 kDa), D-penicillamine (D-pen), D-penicillamine disulfide, tris(2-carboxyethyl)phosphine hydrochloride (TCEP), 1-ethyl-3-[3-dimethylaminopropyl]carbodiimide hydrochloride (EDC), *N*-hydroxysuccinimide (NHS), DL-dithiothreitol (DTT), sodium borohydride ($NaBH_4$), Sephadex G-25 medium, chloroquine diphosphate and ammonium dihydrogen phosphate were purchased from Sigma-Aldrich (St. Louis, MO). NHS-fluorescein and BCA protein assay kit was purchased from Pierce Biotech Inc. (Rockford, IL). Acetonitrile, *N*,*N*-dimethylformamide (DMF), dimethylsulfoxide (DMSO) and *o*-phosphoric acid (85%) were purchased from Fisher Scientific (Pittsburgh, PA). Carboxy-H_2DCFDA and propidium iodide were purchased from Invitrogen (Carlsbad, CA). Annexin-V-FITC was purchased from BD Pharmingen (San Diego, CA).

2.3.2. Synthesis of PGA-D-Pen Conjugate

PGA-D-pen conjugate was synthesized as shown in **Figure 2.1**. 2-(2-Pyridyldithio) ethylamine (PDE) hydrochloride was synthesized according to a previously published method (Gnaccarini et al., 2006). PDE was covalently conjugated to PGA via an amide bond. A large molar excess of D-pen was used to conjugate it to the modified PGA via thiol-disulfide exchange. Briefly, PGA (100 mg, 0.63 mmol of carboxy monomer), PDE hydrochloride (279.78 mg, 1.26 mmol), *N*-hydroxysuccinimide (NHS) (36.15 mg, 0.314 mmol) and 1-ethyl-3-[3-dimethylaminopropyl]carbodiimide hydrochloride (EDC) (120.45 mg, 0.63 mmol) were added to 5 mL of DMF. Triethylamine (1.5 mmol) was added to the

reaction. The mixture was then stirred for 12 hr at room temperature under nitrogen. After the reaction, the solvent was removed by vacuum evaporation, and the product washed three times with dichloromethane to remove excess reactants. The product was then resuspended in 0.05 M borate buffer pH 9.0, and D-pen (234.4 mg, 1.26 mmol) was added. The mixture was stirred for 12 hr at room temperature. PGA-D-pen was purified and exchanged with PBS pH 7.4 using a Sephadex G-25 column (1.5 x 30 cm).

To synthesize fluorescently labeled PGA-D-pen conjugate, 0.04 mL of NHS-fluorescein in DMSO (3.2 mM) was added to 0.45 mL of PGA-D-pen conjugate in PBS buffer pH 7.4. The reaction mixture was stirred in the dark for 1 hr at room temperature. The fluorescently labeled conjugate was purified using a Sephadex G-25 column (1.5 x 30 cm). The moles of fluor per mole of PGA were determined spectrophotometrically (ε=68000 M^{-1} cm^{-1}, λ_{max}= 494 nm).

2.3.3. Choice of Reducing Agent to Measure the Extent of Conjugation

Three different reducing agents, sodium borohydride ($NaBH_4$), DL-dithiothreitol (DTT) and Tris(2-carboxyethyl)phosphine hydrochloride (TCEP) were screened. Briefly, PGA-D-pen conjugate was incubated with increasing concentration (5 mM to 25 mM) of the reducing agent for varying time (30 min to 4 hr) and the amount of D-pen released was determined using HPLC. Based on the results, TCEP was chosen for further studies.

2.3.4. Quantification of D-pen Conjugation by HPLC

100 mM TCEP (0.25 mL) was added to PGA-D-pen conjugate (0.75 mL) and stirred for 1 hr at room temperature. D-pen released upon reduction of the PGA-D-pen conjugate

was analyzed with a modification of our previously reported HPLC method (Gupte and Mumper, 2007b). The HPLC analysis was performed using a Finnigan^{TM} Surveyor HPLC System (Thermo Electron Corp., San Jose, CA) with a Gemini C18 column (250 x 4.6 mm; 5 μM; 20 μL sample; Phenomenex, Torrance, CA). The mobile phase employed was 20 mM ammonium dihydrogen phosphate +3% acetonitrile adjusted to pH 2.5 using o-phosphoric acid, and pumped at a flow rate of 1 mL/min. D-pen and D-pen disulfide were detected by UV absorption at 214 nm with retention times of 5.2 and 4.8 min, respectively.

2.3.5. Cell Uptake Studies

The uptake of the fluorescently labeled PGA-D-pen conjugate was determined qualitatively using confocal microscopy. HL-60 cells (5×10^5) cultured in RPMI-1640 without phenol red and supplemented with 10% fetal bovine serum, 100 units/mL penicillin and 100 μg/mL streptomycin, were plated in a 24 well plate and treated with fluorescently labeled PGA-D-pen conjugate (500 μM D-pen equivalent). Cells were washed with PBS and resuspended in RPMI 1640 without phenol red and immediately observed under a confocal microscope. Cells were transferred onto a slide for visualizing using Zeiss 510 Meta Laser Scanning Confocal Microscope (63 x 1.4 NA oil Plan-Apochromat objective; excitation =488 nm and emission =515 nm; Carl Zeiss, Thornwood, NY). Differential Interference Contrast (DIC) images, fluorescence images and the overlapped images taken from the microscope were visualized using the Zeiss AIM Viewer (Carl Zeiss, Thornwood, NY).

To quantitatively determine D-pen associated with HL-60 cells, 5 x 10^5 cells were incubated with PGA-D-pen (500 μM D-pen equivalent) for predetermined time points. The cells were centrifuged at 1000 g x 10 min and the supernatant was reduced with TCEP to

release free D-pen which was analyzed by HPLC. This was subtracted from the original amount to obtain the cell-associated PGA-D-pen.

2.3.6. Cytotoxicity Studies in Cells

The HL-60 and MDA-MB-468 cells were obtained from American Type Cell Culture Collection (ATCC; Rockville, MD). The P388 cells were obtained from National Cancer Institute-Frederick Cancer Research Facility, DCT Tumor Repository (NCI, Bethesda, MD). HL-60 and P388 cells were cultured in RPMI-1640 (Invitrogen) while MDA-MB-468 cells were cultured in DMEM (Invitrogen). The media were supplemented with 100 U/mL penicillin, 100 μg/mL streptomycin and 10% Fetal Bovine Serum (FBS) (ATCC). All cell lines were maintained at 37^{o}C in a humidified 5% CO_2 incubator. Cell viability was regularly determined by trypan blue dye (0.4% in phosphate buffered saline) (ATCC).The P388 cells and HL-60 cells were plated at 1 x 10^4 and 4 x 10^4 cells respectively in 200 μL of medium per well in round-bottom 96-well microwell plates. The MDA-MB-468 cells were plated at 1 x 10^4 cells/well in 96-well flat bottom microwell plates and allowed to attach overnight. Equal volumes of PGA-D-pen conjugate, PGA, D-pen, PGA+D-pen or PBS were added and the plates were incubated for 48 hr (37^{o}C, 5% CO_2). Twenty (20) μL of MTT reagent (5 mg/mL in PBS) was added to each well and reincubated for 3-4 hr to allow formation of formazan crystals. The round-bottom plates were centrifuged at 200 g x 5 min. Subsequently, the supernatant was aspirated and 200 μL DMSO was added to each well and the plate was incubated at room temperature for 1 hr to lyse the cells and solubilize formazan. The optical density of each well at 570 nm was measured on a Synergy^{TM} 2 Multi-Detection Microplate

Reader (Biotek; Winooski, VT). The results were analyzed in terms of percentage of viable cells after 48 hr of incubation as compared to control cells.

2.3.7. Intracellular ROS Generation

ROS generation was assessed using 5-(and-6)-carboxy-2′, 7′-dichlorodihydrofluorescein diacetate (carboxy-H_2DCFDA) (Molecular Probes). Carboxy-H_2DCFDA is a cell permeant probe and has improved intracellular retention due to additional negative charges at cytosolic pH. It is converted to a highly fluorescent form upon deacetylation by cellular esterases and oxidation. Stock solutions of carboxy-H_2DCFDA (2 mM) were prepared in DMSO. Further dilutions were prepared in PBS. For ROS measurement, HL-60 cells were incubated for 30 min in PBS containing 25 μM carboxy-H_2DCFDA. Subsequently, the cells were washed with PBS and resuspended in RPMI-1640 without phenol red and serum. Three x 10^4 cells were plated in 96-well dark flat bottom plates and treated with different concentrations of D-pen and PGA-D-pen conjugate. Fluorescence was determined at various time points post-treatment using Synergy^{TM} 2 Multi-Detection Microplate Reader at excitation wavelength of 485 ± 20 nm and an emission wavelength of 530 ± 30 nm. RPMI-1640 and cells not incubated with the probe were used as negative controls while 100 μM H_2O_2 was used as positive control.

2.3.8. Apoptosis Assay

HL-60 cells (5×10^5) were incubated with PGA-D-pen (100−1000 μM D-pen equivalent) for 2 hr, 6 hr, 14 hr and 24 hr followed by double staining with Annexin-V-FITC and propidium iodide (PI) to differentiate between live, necrotic and apoptotic cells. Briefly,

the cells were centrifuged, washed with PBS and resuspended in 0.1 mL Annexin-V binding buffer. Annexin-V-FITC (5 μL) was added and incubated for 15 min in dark at room temperature. PI (10 μL of 50 μg/mL stock solution in binding buffer) and 0.4 mL of binding buffer were added and cells were immediately analyzed by flow cytometry (Becton-Dickinson). Untreated HL-60 cells (negative control), cells treated with 10 μM etoposide (Annexin-V-FITC positive control) and cells treated with ethanol for 20 min (PI positive control) were analyzed to adjust instrument compensation and setting up the quadrant statistics. The results were processed by Cellquest (Becton-Dickinson) and FlowJo (Tree Star).

2.3.9. *In-vivo* Anticancer Efficacy

To determine the acute toxicity, PGA-D-pen conjugate in 0.9% sodium chloride (300 mOsmol, pH 7.4, sterile filtered) was administered i.p. to CD2F1 mice (16-18 g) at doses of 1, 2, 5, and 10 mg/kg D-pen equivalent on day 1, 5, and 9. Sodium chloride (0.9%) was administered i.p. as vehicle control to untreated animals. The mice were monitored for 14 days for mortality and were assigned a body condition score (BCS) (Ullman-Cullere and Foltz, 1999) every 48 hr based on body weight and general health criteria. A loss of 10% body weight over 3 days or loss of 20% of initial weight and a BCS score of less than 2 was considered to be criteria for euthanasia.

Anticancer efficacy of the PGA-D-pen conjugate was assessed using the intraperitoneal P388 murine leukemia model. Briefly, 1 x 10^5 P388 murine leukemia cells were implanted in the i.p. cavity of CD2F1 mice (16-18 g) on day 0. PGA-D-pen was administered i.p. on day 1, 5, and 9 at 5 mg/kg and 10 mg/kg D-pen equivalent respectively.

The mice were observed daily for mortality and were assigned a BCS every 48 hr. The percent survival curves were plotted and median survival was determined. All experiments involving mice were performed with the approval of the University of North Carolina Institutional Animal Care and Use Committee.

2.3.10. Statistical Analysis

Statistical analysis was performed with GraphPad Prism 4 Software (GraphPad software Inc. San Diego, CA). Results were depicted as mean ± SD. IC_{50} values were derived from the percent viability data by non-linear regression curve fitting. ROS generation was analyzed by one-way ANOVA followed by Dunnet's post test to compare the different dose levels to control. Survival curves from the anticancer efficacy studies were plotted by Kaplan-Meier's method and analyzed by Mantel-Cox log-rank test.

2.4. Results

2.4.1. Synthesis and Characterization of PGA−d-pen Conjugate

PGA-D-pen conjugate was synthesized by modifying PGA with PDE as shown in **Figure 2.1**. PDE is a heterobifunctional cross-linker as the amine group can be used to conjugate with carboxy groups while the pyridyl thiol functionality provides an opportunity to conjugate thiol groups via thiol-disulfide exchange in the presence of molar excess of another thiol like D-pen. The second conjugation reaction was performed in the presence of borate buffer pH 9.0 to provide favorable conditions for thiol-disulfide exchange (pK_a of D-pen thiol is 7.9). The final conjugate was completely soluble in water.

To determine the efficiency of conjugation, different disulfide reducing agents were screened. Among the agents tested, TCEP was selected for further studies as it was the most efficient reducing agent and did not interfere with the HPLC assay (**Figure 2.2**). The previously developed HPLC assay (Gupte and Mumper, 2007b) was modified to determine D-pen, D-pen disulfide and TCEP before and after reduction. The final conjugate had 35 moles of D-pen per mole of PGA. The theoretical maximum weight loading of D-pen on PGA was 8 wt % (9.3% of the pendant carboxyl groups were modified per chain of PGA). ^{1}H NMR (Inova 500 spectrometer; 500 MHz in D_2O) of the conjugate showed resonance of D-pen at 3.81 ppm (1 H, C2), 1.85 ppm (3 H, C3-methyl) and 1.68 ppm (3 H, C3-methyl), resonance of methylene protons of PDE at 3.03 ppm (2 H, CH_2-S) and 3.13 ppm (2 H, CH_2-N) and resonance of PGA at 4.20 ppm (1 H, C_α-H), 2.16 ppm (2 H, C_γ-H_2) and 1.84 ppm (2 H, C_β-H_2).

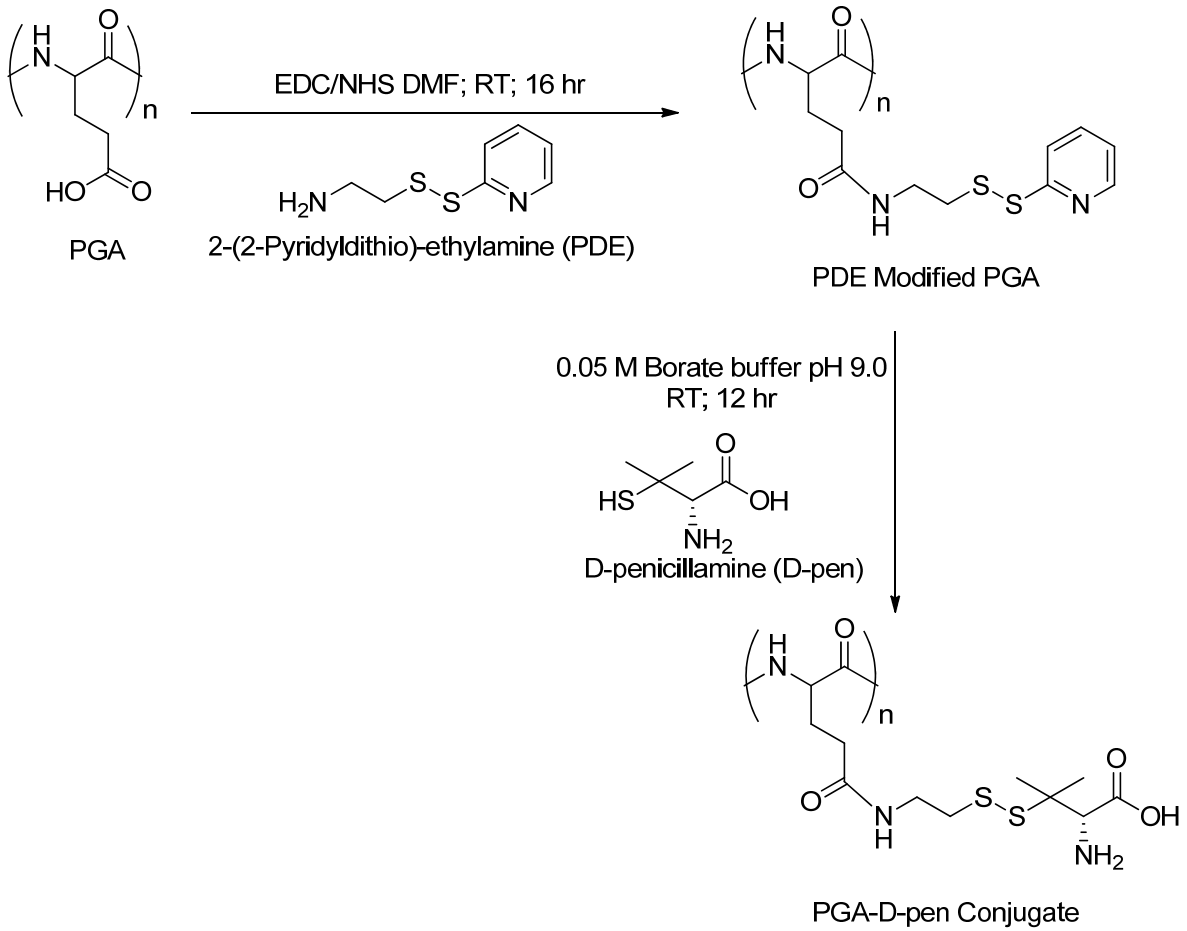

Figure 2.1 Synthesis of PGA-D-Pen Conjugate.
PGA was covalently linked to PDE using EDC/NHS chemistry. D-Pen was conjugated to modified PGA via thiol−disulfide exchange of pyridine-2-thione with D-pen at pH 9.0. Abbreviations: PGA, poly-L-glutamic acid; EDC, 1-ethyl-3-[3-dimethylaminopropyl] carbodiimide hydrochloride; NHS, *N*-hydroxysuccinimide.

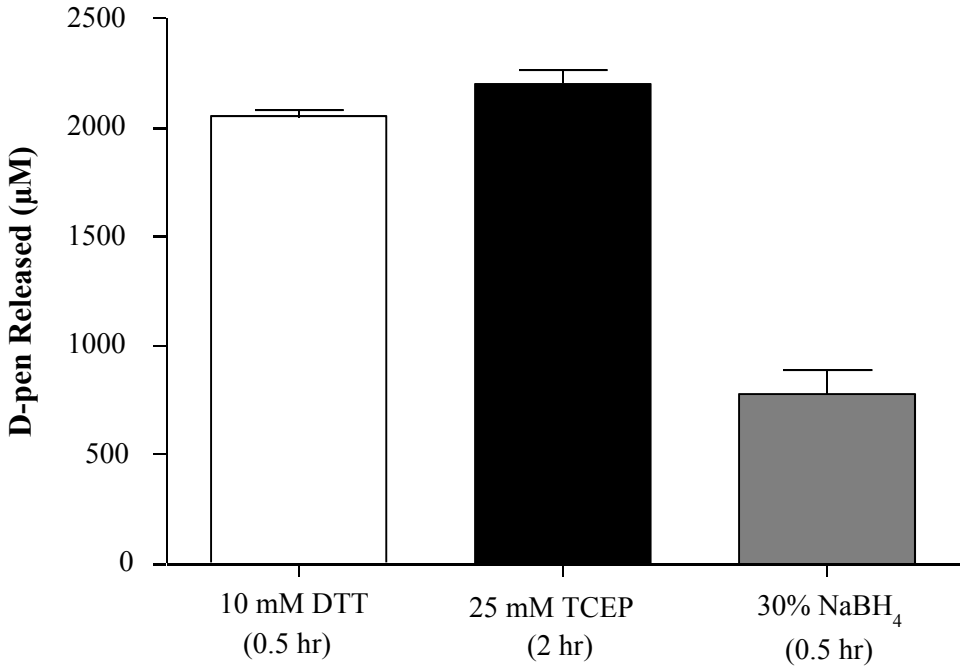

Figure 2.2 Screening of disulfide reducing agents.
PGA-D-pen was incubated separately with different concentrations of three reducing agents for predetermined time and released free D-pen was analyzed by HPLC. Each bar represents mean ± SD (n = 3) of the concentration and time at which the highest amount of D-pen was released.

2.4.2. Cell Uptake Studies

PGA-D-pen was fluorescently labeled using NHS-fluorescein. The number of moles of fluorescein per mole of PGA was 1.34, which was determined spectrophotometrically. The intracellular uptake was visualized by confocal microscopy. Live cells were visualized under the microscope after exposure to the conjugate for a predetermined time. The control cells were visualized to confirm that the cells were healthy and to rule out any background fluorescence. The conjugate exhibited time dependent uptake in HL-60 cells (**Figure 2.3**). To further confirm the results obtained by confocal microscopy, cell associated PGA-D-pen was determined by HPLC. Up to 25% PGA-D-pen was found to be associated with the cells at 8 hr. These results support the hypothesis that polymer conjugation increases the cellular uptake of D-pen.

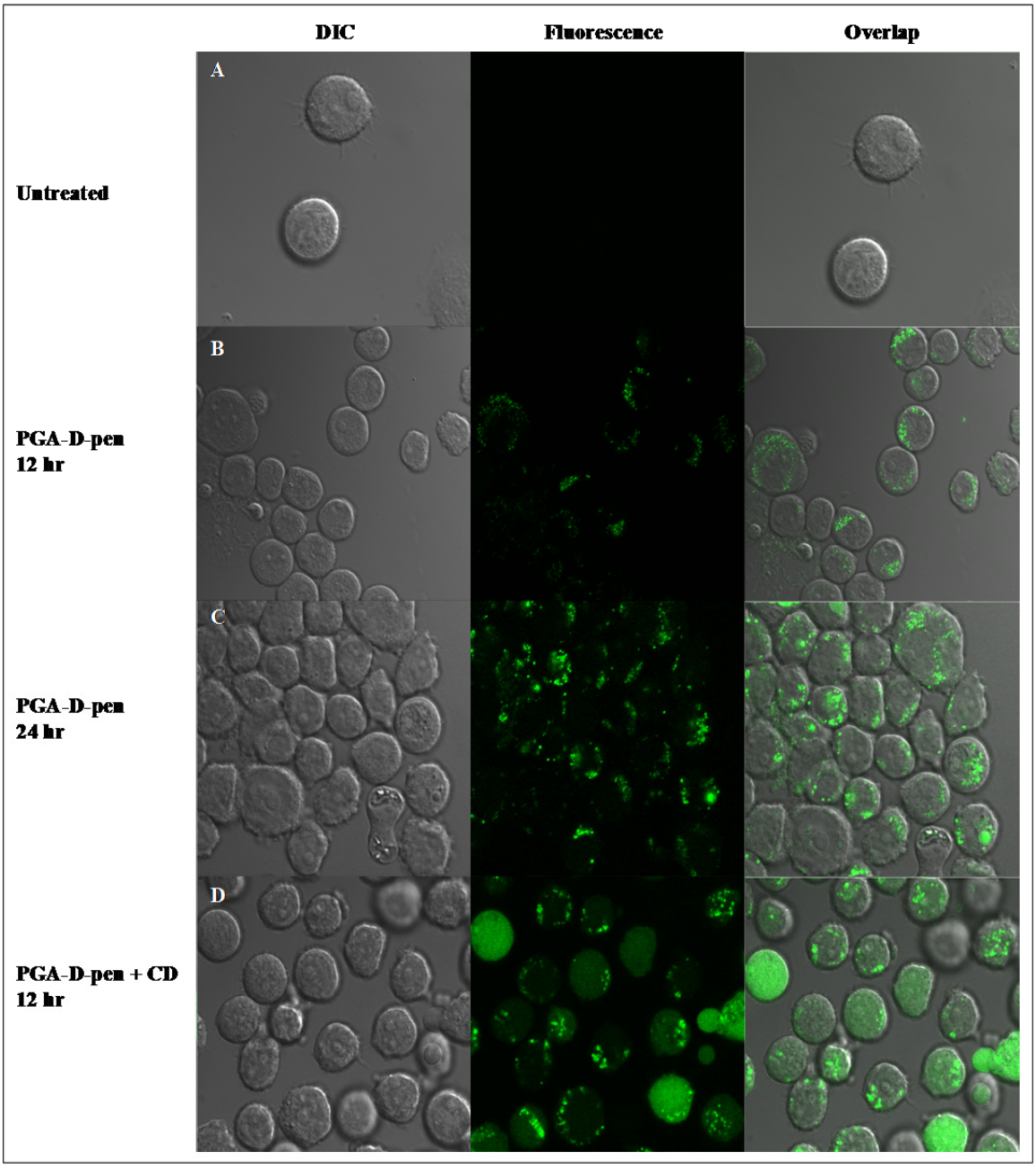

Figure 2.3 Intracellular uptake of PGA-D-pen conjugate by confocal microscopy. Differential interference contrast (DIC) images, fluorescence images and the overlapped images of untreated HL-60 cells (A), HL-60 cells treated with fluorescently labeled PGA-D-pen conjugate for 12 hr (B), 24 hr (C) and 12 hr in the presence of chloroquine diphosphate (D)

2.4.3. Cytotoxicity Studies in Cells

The *in-vitro* cytotoxicity of the conjugate was investigated in leukemia (HL-60 and P388) and human breast cancer cells (MDA-MB-468). The PGA-D-pen conjugate treatment resulted in a dose-dependent reduction in viability of the cells (**Figure 2.4**). The IC_{50} values for HL-60 (4 x 10^4 cells), P388 (1 x 10^4 cells) and MDA-MB-468 (1 x 10^4 cells) were 106.1 μM, 106.3 μM, 156.7 μM, respectively. Similar concentrations of free D-pen, PGA or D-pen + PGA did not cause significant reduction in cell viability over the duration of study. Our previous studies have shown that D-pen alone is cytotoxic to cancer cells only at low millimolar concentrations (Gupte and Mumper, 2007a).

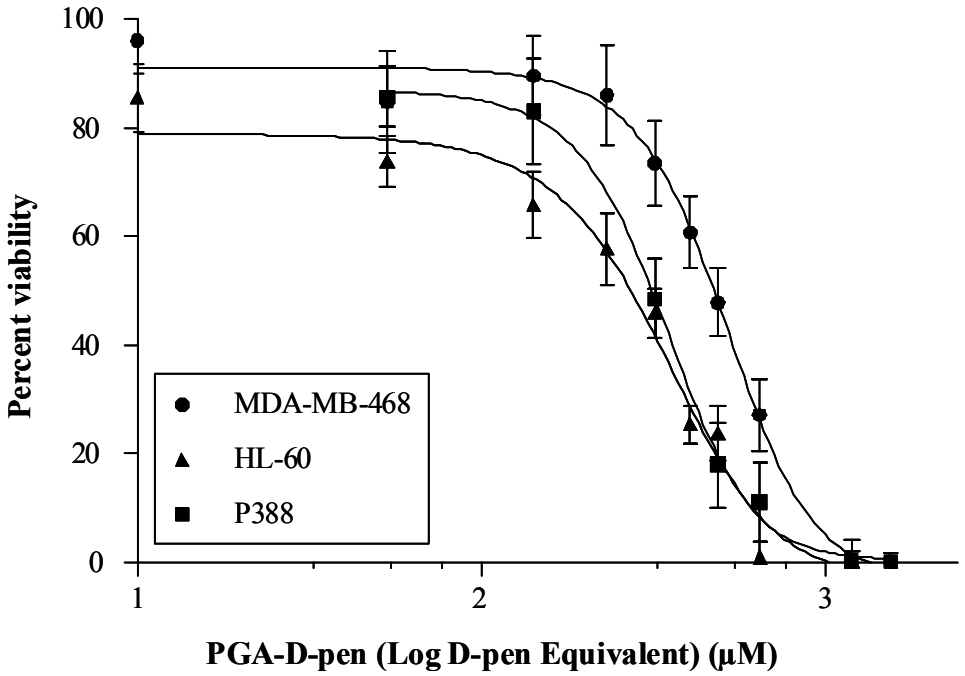

Figure 2.4 Cytotoxicity of PGA-D-pen conjugate in a) HL-60 cells; b) P388 cells and c) MDA-MB-468 cells.

Cytotoxicity was determined by MTT assay 48 hr after treatment with PGA-D-pen. The log of equivalent D-pen concentration was plotted on X-axis. Each point represents mean ± S.D. (n=3).

2.4.4. Intracellular ROS Generation

Generation of ROS upon treatment with the conjugate was investigated using carboxy-H_2DCFDA, a nonfluorescent probe which gets converted to highly fluorescent derivative following deacetylation by intracellular esterases and oxidation. This dye was chosen due to its longer intracellular retention compared to H_2DCFDA used in our previous studies. The time and dye concentration required for the study were optimized using H_2O_2, which was also used as a positive control. The ROS levels were significantly higher compared to the control at all concentrations tested (**Figure 2.5**). Maximal levels of ROS were observed at 8 hr after treatment with PGA-D-pen. The ROS levels at the highest concentration of the conjugate, i.e. 500 μM (D-pen equivalent), were not significantly different from the levels produced by 100 μM H_2O_2, which suggests the strong potential of the synthesized conjugate to generate intracellular ROS upon release of D-pen.

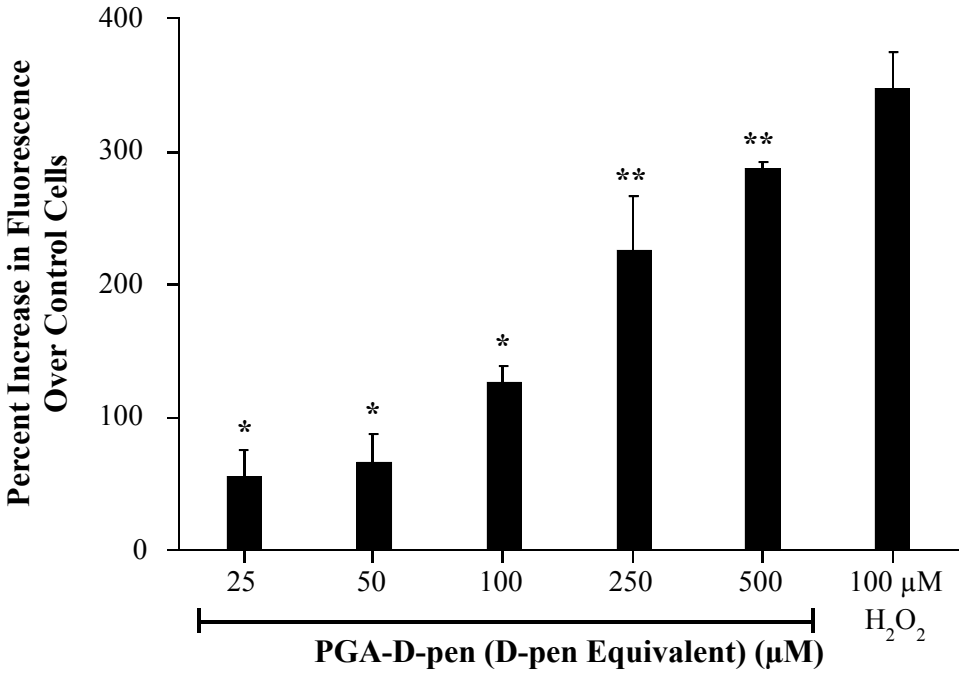

Figure 2.5 Intracellular ROS generation by PGA-D-pen conjugate in HL-60 cells. Cells were incubated with 25 µM carboxy-H_2DCFDA for 30 min before exposure to PGA-D-pen conjugate. H_2O_2 (100 µM) was used as positive control. The fluorescence values were measured post-incubation at 8 hr with the conjugate and at 30 min with H_2O_2 respectively. Each bar represent mean ± S.D. (n=3). *$p<0.01$ and **$p<0.001$ compared to the control untreated cells.

2.4.5. Apoptosis Induction

Phosphatidylserine (PS) is distributed asymmetrically in the plasma membrane of live cells and inverts toward the outer surface during apoptosis. PS inversion is one of the early markers of apoptosis. It is possible to distinguish apoptotic and necrotic cells by staining with Annexin-V-FITC followed by counterstaining with PI as the former binds PS while PI is permeable only to cells with compromised membrane integrity. The HL-60 cells were incubated with three different D-pen equivalent concentrations of PGA-D-pen and analyzed at different time points to determine time and dose dependence. The number of apoptotic cells increased significantly in the PGA-D-pen treated samples (**Figure 2.6**) with dose and time. The percent of apoptotic cells upon treatment with 1000 μM PGA-D-pen (D-pen equivalent) for 14 hr was 22.5 ± 2.95%.

Fig. 2.6A

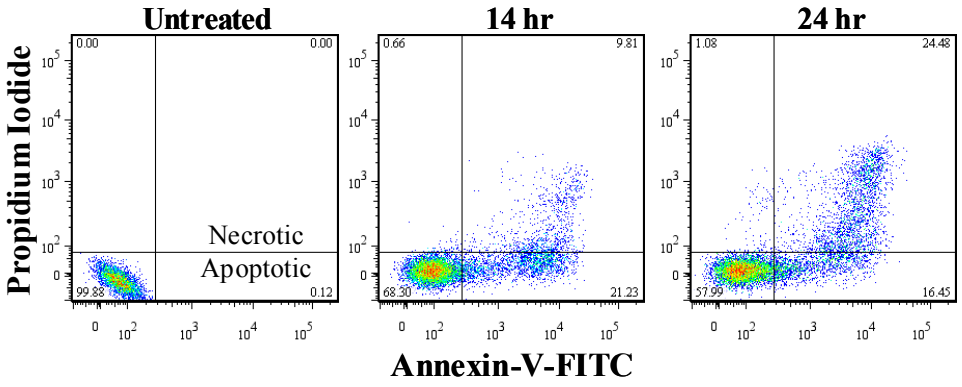
Untreated
14 hr
24 hr
Propidium Iodide
Annexin-V-FITC
Necrotic
Apoptotic
0.00
0.00
99.88
0.12
0.66
9.81
68.30
21.23
1.08
24.48
57.99
16.45

Fig. 2.6B

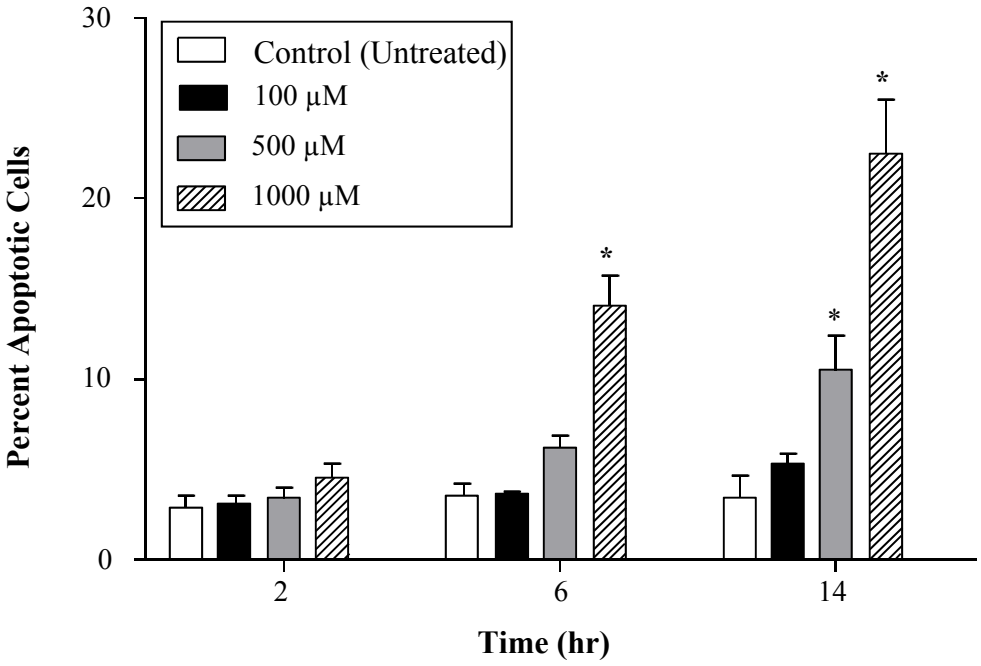

Figure 2.6 Apoptosis induction by PGA-D-pen.
Human leukemia cells (HL-60; 5 x 10^5) were treated with three different concentrations of PGA-D-pen followed by double staining with Annexin-V-FITC/PI at different time points. A: Flow cytometric analysis of HL-60 cells treated with 1000 µM PGA-D-pen conjugate (D-pen equivalent). B: The percent apoptotic cells (FITC positive, PI negative) at different time points. Each bar represents mean ± SD (n=3). *$p<0.001$ compared to the control untreated cells.

2.4.6. In Vivo Evaluation

The PGA-D-pen conjugate was dosed i.p. in CD2F1 mice at 4 different dose levels (1, 2, 5, and 10 mg/kg) to determine the acute toxicity. Mice receiving a 10 mg/kg dose showed signs of toxicity (consistently lower BCS scores), but no mortality was observed after 14 days. The mice in this group showed no weight loss, but the mean percent weight gain was less than that of the control group. Therefore, 10 mg/kg was used to evaluate the *in-vivo* anticancer efficacy of PGA-D-pen conjugate. The conjugate was also dosed at the 5 mg/kg dose level to determine a dose response in the enhancement of survival.

P388 i.p. model is a widely used animal model and involves implantation of cells in the ip cavity (Dykes and Waud, 2002). The tumor doubling time is 0.4 to 0.5 day, and the survival span is between 9 and 11 days in CD2F1 mice (Waud et al., 1992). The median survival upon treatment with 10 mg/kg and 5 mg/kg of PGA-D-pen on days 1, 5, and 9 increased by 28.5% (13.5 days) and 24% (13 days) respectively over control, which was significant ($p < 0.05$) based on log-rank analysis of the survival curves (**Figure 2.7**).

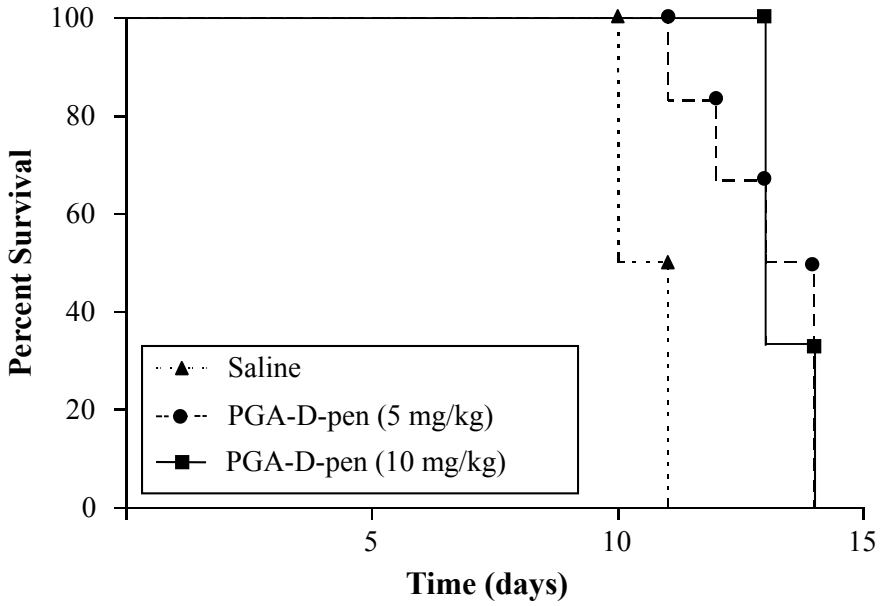

Figure 2.7 Percent survival curves in CD2F1 mice upon i.p. administration of PGA-D-pen.
Mouse leukemia cells (P388) were implanted i.p. on day 0. PGA-D-pen conjugate was administered i.p. on day 1, 5 and 9. Control group (saline) was compared to the groups treated with PGA-D-pen (6 mice/group).

2.5. Discussion

We and others have previously shown that D-pen is impermeable to cancer cells (Gupte et al., 2008; Lodemann, 1981). The impermeability results from a combination of high hydrophilicity (log *P* -0.39) (Chvapil et al., 2005) and the D-isoform being stereochemically less favored for cellular uptake by the amino acid transporters (Lodemann, 1981). Polymer bound drugs have been shown to be taken up by the cells via fluid phase endocytosis (Omelyanenko et al., 1998). Therefore, PGA-D-pen conjugate was synthesized to enhance the intracellular uptake of D-pen. Additionally, conjugation to PGA via disulfide bonds would provide protection to the thiol group of D-pen before it reaches the target cells and ensure intracellular release by endosomal disulfide reduction (Fivaz et al., 2002; Shen et al., 1985).

D-Pen has been shown to cause cytotoxicity by dose dependent generation of ROS via copper catalyzed one electron oxidation (Gupte and Mumper, 2007a). Cancer cells have an exhausted redox buffer capacity, and further increase in the oxidant load can lead to generation of apoptotic signals that may ultimately lead to cell death. Similar effects were observed with D-pen released intracellularly from the PGA-D-pen conjugate. Thus, it is possible that the major mechanism of cytotoxicity caused by D-pen is apoptosis induction via ROS generation. Leukemia cells were found to be more sensitive to PGA-D-pen treatment with lower IC_{50} values. This is similar to our previously reported *in-vitro* experiments (Gupte and Mumper, 2007a) except that the cells were not supplemented with copper. To investigate if the ROS generation and cytotoxicity were related to the endogenous copper levels in the different cells, we measured the intracellular copper in HL-60, P388 and MDA-MB-468 cells by ICP-MS (inductively coupled plasma mass spectrometry) (data not shown). There was no

direct correlation between the cytotoxicity and the endogenous copper levels suggesting that cytotoxicity of D-pen may be mediated by mechanisms additional to metal catalyzed ROS generation like a p53 dependent apoptosis induction (Havre et al., 2002) and binding to cellular proteins by thiol exchange similar to the endogenous thiols (Brennan et al., 2006) which are all independent of the availability of copper.

The confocal microscopic pictures showed a punctate pattern of fluorescence characteristic of endocytic uptake of macromolecular structures (Nori et al., 2003; Omelyanenko et al., 1998). The punctate pattern still exists at 24 hr suggesting that endosomal release mechanisms may be needed to release the conjugate or released D-pen into the cytosol. These observations suggest that cytosolic delivery of the conjugate and/or released D-pen may be important. To qualitatively assess the effect of endosomal escape on the cell uptake of the fluorescently labeled PGA-D-pen, uptake studies were performed in the presence of 50 μM chloroquine diphosphate (CD) based on preliminary cytotoxicity studies with CD alone in which this concentration did not result in significant reduction in cell viability. CD is a lysosomotropic agent and has been shown to increase cytosolic delivery (Ciftci and Levy, 2001) by raising the endosomal pH (Maxfield, 1982) leading to an osmotic burst of the endosome. In our studies (Figure 2.3D), we found that CD treatment resulted in a diffused pattern of fluorescence of the fluorescently labeled PGA-D-pen in HL-60 cells. Moreover, cotreatment of HL-60 cells (4×10^4) with PGA-D-pen conjugate and 50 μM CD resulted in 20% enhancement in cytotoxicity of the conjugate (at IC_{50} value) when normalized to CD treatment over 48 hr suggesting that endosomal release may be important in the enhancement of the efficacy of the conjugate. We are currently investigating cellular uptake and transport mechanisms of the conjugate including possible strategies to avoid

endosomal accumulation. Future efforts are focused on incorporation of an endosomal release mechanism that would result in the cytosolic delivery and more efficient intracellular reduction of the conjugate.

Based on the results of studies above, it was concluded that PGA-D-pen was able to successfully deliver D-pen to cancer cells. Although high doses of the conjugate (D-pen equivalent) are required to achieve beneficial effect if used alone, it has been reported that tumorigenic cells are 30-100-fold more sensitive to treatment with D-pen compared to normal cells (Havre et al., 2002; Okuyama and Mishina, 1981). This in-built selectivity makes D-pen a potential agent for development as an anticancer drug. However, it may be essential to combine it with a standard chemotherapy regimen when used in the clinic. For example, NOV-002, a new drug formulation under clinical trials, is the disodium salt of glutathione disulfide in complex with cisplatin in a ratio of 1000:1. It has been proposed that NOV-002 acts mainly by disturbing the cellular redox balance and results in increased efficacy when used in combination with cisplatin and other chemotherapeutics (Tew et al., 2008; Townsend et al., 2008). It is important to note that the active component of NOV-002, glutathione disulfide, is not cytotoxic even at very high doses when used alone, and like D-pen, glutathione disulfide is impermeable to the cell membrane (Brennan et al., 2006). This is relevant as we have found that treatment with D-pen in the presence of copper results in a decrease in cellular thiols and has the potential to perturb cellular redox balance while generating cytotoxic ROS (Gupte and Mumper, 2007a). Therefore, in an attempt to further enhance the efficacy of PGA-D-pen, we are currently developing dual drug conjugates where an anticancer anthracycline derivative will be conjugated to the PGA-D-pen conjugate via acid-cleavable hydrazone linkages. It has been reported that iron complexes of anthracyclines

especially doxorubicin catalyze oxygen consumption and ROS generation by thiols (Myers et al., 1982). Codelivery of an anthracycline with D-pen bound to a single polymer may synergistically enhance the anticancer efficacy, tolerability and an overall dose reduction of the chemotherapeutic.

2.6. Conclusions

A polymeric conjugate of D-pen with PGA was synthesized to achieve enhanced intracellular accumulation and anticancer efficacy. D-Pen was linked to the polymer by disulfide bonds using a heterobifunctional linker. The conjugate increased cell uptake of polymer bound D-pen as observed by confocal microscopy and HPLC. The ROS generation by PGA-D-pen upon cellular uptake results in apoptosis mediated cytotoxicity in P388 murine leukemia cells. PGA-D-pen significantly enhanced the survival of CD2F1 mice over control animals. Future efforts are focused toward investigating the intracellular release of D-pen from the conjugate and improving the anticancer efficacy of PGA-D-pen by synthesizing dual drug conjugates.

2.7. References

Brennan, J.P., J.I. Miller, W. Fuller, R. Wait, S. Begum, M.J. Dunn, and P. Eaton. 2006. The utility of N,N-biotinyl glutathione disulfide in the study of protein S-glutathiolation. Mol Cell Proteom. 5:215-225.

Chvapil, M., F. Kielar, F. Liska, A. Silhankova, and K. Brendel. 2005. Synthesis and evaluation of long-acting D-penicillamine derivatives. Connect Tissue Res. 46:242-250.

Ciftci, K., and R.J. Levy. 2001. Enhanced plasmid DNA transfection with lysosomotropic agents in cultured fibroblasts. Int J Pharm. 218:81-92.

Duncan, R. 2006. Polymer conjugates as anticancer nanomedicines. Nat Rev Cancer. 6:688-701.

Duncan, R., H. Ringsdorf, and R. Satchi-Fainaro. 2006. Polymer therapeutics--polymers as drugs, drug and protein conjugates and gene delivery systems: past, present and future opportunities. J Drug Target. 14:337-341.

Dykes, D.J., and W.R. Waud. 2002. Murine L1210 and P388 leukemias. Humana Press, Totowa, NJ. 23-40 pp.

Fivaz, M., F. Vilbois, S. Thurnheer, C. Pasquali, L. Abrami, P.E. Bickel, R.G. Parton, and F.G. van der Goot. 2002. Differential sorting and fate of endocytosed GPI-anchored proteins. Embo J. 21:3989-4000.

Gnaccarini, C., S. Peter, U. Scheffer, S. Vonhoff, S. Klussmann, and M.W. Gobel. 2006. Site-specific cleavage of RNA by a metal-free artificial nuclease attached to antisense oligonucleotides. J Am Chem Soc. 128:8063-8067.

Gupta, S.K., V.K. Shukla, M.P. Vaidya, S.K. Roy, and S. Gupta. 1991. Serum trace elements and Cu/Zn ratio in breast cancer patients. J Surg Oncol. 46:178-181.

Gupte, A., and R.J. Mumper. 2007a. Copper chelation by D-penicillamine generates reactive oxygen species that are cytotoxic to human leukemia and breast cancer cells. Free Radic Biol Med. 43:1271-1278.

Gupte, A., and R.J. Mumper. 2007b. An investigation into copper catalyzed D-penicillamine oxidation and subsequent hydrogen peroxide generation. J Inorg Biochem. 101:594-602.

Gupte, A., and R.J. Mumper. 2009. Elevated copper and oxidative stress in cancer cells as a target for cancer treatment. Cancer Treat Rev. 35:32-46.

Gupte, A., S. Wadhwa, and R.J. Mumper. 2008. Enhanced intracellular delivery of the reactive oxygen species (ROS)-generating copper chelator D-penicillamine via a novel gelatin-D-penicillamine conjugate. Bioconjug Chem. 19:1382-1388.

Havre, P.A., S. O'Reilly, J.J. McCormick, and D.E. Brash. 2002. Transformed and tumor-derived human cells exhibit preferential sensitivity to the thiol antioxidants, N-acetyl cysteine and penicillamine. Cancer Res. 62:1443-1449.

Held, K.D., F.C. Sylvester, K.L. Hopcia, and J.E. Biaglow. 1996. Role of Fenton chemistry in thiol-induced toxicity and apoptosis. Radiat Res. 145:542-553.

Hu, G.F. 1998. Copper stimulates proliferation of human endothelial cells under culture. J Cell Biochem. 69:326-335.

Hurwitz, E., M. Wilchek, and J. Pitha. 1980. Soluble macromolecules a carriers for daunorubicin. J Appl Biochem. 2:25-35.

Joyce, D.A., R.O. Day, and B.R. Murphy. 1991. The pharmacokinetics of albumin conjugates of D-penicillamine in humans. Drug Metab Disp. 19:309-311.

Joyce, D.A., D.N. Wade, and B.R. Swanson. 1989. The pharmacokinetics of albumin conjugates of D-penicillamine in rats. Drug Metab Disp. 17:208-211.

Kato, Y., M. Saito, H. Fukushima, Y. Takeda, and T. Hara. 1984. Antitumor activity of 1-beta-D-arabinofuranosylcytosine conjugated with polyglutamic acid and its derivative. Cancer Res. 44:25-30.

Li, C. 2002. Poly(L-glutamic acid)--anticancer drug conjugates. Adv Drug Deliv Rev. 54:695-713.

Li, C., J.E. Price, L. Milas, N.R. Hunter, S. Ke, D.F. Yu, C. Charnsangavej, and S. Wallace. 1999. Antitumor activity of poly(L-glutamic acid)-paclitaxel on syngeneic and xenografted tumors. Clin Cancer Res. 5:891-897.

Lodemann, E. 1981. Transport of D- and L-penicillamine by mammalian cells. Biochem Biophys Res Commun. 102:775-783.

Lowndes, S.A., and A.L. Harris. 2004. Copper chelation as an antiangiogenic therapy. Oncol Res. 14:529-539.

Maeda, H., G.Y. Bharate, and J. Daruwalla. 2009. Polymeric drugs for efficient tumor-targeted drug delivery based on EPR-effect. Eur J Pharm Biopharm. 71:409-419.

Maeda, H., L.W. Seymour, and Y. Miyamoto. 1992. Conjugates of anticancer agents and polymers: advantages of macromolecular therapeutics in vivo. Bioconjug Chem. 3:351-362.

Mamou, F., K.S. May, M.J. Schipper, N. Gill, M.S. Kariapper, B.M. Nair, G. Brewer, D. Normolle, and M.K. Khan. 2006. Tetrathiomolybdate blocks bFGF- but not VEGF-induced incipient angiogenesis in vitro. Anticancer Res. 26:1753-1758.

Matsubara, T., R. Saura, K. Hirohata, and M. Ziff. 1989. Inhibition of human endothelial cell proliferation in vitro and neovascularization in vivo by D-penicillamine. J Clin Invest. 83:158-167.

Maxfield, F.R. 1982. Weak bases and ionophores rapidly and reversibly raise the pH of endocytic vesicles in cultured mouse fibroblasts. J Cell Biol. 95:676-681.

Myers, C.E., L. Gianni, C.B. Simone, R. Klecker, and R. Greene. 1982. Oxidative destruction of erythrocyte ghost membranes catalyzed by the doxorubicin-iron complex. Biochemistry. 21:1707-1712.

Nori, A., K.D. Jensen, M. Tijerina, P. Kopeckova, and J. Kopecek. 2003. Tat-conjugated synthetic macromolecules facilitate cytoplasmic drug delivery to human ovarian carcinoma cells. Bioconjug Chem. 14:44-50.

Okuyama, S., and H. Mishina. 1981. Probable superoxide therapy of experimental cancer with D-penicillamine. Tohoku J Exp Med. 135:215-216.

Omelyanenko, V., P. Kopeckova, C. Gentry, and J. Kopecek. 1998. Targetable HPMA copolymer-adriamycin conjugates. Recognition, internalization, and subcellular fate. J Control Release. 53:25-37.

Pan, Q., C.G. Kleer, K.L. van Golen, J. Irani, K.M. Bottema, C. Bias, M. De Carvalho, E.A. Mesri, D.M. Robins, R.D. Dick, G.J. Brewer, and S.D. Merajver. 2002. Copper deficiency induced by tetrathiomolybdate suppresses tumor growth and angiogenesis. Cancer Res. 62:4854-4859.

Pelicano, H., D. Carney, and P. Huang. 2004. ROS stress in cancer cells and therapeutic implications. Drug Resist Updat. 7:97-110.

Raju, K.S., G. Alessandri, M. Ziche, and P.M. Gullino. 1982. Ceruloplasmin, copper ions, and angiogenesis. J Natl Cancer Inst. 69:1183-1188.

Santoliquido, P.M., H.W. Southwick, and J.H. Olwin. 1976. Trace metal levels in cancer of the breast. Surg Gynecol Obstet. 142:65-70.

Shen, W.C., H.J. Ryser, and L. LaManna. 1985. Disulfide spacer between methotrexate and poly(D-lysine). A probe for exploring the reductive process in endocytosis. J Biol Chem. 260:10905-10908.

Siddiqui, M.K.J., Jyoti, S. Singh, P.K. Mehrotra, K. Singh, and R. Sarangi. 2006. Comparison of some trace elements concentration in blood, tumor free breast and tumor tissues of women with benign and malignant breast lesions: An Indian study. Environ Int. 32:630-637.

Singer, J.W., R. Bhatt, J. Tulinsky, K.R. Buhler, E. Heasley, P. Klein, and P. de Vries. 2001. Water-soluble poly-(L-glutamic acid)-Gly-camptothecin conjugates enhance camptothecin stability and efficacy in vivo. J Control Release. 74:243-247.

Singer, J.W., P. De Vries, R. Bhatt, J. Tulinsky, P. Klein, C. Li, L. Milas, R.A. Lewis, and S. Wallace. 2000. Conjugation of camptothecins to poly-(L-glutamic acid). Ann N Y Acad Sci. 922:136-150.

Starkebaum, G., and R.K. Root. 1985. D-Penicillamine: analysis of the mechanism of copper-catalyzed hydrogen peroxide generation. J Immunol. 134:3371-3378.

Tew, K.D., L. He, S. Hutchens, T.E. VandenBerg, C.J. Pazoles, and D.M. Townsend. 2008. NOV-002, a glutathione disulfide mimetic, is a pleiotropic modulator of cellular redox balance. Biomed Pharmacother. 62:427-427.

Townsend, D.M., C.J. Pazoles, and K.D. Tew. 2008. NOV-002, a mimetic of glutathione disulfide. Expert Opin Invest Drugs. 17:1075-1083.

Ullman-Cullere, M.H., and C.J. Foltz. 1999. Body condition scoring: a rapid and accurate method for assessing health status in mice. Lab Anim Sci. 49:319-323.

Waud, W.R., S.D. Harrison, Jr., C.G. Temple, Jr., and D.P. Griswold, Jr. 1992. Antitumor drug cross-resistance in vivo in a murine P388 leukemia resistant to ethyl 5-amino-1,2-dihydro-2-methyl-3-phenylpyrido[3,4-b]pyrazin-7-ylcarbamate 2-hydroxyethane sulfonate hydrate (NSC 370,147) 370147. Cancer Chemother Pharmacol. 29:190-194.

Winterbourn, C.C., and D. Metodiewa. 1999. Reactivity of biologically important thiol compounds with superoxide and hydrogen peroxide. Free Radic Biol Med. 27:322-328.

Yucel, I., F. Arpaci, A. Ozet, B. Doner, T. Karayilanoglu, A. Sayar, and O. Berk. 1994. Serum copper and zinc levels and copper/zinc ratio in patients with breast cancer. Biol Trace Elem Res. 40:31-38.

Zou, Y.Y., Q.P. Wu, W. Tansey, D. Chow, M.C. Hung, C.C. Vej, S. Wallace, and C. Li. 2001. Effectiveness of water soluble poly(L-glutamic acid)camptothecin conjugate against resistant human lung cancer xenografted in nude mice. Int J Oncol. 18:331-336.

Zuo, X.L., J.M. Chen, X. Zhou, X.Z. Li, and G.Y. Mei. 2006. Levels of selenium, zinc, copper, and antioxidant enzyme activity in patients with leukemia. Biol Trace Elem Res. 114:41-53.

Chapter 3

Polypeptide-Conjugates of D-penicillamine and Idarubicin for Anticancer Therapy

3.1. Abstract

We investigated oxidative stress therapy of cancer with a novel combination of D-pen and ida in a synthetic dual drug conjugate (DDC). D-pen and Ida were covalently linked to poly(α)-L-glutamic acid (PGA), a completely biodegradable and biocompatible homopolypeptide, via reducible disulfide and acid-sensitive hydrazone bonds respectively. The DDCs showed sustained release of the bound drugs in conditions mimicking the intracellular release media (10 mM glutathione and pH 5.2) and were taken up by cancer cells in a time-dependent manner. The *in-vitro* cytotoxicity of DDCs was comparable to unconjugated Ida in several sensitive and resistant cancer cell lines and correlated with the rate of cell uptake. In a single equivalent-dose pharmacokinetic (PK) study, DDCs enhanced the drug exposure by 7-fold and prolonged the plasma circulation half-life ($t_{1/2}$) by 5-fold over unconjugated Ida. The therapeutic index (maximum tolerated dose; MTD) of DDCs was 2-3-fold higher than unconjugated drugs. When dosed at MTD, DDCs caused 89% tumor growth inhibition compared to 60% by unconjugated Ida alone and led to significant enhancement in the median survival (17%) of athymic *nu/nu* mice bearing NCI-H460 tumor xenografts.

3.2. Introduction

Oxidative stress therapy of cancer involves treatment with xenobiotics that cause elevation of intracellular reactive oxygen species (ROS). ROS are natural by-products of mitochondrial metabolism and cells maintain a low level of ROS as they have an important role in cell signaling pathways (Martin and Barrett, 2002; Murphy, 2009). However, at higher levels, ROS may cause direct damage to DNA, cause lipid peroxidation leading to membrane destabilization, and initiate apoptotic signals (Cejas et al., 2004; Chandra et al., 2000). We have shown that D-penicillamine (D-pen), an aminothiol, generates dose-dependent ROS in cancer cells and is cytotoxic (Gupte and Mumper, 2007). Recently, the involvement of p53 tumor suppressor protein that is highly sensitive to cellular ROS levels has also been implicated in apoptotic cell death induced by D-pen (Havre et al., 2002). However, a reactive thiol group, rapid clearance, low cellular permeability, strong plasma protein binding and higher effective concentrations are major barriers to the successful delivery of D-pen to cancer cells (Gupte and Mumper, 2007; Joyce et al., 1991; Joyce et al., 1989; Lodemann, 1981). We previously reported the synthesis of poly-α-L-glutamic acid-D-pen (PGA-D-pen) conjugate, where D-pen is covalently linked to PGA via intracellularly reducible disulfide bonds. PGA-D-pen enhanced the cell permeability of D-pen. Elevated cellular ROS levels upon uptake leading to the induction of apoptosis and enhancement in survival of mice bearing i.p. leukemia was reported (Wadhwa and Mumper, 2010). In the present study, we investigated a novel combination of ida and D-pen, delivered as dual drug conjugates (DDCs) of PGA, to further enhance the anticancer efficacy.

Ida, an anthracycline derivative, has been effective as first line treatment for acute leukemia and several other cancers (Borchmann et al., 1997). Anthracyclines act by several

mechanisms including DNA intercalation, topoisomerase II inhibition and p53 mediated apoptosis induction (Gewirtz, 1999). Cellular damage by anthracycline-iron (Fe) complexes via generation of ROS has been considered an important mechanism in their cytotoxicity (Minotti et al., 2004). The ROS generation is dependent on and is augmented by thiol mediated reduction of the anthracycline-Fe (III) complex to anthracycline-Fe (II) which is redox active. This reduction results in further generation of hydroxyl radicals that are the most damaging among ROS (Muindi et al., 1984; Xu et al., 2005), via Fenton type reactions (Held et al., 1996). Moreover, it has been shown that the anthracycline-iron complex can catalyze oxygen consumption by thiols and thus may augment ROS generation (Eliot et al., 1984). We hypothesized that DDCs co-delivering D-pen and Ida will be highly effective anticancer agents and reduce adverse events associated with administration of Ida leading to an increase in the therapeutic index. To the best of our knowledge, this is the first report investigating the combination of an anthracycline with an aminothiol for anticancer therapy through DDCs.

Conjugation of drugs to linear polymers like PGA, HPMA copolymer and polyethylene glycol via releasable linkers has several advantages. It has been shown to prolong plasma circulation, improve tumor accumulation and drug solubility (Duncan, 2003; Rodrigues et al., 1999; Ulbrich et al., 2003; Ulbrich et al., 2000). Longer circulation enables increased passive accumulation in the tumors. Further enhancement in tumor uptake may be achieved due to the presence of leaky, distorted vasculature in solid tumors and poor lymphatic drainage, the major source of clearance for macromolecules (Maeda et al., 2009; Maeda et al., 1992). Polymer drug conjugates (PDCs) have also been investigated for combination therapy of cancer to enhance therapeutic responses (Vicent, 2007). This

includes using single drug polymer conjugates in combination with chemotherapy (Herzog et al., 2005), synthesis of multi-functional conjugates (Vicent et al., 2005) and simultaneous delivery of two separate PDCs (Dharap et al., 2005). PGA is a linear homopolypeptide composed of L-glutamic acid monomer, an endogenous amino acid. It is very sensitive to cleavage by lysosomal cysteine proteases, cathepsins, and can be dosed at very high levels with no adverse events (Kishore et al., 1990; Wen et al., 2004). PGA has been widely investigated for drug conjugation (Li, 2002). PGA-PTX conjugate showed strong antitumor effect in preclinical studies and results of a phase III clinical trial in NSCLC patients were published recently whereby the conjugate was equally effective as chemotherapy controls, however, a greater anticancer effect was observed in the female patients (Chipman et al., 2006; Langer et al., 2008; Sabbatini et al., 2004).

The DDCs of the present study were investigated for anticancer efficacy in a non-small cell lung cancer (NCI-H460) model. Detailed analysis of the plasma and organ disposition kinetics was performed to study the *in-vivo* behavior.

3.3. Materials and Methods

3.3.1. Materials

Poly-α-L-glutamic acid sodium salt (MW 50-70 kDa), D-penicillamine (D-pen), tris(2-carboxyethyl)phosphine hydrochloride (TCEP), 1-ethyl-3-[3-dimethylaminopropyl] carbodiimide hydrochloride (EDC), glutathione and *N*-hydroxysuccinimide (NHS) were purchased from Sigma-Aldrich (St. Louis, MO). Slide-A-Lyzer® dialysis cassettes, 4-maleimidophenylbutyric acid hydrazide hydrochloride (MPBH), sepharose Cl-4B, buffers and all solvents were purchased from Thermo Fisher Scientific (Rockford, IL). Idarubicin hydrochloride was purchased from Synbias Pharma (Donetsk, Ukraine).

3.3.2. Synthesis of Idarubicin MPBH (1)

Idarubicin hydrochloride (16 mg, 0.03 mmol) and 4-maleimidophenylbutyric acid hydrazide hydrochloride (MPBH) (50 mg, 0.15 mmol) were dissolved in anhydrous methanol (10 mL). A few drops of trifluoroacetic acid were added and the reaction was stirred for 96 hr at room temperature under argon. The mixture was concentrated to 2 mL and precipitated from anhydrous ethyl acetate. The precipitate was separated by centrifugation. The precipitation was repeated three times and the product (**1**) was dried under vacuum (14 mg, 62%). ^{1}H NMR (400 MHz, CD_3OD): δ (ppm) = 1.17 (m, 3H), 1.93-2.03 (m, 7H), 2.32 (t, 2H), 2.65 (m, 2H), 3.0-3.12 (m, 3H), 3.52 (t, 1H), 6.96 (s, 2H), 7.21 (m, 4H), 7.89 (m, 2H), 8.29 (m, 2H); m/e (ESI): 753.37.

3.3.3. Synthesis of DDC (4)

2-(2-Pyridyldithio) ethylamine (PDE) hydrochloride was synthesized as described previously (Gnaccarini et al., 2006). PGA sodium (0.5 g) was dissolved in 5 mL deionized water cooled to 4^{o}C. Hydrochloric acid (1 N) was added drop-wise to precipitate PGA. The precipitate was washed with water until the pH was >5.0. The precipitate was lyophilized on a VirTis^{TM} AdVantage Freeze Dryer (SP Scientific, Gardiner, NY). Lyophilized PGA (50 mg, 0.83 μmol) was dissolved in anhydrous dimethylformamide (DMF) (5 mL). Then, 1-ethyl-3-[3-dimethylaminopropyl] carbodiimide hydrochloride (EDC) (63.9 mg, 0.33 mmol), N-hydroxysuccinimide (NHS) (18.10 mg, 0.16 mmol) and PDE (37.8 mg, 0.17 mmol) were added to the flask. The mixture was stirred for 12 hr at room temperature under an atmosphere of argon. The PGA-PDE conjugate (**2**) was precipitated by addition of ether and subsequent washing with water. The conjugate was dissolved by adding a few drops of 0.5 M sodium bicarbonate and pH was adjusted to 7.4 using 0.1 M PBS. The extent of conjugation was determined spectrophotometrically (ε = 8080 M^{-1} cm^{-1}, λ_{max} = 343 nm) by measuring the absorbance of pyridine-2-thione released upon the reduction of the conjugate in presence of 25 mM tris(2-carboxyethyl)phosphine hydrochloride (TCEP) for 1 hr.

To the solubilized PGA-PDE conjugate, D-pen (124 mg, 0.83 mmol) was added and the mixture was stirred for 12 hr at room temperature. The PGA-D-pen conjugate (**3**) was dialyzed against 10 mM PBS for 48 hr using a Slide-A-Lyzer dialysis cassette (Thermo Scientific, Rockford, IL). The extent of D-pen conjugation was determined by HPLC as described previously (Wadhwa and Mumper, 2010). To synthesize DDCs (**4**), the PGA-D-pen conjugate (containing 0.05 mmol D-pen) was reduced in the presence of TCEP (1 mM) for 5 min. TCEP was removed by centrifugation using an Amicon^{TM} Ultra-15 centrifugal

filter (Millipore, Bedford, MA) and Ida-MPBH (11.54 mg, 0.015 mmol) was added. The reaction was stirred for 12 hr at room temperature. The DDCs were purified by filtration with a sepharose CL-4B column (15 x 1.5 cm) using PBS pH 7.4 as the mobile phase, lyophilized and stored at -20^{o}C until further use. ^{1}H NMR (400 MHz, CD_3OD): δ (ppm) = 1.23-1.43 (m, 6H), 1.83-2.38 (s, broad, ~30H), 3.31-3.49 (m, broad ~12H), 3.56-3.67 (m, broad, ~6H), 7.86-8.26 (m, broad, ~21H). The molecular weight of PGA measured by viscosity and multi-angle laser light scattering (MALLS), as reported by the manufacturer, was 50-70 kDa. We determined the molecular weight before and after conjugation with dynamic light scattering (DLS) using a Nano-ZS^{TM} Zetasizer (Malvern, Worcestershire, UK). Toluene was used as a scattering standard. The refractive index increment (dn/dc) of 0.176 was used to run ten different standards in the concentration range of 5 mg/ml to 0.05 mg/ml (Van et al., 2010). The DDCs at concentration within the standard curve were analyzed to obtain the molecular weight after conjugation. The average molecular weight of DDCs determined by DLS, was found to be 68 ± 8.9 kDa before conjugation and 101.6 ± 1.67 kDa after conjugation. Although ^{1}H-NMR showed the presence of aromatic protons of Ida, it was difficult to estimate the extent of conjugation. Therefore, a spectrophotometric method was used to determine Ida concentrations in the conjugate (ε = 8887.8 M^{-1} cm^{-1}, λ_{max} = 483 nm). Additionally, the Ida content was also measured by HPLC following acidification of DDC with 1 N HCl for 30 min. The final conjugate had approximately 4 moles of Ida (35 mg Ida/g PGA) and 36 moles (89 mg D-pen/g of PGA) of D-pen per PGA chain (theoretical average molecular weight of 60 kDa). This converts to a weight ratio of 2.515 for D-pen:Ida.

3.3.4. Circular Dichroism Study

Spectra were acquired on a Chirascan™-plus Circular Dichroism (CD) Spectrometer (Applied Photophysics, Leatherhead, UK). The spectra were measured from 185 nm to 260 nm at 25°C, pH 7.4 and PGA concentration of approximately 50 µM. Two independent measurements were performed for each sample. Simultaneous UV absorbance spectra were measured in the same wavelength range to monitor scattering and optimize sample concentrations.

3.3.5. Cell Culture

The HL-60, P388 and NCI-H460 cells were obtained from American Type Cell Culture Collection (ATCC; Rockville, MD). HL-60/VCR (P-gp) and P388/ADR (MRP-1) cells were provided by Dr. Baer (Roswell Park Cancer Institute, Buffalo, NY). The cells were cultured in RPMI 1640 medium (Invitrogen, Carlsbad, CA). The media were also supplemented with 10% Fetal Bovine Serum, 100 U/mL of penicillin and 100 µg/mL of streptomycin (ATCC, Rockville, MD). All cell lines were maintained at 37°C in a humidified 5% CO_2 incubator.

3.3.6. HPLC Method

Analysis of Ida concentration was performed by HPLC on Finnigan Surveyor™ HPLC system (Thermo Electron Corp., San Jose, CA) equipped with a fluorescence detector using a Synergi® Hydro-RP column (250 mm x 4.6 µm; 4 µm; 25 µL injection volume; Thermo Electron Corp., San Jose, CA). The mobile phase containing (v/v) 65% 0.1 M sodium dihydrogen phosphate (adjusted to pH 2.2 using o-phosphoric acid) + 35%

acetonitrile was pumped at 1 mL/min. The retention time of Ida was 6.5 min and standard curve was constructed in the range 5 ng/mL – 1000 ng/mL. The limit of detection was 1 ng/mL. D-pen was analyzed by the HPLC method described previously (Wadhwa and Mumper, 2010).

3.3.7. Mice Plasma and Tissue Sample Analysis

To analyze DDCs in the plasma, samples were acidified with 1 N HCl and incubated for 30 min to release the conjugated Ida. Acetonitrile (five volumes) was added to the samples to precipitate proteins. The samples were diluted in mobile phase, vortexed and centrifuged (14,000 g x 10 min) after 15 min. The supernatants were analyzed by HPLC. Spike standard curves of Ida and DDCs were prepared in mouse plasma and the percent recovery was calculated prior to actual sample analysis.

Weighed tissue samples were added to lysis vials containing zirconium oxide beads and homogenized in the presence of water on a Precellys®-24 Tissue Homogenizer (Bertin Technologies, France). Further processing of the homogenized tissue was similar to plasma samples.

3.3.8. *In-vitro* Release of the Conjugated Drugs

The DDCs were incubated in 0.1 M MES buffer pH 5.2 to mimic the acidic endosomal environment. The samples were also incubated in 10 mM phosphate buffer pH 7.4 to validate the pH specific release of Ida. At predetermined time, the sample was injected into HPLC column to determine the amount of Ida released from the conjugate. D-pen

release from the conjugate in the presence of 10 mM glutathione (GSH) was determined. Samples were analyzed by HPLC.

3.3.9. Cell Uptake

To investigate the cellular uptake of DDCs, human leukemia (HL-60) cells (1 x 10^6) were incubated with 1 μM DDCs (Ida equivalent dose) for 4 hr and 12 hr. The cells were visualized live using Zeiss 510 Meta Laser Scanning Confocal Microcope (63 x 1.4 NA oil Plan-Apochromat objective; Excitation: 488 nm and emission: 540 nm; Carl Zeiss, Thornwood, NY). The images were processed using Zeiss AIM Viewer (Carl Zeiss, Thornwood, NY).

Quantitative analysis of cell uptake was performed by flow cytometric analysis. Briefly, HL-60 cells were treated with either Ida or DDCs for a predetermined time. Further processing was done at 4^{o}C. The cells were washed two times with and resuspended in cold 10 mM PBS containing 2% sodium edetate and 10% FBS. Analysis was immediately performed on a BD^{TM} LSR II Flow Cytometer (BD Biosciences, Franklin Lakes, NJ) using the 488 nm laser for excitation.

3.3.10. Stability of DDCs in Mouse Plasma

To determine the stability of the hydrazone linkage between Ida and PGA, 0.1 mL of DDCs were incubated with 0.9 mL mouse plasma at 37^{o}C for selected times (0.25, 0.5, 1, 2, 4, 8 and 24 hr). Samples were divided in two equal parts. One part was acidified with 1 N HCl for 30 min. Both samples were further processed as described above. Analysis was

performed by HPLC. The percent of Ida conjugated was calculated by subtracting the results of acidified samples from those not acidified.

3.3.11. Cytotoxicity Studies

Leukemia cells were incubated in 96 well round-bottom cell culture plates at 1 x 10^4 cells/well few hours before treatment. NCI-H460 cells were incubated in 96 well flat-bottom cell culture plates at 1 x 10^4 cells/well overnight to allow for attachment. The final dilutions for all the treatment groups were made in the culture medium. The cell viability was measured at 48 and 72 hr following treatment by addition of (3-(4, 5-dimethylthiazolyl-2)-2, 5-diphenyltetrazolium bromide) (MTT) reagent at a final concentration of 0.5 mg/mL. The media was removed (centrifugation preceded aspiration in case of leukemia cells) and resulting formazan crystals were dissolved in DMSO and the absorbance was measured at 570 nm on a Synergy^{TM} 2 Multi-Detection Microplate Reader (Biotek, Vinooski, VT). The results were expressed as percent viable cells compared to untreated control.

3.3.12. Plasma Disposition and Biodistribution Studies

NCI-H460 cells (1 x 10^6) were implanted subcutaneously (s.c.) in the right flank of male athymic *nu/nu* mice (20-25 g). When the tumors attained a size of approximately 200 mm^3 (day 13), the mice were injected i.v. with Ida (3 mg/kg) or DDC (3 mg Ida equivalent/kg and 7.5 mg D-pen equivalent/kg). The mice (n=3/time point) were sacrificed at selected times between days 13 and 15 (t= 0.08, 0.25, 0.5, 1, 4, 8, 24 and 48 hr). Blood was collected by cardiac puncture. Subsequently, tumors and organs (heart, liver, kidneys, lungs and spleen) were blotted with a filter paper and collected in pre-weighed lysis tubes

containing zirconium oxide beads. Plasma was separated from blood with Lithium-Heparin microtubes (Sarstedt, NC). Plasma and organ samples were stored at -80^{o}C until further analysis. The samples were analyzed for Ida concentration by HPLC as described above. The data were analyzed by non-compartmental pharmacokinetic analysis using WinNonlin® 4.0 (Pharsight, Mountain View, CA).

3.3.13. Antitumor Efficacy

Athymic *nu/nu* mice bearing NCI-H460 tumor xenografts (40 ± 10 mm^3) were intravenously administered different treatment groups. A dosing regimen of Q2dx3 was followed based on a dose escalation study performed in BALB/c mice (20-25 g; n= 3-4/dose). The mice were monitored for tumor volume, body weight and a body condition score (BCS) was assigned every 24-48 hr (Ullman-Cullere and Foltz, 1999). The length of the study was 60 days from tumor implantation. A loss of body weight that is 20% or greater, a 10% or greater loss over three consecutive days, or a BCS of 2 or lower was considered as a criteria for euthanasia. Tumors were not allowed to grow larger than 1500 mm^3. All experiments involving mice were performed with the approval of the University of North Carolina Institutional Animal Care and Use Committee.

3.3.14. Statistical Analysis

Organ pharmacokinetic data was analyzed by regular two-way ANOVA followed by Bonferroni post-test to compare the means at individual time points between different treatments. Tumor volume (TV) were calculated as, TV (mm^3) = ((length (mm) x width^2 (mm))/2). Tumor growth inhibition (TGI) was calculated as, TGI (%) = (($TV_{untreateed}$ –

$TV_{treatment}$)/$TV_{untreated}$) x 100. Differences between TVs in the anticancer efficacy studies were analyzed by one-way ANOVA followed by Dunnett's post-test. Survival curves were plotted by Kaplan-Meier method and analyzed by Mantel-Cox log rank test. Differences were considered significant if the p values were less than 0.05.

3.4. Results and Discussion

3.4.1. Synthesis of Dual Drug Conjugates

The DDCs were synthesized to contain two drugs – D-pen and Ida. Two distinct mechanisms for the release of the conjugated drugs were incorporated in the DDCs. Ida was derivatized with MPBH (**Figure 3.1**) to incorporate acid cleavable hydrazone linkage in the DDC. The hydrazone linkage is expected to cleave in the acidic endosomal compartment upon cellular uptake (Ulbrich and Subr, 2004). Ida-MPBH (**1**) was conjugated to DDCs (**4**) via thioether linkage (**Figure 3.2**). D-pen was conjugated to PGA through disulfide linkage as described previously. The disulfide bond has been shown to release upon cellular uptake in the endosomes by an enzymatic pathway mediated by GILT as well as in the cytosol by GSH and thioredoxin (Arunachalam et al., 2000; Gao et al., 2010). Two separate HPLC assays were developed to analyze both the drugs released from the conjugate.

Previously reported PGA-D-pen conjugate was used as the starting material for the synthesis of DDCs (Wadhwa and Mumper, 2010). Derivatization with MPBH provides a maleimide end group that can be covalently linked to the exposed sulfhydryl groups on PGA-D-pen (**3**) under controlled reduction using TCEP. The reduction reaction was optimized to release 10-12% of the conjugated D-pen that can be analyzed by HPLC. It is important to perform the disulfide reduction in the presence of a metal chelator like EDTA and immediately purify the partially reduced conjugate to avoid oxidative cross-linking of the polymer chains. The conjugate was buffer exchanged with PBS pH 7.4 using a sepharose CL-4B column before reaction with Ida-MPBH (**1**) to provide an optimum pH for maleimide-thiol reaction. The pH range of 6.5 to 7.5 provides high specificity of maleimides towards sulfhydryls and reaction with free amines is negligible (Partis et al., 1983).

Derivatization of daunorubicin to provide maleimide end groups was reported by Kratz and co-workers who developed highly active drug-transferrin conjugates while the amide linked conjugates were inactive (Kratz et al., 1997). Similar derivatives of doxorubicin developed to bind albumin *in-situ*, showed superior antitumor efficacy (Kratz et al., 2002). Derivatization of doxorubicin with maleimide end group and conjugation to elastin like polypeptides (ELPs) has been reported with increased antitumor efficacy (Dreher et al., 2003; Mackay et al., 2009).

PGA has been reported to undergo a pH dependent helix-coil transition with an almost complete conversion to α-helix below pH 4.5 and greatly reduced water solubility (Krejtschi and Hauser, 2011; Lumry et al., 1964). As the PGA used in the synthesis of PGA-D-pen was previously acid-precipitated, lyophilized and solubilized in DMF, it was expected to be in the helix conformation during the reaction. The PGA-D-pen conjugate was solubilized in sodium bicarbonate with a resulting pH of 8.0 - 8.5. Interestingly, CD spectra measurements showed the presence of PGA in helical conformation in a completely water soluble state (**Figure 3.3**). This may be due to hydrophilicity imparted by the D-pen molecules on the outer side of the helix that may lead to the solubilization while the core may contain some unionized carboxyl groups that help stabilize the helix.

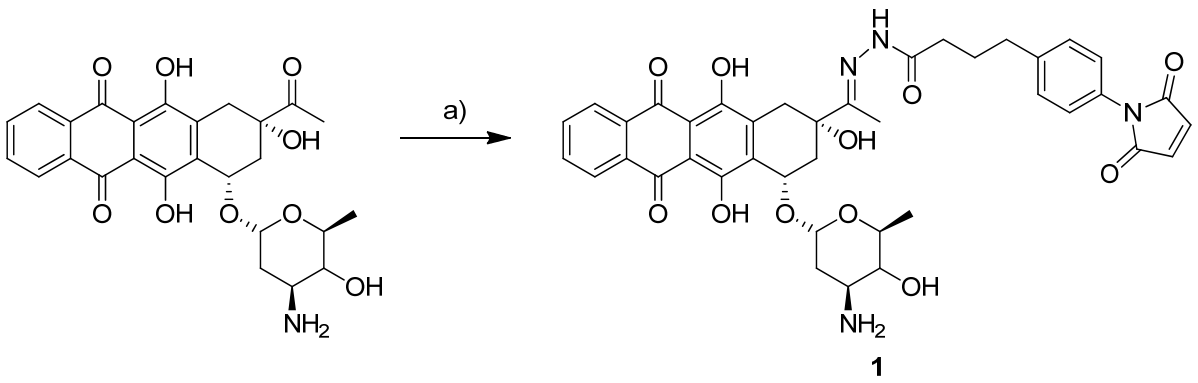

Figure 3.1 Synthesis of Ida-MPBH.
Reagents: a) Anhydrous methanol, trifluoroacetic acid and MPBH

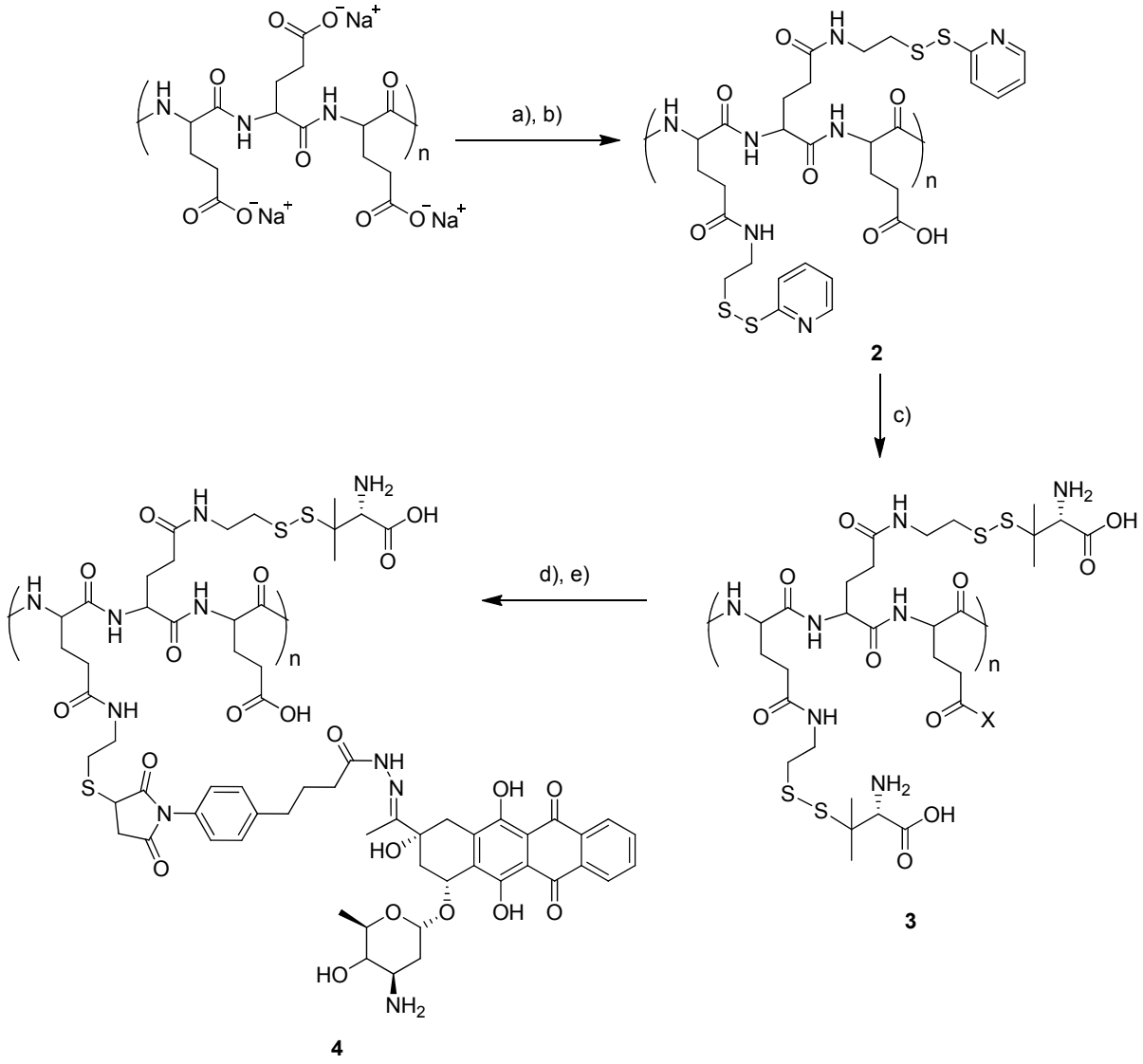

Figure 3.2 Synthesis of dual drug conjugates (DDCs).
Reagents: a) 1 N HCl, Lyophilization; b) PDE, EDC, NHS, DMF; c) D-pen, PBS pH 7.4; d) 1 mM TCEP, 5 min; e) Ida-MPBH.

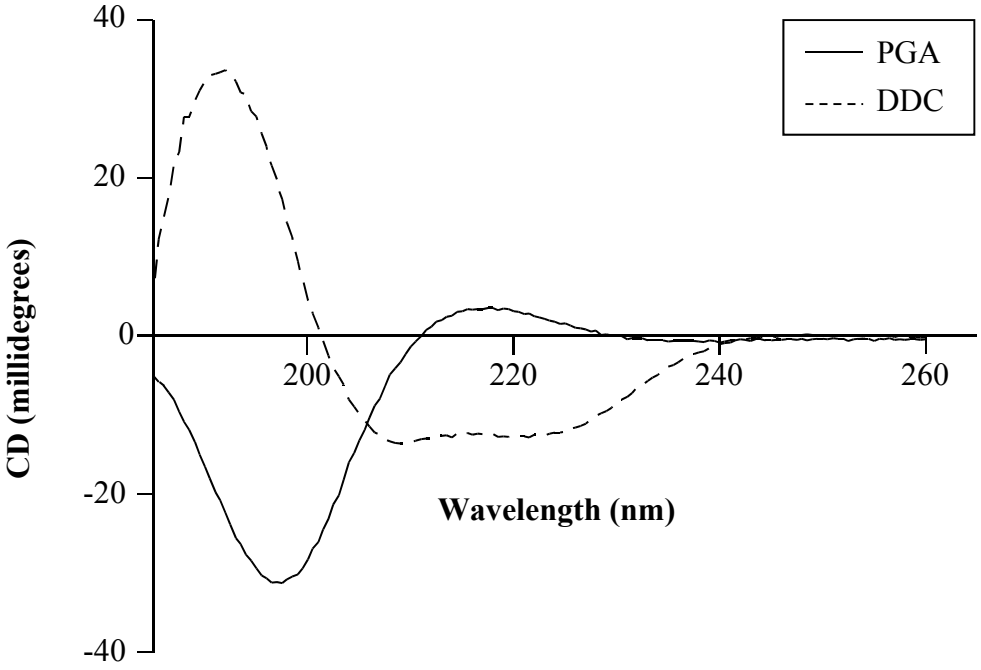

Figure 3.3 Circular dichroism spectra of PGA and DDC.
The spectra before conjugation were compared with that of dual drug conjugate at 25^{o}C and PGA concentration of approximately 50 μM. Each value is a mean of two independent measurements.

3.4.2. *In-vitro* Drug Release

The DDCs released 90% of hydrazone-conjugated Ida within 14-16 hr of incubation (**Figure 3.4A**). However, the conjugate was stable at pH 7.4 with less than 10% Ida being released at the end of 16 hr. This is in agreement with what has been observed with several polymeric conjugates where doxorubicin was conjugated via hydrazone linkage (Rodrigues et al., 1999; Etrych et al., 2002). The rate of hydrolysis of hydrazone (imine) bond increases with a decrease in the pH as the rate limiting step in the hydrolysis changes from attack of hydroxyl anion on the protonated imine leading to carbinolamine formation to the decomposition of carbinolamine to the starting products i.e. the ketone and free amine (D'Souza and Topp, 2004). Therefore, the conjugate is expected to be stable in circulation and only release the bound drug upon cellular uptake. Some degree of release may occur in the extracellular matrix environment in areas of low pH within the tumor. Several studies have reported conjugation of doxorubicin to drug carriers via hydrazone bonds and subsequent intracellular release.

D-pen was completely released in the presence of 10 mM GSH within 3 hr (**Figure 3.4B**). The normal range of intracellular GSH concentrations is 1–10 mM. Cancer cells usually have low concentrations of reduced GSH due to metabolic stress. Therefore, the cellular release is expected to occur at a reduced rate. However, disulfide reduction is also mediated enzymatically by GILT and thioredoxin as discussed above. Some degree of disulfide reduction has also been shown to occur at the cell surface mediated by thiols associated with membrane proteins. Based on this observation, the two drugs are expected to be released from the conjugate if similar conditions are encountered intracellularly.

Fig. 3.4A

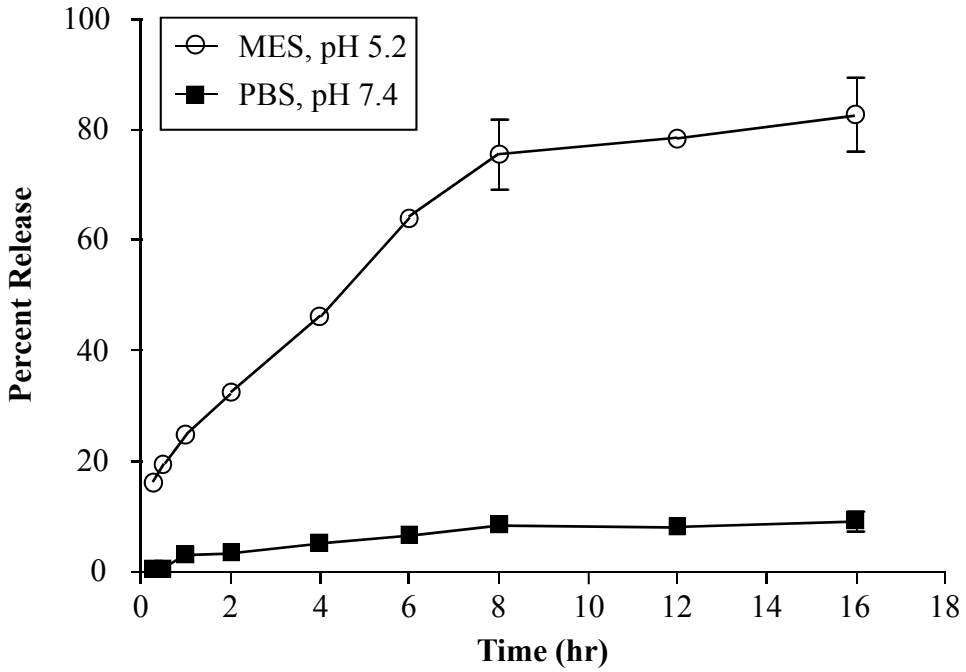
MES, pH 5.2
PBS, pH 7.4
Percent Release
Time (hr)
0
20
40
60
80
100
0
2
4
6
8
10
12
14
16
18

Fig. 3.4B

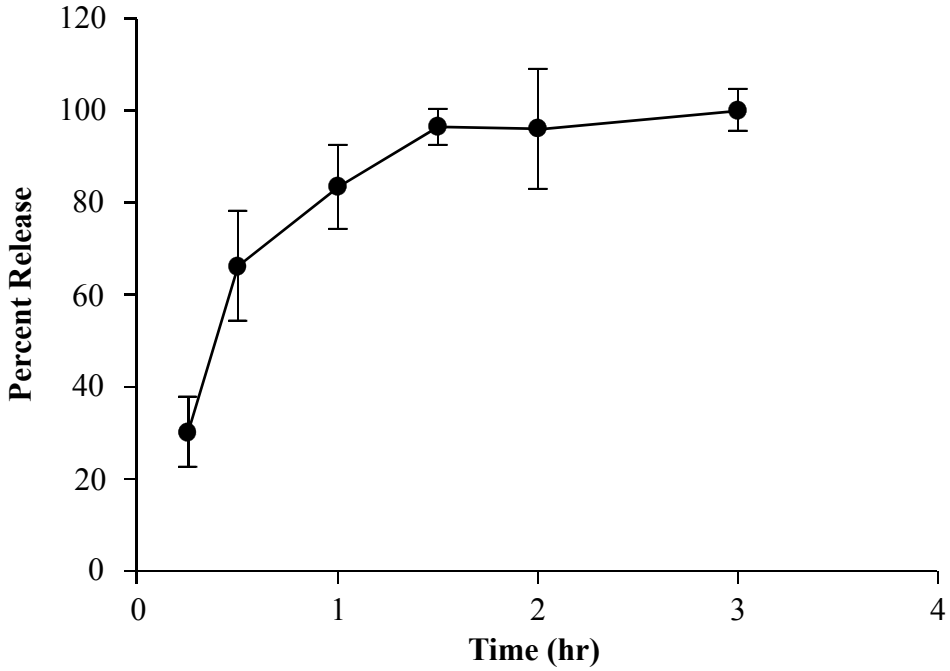

Figure 3.4 *In-vitro* release of D-pen and Ida from DDC.
Values represent mean ± SD (n=3).
A. Release of D-pen was investigated in the presence of 10 mM GSH.
B. Dependence of Ida release on pH was investigated at pH 5.2 and 7.4, respectively.

3.4.3. Cell Uptake

Fluid-phase endocytosis is the major mechanism of cellular entry for PDCs that do not have cell-specific moieties attached to them. In case of fluorescently labeled PDCs, endocytic uptake is characterized by pitted pattern of fluorescence while a diffused fluorescence indicates predominantly cytosolic delivery (Nori et al., 2003). Time dependent cell uptake of DDCs was monitored by tracking the fluorescence of Ida. The cellular uptake of DDCs was qualitatively assessed by confocal microscopy in HL-60 cells previously shown to be sensitive to treatment with PGA-D-pen conjugate. Endocytic uptake is evident by the pitted pattern of fluorescence. The cells showed a time dependent increase in the fluorescence upon treatment with the DDC as observed after 4 hr and 12 hr of treatment (**Figure 3.5A**). The cell uptake was quantitatively assessed by flow cytometry. The fluorescence intensity (FI) increased 3-fold over 24 hr treatment (**Figure 3.5B**). However, the FI was 4-fold lower than free Ida at similar dose and time. Ida is a hydrophobic compound and is expected to be cell permeable with faster cell uptake compared to DDCs (Hollingshead and Faulds, 1991). In addition to the uptake barrier, drug release also contributes as a barrier in successful drug delivery with PDCs. Although this may profoundly affect the effectiveness *in-vitro*, this may lead to fewer adverse events due to reduced non-target organ uptake and an increase in the overall therapeutic index as has been observed with some other PDCs. Further, based on the concept of EPR effect, a higher tumor accumulation of macromolecules due to leaky vasculature and poor lymphatic drainage may enhance the overall efficacy of DDCs (Maeda et al., 2009).

Fig. 3.5A

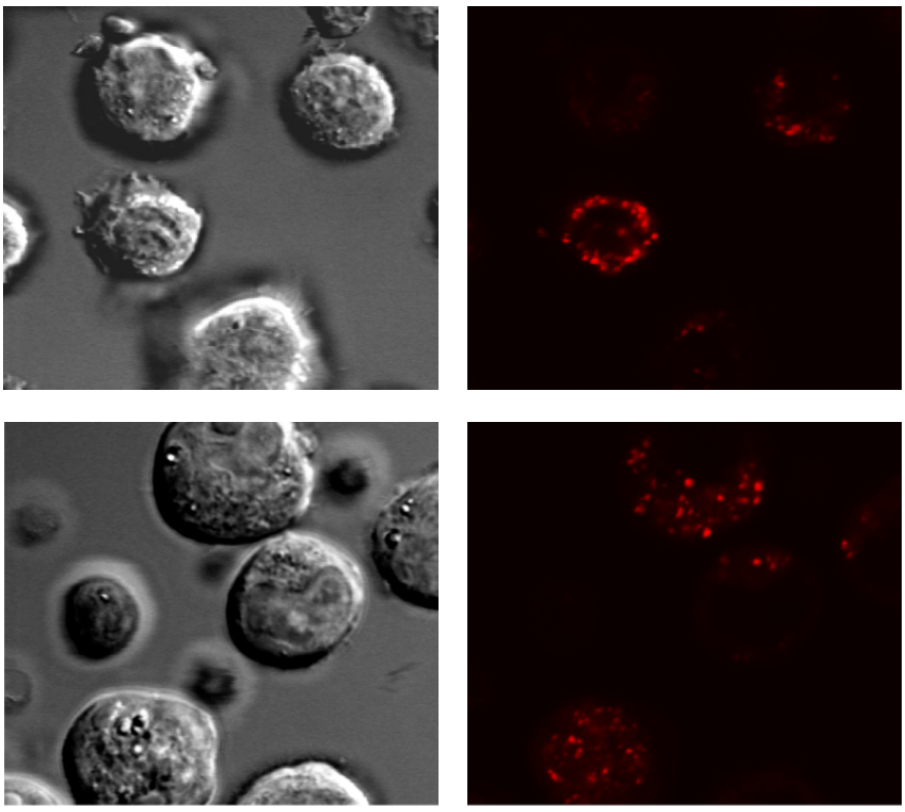

Fig. 3.5B

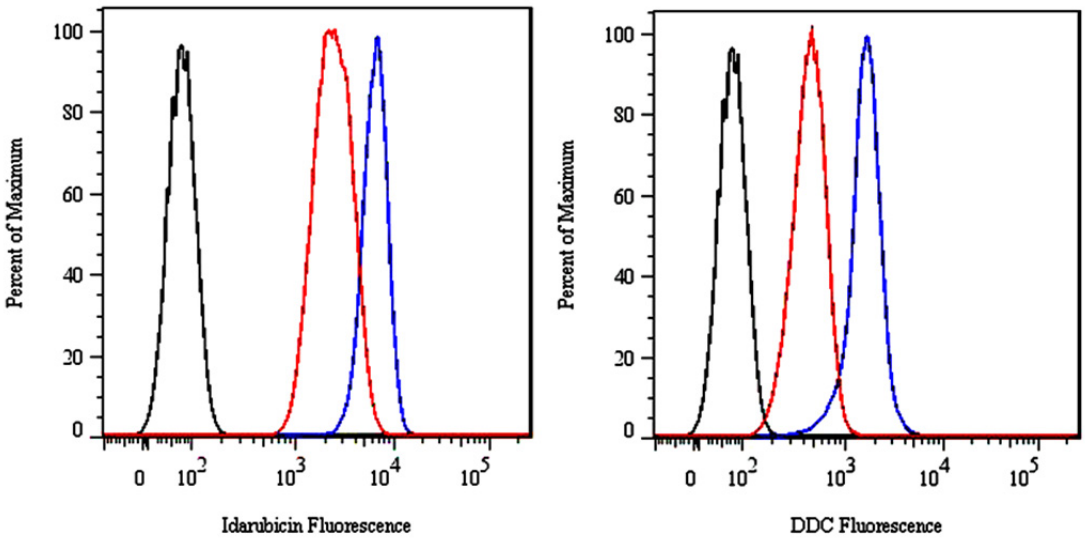

Fig. 3.5C

Time (hr)	Mean Fluorescence Intensity	
	Ida	DDC
1	2,470.3	453.8
24	6,307.8	1,599.3

Figure 3.5 Cell uptake of DDC.
A. Confocal microscopic visualization of HL-60 cells for the uptake of DDC showing the differential interference contrast (left) and fluorescence images respectively after 4 hr (top) and 12 hr (bottom) of treatment with DDC.
B. Quantitation of cell uptake by flow cytometric analysis of HL-60 cells showing fluorescence intensity (FI) of untreated cells (black), at 1 hr (red) and 24 hr (blue) after treatment with idarubicin (left) or DDCs (right).
C. Table showing the FI representing the flow cytometric histograms in (B).

3.4.4. Stability of DDCs in Mouse Plasma

The stability of DDCs in mouse plasma at 37^{o}C was determined using the HPLC assay. The results showed that the DDCs were stable in mouse plasma for 24 hr with no significant drug release (**Figure 3.6**). This ensures the stability during the longer circulation of DDCs and higher concentrations of conjugated drug to accumulate in the tumor. In aqueous solutions, acylhydrazones are susceptible to hydrolysis in acidic conditions leading to the formation of starting products. This provides specific release of conjugated drugs upon acidification of endosomes thus minimizing extracellular drug release. The range of sensitivity for hydrazone linkages in PDCs has been studied and Although hydrazone linakges have been reported to be stable in serum for at least 24 hr (Greenfield et al., 1990), it is important to determine the stability for individual conjugates as involvement of physicochemical and steric factors may lead to increase or decrease in stability (Rodrigues et al., 1999). Drugs have also been conjugated to polymers through *cis*-aconityl linkage, which also leads to the release of bound drug at endosomal pH. However, Ulbrich and co-workers recently showed that hydrazone bound HPMA copolymer-dox conjugates were more active than *cis*-aconityl conjugates (Ulbrich et al., 2003).

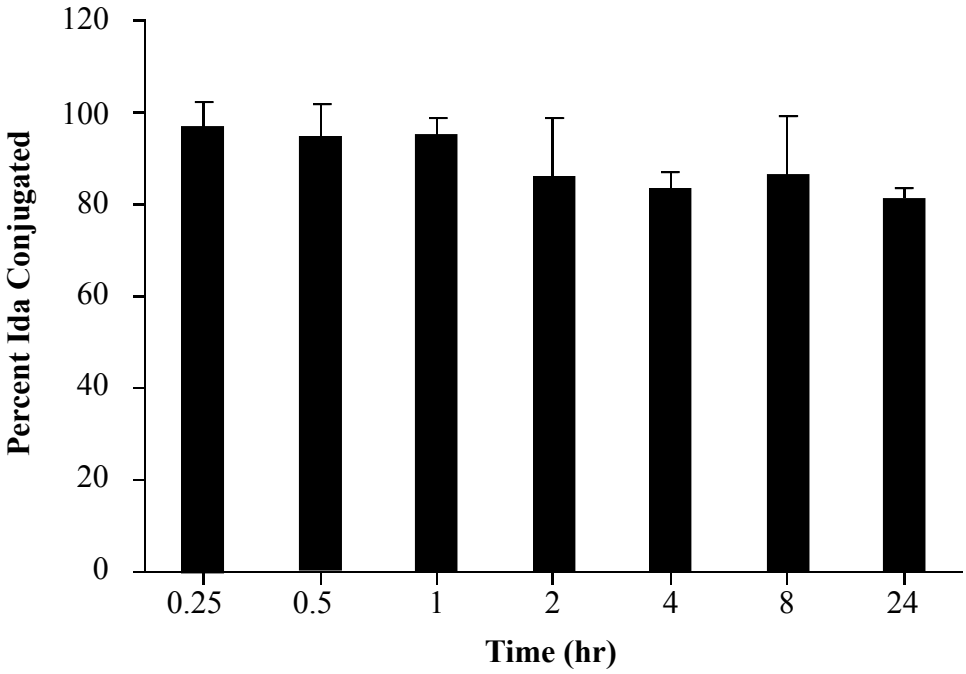

Figure 3.6 Stability of DDC in mouse plasma.
Stability of the hydrazone linkage between Ida and PGA was investigated *in-vitro* in mouse plasma in shaking water bath at 37^{o}C. Analysis was performed by HPLC.

3.4.5. Cytotoxicity Studies

The *in-vitro* cytotoxicity of DDCs was determined in both sensitive and resistant cancer cells. As the cellular entry mechanism of DDCs is distinct from small molecules, they are expected to avoid the efflux mechanisms and thus overcome resistance. This has been shown with HPMA copolymer conjugates of ADR that were comparably less sensitive to resistance mechanisms (Minko et al., 1999). However, the drug released in the cytosol is still subject to efflux.

In our studies, DDCs were comparable in cytotoxic potential to free Ida while D-pen was inactive (data not shown) at the corresponding doses in murine leukemia (both sensitive and resistant) and NSCLC cells (**Table 3.1**). However, both the sensitive and resistant human leukemia cells (HL-60) were significantly less sensitive to DDCs than Ida. The overall cytotoxicity of DDCs may be dependent on a combination of the rate of endocytic uptake, rate of drug release and the efficiency of the efflux mechanism. As noted above, the rate of cell uptake of the DDCs in HL-60 cells was 4-fold less than Ida. This correlates well with the almost 3-fold difference in the cytotoxic potential. To further examine the lag phase involved in the cytotoxicity of DDCs, we determined cell viability at 72 hr after treatment and compared in to the effect at 48 hr after treatment. In most of the cell lines tested, the IC_{50} values at 72 hr were lower than at 48 hr and for human leukemia cells. Additionally, the difference between the IC_{50} of Ida and DDCs at 72 hr reduced indicating a relatively decreased sensitivity towards resistance mechanisms.

Cell line	48 hr, IC_{50} (nM)		72 hr, IC_{50} (nM)	
	Ida	**DDC**	**Ida**	**DDC**
HL-60	32.7 ± 1.7	98.9 ± 4.4	27.5 ± 2.1	53.7 ± 4.3
HL-60/VCR	64.5 ± 3.1	199.3 ± 13.4	45.4 ± 2.8	97.7 ± 6.0
P388	9.4 ± 2.7	9.7 ± 2.1	7.3 ±2.1	10.1 ± 3.2
P388/ADR	281 ± 48.5	294.2 ± 75.21	162.6 ±5.6	213.2 ± 8.5
NCI-H460	61.3 ± 22.1	86.6 ± 18.36	55.2 ±15.1	96.2 ± 7.4

Table 3.1 Effect of Dual Drug Conjugate (DDC) treatment on cancer cell via**bility.**
Dose and time dependent effect of DDC treatment on cancer cell viability was investigated by MTT assay in resistant (HL-60/VCR and P388/ADR) and sensitive (HL-60 and P388) leukemia and non-small cell lung cancer (NCI-H460) cells. Values represent mean ± SD (n=6).

3.4.6. Plasma Disposition of DDCs

A dose-equivalent pharmacokinetic study was performed where a single dose of DDCs or Ida was injected i.v. and blood was collected at different time points after administration. In case of DDCs, total Ida (conjugated + unconjugated) in plasma was determined by acidification prior to analysis. DDCs showed a rapid distribution followed by a slower elimination phase (**Figure 3.7A**). The $t_{1/2}$ of DDCs was 15.6 hr which is almost 5-fold longer than Ida. DDCs enhanced the drug exposure by 7-fold as indicated by the area under the plasma concentration-time curve ($AUC_{0\text{-last}}$) (**Table 3.2**). In comparison, similar PGA-CPT conjugates synthesized using a 50 kDa PGA, showed just over 1.8-fold enhancement in the plasma AUC over CPT (Bhatt et al., 2003). Liposomal and nanoparticulate (solid lipid) formulations of Ida have also been reported previously with prolonged circulation and enhanced drug exposure (Santos et al., 2005; Zara et al., 2002). However, due to the lipophilicity of Ida, it is challenging to keep it entrapped in the delivery system and achieve reproducible drug release. The plasma concentrations after 5 min of administration, were 21.5-fold higher for DDC (3015 ng/mL) than Ida (140.2 ng/mL). The plasma circulation half-life ($t_{1/2}$) of Ida was 3.2 hr. Xenobiotics with small molecular weight are efficiently cleared by glomerular filtration and therefore, it was not surprising to observe a rapid decline in the blood levels of Ida with no detectable levels after 8 hr. The formation of its major metabolite, idarubicinol, and its effect on the overall circulation time was not taken into account (Hollingshead and Faulds, 1991).

DDCs are expected to be negatively charged in physiological conditions due to residual carboxyl groups on PGA. This may increase their uptake by the components of the reticuloendothelial (RES) system. A faster distribution may also be caused by metabolism of

the polymer in plasma leading to the formation of smaller entities with different rates of elimination. It has been previously reported for PGA that the amide bonds in the polymer chain are more susceptible to hydrolysis than the covalent bonds linking the drugs. An interesting example is the PGA-PTX conjugate where PTX is attached to PGA through an ester bond, however, the major degradation products *in-vivo* are mono and diglutamyl-PTX derivatives (Shaffer et al., 2007).

3.4.7. Biodistribution Studies

The distribution kinetics of DDCs vs. Ida was studied in liver, kidney, heart, lungs and spleen which constitute the most perfused organs of the body. The tumor accumulation at 4, 8 and 24 hr after administration was significantly higher for DDCs (5.7-fold at 24 hr) than Ida (**Figure 3.7B**). This may be explained by the passive accumulation as a result of a combination of longer plasma $t_{1/2}$ and possibly, the EPR effect. For comparison, a 6-fold enhancement in tumor exposure was reported for PGA-CPT conjugates compared to CPT (Bhatt et al., 2003).

In clinical setting, treatment with Ida is associated with cardiotoxicity that can be a dose-limiting factor although the severity in comparison to doxorubicin is lower (Chan-Lam et al., 1992; Platel et al., 1999). The short-term single equivalent dose pharmacokinetic study showed that the cardiac accumulation of Ida was significantly reduced with DDCs (**Figure 3.7C**). The peak levels of Ida detected in heart were 4.8-fold higher than the peak levels with DDC ($p<0.001$). This may lead to significant enhancement in the doses that can be delivered to patients in the clinic. However, the levels in heart with DDCs were sustained at lower levels due to slower clearance with the concentrations becoming higher than free Ida at 24 hr

and beyond. This is the reason that the predicted PK parameters calculated by the non-compartmental analysis show comparable AUC values while an increased MRT and $t_{1/2}$ for DDCs (**Table 3.2**). A long-term multiple dosing study will perhaps indicate if these sustained levels stay effectively lower than those that can cause clinical toxicity.

The liver uptake of DDCs was significantly higher than Ida with almost 15% of the injected dose (i.d.) found in liver at 1 hr compared to 4% i.d. of Ida at 30 min after administration (**Figure 3.7E**). Accumulation in liver and spleen has been shown for poly-γ-D-glutamic acid and its possible that PGA may have similar effects (Sutherland et al., 2008). As mentioned above, the charge and the molecular size make DDCs prone to uptake by phagocytic cells in the circulation and in the organs of the RES system. The difference in accumulation of DDCs and Ida in spleen was not as significant as that observed in liver. Significant accumulation of Ida in kidneys is reflective of the rapid clearance from plasma while DDCs showed a sustained slow rate of kidney accumulation (**Figure 3.7G**). Higher kidney concentrations may manifest as urotoxicity in clinical settings.

Fig. 3.7A

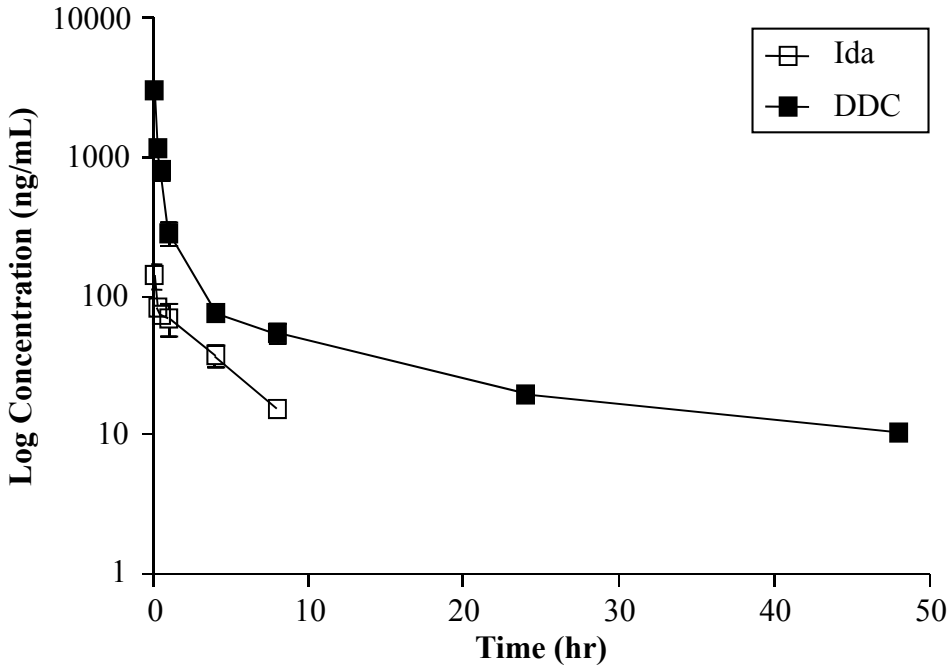
10000
1000
100
10
1
Log Concentration (ng/mL)
0
10
20
30
40
50
Time (hr)
Ida
DDC

Fig. 3.7B

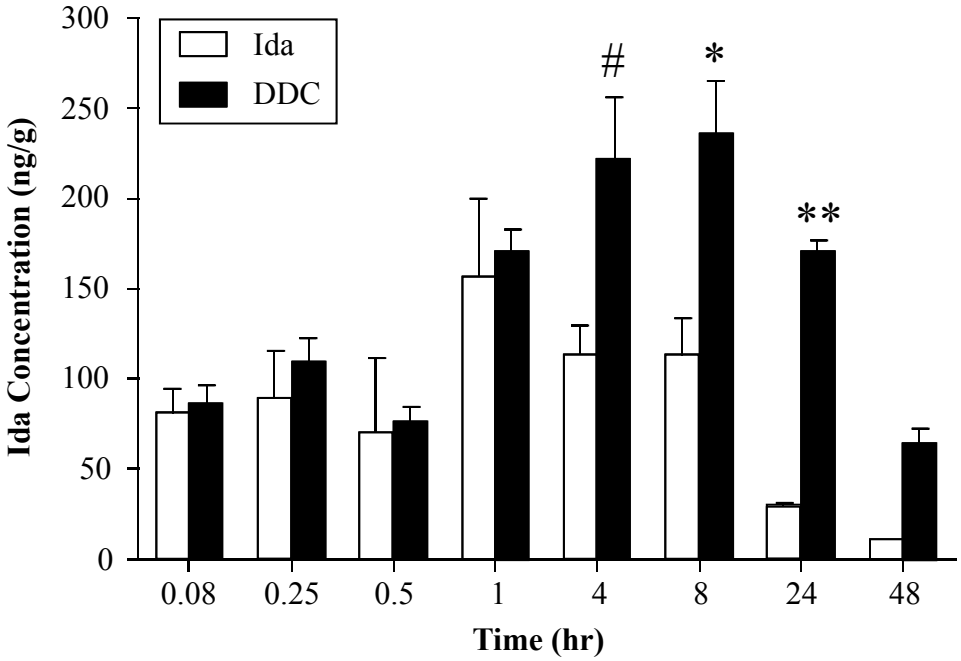
Ida
DDC
Ida Concentration (ng/g)
300
250
200
150
100
50
0
#
*
**
0.08
0.25
0.5
1
4
8
24
48
Time (hr)

Fig. 3.7C

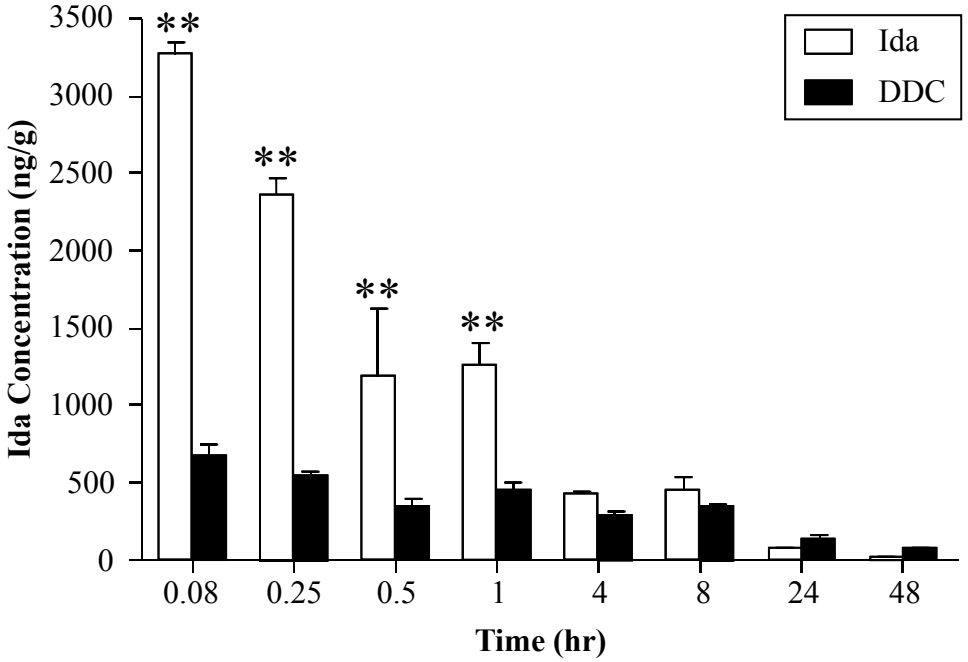
Ida
DDC
Ida Concentration (ng/g)
3500
3000
2500
2000
1500
1000
500
0
**
**
**
**
0.08
0.25
0.5
1
4
8
24
48
Time (hr)

Fig. 3.7D

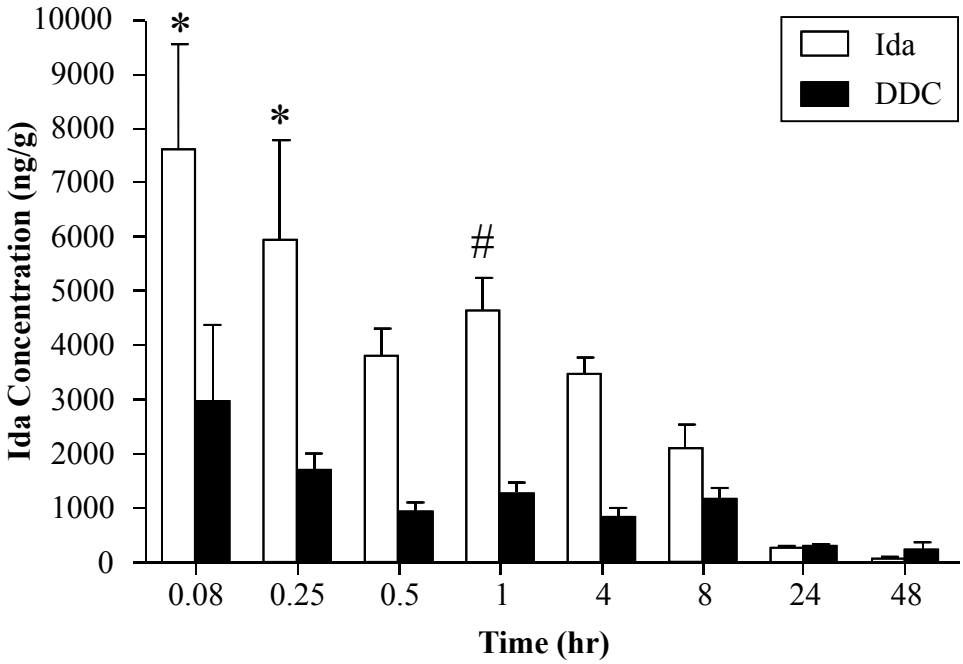
10000
9000
8000
7000
6000
5000
4000
3000
2000
1000
0
Ida Concentration (ng/g)
*
*
#
Ida
DDC
0.08
0.25
0.5
1
4
8
24
48
Time (hr)

Fig. 3.7E

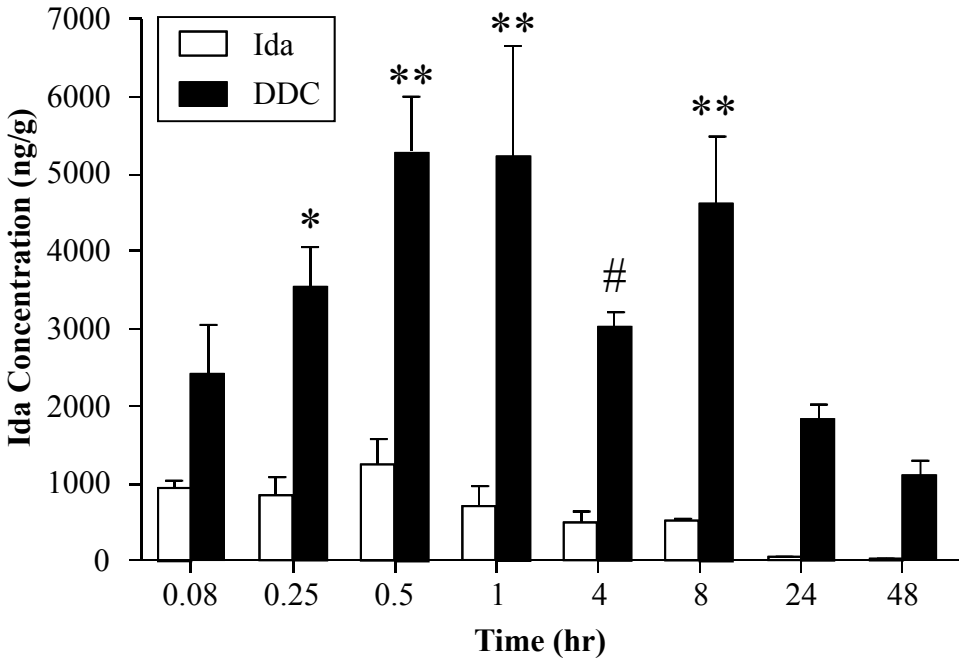
Ida
DDC
Ida Concentration (ng/g)
7000
6000
5000
4000
3000
2000
1000
0
*
**
**
#
**
0.08
0.25
0.5
1
4
8
24
48
Time (hr)

Fig. 3.7F

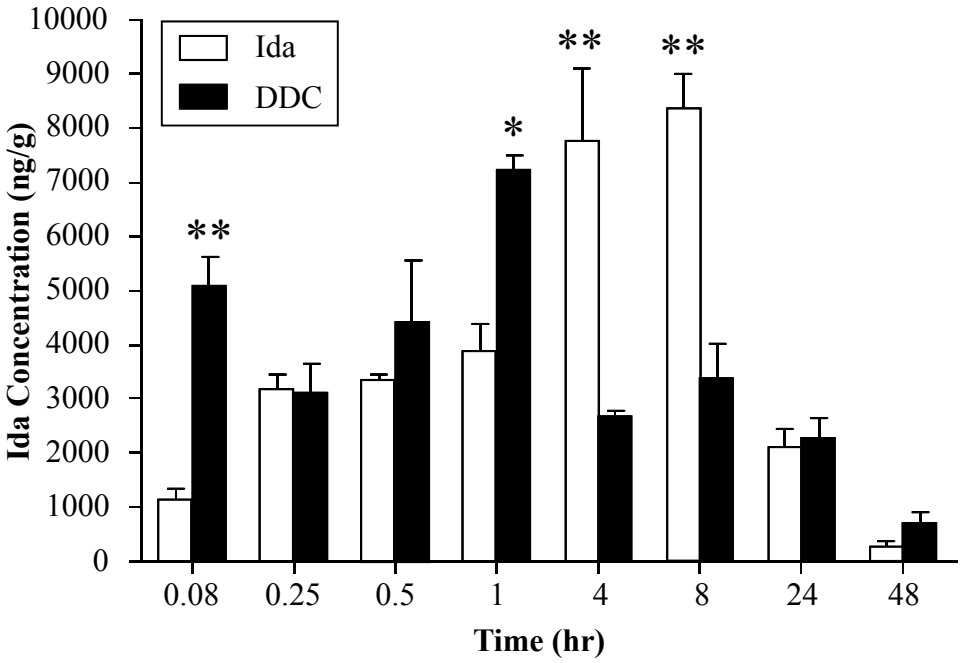
Ida
DDC
Ida Concentration (ng/g)
10000
9000
8000
7000
6000
5000
4000
3000
2000
1000
0
**
*
**
**
0.08
0.25
0.5
1
4
8
24
48
Time (hr)

Fig. 3.7G

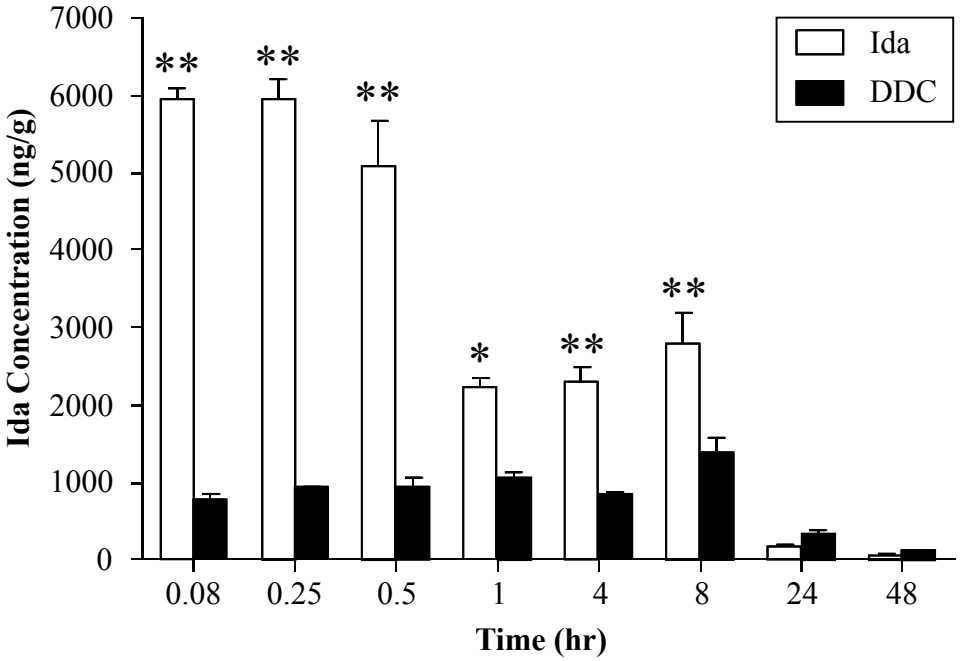

Figure 3.7 *In-vivo* plasma and tissue disposition kinetics of DDC and Idarubicin.
The pharmacokinetic behavior of DDC (3 mg/kg Ida and 7.5 mg/kg D-pen) and Ida (3 mg/kg) administered as a single i.v. dose was monitored. Values represent mean ± SEM (n=3-4/time point). # $p<0.05$, * $p<0.01$, ** $p<0.001$.
A. Plasma disposition of DDC and Ida administered as i.v. injection.
B. Disposition kinetics of DDC and Ida in NCI-H460 xenografts.
C. Disposition kinetics of DDC and Ida in heart tissue.
D. Disposition kinetics of DDC and Ida in lung tissue.
E. Disposition kinetics of DDC and Ida in liver tissue.
F. Disposition kinetics of DDC and Ida in spleen tissue.
G. Disposition kinetics of DDC and Ida in kidney tissue.

Organ	$AUC_{(0\text{-last})}$ (hr*ng/mL)		MRT (hr)		Cl (ml/hr/kg)		$t_{1/2}$ (hr)	
	Ida	**DDC**	**Ida**	**DDC**	**Ida**	**DDC**	**Ida**	**DDC**
Plasma	415	2,993	4.6	13.3	7,224	1,002	3.2	15.6
Tumor	2,617	9,426	17.6	32.1	1,146	318	12.2	21.1
Liver	9,063	148,348	11.6	31.8	331	20	8.5	21.3
Lungs	46,751	31,982	9.9	29.1	64	94	7.6	19.7
Heart	10,605	11,280	11.7	28.6	283	266	10.1	19.6
Kidney	39,834	27,747	10.1	19.2	75	108	7.3	12.1
Spleen	150,046	125,163	14.4	25.3	20	24	8.1	17.3

Table 3.2 Pharmacokinetic parameters for plasma and tissue disposition of DDC and Idarubicin.
Noncompartmental analysis of pharmacokinetic data was performed to calculate and predict parameters that are indicators of *in-vivo* behavior.

3.4.8. Antitumor Efficacy

The therapeutic index of DDCs, in terms of Ida, was found to be 2-3-fold (3-6 mg/kg) higher than Ida (1.5 mg/kg) when tested in a Q2dx3 regimen and a dose escalation study. The mice treated with 6 mg/kg (Ida equivalent) showed >15% loss in their body weight following a second dose. The body weight was partially recovered by the end of the study at 30 days. Initial dose selection was based on our previously published detailed analysis of dose escalation with unconjugated Ida in CD2F1 mice (Ma et al, 2009).

Anticancer efficacy studies were performed in athymic *nu/nu* mice bearing NCI-H460 tumor xenografts. **Figure 3.8** shows the tumor growth curves for different treatments. A previous efficacy study (data not shown) indicated no improvement in anticancer efficacy or survival upon co-administration of D-pen and Ida as a single solution in saline. Therefore, this treatment group was excluded from the later studies. DDCs showed potent antitumor effect by completely suppressing the tumor growth at the highest dose. The tumor suppression at this dose was significantly higher than any other group tested. Mean tumor volumes were used to calculate the TGI among different treatment groups on the last day at which all mice were alive (day 16). The DDCs, at the highest dose tested, resulted in 89% TGI compared to 60% by Ida (**Table 3.3**). Higher doses of DDC showed weight loss after second dosing as observed with the dose escalation studies. However, 50% of the mice recovered from the loss but others had to be euthanized. This is reflected in an overall decrease in the median survival of this treatment group predicted from the Kaplan-Meier curve (**Table 3.3**). The lower dose of DDCs, however, resulted in a comparable antitumor efficacy with no significant loss in body weight and significantly enhanced median survival (41 days) over other groups.

Previous studies have reported that the tumor IFP increases with increasing size due to edema associated with an increase in water content (Boucher et al., 1991). Increased IFP can further diminish macromolecular drug delivery to the tumors (Jain, 1987). Therefore, we examined the anticancer effects of DDC on the growth of larger tumors. The lower, better tolerated dose of DDC was chosen for this study and compared with Ida treatment. Administration of D-pen alone was not tested as it failed to show significant anticancer effects in the previous study (**Figure 3.8A**). Our observations indicated that DDCs may be able to suppress the growth of large tumors as well. The TGI on day 18 was 64% with DDC and 48% with Ida alone (**Figure 3.8C**).

Fig. 3.8A

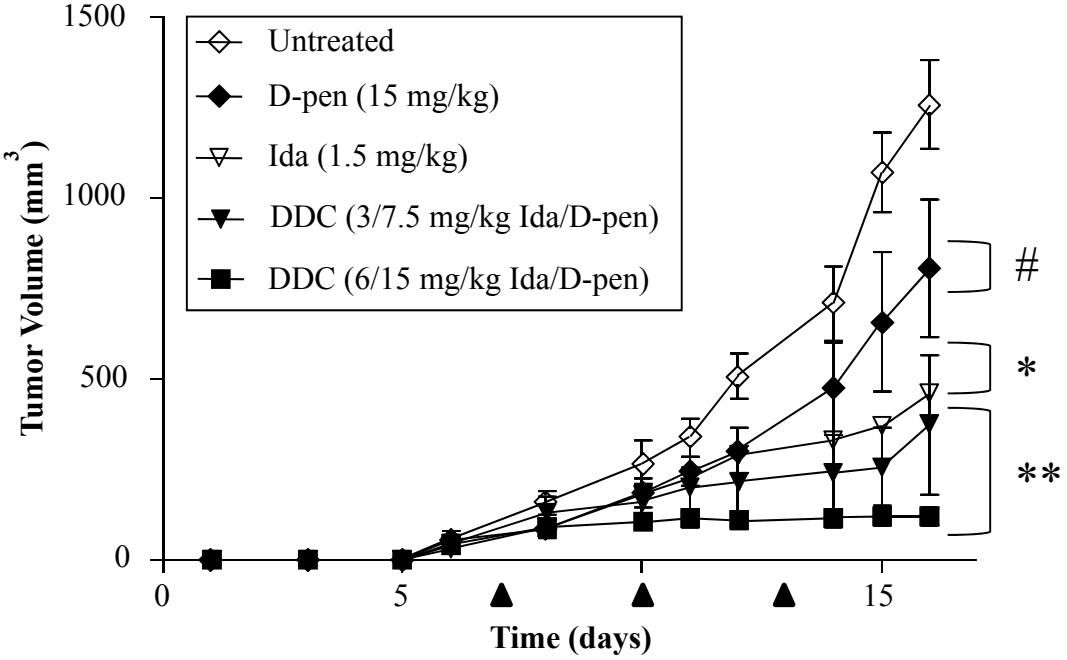
1500
1000
500
0
Tumor Volume (mm3)
Untreated
D-pen (15 mg/kg)
Ida (1.5 mg/kg)
DDC (3/7.5 mg/kg Ida/D-pen)
DDC (6/15 mg/kg Ida/D-pen)
#
*
**
0
5
15
Time (days)

Fig. 3.8B

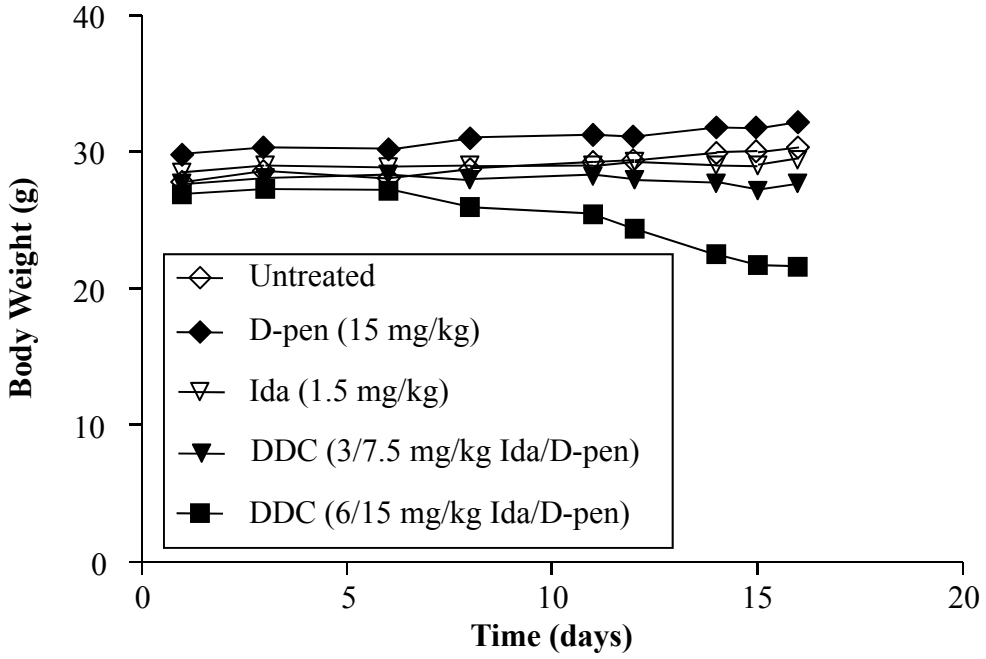
40
30
20
10
0
Body Weight (g)
0
5
10
15
20
Time (days)
Untreated
D-pen (15 mg/kg)
Ida (1.5 mg/kg)
DDC (3/7.5 mg/kg Ida/D-pen)
DDC (6/15 mg/kg Ida/D-pen)

Fig. 3.8C

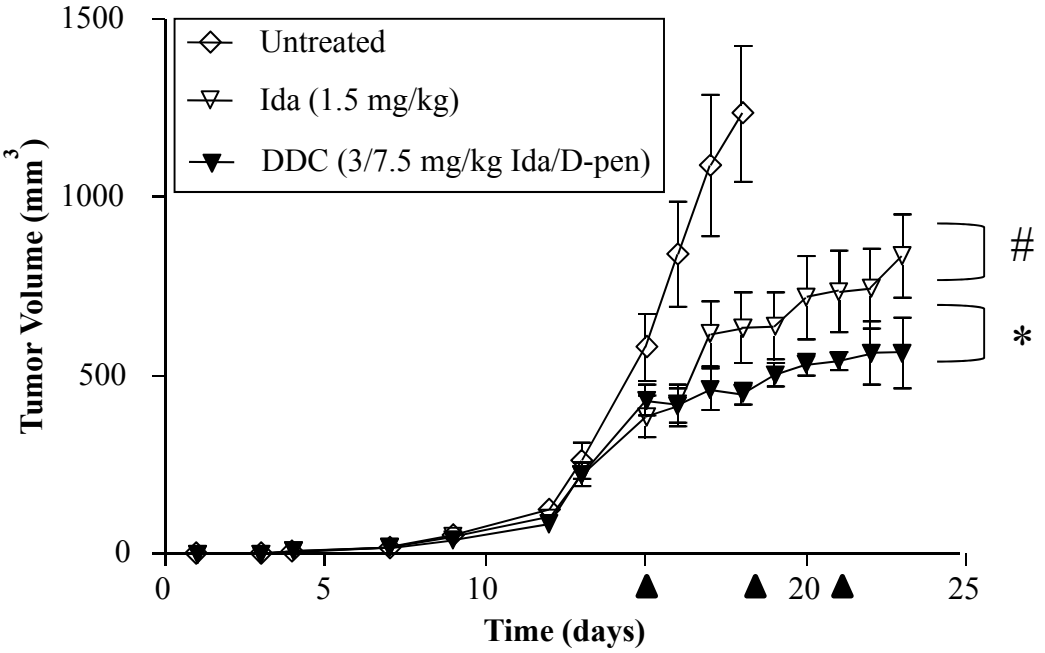

Figure 3.8 Anticancer efficacy in NCI-H460 tumor model.
Athymic *nu/nu* mice bearing NCI-H460 xenografts (50-100 mm^3) were administered different treatments following a Q2dx3 dosing schedule. Tumors were measured and body weight recorded every 24-48 hr. Values represent mean (n=6-8). # $p<0.05$, * $p<0.01$, **$p<0.001$.
A. Tumor growth curve (Mean ± SEM, n=6-8).
B. Body weight curve. The body weight was monitored every 24-48 hr and the mice were assigned a Body Condition Score in the range of 0-5 based on body weight loss and physical assessment.
C. Tumor growth curve (Mean ± SEM, n=8).

Parameters/ Treatment Group	Untreated	D-pen	Ida	DDC	DDC
Dose or Dose Equivalent (mg/kg)	None	15	1.5	Ida: 3 D-pen: 7.5	Ida: 6 D-pen: 15
Mean Tumor Volume (n=6, ± SEM, d16; mm^3)	562 ± 54	330 ± 78 ($p>0.05$)	220 ± 55 ($p<0.05$)	154 ± 74 ($p<0.01$)	60 ± 13 ($p<0.01$)
Tumor Growth Inhibition at day 16 (%)	None	41.3	60.8	72.5	89.4
Median Survival (days)	23	26	35	41	26

Table 3.3 Quantitative parameters of anticancer efficacy in the NCI-H460 tumor model.

3.5. Conclusions

DDCs containing D-pen and Ida conjugated to PGA were synthesized and evaluated for their anticancer properties. The DDCs released the conjugated drugs *in-vitro* in a sustained manner and were cytotoxic to cancer cells. PK analysis indicated longer circulation, enhanced drug exposure and tumor accumulation. This led to an increase in the antitumor activity characterized by 89% TGI and significant enhancement in the survival NCI-H460 tumors in mice. We are currently examining the effect of the presence of Sigma-1 receptor targeting ligand on the cell uptake and *in-vivo* anticancer efficacy of DDCs. Further studies will be conducted to investigate the *in-vivo* fate of DDCs in terms of rate of drug release and metabolism of the residual polymer.

3.6 References

Arunachalam, B., U.T. Phan, H.J. Geuze, and P. Cresswell. 2000. Enzymatic reduction of disulfide bonds in lysosomes: characterization of a gamma-interferon-inducible lysosomal thiol reductase (GILT). Proc Natl Acad Sci U S A. 97:745-750.

Bhatt, R., P. de Vries, J. Tulinsky, G. Bellamy, B. Baker, J.W. Singer, and P. Klein. 2003. Synthesis and in vivo antitumor activity of poly(l-glutamic acid) conjugates of 20S-camptothecin. J Med Chem. 46:190-193.

Borchmann, P., K. Hubel, R. Schnell, and A. Engert. 1997. Idarubicin: a brief overview on pharmacology and clinical use. Int J Clin Pharmacol Ther. 35:80-83.

Boucher, Y., J.M. Kirkwood, D. Opacic, M. Desantis, and R.K. Jain. 1991. Interstitial hypertension in superficial metastatic melanomas in humans. Cancer Res. 51:6691-6694.

Cejas, P., E. Casado, C. Belda-Iniesta, J. De Castro, E. Espinosa, A. Redondo, M. Sereno, M.A. Garcia-Cabezas, J.A. Vara, A. Dominguez-Caceres, R. Perona, and M. Gonzalez-Baron. 2004. Implications of oxidative stress and cell membrane lipid peroxidation in human cancer. Cancer Causes Control. 15:707-719.

Chan-Lam, D., J.A. Copplestone, A. Prentice, R. Price, S. Johnson, and M. Phillips. 1992. Idarubicin cardiotoxicity in acute myeloid leukaemia. Lancet. 340:185-186.

Chandra, J., A. Samali, and S. Orrenius. 2000. Triggering and modulation of apoptosis by oxidative stress. Free Radic Biol Med. 29:323-333.

Dharap, S.S., Y. Wang, P. Chandna, J.J. Khandare, B. Qiu, S. Gunaseelan, P.J. Sinko, S. Stein, A. Farmanfarmaian, and T. Minko. 2005. Tumor-specific targeting of an anticancer drug delivery system by LHRH peptide. Proc Natl Acad Sci U S A. 102:12962-12967.

Dos Santos, N., D. Waterhouse, D. Masin, P.G. Tardi, G. Karlsson, K. Edwards, and M.B. Bally. 2005. Substantial increases in idarubicin plasma concentration by liposome encapsulation mediates improved antitumor activity. J Control Release. 105:89-105.

D'Souza, A.J., and E.M. Topp. 2004. Release from polymeric prodrugs: linkages and their degradation. J Pharm Sci. 93:1962-1979.

Duncan, R. 2003. The dawning era of polymer therapeutics. Nat Rev Drug Discov. 2:347-360.

Eliot, H., L. Gianni, and C. Myers. 1984. Oxidative destruction of DNA by the adriamycin-iron complex. Biochemistry. 23:928-936.

Etrych, T., P. Chytil, M. Jelinkova, B. Rihova, and K. Ulbrich. 2002. Synthesis of HPMA copolymers containing doxorubicin bound via a hydrazone linkage. Effect of spacer on drug release and in vitro cytotoxicity. Macromol Biosci. 2:43-52.

Gao, W., R. Langer, and O.C. Farokhzad. 2010. Poly(ethylene glycol) with observable shedding. Angew Chem Int Ed Engl. 49:6567-6571.

Gewirtz, D.A. 1999. A critical evaluation of the mechanisms of action proposed for the antitumor effects of the anthracycline antibiotics adriamycin and daunorubicin. Biochem Pharmacol. 57:727-741.

Gnaccarini, C., S. Peter, U. Scheffer, S. Vonhoff, S. Klussmann, and M.W. Gobel. 2006. Site-specific cleavage of RNA by a metal-free artificial nuclease attached to antisense oligonucleotides. J Am Chem Soc. 128:8063-8067.

Gupte, A., and R.J. Mumper. 2007. Copper chelation by D-penicillamine generates reactive oxygen species that are cytotoxic to human leukemia and breast cancer cells. Free Radic Biol Med. 43:1271-1278.

Greenfield, R.S., T. Kaneko, A. Daues, M.A. Edson, K.A. Fitzgerald, L.J. Olech, J.A. Grattan, G.L. Spitalny, and G.R. Braslawsky. 1990. Evaluation in vitro of adriamycin immunoconjugates synthesized using an acid-sensitive hydrazone linker. Cancer Res. 50:6600-6607.

Havre, P.A., S. O'Reilly, J.J. McCormick, and D.E. Brash. 2002. Transformed and tumor-derived human cells exhibit preferential sensitivity to the thiol antioxidants, N-acetyl cysteine and penicillamine. Cancer Res. 62:1443-1449.

Held, K.D., F.C. Sylvester, K.L. Hopcia, and J.E. Biaglow. 1996. Role of Fenton chemistry in thiol-induced toxicity and apoptosis. Radiat Res. 145:542-553.

Herzog, T., R.J. Barret, R. Edwards, and F.B. Oldham. 2005. Phase II study of paclitaxel poliglumex (PPX)/carboplatin (C) for 1st line induction and maintenance therapy of stage III/IV ovarian or primary peritoneal carcinoma. J Clin Oncol. 23:458s-458s.

Hollingshead, L.M., and D. Faulds. 1991. Idarubicin. A review of its pharmacodynamic and pharmacokinetic properties, and therapeutic potential in the chemotherapy of cancer. Drugs. 42:690-719.

Jain, R.K. 1987. Transport of molecules in the tumor interstitium: a review. Cancer Res. 47:3039-3051.

Joyce, D.A., R.O. Day, and B.R. Murphy. 1991. The pharmacokinetics of albumin conjugates of D-penicillamine in humans. Drug Metab Disp. 19:309-311.

Joyce, D.A., D.N. Wade, and B.R. Swanson. 1989. The pharmacokinetics of albumin conjugates of D-penicillamine in rats. Drug Metab Disp. 17:208-211.

Kishore, B.K., P. Lambricht, G. Laurent, P. Maldague, R. Wagner, and P.M. Tulkens. 1990. Mechanism of protection afforded by polyaspartic acid against gentamicin-induced phospholipidosis. II. Comparative in vitro and in vivo studies with poly-L-aspartic, poly-L-glutamic and poly-D-glutamic acids. J Pharmacol Exp Ther. 255:875-885.

Kratz, F., U. Beyer, P. Schumacher, M. Kruger, H. Zahn, T. Roth, H.H. Fiebig, and C. Unger. 1997. Synthesis of new maleimide derivatives of daunorubicin and biological activity of acid labile transferrin conjugates. Bioorg Med Chem Lett. 7:617-622.

Kratz, F., A. Warnecke, K. Scheuermann, C. Stockmar, J. Schwab, P. Lazar, P. Druckes, N. Esser, J. Drevs, D. Rognan, C. Bissantz, C. Hinderling, G. Folkers, I. Fichtner, and C. Unger. 2002. Probing the cysteine-34 position of endogenous serum albumin with thiol-binding doxorubicin derivatives. Improved efficacy of an acid-sensitive doxorubicin derivative with specific albumin-binding properties compared to that of the parent compound. J Med Chem. 45:5523-5533.

Krejtschi, C., and K. Hauser. 2011. Stability and folding dynamics of polyglutamic acid. Eur Biophys J. 40:673-685.

Li, C. 2002. Poly(L-glutamic acid)--anticancer drug conjugates. Adv Drug Deliv Rev. 54:695-713.

Lodemann, E. 1981. Transport of D- and L-penicillamine by mammalian cells. Biochem Biophys Res Commun. 102:775-783.

Lumry, R., R. Legare, and W.G. Miller. 1964. The dynamics of the helix-coil transition in poly-α, L-glutamic acid. Biopolymers. 2:489-500.

Ma, P., X. Dong, C.L. Swadley, A. Gupte, M. Leggas, H.C. Ledebur, and R.J. Mumper. 2009. Development of idarubicin and doxorubicin solid lipid nanoparticles to overcome Pgp-mediated multiple drug resistance in leukemia. J Biomed Nanotechnol. 5:151-161.

MacKay, J.A., M. Chen, J.R. McDaniel, W. Liu, A.J. Simnick, and A. Chilkoti. 2009. Self-assembling chimeric polypeptide-doxorubicin conjugate nanoparticles that abolish tumours after a single injection. Nat Mater. 8:993-999.

Maeda, H., G.Y. Bharate, and J. Daruwalla. 2009. Polymeric drugs for efficient tumor-targeted drug delivery based on EPR-effect. Eur J Pharm Biopharm. 71:409-419.

Maeda, H., L.W. Seymour, and Y. Miyamoto. 1992. Conjugates of anticancer agents and polymers: advantages of macromolecular therapeutics in vivo. Bioconjug Chem. 3:351-362.

Martin, K.R., and J.C. Barrett. 2002. Reactive oxygen species as double-edged swords in cellular processes: low-dose cell signaling versus high-dose toxicity. Hum Exp Toxicol. 21:71-75.

Minko, T., P. Kopeckova, and J. Kopecek. 1999. Chronic exposure to HPMA copolymer-bound adriamycin does not induce multidrug resistance in a human ovarian carcinoma cell line. J Control Release. 59:133-148.

Minotti, G., P. Menna, E. Salvatorelli, G. Cairo, and L. Gianni. 2004. Anthracyclines: molecular advances and pharmacologic developments in antitumor activity and cardiotoxicity. Pharmacol Rev. 56:185-229.

Muindi, J.R., B.K. Sinha, L. Gianni, and C.E. Myers. 1984. Hydroxyl radical production and DNA damage induced by anthracycline-iron complex. FEBS Lett. 172:226-230.

Murphy, M.P. 2009. How mitochondria produce reactive oxygen species. Biochem J. 417:1-13.

Nori, A., K.D. Jensen, M. Tijerina, P. Kopeckova, and J. Kopecek. 2003. Tat-conjugated synthetic macromolecules facilitate cytoplasmic drug delivery to human ovarian carcinoma cells. Bioconjug Chem. 14:44-50.

Partis, M.D., D.G. Griffiths, G.C. Roberts, and R.B. Beechey. 1983. Cross-Linking of protein by omega-maleimido alkanoyl N-hydroxysuccinimido esters. J Protein Chem. 2:263-277.

Platel, D., P. Pouna, S. Bonoron-Adele, and J. Robert. 1999. Comparative cardiotoxicity of idarubicin and doxorubicin using the isolated perfused rat heart model. Anti-Cancer Drugs. 10:671-676.

Rodrigues, P.C., U. Beyer, P. Schumacher, T. Roth, H.H. Fiebig, C. Unger, L. Messori, P. Orioli, D.H. Paper, R. Mulhaupt, and F. Kratz. 1999. Acid-sensitive polyethylene glycol conjugates of doxorubicin: preparation, in vitro efficacy and intracellular distribution. Bioorg Med Chem. 7:2517-2524.

Sabbatini, P., C. Aghajanian, D. Dizon, S. Anderson, J. Dupont, J.V. Brown, W.A. Peters, A. Jacobs, A. Mehdi, S. Rivkin, A.J. Eisenfeld, and D. Spriggs. 2004. Phase II study of CT-2103 in patients with recurrent epithelial ovarian, fallopian tube, or primary peritoneal carcinoma. J Clin Oncol. 22:4523-4531.

Shaffer, S.A., C. Baker-Lee, J. Kennedy, M.S. Lai, P. de Vries, K. Buhler, and J.W. Singer. 2007. In vitro and in vivo metabolism of paclitaxel poliglumex: identification of metabolites and active proteases. Cancer Chemother Pharmacol. 59:537-548.

Sutherland, M.D., P. Thorkildson, S.D. Parks, and T.R. Kozel. 2008. In vivo fate and distribution of poly-gamma-D-glutamic acid, the capsular antigen from Bacillus anthracis. Infect Immun. 76:899-906.

Ulbrich, K., T. Etrych, P. Chytil, M. Jelinkova, and B. Rihova. 2003. HPMA copolymers with pH-controlled release of doxorubicin: in vitro cytotoxicity and in vivo antitumor activity. J Control Release. 87:33-47.

Ulbrich, K., and V. Subr. 2004. Polymeric anticancer drugs with pH-controlled activation. Adv Drug Deliv Rev. 56:1023-1050.

Ulbrich, K., V. Subr, J. Strohalm, D. Plocova, M. Jelinkova, and B. Rihova. 2000. Polymeric drugs based on conjugates of synthetic and natural macromolecules. I. Synthesis and physico-chemical characterisation. J Control Release. 64:63-79.

Ullman-Cullere, M.H., and C.J. Foltz. 1999. Body condition scoring: a rapid and accurate method for assessing health status in mice. Lab Anim Sci. 49:319-323.

Van, S., S.K. Das, X. Wang, Z. Feng, Y. Jin, Z. Hou, F. Chen, A. Pham, N. Jiang, S.B. Howell, and L. Yu. 2010. Synthesis, characterization, and biological evaluation of poly(L-gamma-glutamyl-glutamine)- paclitaxel nanoconjugate. Int J Nanomedicine. 5:825-837.

Vicent, M.J. 2007. Polymer-drug conjugates as modulators of cellular apoptosis. AAPS J. 9:E200-207.

Vicent, M.J., F. Greco, R.I. Nicholson, A. Paul, P.C. Griffiths, and R. Duncan. 2005. Polymer therapeutics designed for a combination therapy of hormone-dependent cancer. Angew Chem Int Ed Engl. 44:4061-4066.

Wadhwa, S., and R.J. Mumper. 2010. Intracellular delivery of the reactive oxygen species generating agent D-penicillamine upon conjugation to poly-L-glutamic acid. Mol Pharm. 7:854-862.

Wen, X., E.F. Jackson, R.E. Price, E.E. Kim, Q. Wu, S. Wallace, C. Charnsangavej, J.G. Gelovani, and C. Li. 2004. Synthesis and characterization of poly(L-glutamic acid) gadolinium chelate: a new biodegradable MRI contrast agent. Bioconjug Chem. 15:1408-1415.

Xu, X., H.L. Persson, and D.R. Richardson. 2005. Molecular pharmacology of the interaction of anthracyclines with iron. Mol Pharmacol. 68:261-271.

Zara, G.P., A. Bargoni, R. Cavalli, A. Fundaro, D. Vighetto, and M.R. Gasco. 2002. Pharmacokinetics and tissue distribution of idarubicin-loaded solid lipid nanoparticles after duodenal administration to rats. J Pharm Sci. 91:1324-1333.

Chapter 4

Dual Drug Conjugates of D-penicillamine and Idarubicin Targeted to Sigma-1 Receptor Over-expressing Cancer Cells Enhance Drug Uptake and Cytotoxicity

4.1. Abstract

Sigma receptors are over-expressed in several malignant human and non-human cell lines including breast, lung, prostate, renal and brain. Their expression correlates with the metastatic potential and growth of tumors. However, neither the endogenous ligand nor the exact physiological function of sigma receptors is known. Several benzamide analogues have been shown to bind the sigma receptor with very high affinity (K_d = 15 nm). In this report, we investigated a novel benzamide derivative, trivalent anisamide (TA), for the delivery of dual drug conjugates (DDCs) of D-pen and Ida bound to poly-α-L-glutamic acid. Sigma expression was measured by western blotting in human (HL-60, HL-60/VCR, HL-60/ADR, ThP-1 and K562) and murine (P388 and P388/ADR) leukemia, breast (MCF-7) and non-small cell lung cancer (NSCLC; NCI-H460) cell lines. High expression was observed in HL-60, ThP-1, MCF-7 and NCI-H460 cells. TA-DDCs showed higher specific uptake in cells that could be completely inhibited by haloperidol. TA-DDCs led to a 2-fold enhancement in the cytotoxicity over untargeted DDCs. Preliminary pharmacokinetic study showed that TA-DDCs were long-circulating ($t_{1/2}$ 14.8 hr) in mice bearing NCI-H460 xenografts.

4.2. Introduction

Targeted macromolecular therapy of cancer, analogous to the concept of 'magic bullet' first proposed by Paul Ehrlich, involves incorporation of a molecular recognition component to focus the drug delivery to specific cell populations. In the past two decades, there has been a tremendous interest in utilizing this concept to increase the effectiveness of drug delivery systems including liposomes, nanoparticles and polymer drug conjugates (PDCs) (Duncan et al., 1996). We have recently developed dual drug conjugates (DDCs) for the co-delivery of D-pen and Ida with significantly enhanced therapeutic index and anticancer efficacy. We hypothesized that targeting DDCs to receptors over-expressed in cancer cells will further improve the anticancer effect of DDCs. PDCs that are designed to target specific receptors over-expressed in cancer cells may overcome drug efflux via multi-drug resistance (MDR), reduce non-specific organ uptake and lead to further increased drug concentration in the tumor via active accumulation. This can result in an overall dose reduction and decreased associated adverse events. The present study investigated the effect of targeting DDCs to cells over-expressing sigma-1 receptors.

Sigma receptors were originally classified as opiate receptors but were later differentiated (Su et al., 1988). Two different subtypes, sigma-1 and sigma-2 have been identified. Sigma-1 receptor has been cloned (25,330 kDa) and more widely investigated (Hanner et al., 1996; Maurice and Su, 2009). The exact physiological function of sigma receptors and the endogenous ligand is still unknown. However, interaction with various ion channels may play an important role in mediating its functions (Aydar et al., 2004).

Treatment with antagonists of sigma-1 receptors has resulted in reduction in viability and tumor growth inhibition indicating their potential role in cell growth (Spruce et al., 2004;

Wang et al., 2004). Sigma-1 receptors have been shown to be over-expressed in several human and non-human cancer cell lines including breast, lung, prostrate, renal and brain (Vilner et al., 1995). They have been successfully targeted to deliver high concentrations of chemotherapeutics to cancer cells using benzamide derivatives shown to bind sigma-1 receptor with very high affinity (K_d = 15 nM), as ligands (Mach et al., 2004). Huang and co-workers showed that doxorubicin-containing liposomes targeted to sigma receptors using anisamide conjugated to DSPE-PEG(3500) resulted in significant reduction in tumor (DU-145) growth compared to untargeted liposomes (Banerjee et al., 2004). They recently also showed a 3-fold enhancement in cell uptake and strong epidermal growth factor receptor (EGFR) silencing by siRNA-containing liposomes formulated with anisamide-lipid (DSGLA) conjugate (Chen et al., 2009).

Although several attempts have been made to deliver drugs to sigma-1 receptor, targeting polymer bound drugs to sigma-1 receptors has not been investigated. We evaluated DDCs targeted to sigma-1 receptors using a novel benzamide analog as ligand and investigated the effect of targeting on cellular uptake and viability.

4.3. Materials and Methods

4.3.1. Materials

Poly-α-L-glutamic acid sodium salt (MW 50-70 kDa), D-penicillamine (D-pen), tris(2-carboxyethyl)phosphine hydrochloride (TCEP), 1-ethyl-3-[3-dimethylaminopropyl] carbodiimide hydrochloride (EDC) and *N*-hydroxysuccinimide (NHS) were purchased from Sigma-Aldrich (St. Louis, MO). Sepharose Cl-4B, buffers and all solvents were purchased from Thermo Fisher Scientific (Rockford, IL).

4.3.2. Synthesis of N-boc-2-amino ethyl-4-methoxy Benzamide (Compound 1)

4-methoxybenzoyl chloride (0.8 g, 4.7 mmol) in 5 mL dry DCM was added slowly to the solution of N-boc ethylene diamine (0.5 g, 3.1 mmol) and triethyl amine (0.5 mL) in 5 mL dry DCM under nitrogen atmosphere at 0^{o}C.The resultant solution was stirred for another 3 hr. The reaction mixture was diluted with excess DCM and washed with 1N HCl (1 x 50 mL) followed by saturated sodium bicarbonate and brine solution and the organic layer was dried over anhydrous sodium sulphate. The solvent was removed and purified by column chromatography. The compound **1** (N-boc-2-aminoethyl-4-methoxy benzamide) was eluted with 2% methanol in chloroform as a white solid (0.8 g, 87%). ^{1}H NMR (400 MHz, $CDCl_3$): δ (ppm) = 1.41(s, 9H), 3.4 (m, 2H), 3.6 (m, 2H), 3.82 (s, 3H), 5.0(bs, NH), 6.9 (dd, 2H), 7.8 (dd, 2H).

4.3.3. Synthesis of N-1-(4-Methoxybenzoyl) Ethylenediamine

N-boc-2-amino ethyl-4-methoxy benzamide (0.7 g, 2.3 mmol) was dissolved in 4 mL dry DCM under nitrogen atmosphere. Trifluoro acetic acid (1 mL) was slowly added to the

reaction mixture at 0°C and stirred for 4 hr. Solvent was removed and purified by the column chromatography. The compound (N-1-(4-Methoxybenzoyl) ethylenediamine) was eluted with 8% methanol in chloroform as a white solid. (0.42 g, 91%). ^{1}H NMR (400 MHz, D_2O): δ (ppm) = 3.1 (t, 2H), 3.5-3.6 (m, 2H), 3.8 (s, 3H), 6.9-6.95 (dd, 2H), 7.6-7.7 (dd, 2H).

4.3.4. Synthesis of Compound 2

N-1-(4-Methoxybenzoyl) ethylenediamine (0.5 g, 2.6 mmol) was dissolved in 5 mL of dry DMF. Tri ethyl amine (300 μL) and glutaric anhydride (0.45 g, 3.9 mmol) were added and the reaction mixture was stirred for 12 hr. Water was added and the compound was extracted with ethyl acetate (3 x 50 mL). The organic layer washed with water (1 x 20 mL) and followed by brine solution. The organic layer was dried over anhydrous sodium sulphate and solvent was removed by vacuum evaporation to obtain compound **2** as a white solid (0.6 g, 75%). ^{1}H NMR (400 MHz, CD_3OD): δ (ppm) = 1.8-1.9 (m, 2H), 2.1-2.4 (m, 4H), 3.3-3.5 (m, 4H), 3.8 (s, 3H), 6.9 (dd, 2H), 7.8 (dd, 2H). ESI-mass: 639 (M+23).

4.3.4. Synthesis of Compound 3

Compound **2** (0.43 g, 1.4 mmol), EDC (0.27 g, 1.4 mmol) and catalytic amount of DMAP were dissolved in 3 mL of dry DMF under nitrogen atmosphere. After 15 min, the Tris (5-hydroxy-2-oxapentyl)-N-boc-methylamine (0.14 g, 0.35 mmol) (Khorev et al., 2008) in 1 mL dry DMF was added slowly to the reaction mixture and stirred overnight. Water was added and the compound was extracted with ethyl acetate (3 x 30mL). The organic layer was washed with water (2 x 30mL) followed by a brine solution. The organic layer was dried over anhydrous sodium sulphate, the solvent was removed, and the compound was purified

by column chromatography. Compound **3** was eluted with 3% methanol in chloroform as a pale yellow solid. (0.39 g, 89%). ^{1}H NMR (400 MHz, $CDCl_3$): δ (ppm) = 1.4 (s, 9H), 1.7 (s, 2H), 1.8-2.0 (m, 12H), 2.2-2.4 (m, 12H), 3.4-3.5 (m, 12H), 3.5-3.6 (m, 12H), 3.82 (s, 3H), 4.1 (t, 6H), 6.9 (dd, 2H), 7.8 (dd, 2H). ESI-mass: 1289(M+23).

4.3.5. Synthesis of Trivalent Anisamide (Compound 4)

Compound **3** (0.3 g, 0.23 mmol) was dissolved in 2 mL of dry DCM under nitrogen atmosphere and TFA (0.5 mL) was added at 0^{o}C and stirred for 3 hr. The solvent was removed by N_2 flushing and the final compound was obtained as a pale yellow semi solid (0.25 g, quantitative yield). ^{1}H NMR (400 MHz, $CDCl_3$): δ (ppm) = 1.8-1.9 (m, 12H), 2.2-2.4 (m, 12H), 3.4-3.6 (m, 24H), 3.82 (s, 3H), 4.2 (t, 6H), 6.9 (dd, 2H), 7.8 (dd, 2H). ESI-mass: 1167(M+1).

4.3.6. Synthesis of Sigma Targeted DDC

PGA was obtained from PGA sodium as described in section 3.3.3. PGA (50 mg, 0.83 μmol), EDC (63.9 mg, 0.33 mmol), NHS (18.10 mg, 0.16 mmol) and PDE (55.7 mg, 0.25 mmol) were dissolved in 5 mL anhydrous DMF. Immediately, TA (**4**) (53.7 mg, 0.042 mmol) was added to the reaction and stirred for 12 hr at room temperature under an atmosphere of argon. The TA-PGA-PDE conjugate (**5**) was precipitated by the addition of ether and subsequent washing with water. The conjugate was dissolved by adding a few drops of 0.5 M sodium bicarbonate and pH was adjusted to 7.4 using 0.1 M PBS. The extent of conjugation was determined spectrophotometrically (ε = 8080 M^{-1} cm^{-1}, λ_{max} = 343 nm) by measuring the absorbance of pyridine-2-thione released upon the reduction of the conjugate

in presence of 25 mM TCEP for 1 hr. The extent of conjugation of TA was also determined spectrophotometrically ($\varepsilon = 24810.07\ M^{-1}\ cm^{-1}$, $\lambda_{max} = 252$ nm).

To the solubilized TA-PGA-PDE (**5**) conjugate, D-pen (124 mg, 0.83 mmol) was added and the mixture was stirred for 12 hr at room temperature. The TA-PGA-D-pen conjugate (**6**) was separated from unreacted components with Amicon^{TM} Ultra-15 Centrifugal Filter Device (Millipore, Bedford, MA). The extent of D-pen conjugation was determined by HPLC as described previously (Wadhwa and Mumper, 2010). To synthesize TA-DDCs (**7**), the TA-PGA-D-pen conjugate (containing 0.05 mmol D-pen) was reduced in the presence of TCEP (1 mM) for 5 min to release 10-12% of conjugated D-pen. TCEP was removed by centrifugation using Amicon Ultra-15 and Ida-MPBH (11.54 mg, 0.015 mmol) was added. The reaction was stirred for 12 hr at room temperature. The TA-DDCs were purified by filtration with sepharose CL-4B column (15 x 1.5 cm) using PBS pH 7.4 as the mobile phase, lyophilized and stored at -20^{o}C until further use.

4.3.7. Sigma Receptor Expression by Western Blot Analysis

Sigma receptor expression in human leukemia (HL-60, THP-1 and K562) and non-small cell lung cancer (NCI-H460) cells was determined by Western Blot analysis using a sigma receptor specific polyclonal antibody (SC-22948, Santa Cruz Biotechnology, Santa Cruz, CA). As a positive control, sigma expression levels were also determined in human breast cancer cells (MCF-7) (Aydar et al., 2004). Cells were lysed with RIPA lysis buffer (Santa Cruz Biotechnology, Santa Cruz, CA) and 25-50 μg of total protein from each cell line was separated by electrophoresis on Ready Gel® (4-20%) (Bio-Rad, Hercules, CA) and transferred to a PVDF membrane. The membrane was blocked with 5% non-fat milk and

incubated overnight at 4°C with the primary antibody diluted to 1:50 in 5% non-fat milk followed by incubation for 30 min with secondary antibody diluted to 1:1000 in 5% non-fat milk. The protein bands were detected by chemiluminescence using VersaDoc™ Imaging System (Bio-Rad Laboratories, Hercules, CA). The membrane was incubated with Restore™ PLUS western blot stripping buffer (Thermo Scientific, Rockford, IL) and re-probed for β-actin using a mouse monoclonal antibody (SC-47778, Santa Cruz Biotechnology, Santa Cruz, CA) and secondary antibody diluted to 1:1000 with 5% non-fat milk. The band intensities for sigma were normalized to the β-actin and compared among different cell lines.

4.3.8. Cell Uptake Studies

NCI-H460 cells (1 x 10^6) cultured on Lab-Tek™ Chambered Coverglass (Nalge Nunc International, NY) were incubated with 2 μM of TA-DDCs or DDCs (Ida equivalent dose) for 0.5, 2 and 4 hr. The cells were subsequently washed five times with PBS. The cells were visualized live using Zeiss 510 Meta Laser Scanning Confocal Microcope (63 x 1.4 NA oil Plan-Apochromat objective; Excitation: 488 nm and emission: 540 nm; Carl Zeiss, Thornwood, NY). The images were processed using Zeiss AIM Viewer (Carl Zeiss, Thornwood, NY).

Quantitative cell uptake was studied by confocal microscopy. NCI-H460 cells (1 x 10^6) were plated in 12-well cell culture plates and allowed to attach overnight. Cell were treated with TA-DDCs or DDCs (1 μM Ida equivalent) in the presence of absence of haloperidol (50 μM) for 0.5, 2 and 4 hr. Further processing was performed at 4°C. Cells were trypsinized and, washed two times with and resuspended in cold 10 mM PBS containing 2%

sodium edetate and 10% FBS. Analysis was immediately performed on a BD^{TM} LSR II Flow Cytometer (BD Biosciences, Franklin Lakes, NJ) using the 488 nm laser for excitation.

4.5.9. Plasma Disposition Study

NCI-H460 cells (1 x 10^6) were implanted subcutaneously (s.c.) in the right flank of male athymic *nu/nu* mice (20-25 g). When the tumors attained a size of approximately 200 mm^3 (day 13), the mice were injected i.v. with TA-DDCs (3 mg Ida equivalent/kg and 7.5 mg D-pen equivalent/kg). The mice (n=3/time point) were sacrificed at selected times between days 13 and 15 (t= 0.08, 0.25, 0.5, 1, 4, 8, 24 and 48 hr). Blood was collected by cardiac puncture. Plasma was separated from blood with Lithium-Heparin microtubes (Sarstedt, NC). Samples were stored at -80^{o}C until further analysis. The samples were analyzed for Ida concentration by HPLC as described in section 3.3.6. The data were analyzed by non-compartmental pharmacokinetic analysis using WinNonlin® 4.0 (Pharsight, Mountain View, CA).

4.5.10. Statistical Analysis

The cell uptake of TA-DDCs was compared with DDCs by regular two-way ANOVA followed by Bonferroni post-test to analyze effect of time. Differences were considered significant at p values of <0.05.

4.4. Results and Discussion

4.4.1. Synthesis of Sigma-1 Receptor Targeted DDCs

Anisamide has been previously used to effectively target chemotherapy to cells over-expressing sigma receptors. The new ligand was synthesized to enhance the receptor binding by increasing the valency of receptor-ligand interaction, a concept that has been popularly applied to nanoparticulate drug delivery systems (Simnick et al., 2010). Conjugation of multiple trivalent ligands to polymer chain is expected to further enhance the avidity of binding. Moreover, a recent report showed that a similar trivalent benzamide derivative conjugated to oligonucleotides significantly enhanced the uptake in sigma receptor over-expressing prostate cancer cells (Nakagawa et al., 2010). The number of ligands per polymer chain was optimized by performing cell uptake studies by flow cytometry and it was found that 4-6 TA per chain resulted in the maximal enhancement in the uptake while at higher levels of conjugation led to decrease in uptake with a decrease in aqueous solubility. The final TA-DDCs had 4 moles of TA, 4 moles of Ida and 35 moles of D-pen per polymer chain as determined by HPLC and spectrophotometry.

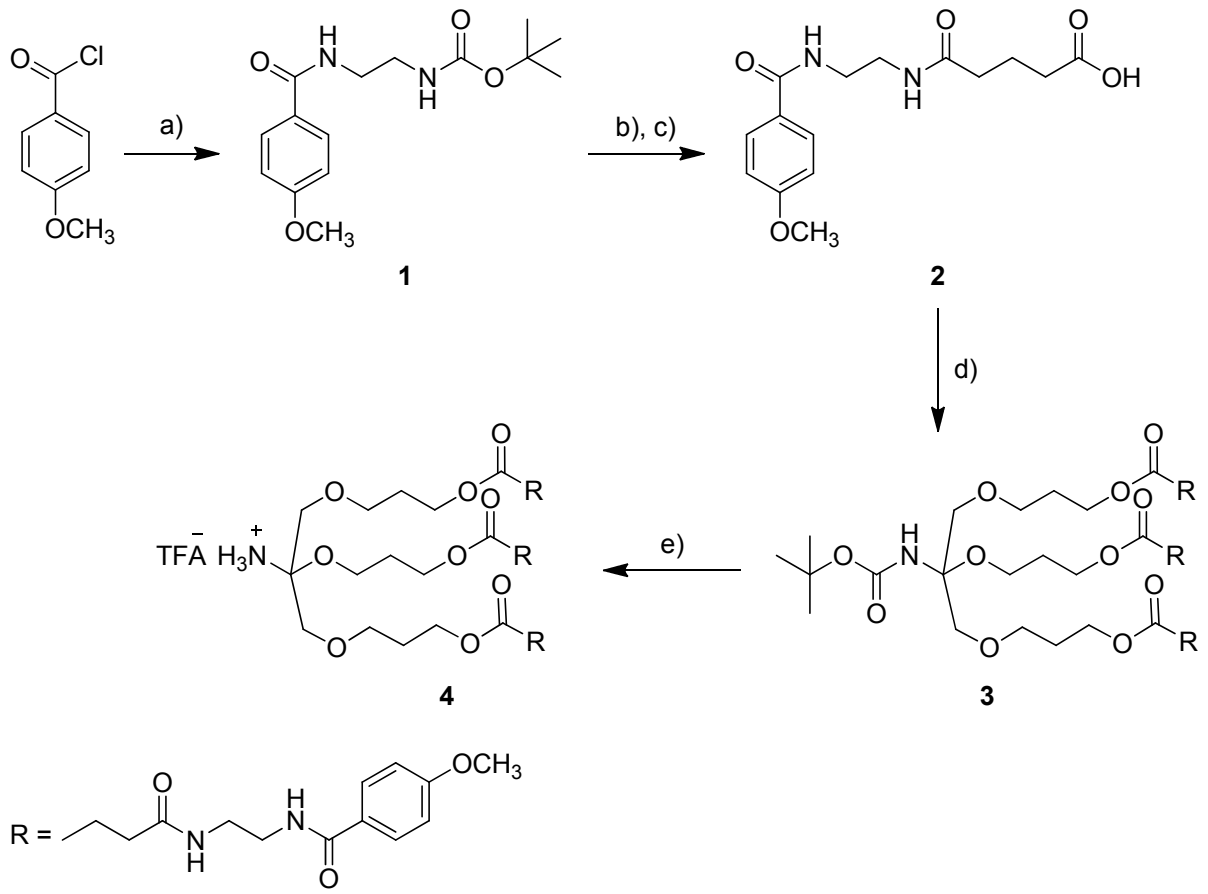

Figure 4.1 Synthesis of trivalent anisamide (TA)
Reagents: a) N-boc ethylene diamine, TEA, DCM, 0^{o}C; b) TFA, DCM; c) Glutaric anhydride, TEA, DMF; d) Tris (5-hydroxy2-oxapentyl)-N-boc methylamine, EDC, DCM; e) TFA, DCM.

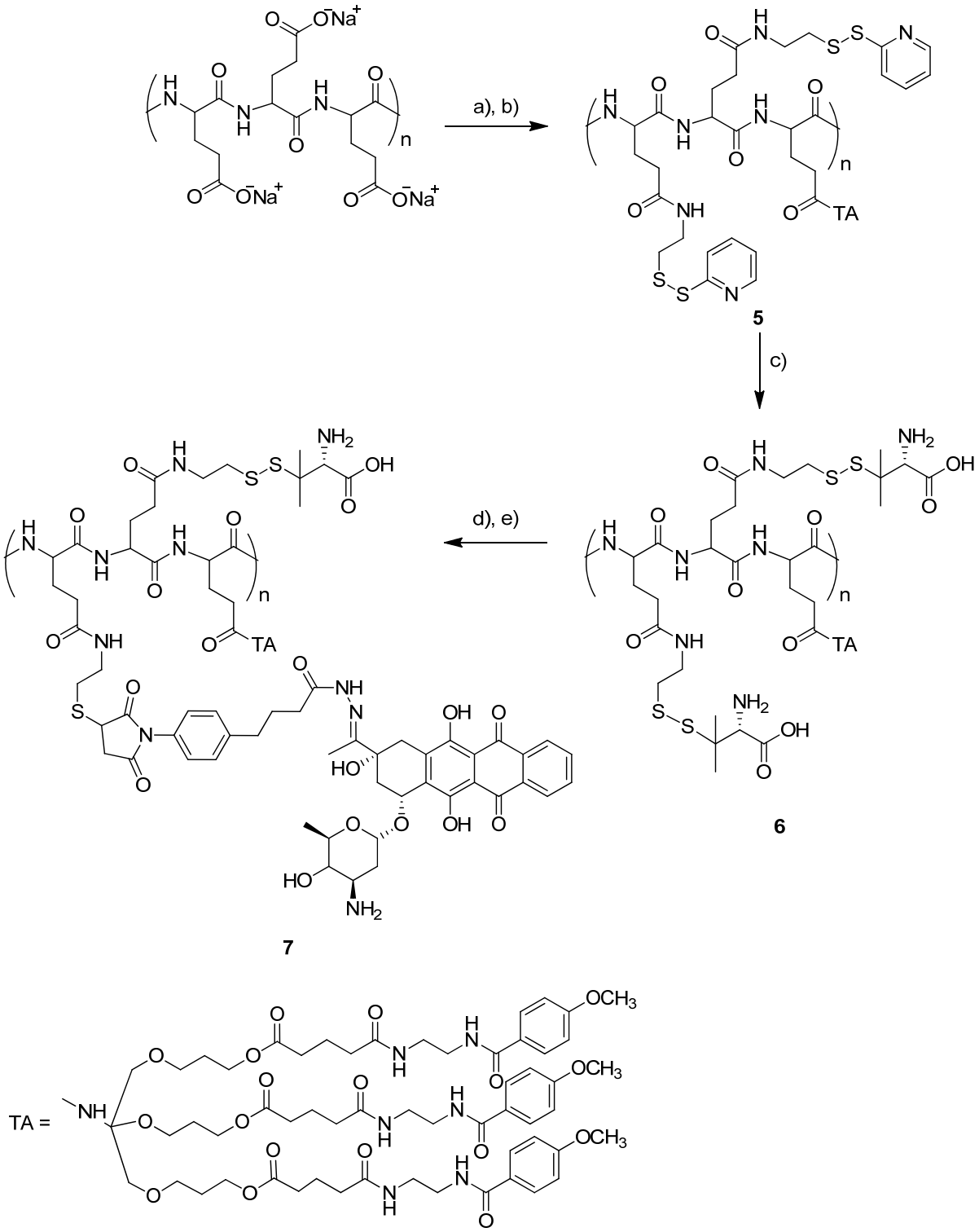

Figure 4.2 Synthesis of DDCs targeted to sigma-1 receptors using trivalent anisamide. Reagents: a) 1 N HCl, Lyophilization; b) PDE, TA, EDC, NHS, DMF; c) D-pen, PBS pH 7.4; d) 1 mM TCEP, 5 min; e) Ida-MPBH.

4.4.2. Sigma Receptor Expression by Western Blot Analysis

The sigma-1 receptor gene has been cloned and the receptor is shown to be a protein of 25,300 Da (Hanner et al., 1996). Sigma-1 expression has previously been shown to be elevated in several different cancer cell lines (Vilner et al., 1995). The sigma receptor protein band was detected in all cell lines at the expected molecular size (25 kDa) (**Figure 4.3**). Protein concentration levels were normalized to β-actin thus revealing robust expression in HL60, ThP-1 and NCI-H460 cells and moderate expression in the K562 cells. The sigma-1 receptors are predominantly located at the interface of ER and mitochondria but can translocate to the plasma membrane when they are over-expressed as has been reported in breast cancer cells (Aydar et al., 2006; Su et al., 2009). An enhanced expression of sigma-1 receptors provides an opportunity to target chemotherapy to cancer cells while sparing non-target cells.

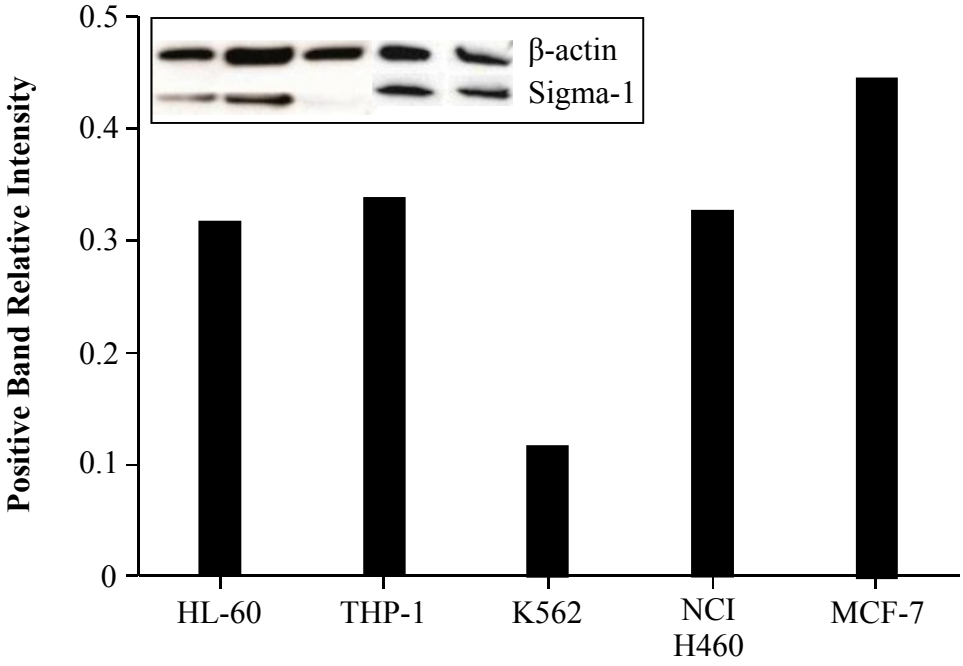

Figure 4.3 Sigma-1 receptor expression study by Western Blot analysis in different cancer cells.

4.4.3. Cell Uptake Studies

Confocal microscopic pictures showed significantly high fluorescence intensity in NCI-H460 cells treated with TA-DDCs compared to DDCs after 0.5 hr. It is interesting to note that the non-specific uptake of the untargeted DDCs is significant thus making differentiation difficult at later time points (2 hr and 4 hr). Ida, a lipophilic anthracycline derivative, is expected to passively accumulate in the cells and it was not surprising to see high FI in Ida treated cells at shorter time points (data not shown). Therefore, lower doses were used for quantitative studies with flow cytometry to identify differences between the treatment groups at time points beyond 0.5 hr. TA-DDCs showed 2-3-fold enhancement in the FI over DDCs. To investigate if the enhancement could be attributed to sigma receptors, uptake studies were performed in the presence of haloperidol. Haloperidol is a potent but non-selective inhibitor of sigma-1 receptors ($K_{i\sigma\text{-}1}$ = 644 nM; $K_{i\sigma\text{-}2}$ = 221 nM) (Aydar et al., 2004). We did not determine the expression of sigma-2 receptors and therefore, some contribution to the uptake by sigma-2, if present, cannot be ruled out.

In-vitro cytotoxicity of TA-DDCs was determined in NCI-H460 cells and compared to DDCs and Ida. The IC_{50} values for TA-DDCs, DDCs and Ida were 41.27 nM, 86.57 nM, and 61.28 nM, respectively. The difference between the targeted and untargeted conjugates may be attributed to enhanced uptake as seen by flow cytometry. However, the lower IC_{50} values compared to Ida is an indirect evidence of a combination effect of Ida and D-pen.

Fig. 4.4A

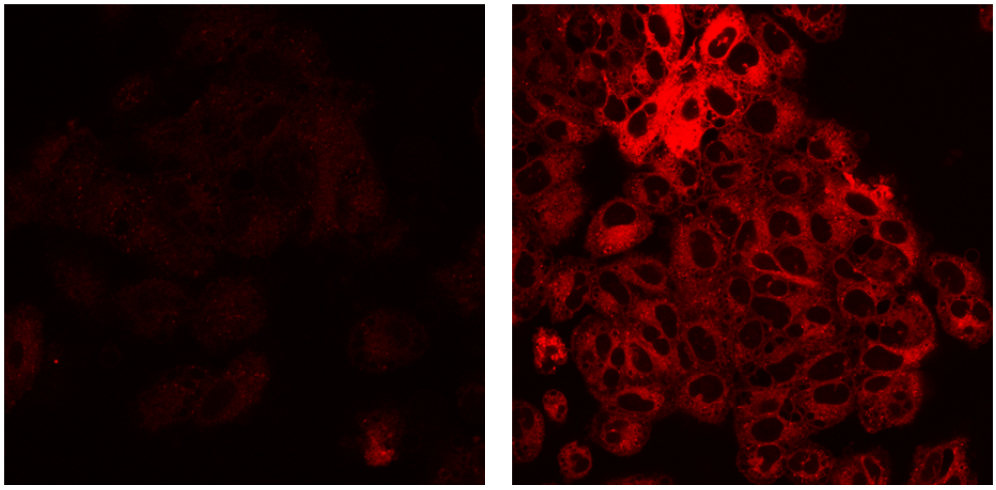

Fig. 4.4B

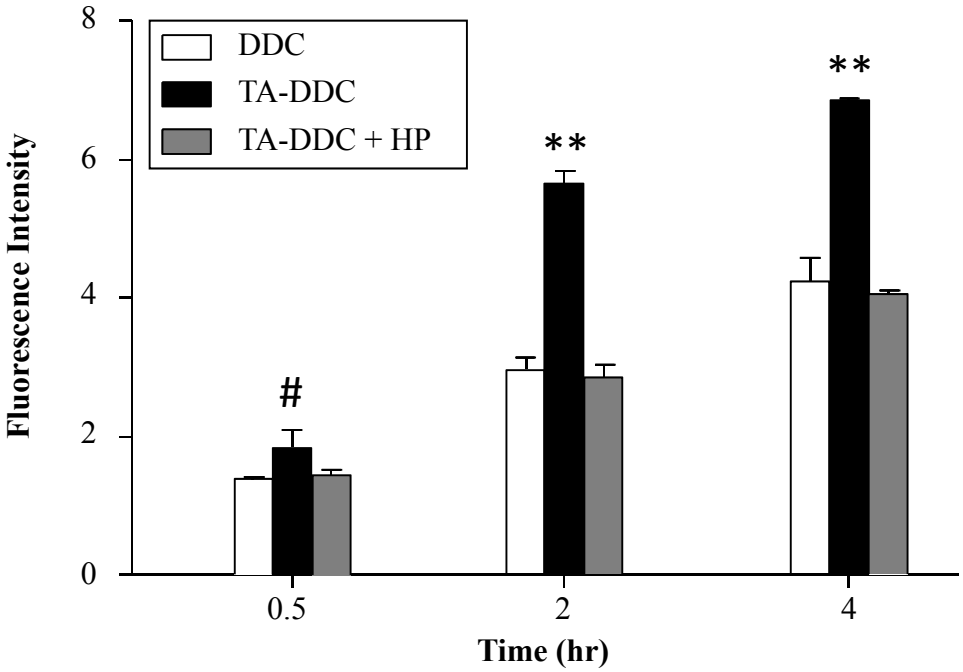

Figure 4.4 Uptake of targeted vs untargeted DDCs in NCI-H460 cells.
A. NCI-H460 cells treated with TA-DDCs and DDCs for 0.5 hr were visualized by confocal microscopy.
B. NCI-H460 cells were treated with DDCs or TA-DDCs for 0.5, 2 hr and 4 hr in the presence or absence of haloperidol (50 μM) and analyzed by flow cytometry. The y-axis represents fold increase in fluorescence intensity over untreated cells.

4.4.4. Plasma Disposition of DDCs

Plasma disposition study was performed to investigate the long-circulating property of TA-DDCs (**Figure 4.5**). The TA-DDCs showed a rapid distribution followed by a sustained plasma profile upto 48 hr and circulation $t_{1/2}$ of 14.8 hr (12-fold) compared to 1.23 hr for Ida reported previously in BALB/c mice (Dos Santos et al., 2005). Although sigma receptors have been shown to be expressed in other organs of the body (Su et al., 1988), we expect that the large molecular size of DDCs will minimize the uptake in non-target organs. This will result in an increased accumulation in the tumors and lead to further enhancement of the therapeutic index allowing higher doses to be administered.

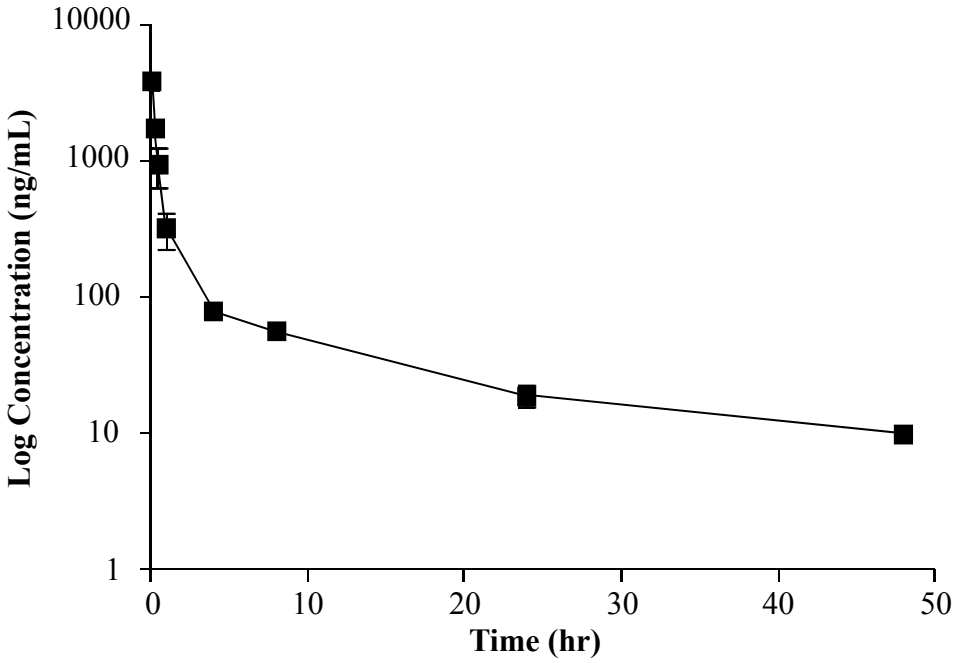

Figure 4.5 Plasma disposition of TA-DDCs in mice bearing NCI-H460 tumors.
TA-DDCs were dosed at 3 mg/kg Ida equivalent and 7.5 mg/kg D-pen equivalent dose in anthymic *nu/nu* mice bearing NCI-H460 tumor xenografts. A dosing schedule of Q2dx3 was followed.

4.5. Conclusions

Preliminary investigations showed that DDCs targeted to sigma-1 receptor enhanced the cellular uptake and cytotoxicity. The TA-DDCs were longer circulating and are, therefore, expected to increase the tumor accumulation of conjugated drugs. Future studies will focus on determining the binding properties of conjugates and further optimization of the conjugate to enable *in-vivo* anticancer efficacy.

4.6. References

Aydar, E., P. Onganer, R. Perrett, M.B. Djamgoz, and C.P. Palmer. 2006. The expression and functional characterization of sigma (sigma) 1 receptors in breast cancer cell lines. Cancer Lett. 242:245-257.

Aydar, E., C.P. Palmer, and M.B. Djamgoz. 2004. Sigma receptors and cancer: possible involvement of ion channels. Cancer Res. 64:5029-5035.

Banerjee, R., P. Tyagi, S. Li, and L. Huang. 2004. Anisamide-targeted stealth liposomes: a potent carrier for targeting doxorubicin to human prostate cancer cells. Int J Cancer. 112:693-700.

Chen, Y., J. Sen, S.R. Bathula, Q. Yang, R. Fittipaldi, and L. Huang. 2009. Novel cationic lipid that delivers siRNA and enhances therapeutic effect in lung cancer cells. Mol Pharm. 6:696-705.

Dos Santos, N., D. Waterhouse, D. Masin, P.G. Tardi, G. Karlsson, K. Edwards, and M.B. Bally. 2005. Substantial increases in idarubicin plasma concentration by liposome encapsulation mediates improved antitumor activity. J Control Release. 105:89-105.

Duncan, R., T.A. Connors, and H. Meada. 1996. Drug targeting in cancer therapy: the magic bullet, what next? J Drug Target. 3:317-319.

Hanner, M., F.F. Moebius, A. Flandorfer, H.G. Knaus, J. Striessnig, E. Kempner, and H. Glossmann. 1996. Purification, molecular cloning, and expression of the mammalian sigma1-binding site. Proc Natl Acad Sci U S A. 93:8072-8077.

Khorev, O., D. Stokmaier, O. Schwardt, B. Cutting, and B. Ernst. 2008. Trivalent, Gal/GalNAc-containing ligands designed for the asialoglycoprotein receptor. Bioorg Med Chem. 16:5216-5231.

Mach, R.H., Y. Huang, R.A. Freeman, L. Wu, S. Vangveravong, and R.R. Luedtke. 2004. Conformationally-flexible benzamide analogues as dopamine D3 and sigma 2 receptor ligands. Bioorg Med Chem Lett. 14:195-202.

Maurice, T., and T.P. Su. 2009. The pharmacology of sigma-1 receptors. Pharmacol Ther. 124:195-206.

Nakagawa, O., X. Ming, L. Huang, and R.L. Juliano. 2010. Targeted intracellular delivery of antisense oligonucleotides via conjugation with small-molecule ligands. J Am Chem Soc. 132:8848-8849.

Simnick, A.J., C.A. Valencia, R. Liu, and A. Chilkoti. 2010. Morphing low-affinity ligands into high-avidity nanoparticles by thermally triggered self-assembly of a genetically encoded polymer. ACS Nano. 4:2217-2227.

Spruce, B.A., L.A. Campbell, N. McTavish, M.A. Cooper, M.V. Appleyard, M. O'Neill, J. Howie, J. Samson, S. Watt, K. Murray, D. McLean, N.R. Leslie, S.T. Safrany, M.J. Ferguson, J.A. Peters, A.R. Prescott, G. Box, A. Hayes, B. Nutley, F. Raynaud, C.P. Downes, J.J. Lambert, A.M. Thompson, and S. Eccles. 2004. Small molecule antagonists of the sigma-1 receptor cause selective release of the death program in tumor and self-reliant cells and inhibit tumor growth in vitro and in vivo. Cancer Res. 64:4875-4886.

Su, T.P., T. Hayashi, and D.B. Vaupel. 2009. When the endogenous hallucinogenic trace amine N,N-dimethyltryptamine meets the sigma-1 receptor. Sci Signal. 2:pe12.

Su, T.P., E.D. London, and J.H. Jaffe. 1988. Steroid binding at sigma receptors suggests a link between endocrine, nervous, and immune systems. Science. 240:219-221.

Vilner, B.J., C.S. John, and W.D. Bowen. 1995. Sigma-1 and sigma-2 receptors are expressed in a wide variety of human and rodent tumor cell lines. Cancer Res. 55:408-413.

Wang, B., R. Rouzier, C.T. Albarracin, A. Sahin, P. Wagner, Y. Yang, T.L. Smith, F. Meric-Bernstam, C. Marcelo Aldaz, G.N. Hortobagyi, and L. Pusztai. 2004. Expression of sigma 1 receptor in human breast cancer. Breast Cancer Res Treat. 87:205-214.

APPENDIX A

Lipid Nanocapsules as Vaccine Carriers for His-Tagged Proteins: Evaluation of Antigen Specific Immune Responses to HIV I His-Gag p41 and Systemic Inflammatory Responses

A.1 Abstract

The purpose of this study was to design novel nanocapsules (NCs) with surface-chelated nickel (Ni-NCs) as a vaccine delivery system for histidine (His)-tagged protein antigens. Ni-NCs were characterized for binding His-tagged model proteins through high affinity non-covalent interactions. The mean diameter and zeta potential of the optimized Ni-NCs was 214.9 nm and -14.8 mV, respectively. The optimal binding ratio of His-tagged Green Fluorescent Protein (His-GFP) and His-tagged HIV-1 Gag p41 (His-Gag p41) to the Ni-NCs was 1:221 and 1:480 w/w, respectively. The uptake of Ni-NCs by DC2.4 dendritic cells was visualized by microscopy. Treatment of DC2.4 cells with Ni-NCs did not result in significant loss in the cell viability up to 24 h (<5%). We further evaluated the antibody response of the Ni-NCs using His-Gag p41 as a model antigen. Formulations were administered subcutaneously to BALB/c mice at day 0 (prime) and 14 (boost) followed by serum collection on day 28. Serum His-Gag p41 specific antibody levels were found to be significantly higher at 1 and 0.5 μg doses of Gag p41-His-Ni-NCs (His-Gag p41 equivalent) compared to His-Gag p41 (1 μg) adjuvanted with aluminum hydroxide (AH). The serum IgG2a levels induced by Gag p41-His-Ni-NCs (1 μg) were significantly higher than AH adjuvanted His-Gag p41. The Ni-NCs alone did not result in elevation of systemic IL-12/p40 and CCL5/RANTES inflammatory cytokine levels upon subcutaneous administration in BALB/c mice. In conclusion, the proposed Ni-NCs can bind His-tagged proteins and have the potential to be used as antigen delivery system capable of generating strong antigen specific antibodies at doses much lower than with aluminum based adjuvant and causing no significant elevation of systemic proinflammatory IL-12/p40 and CCL5/RANTES cytokines.

A.2. Introduction

Subunit vaccines containing soluble protein antigens have been proposed as alternatives to using whole organisms to generate immune responses because of reproducible immune responses and better characterization (Peek et al., 2008). However, many of these antigens are poorly immunogenic if administered alone. Particulate antigen delivery systems like nanoparticles (NPs), emulsions, microparticles and liposomes have been shown to enhance the recognition of the antigens by the antigen presenting cells (APCs) and result in improved immune response (Aline et al., 2009; Alving, 1995; Audran et al., 2003; Ott et al., 1995). Formation of a depot at the site of injection has been proposed as a possible mechanism of enhanced antigen recognition by particulate systems (Panyam and Labhasetwar, 2003). In addition to being taken up efficiently by the APCs, NPs have the potential to release the entrapped antigen over prolonged time. Moreover, surface modification allows incorporation of a variety of antigens on the same particle and surface-coated ligands to target the APCs (Klippstein and Pozo, 2010; Yan et al., 2009).

The antigen can be either entrapped inside the matrix/core of the particle or coated on the surface. The entrapment of protein in the core of a particle has problems associated with the stability of the protein during the preparation of particles and poor entrapment (Duncan et al., 2005). The surface coating of the antigen on the particle may be achieved by ionic interactions (Patel et al., 2007a), covalent conjugation (Sloat et al., 2010) or non-covalent attachment (Patel et al., 2007b). We have previously reported that increasing the affinity of the antigen to the surface of solid lipid NPs contributes to enhanced immune responses as compared to the antigens associated on the surface via simple adsorption or charge-charge interactions (Patel et al., 2007a; Patel et al., 2007b).

In the present study, we investigated the formulation of novel nanocapsules (NCs) with surface chelated nickel (Ni-NCs) in the outer shell and their potential to bind histidine (His)-tagged proteins with high affinity through non-covalent attachment. The strong non covalent interaction ($K_d \sim 10^{-6} – 10^{-14}$ M) between nucleophilic ligands such as the His-tag on a protein and transition metal ions like Ni and Cu has been investigated in detail and has been successfully applied to protein purification (Hochuli et al., 1987; Knecht et al., 2009; Porath et al., 1975). This interaction is highly dependent on individual protein, the site and length of His-tag and pH (Knecht et al., 2009; Lauer and Nolan, 2002). Liposomes and iron oxide NPs with surface chelated Ni have been previously proposed for the delivery and purification of His-tagged proteins (Kim et al., 2007; Platt et al., 2010). We formulated the Ni-NCs using 1,2-dioleoyl-*sn*-glycero-3-[(N-(5-amino-1-carboxypentyl) iminodiacetic acid) succinyl] (nickel salt) (DGS-NTA-Ni), a lipid with NTA end group that can chelate Ni. Platt and co-workers concluded that the association of NTA-Ni and his-tagged proteins is in micromolar range which may be considered weak for *in-vivo* conditions. However, later studies comparing NTA to trivalent NTA ligands suggested that increasing the affinity of this interaction did not lead to an increase in immune responses (Platt et al., 2010; Watson et al., 2011). Although this report showed that covalently bound antigen elicits stronger responses, the effect of the nature of association on immune response may be antigen-specific as was reported by Shahum and Therien (Shahum and Therien, 1988). Moreover, it has been previously known that covalent modification of antigens is prone to causing changes in the antigenicity and loss of binding (Cooper et al., 1987). Non-covalent attachment while enhancing the antigen association is expected to preserve the antigenicity by ensuring the presentation of the unmodified antigen.

Aluminum salts remain the only FDA approved particulate adjuvants. They have been shown to induce strong antibody responses but there is uncertainty in induction of cellular immunity (Rabinovich et al., 1994). Additionally, the use of aluminum containing salts has been linked to hypersensitivity reactions and physical or chemical alterations of the adsorbed protein antigen in some cases (Baylor et al., 2002). NPs have been investigated for their superior safety profile and an ability to protect the entrapped antigen (Wang et al., 2008). In addition, we have reported strong humoral and cellular immune responses against several protein antigens like TAT, p24 and Nef coated onto solid lipid NPs and that NP bound antigens have the potential to generate CD8+ T cell responses (Cui et al., 2004).

In the present studies, we investigated a new type of lipid-based NCs developed in our laboratory for their potential to deliver His-tagged proteins. His-Gag p41 was used as a model antigen. We also compared the immune responses from our previously reported (Patel et al., 2007b) nickel decorated solid lipid NPs (Ni-NPs) to the novel Ni-NCs.

A.3. Materials and Methods

A.3.1. Materials and Reagents:

Polyoxyethylene (20) stearyl ether (Brij® 78), d-α-tocopheryl polyethylene glycol 1000 succinate (Vitamin E TPGS) and Miglyol® 812 (caprylic/capric triglycerides) were purchased from Uniqema (Wilmington, DE), Eastman Chemicals (Kingsport, TN) and Sasol (Witten, Germany), respectively. Sepharose® CL-4B and DGS-NTA-Ni were obtained from GE Healthcare (Piscataway, NJ) and Avanti Polar Lipids (Alabaster, AL), respectively. Inductively Coupled Plasma-Mass Spectrometry (ICP-MS) standard for Nickel was purchased from Sigma Aldrich (St. Louis, MO) and N-terminal His-tagged GFP (His-GFP) was purchased from Millipore (Billerica, MA). Aluminum hydroxide gel (Cat. No. AL226) and emulsifying wax (comprised of cetyl alcohol and polysorbate 60 in a molar ratio of 20:1) were purchased from Spectrum Chemicals (Gardena, CA). CpG oligonucleotide (5'- tcc atg acg ttc ctg acg tt -3') (20 mer) (CpG ODN) was purchased from InvivoGen (San Diego, CA).

A.3.2. Preparation of Ni-NCs

To prepare Ni-NCs, Brij 78 (3.5 mg), Vitamin E TPGS (1.5 mg) and Miglyol 812 (2.5 mg) were weighed in a glass vial. DGS-NTA-Ni (varying amounts of 10 mg/mL stock solution in chloroform) and 0.2 mL ethanol were added and mixed. The solvents were later evaporated under nitrogen. The vial was placed in a water bath at 65^{o}C and deionized water (1 mL) preheated to 65^{o}C was added while stirring the contents for 30 min. The Ni-NCs form spontaneously and are composed of liquid core (Miglyol 812) and solid shell (Brij 78 and Vitamin E TPGS). The suspension was cooled to room temperature and separated from free components using a Sepharose CL-4B column (1.5 x 15 cm). The purified Ni-NCs were

characterized for particle size using Beckman Coulter N5 Submicron Particle Size Analyzer (Beckman Coulter, Brea, CA) and zeta potential using a Malvern Nano-Z (Malvern Instruments, Southborough, MA). **Table A.1** lists the representative formulations. For comparison, Ni-NPs were prepared as previously reported (Patel et al., 2007b). Briefly, emulsifying wax (2 mg) and Brij 78 (3.5 mg) were weighed in a glass vial and heated to 65^{o}C. DGS-NTA-Ni (0.106 mg; 10 mg/mL stock solution in chloroform) was added to the mixture. Deionized water (1 mL) was added and the contents were stirred at 65^{o}C to form a clear oil-in-water microemulsion. Ni-NPs were obtained by cooling the microemulsion to room temperature that causes the solidification of the core and the shell components. The Ni-NPs were purified as described above.

A.3.3. Determination of Surface Nickel Content

ICP-MS was used to quantify the amount of Ni on the surface of the Ni-NCs available for binding to His-tagged ligands using Varian 820 Mass Spectrometer (Palo Alto, CA). A standard curve for Ni was prepared using Ni standard solution (1000 mg/L) in the concentration range of 9 – 200 ppb. The recovery of Ni from the Ni-NCs was quantified by spiking the standards with Ni-NCs dissolved in 0.2 mL of ethanol. To quantify the amount of Ni on the surface, the Ni-NCs were diluted with 2% nitric acid, filtered through a 0.2 μm filter and analyzed by ICP-MS. Ni concentrations were calculated from the previously developed standard curve. Formulation NC02 was selected for further studies based on lower polydispersity and higher DGA-NTA-Ni incorporation (wt %) compared to other formulations (**Table A.2**).

Formulation/ Components	NC00	NC01	NC02	NC03
Brij 78 (mg)	3.5	3.5	3.5	3.5
Vitamin E TPGS (mg)	1.5	1.5	1.5	1.5
Miglyol 812 (mg)	2.5	2.5	2.5	2.5
DGS-NTA-Ni (mg)	None	0.1	0.25	0.50

Table A.1 Representative nanocapsule (NC) formulations with various components designed to incorporate surface chelated nickel.

Formulation/ Parameters	NC00	NC01	NC02	NC03
DGS-NTA-Ni (wt % after purification)	None	1.05 ± 0.01	2.73 ± 0.04	3.51 ± 0.04
Particle Size (nm) (Mean ± SD)	197.2 ± 59.3	199.7 ± 67.4	214.9 ± 57.1	270.2 ± 145.2
Zeta Potential (mV)	-7.8	-16.2	-14.8	-35.9
Nickel Content (ng/mg NPs)	ND	29.5 ± 2.8	145.6 ± 19.5	228.4 ± 38.5

Table A.2 Physicochemical characterization of the representative NC formulations with or without the incorporation of surface chelated nickel.
*The calculation of DGS-NTA-Ni incorporation (%) was based on the experimental values obtained by ICP-MS in Ni-NCs before and after the gel filtration chromatography using Sepharose Cl-4B column to separate non-incorporated components.
ND = Not detected

A.3.4. His-GFP Biding to Ni-NCs

To investigate the extent of accessible Ni on the surface, formulation NC02 was mixed with His-GFP in several Ni to His-GFP molar ratios (1:0.1, 1:0.2, 1:0.4 and 1:0.8) and incubated at 4^{o}C overnight to allow for surface binding. Formulation NC00 was also incubated with His-GFP (amount similar to that used in the ratio 1:0.2 above) to determine non-specific association. The GFP-His-Ni-NC02 was separated from unbound His-GFP using a Sepharose CL-4B column (1.5 x 15 cm) equilibrated with 10 mM PBS. Briefly, 0.2 mL mixture was applied to the column and 1 mL fractions were collected. Subsequently, the fluorescence associated with each fraction was measured (Ex 360/40, Em 528/20) on a Synergy^{TM} 2 Multi-Detection Microplate Reader (Biotek, Winooski, VT). The particle intensity of each fraction was also measured and fractions containing GFP-His-Ni-NC02 were pooled and characterized for their particle size and zeta potential, respectively.

A.3.5. Microscopy

Formulation NC02 was visualized by transmission electron microscopy (TEM) to understand the morphology of the particles. Briefly, 5 μL (approximately 1.6 x 10^6 particles) of diluted NC02 suspension was spread on a Pelco formvar coated 300 mesh copper grid (01710-F, Ted Pella, Redding, CA). The suspension was allowed to air dry for 5 min. Any remaining liquid was wicked off. There was no additional staining. The grids were then examined with a Zeiss EM 900 Transmission Electron Microscope using 50 kV accelerating voltage. The images were acquired using photographic film which was subsequently digitized.

A.3.6. Uptake of GFP-His-Ni-NCs by Dendritic Cells

The DC2.4 murine dendritic cell line was obtained from Dr. Kenneth L. Rock (Department of Pathology, University of Massachusetts Medical School). The cells were cultured in RPMI 1640 (ATCC) supplemented with 10% fetal bovine serum, 2 mM glutamine, 55 μM beta-mercaptoethanol, non-essential amino acids, 10 mM HEPES buffer and 100 U/mL penicillin and 100 μg/mL streptomycin (GIBCO). Trypan blue was used to determine viability and cells were used for experiments when 70-80% confluent. Uptake of GFP-His-Ni-NC02 (NC02-02, **Table A.3**) by DC2.4 dendritic cells was determined using confocal microscopy. Briefly, 1 x 10^5 cells were added to chamber slides (Lab-Tek® Chamber Slide System™, Nunc) and incubated overnight to allow for attachment of cells followed by treatment with predetermined concentration of NC02-02 for 2 hr. The cells were fixed with 4% paraformaldehyde and permeabilized using 0.2% Triton X-100. Subsequently, the cells were counterstained using 4,6-diamidino-2-phenylindole (DAPI) and mounted using Prolong® Gold Antifade Reagent (Invitrogen). The slides were visualized on a Leica DM IRB Inverted Microscope using a 100x oil objective.

A.3.7. Effect of GFP-His-Ni-NCs on the Viability of Dendritic Cells

The DC2.4 dendritic cells were incubated with different concentrations of NC02 for up to 48 hr. The cells were trypsinized with 0.05% Trypsin-EDTA (GIBCO), suspended in culture medium, centrifuged at 200 g x 5 min and re-suspended in 10 mM PBS containing 1 mM EDTA and 10% fetal bovine serum. Propidium iodide (PI) was added to the cell suspension as a viability marker at a final concentration of 1 μg/mL immediately before analysis by flow cytometry. Flow cytometric analysis was performed using BD LSRII Flow

Cytometer (BD Biosciences, Mountain View, CA). Data analysis was performed using Flow Jo 7.6Software (Tree Star, Ashland, OR).

A.3.8. His-Gag p41 Binding to Ni-NCs

Purified recombinant His-Gag p41 protein (HXB2 isolate) was generously provided by Dr. Robert Seder (NIH-NIAID) and was used as model antigen. The protein was fluorescently labeled using NHS-fluorescein. Briefly, 16 μg of NHS-fluorescein (186 μg/mL stock solution in DMSO) was added to 325 μg of His-Gag p41 (1.2 mg/mL stock solution in 10 mM PBS). The mixture was incubated overnight at 4^{o}C. Excess reactants were separated from the protein using a desalting spin column. The degree of modification was calculated using the molar extinction coefficient of fluorescein (ε = 68,000 M^{-1} cm^{-1}, λ_{max} = 493 nm). The fluorescein-His-Gag p41 was incubated with NC02 in different weight ratios (His-Gag p41:NC02) as described previously for His-GFP to estimate the binding of fluorescein-His-Gag p41 to NC02.

A.3.9. Mouse Immunization Study

Eight to 10-weeks old female BALB/c mice (n = 5–7/group) from Charles River Laboratories were used for immunization studies. The experimental design is shown in **Table A.4**. Formulations (100 μL) were administered subcutaneously in the nape of the neck on day 0 and 14. Gag p41-His-Ni-NC02 (His-Gag p41:Ni-NCs weight ratio of 1:480) was used to prepare three different concentrations that were subsequently administered to mice to give three different doses of His-Gag p41. Gag p41-His-Ni-NP (His-Gag p41:Ni-NP weight ratio of 1:100) were administered for comparison. Immune responses were compared to His-Gag

p41 adjuvanted with AH. Mice were bled by cardiac puncture on day 28 and sera were collected. All sera were stored at -20^{o}C until further analysis.

A.3.10. Determination of Antibody Levels

His-Gag p41 specific serum IgG, IgG1 and IgG2a antibody levels were determined by ELISA. Briefly, 96-well plates were coated with 50 µL His-Gag p41 (5 µg/mL in PBS) overnight at 4^{o}C. The wells were blocked using 4% BSA prepared in PBS/Tween 20 for 1 hr at 37^{o}C. Subsequently, 50 µL of mouse serum at predetermined dilution was added and plates were incubated for 2 hr at 37^{o}C. Horseradish Peroxidase (HRP) conjugated Anti-mouse IgG $F(ab^{/})_2$ fragment from sheep (50 µL of 1:3000 dilution in 1% BSA in PBS/Tween 20) was added and incubated for 1 hr at 37^{o}C. TMB (3,3,5,5-tetramethylbenzidine) substrate (100 µL) was added to each well and incubated for 30 min at RT. Color development was stopped by addition of 2M sulfuric acid and the absorbance at 450 nm was measured on Synergy^{TM} 2 Multi-Detection Microplate Reader (Biotek, Vinooski, VT). For the determination of IgG1 and IgG2a, the plates were blocked for 1 hr at 37^{o}C as described above followed by incubation with mouse serum for 1 hr at RT. The plates were incubated with biotinylated rat anti-mouse IgG1 or IgG2a for 1 hr at RT followed by incubation with streptavidin HRP for 30 min at RT. The plates were developed as described for IgG. The wells were washed four times with PBS/Tween 20 before each step.

A.3.11. Systemic Cytokine Induction Studies

To investigate the induction of inflammatory cytokines upon s.c. administration of Ni-NCs, 8–10 weeks old female BALB/c mice (n = 3/time point) were used. Briefly, 0.48 mg

of NC02 or 10 μg CpG ODN (0.1 mg/mL in PBS) were administered to mice. Blood was collected by cardiac puncture at 3, 6, 12, 24 and 48 hr after administration. Sera were collected and stored at -20^{o}C.

The serum concentration of IL-12/p40 and RANTES/CCL5 were determined by BD^{TM} cytometric bead array (CBA) flex assay following manufacturer's protocol (BD Pharmingen, La Jolla, CA). Flow cytometric analysis was performed using BD^{TM} LSRII Flow Cytometer (BD Biosciences, Mountain View, CA). Data analysis was performed using Flow Jo 7.6Software (Tree Star, Ashland, OR).

A.3.12. Statistical Analysis

Statistical analysis was performed using GraphPad Prism 4 Software (GraphPad Software, San Diego, CA). Differences in antibody responses among treatment groups were analyzed by one way ANOVA followed by Dunnet's post-test to compare different treatments to the naïve group. Effects on DC2.4 cell viability and cytokine induction results were analyzed by regular two-way ANOVA followed by Bonferroni post-test to compare differences within groups. Differences were considered significant at $p<0.05$.

A.4. Results

A.4.1. Preparation and Characterization of Ni-NCs

Our laboratory has recently reported the formulation of stable spontaneously forming NCs containing a liquid oil core and surfactant-based shell prepared using biocompatible and biodegradable components (Dong et al., 2009a; Dong et al., 2009b). The liquid core consists of Miglyol 812, which is a mixture of caprylic and capric acid triglycerides, while the shell is composed of two nonionic surfactants, Brij 78 and Vitamin E TPGS respectively. We modified the formulation to contain a small amount of surface accessible nickel by incorporating DGS-NTA-Ni in the shell (**Figure A.1**). DGS-NTA-Ni has two out of the six co-ordination sites available to interact with the His residues on proteins. **Table A.1** shows four representative formulations prepared during the optimization of NCs with or without surface accessible nickel. The incorporation of DGS-NTA-Ni was determined by measuring the amount of Ni by ICP-MS. Based on the incorporation efficiency of DGS-NTA-Ni determined by ICP-MS analysis and desired particle size range, formulation NC02 was selected for further studies. The optimized NCs had mean particle size of 214 nm with very low polydispersity upon gel filtration and had negative surface charge density as indicated by zeta potential measurements in 0.5 mM phosphate buffer (**Table A.2**). The negative charges can be due to the formation of small amounts of metal oxides or accumulation of negative ions on the surface of the NCs. We also formulated previously reported Ni-NPs to investigate the effect of particle morphology on antigen delivery (Patel et al., 2007b). The Ni-NPs have a solid matrix core composed of emulsifying wax coated with a single surfactant.

Fig. A.1A

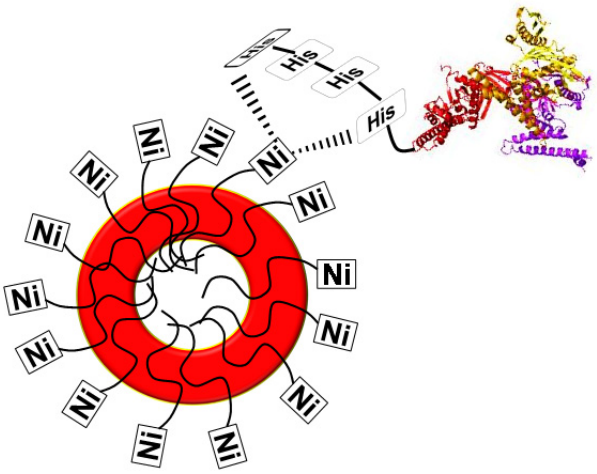

Fig. A.1B

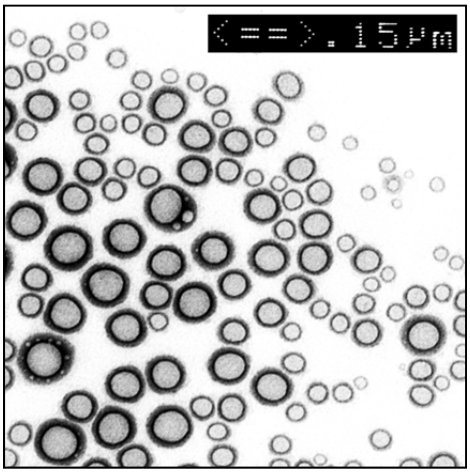

Figure A.1 Nanocapsules (NCs) with surface accessible nickel (Ni-NCs).
A) Ni-NCs having a core and shell morphology were formulated with DGS-NTA-Ni to provide surface accessible nickel for binding to His-tagged proteins. Four out of the six co-ordination sites of Ni in DGS-NTA-Ni are occupied while the two remaining sites are available for His-tagged ligand binding.
B) TEM image of Ni-NCs. The distance between the arrowheads within the blackbox corresponds to 150 nm.

A.4.2. Protein Binding

His-GFP was used as a model protein to study the interaction of His-tag with surface Ni and investigate the binding efficiency of the Ni-NCs. His-GFP can be easily detected by fluorescence making it easier to quantitatively determine the amount of protein bound to the surface and qualitative assessment by microscopy. The GFP-His-Ni-NC02 was separated from unbound His-GFP using gel filtration (Sepharose CL-4B). The fluorescence associated with the particles compared to the fluorescence of the unbound fractions was used to derive the percent of His-GFP bound to the Ni-NCs (**Figure A.2**). The elution of particles from the gel was monitored using particle intensity measurements by light scattering. Based on trials using different ratios of surface Ni to His-GFP, Ni-NCs (NC02-02) incubated at molar ratio of 1:0.2 (Ni:His-GFP) resulted in the highest level of binding (35%). Interestingly, increasing the amount of GFP did not increase the association (**Table A.3**). This indicates that only a limited number of DGS-NTA-Ni are accessible on the surface of the NCs and the binding is therefore, saturable. Theoretical calculations showed that the weight ratio His-GFP: Ni-NC in formulation NC02-02 was 1:221 and the ratio of molecules of Ni (13,300) to molecules of His-GFP (885) was approximately 15. This is expected as the much larger surface area of His-GFP may result in shielding of the surface Ni and the ability of single His-tag residue to complex with multiple Ni atoms. The binding of protein on the surface did not significantly affect the particle size and zeta potential of Ni-NCs (data not shown). Formulation NC00 was used as controls to determine non-specific binding of His-GFP which was found to be negligible (**Figure A.2**). The results from this study provide an evidence of surface binding of His-tagged proteins that was specific to Ni-NCs.

The binding experiments were also performed using fluorescein-His-Gag p41. The weight ratio of 1:480 (His-Gag p41: NC02) resulted in more than 65% of the protein associated with the NC02 (**Figure A.2**).

A.4.3. Microscopy

To examine the morphology of the Ni-NCs, NC02 suspension was observed by TEM. As the Ni-NCs have a soft structure and all the components have lower melting points, the protocol involved air drying of the grids. The TEM images corroborated the sizing parameters obtained by light scattering. Based on TEM analysis, the Ni-NCs ranged in size from 150 – 250 nm (**Figure A.1**). The NCs appeared as hollow spheres that confirms the presence of a fluid core. This is in contrast to similar TEM studies performed with our previous solid lipid nanoparticles where the core is composed of waxy solid and the particles appear as opaque spheres (Oyewumi et al., 2003).

Formulation	Ni:GFP (Molar Ratio)	GFP Associated with NCs (%)
NC02-01	1:0.1	24.87
NC02-02	1:0.2	35.68
NC02-03	1:0.4	32.28
NC02-04	1:0.8	32.70
NC00-01	0:0.2*	2.34

Table A.3 Estimation of accessible nickel on the surface of Ni-NCs using His-GFP as a model protein.

Ni-NCs were incubated with His-GFP at different molar ratios of Ni:His-GFP. The GFP-His-Ni-NCs were purified and the percentage of fluorescence associated with NCs was calculated.

*Formulation NC02 was incubated with His-GFP to estimate non-specific binding in the absence of surface nickel. The amount of GFP incubated with NC00 was equivalent to that used in NC02 (Ni:His-GFP of 1:0.2) trial.

Fig. A.2A

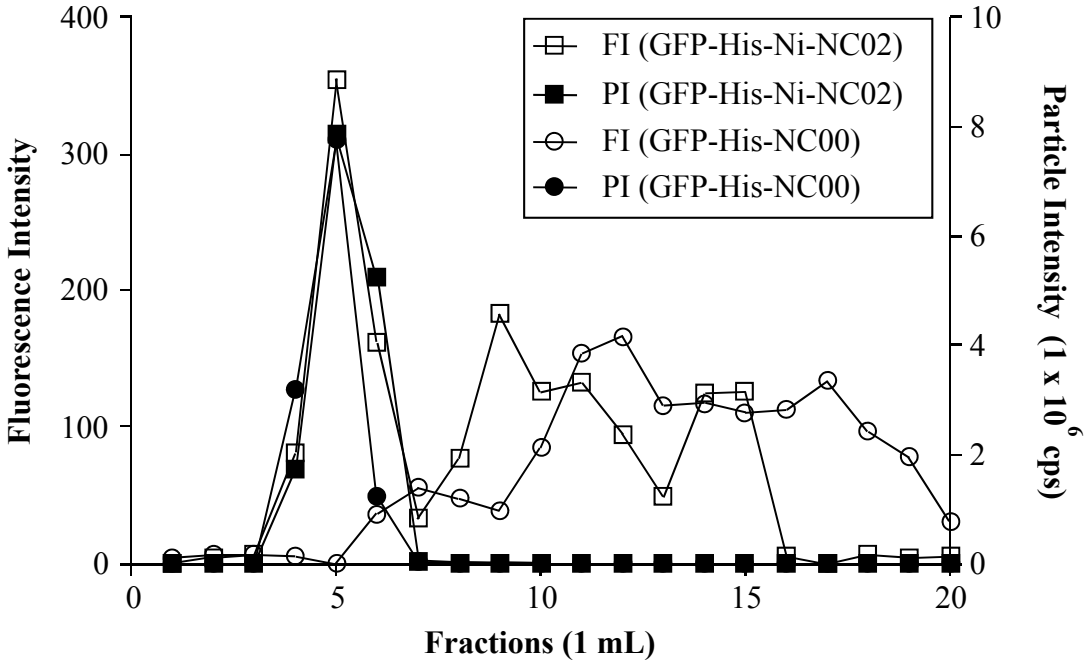
FI (GFP-His-Ni-NC02)
PI (GFP-His-Ni-NC02)
FI (GFP-His-NC00)
PI (GFP-His-NC00)
Fluorescence Intensity
Particle Intensity (1 x 10^6 cps)
Fractions (1 mL)
0
100
200
300
400
0
2
4
6
8
10
0
5
10
15
20

Fig. A.2B

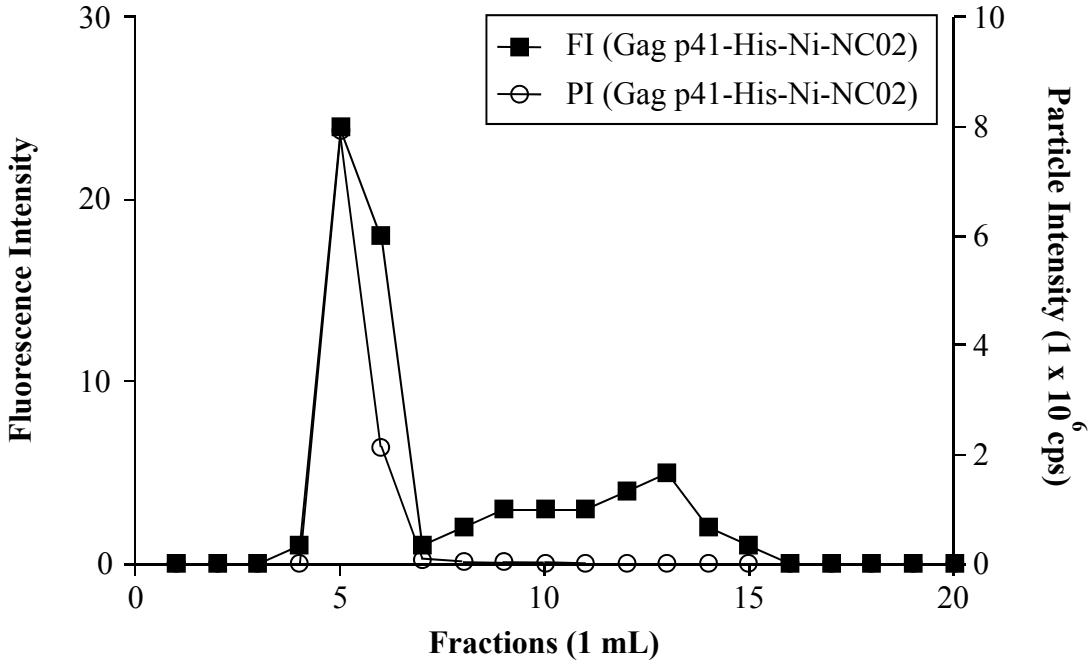

Figure A.2 Binding of His-tagged proteins to Ni-NCs.
A) Ni-NCs formulated with (formulation NC02) or without (formulation NC00) surface Ni were compared to determine specific and non-specific binding of His-GFP as a model protein, and to determine the binding efficiency of the Ni-NCs. The Ni-NCs were separated from unbound His-GFP by elution from a Sepharose CL-4B column (1.5 x 15 cm) using 10 mM PBS as the elution medium. The elution of Ni-NCs was monitored by measuring the particle intensity (PI) while the fluorescence intensity (FI) was measured to determine His-GFP associated with each fraction.
B) Binding of fluorescein-His-Gag p41 to the surface of Ni-NCs (formulation NC02) was determined similarly.

A.4.4. Uptake and Toxicity of NCs in Dendritic Cells

Dendritic cells are the most potent APCs. Particulate delivery systems are suited for rapid uptake by the dendritic cells due to their size. We investigated the uptake of GFP-His-Ni-NC02 by DC2.4 dendritic cells. As shown in **Figure A.3**, the Ni-NCs were taken up by the cells within 2 hr of incubation as indicated by the fluorescence of GFP. The fluorescence was diffused throughout the cytosol with minimal fluorescence in the nucleus. Intact GFP is impermeable to cell membrane (Fuchs and Raines, 2007) and therefore, it can be said that the intact NCs were taken up by the cells possibly via endocytosis. However, we did not evaluate the rate of release of GFP from the NCs upon cell uptake.

The toxicity of the Ni-NCs (NC02) to DCs was investigated by flow cytometry by measuring the fraction of cells that stained positive with PI. NC02 did not show any significant decrease in the viability of the cells up to a concentration of 40 μg/mL for 24 hr. At 48 hr, higher concentrations of NC02 (40 μg/mL) did result in significant PI positive cell population (**Figure A.3**). We have previously shown that Ni-NPs exhibit significant loss of cell viability at comparatively lower concentrations (Yan et al., 2009). This could have implications on adverse events associated with the particle-based delivery systems.

Fig. A.3A

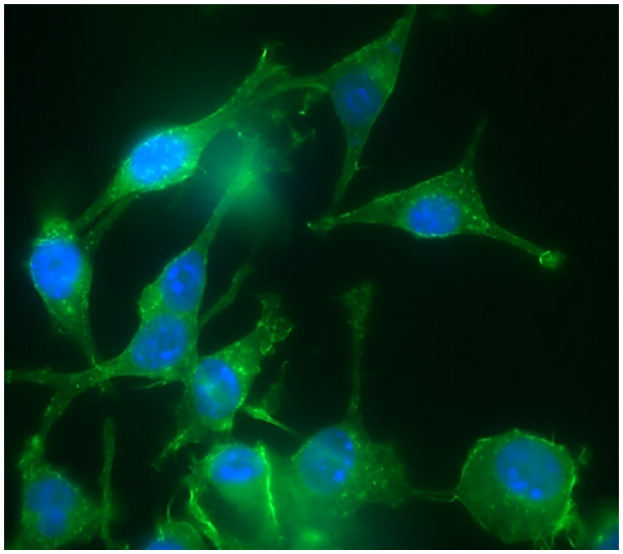

Fig. A.3B

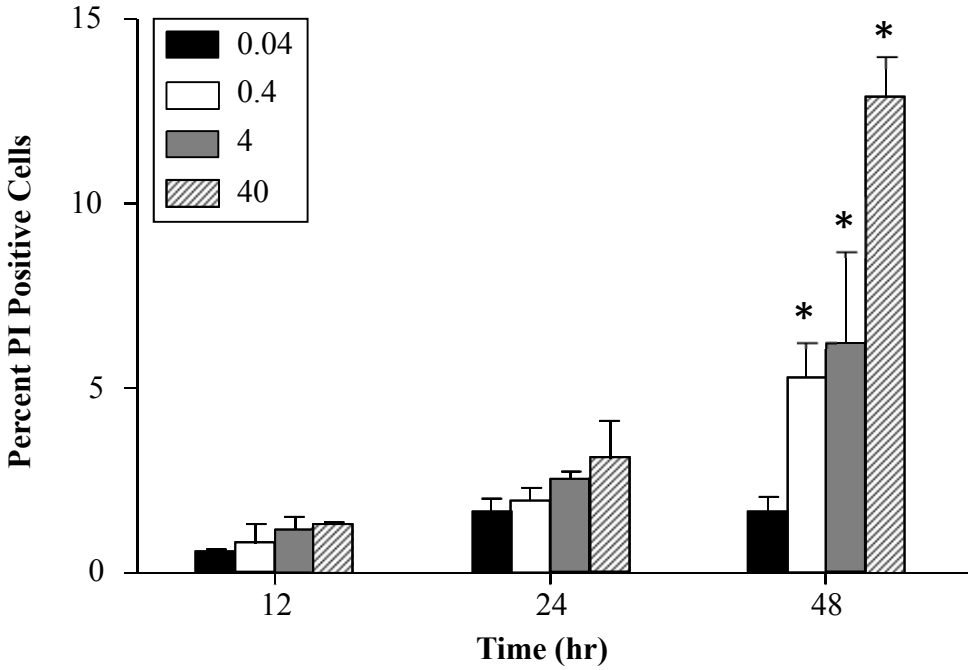

Figure A.3 Interaction of Ni-NCs with DC2.4 dendritic cells.
A) DC2.4 dendritic cells (1 x 10^5) were treated with formulation GFP-His-Ni-NC02 for 2 hr followed by nuclear staining with DAPI. Cells were visualized by confocal microscopy.
B) DC2.4 dendritic cells (1 x 10^5) were treated with formulation NC02 (0.04, 0.4, 4 and 40 μg/ml) following which they were stained with propidium iodide and analyzed by flow cytometry. Data represents mean ± SEM (n = 3). *$p<0.01$

A.4.5. Immunization Study

Mice were immunized with Gag p41-His-Ni-NC02, Gag p41-His-Ni-NPs or His-Gag p41 adjuvanted with AH. Three different doses of His-Gag p41/Ni-NCs (fixed weight ratio of 1:480) were administered to investigate a His-Gag p41 dose response in the antibody generation. When compared at the 1:1000 sera dilution, the Ni-NCs resulted in stronger antibody response compared to AH at both the 1 μg and 0.5 μg His-Gag p41 doses (**Figure A.4**). When compared at the same sera dilution, the OD (450 nm) values for NCs at the 1 μg dose were >4-fold higher than those for Ni-NPs. In contrast to the Ni-NCs used in these studies, the Ni-NPs caused significant loss of viability in DC2.4 dendritic cells at concentrations as low as 4 μg/mL (Yan et al., 2009). Therefore, it is possible that the toxicity to APCs may have contributed to weaker antibody response observed with the Ni-NPs.

The serum isotype levels, IgG1 and IgG2a, were determined by ELISA to investigate the type of immune response. While production of IgG2a isotype has been associated with Th1 response, IgG1 isotype has been associated with Th2 type response. The ratios of IgG2a/IgG1 were used to indicate the Th1 or Th2 bias of the generated immune response (Maassen et al., 2003; Romagnani, 2000). A balanced Th1 and Th2 response is desired following vaccination as excess of either will result in adverse effects. Aluminum containing salts have been reported to generate a Th2 biased response (Marrack et al., 2009; McKee et al., 2009). This is expected to result in a lower IgG2a/IgG1 ratio. In our observations, the ratio IgG2a/IgG1 was 0.14 for AH and 0.55 for Ni-NCs at highest dose of His-Gag p41 (1 μg) respectively (**Figure A.4**).

A.4.6. Systemic Cytokine Induction Studies

To investigate the immunostimulating activity of Ni-NCs, we determined the induction of pro-inflammatory cytokines by Ni-NCs (formulation NC02). CpG ODN was administered as strong inducer of pro-inflammatory cytokines. We determined serum concentrations of IL-12/p40 and CCL5/RANTES upon s.c. injection of Ni-NCs in comparison to CpG ODN and untreated animals. The results demonstrate that Ni-NCs did not result in significant elevation in the level of any of the cytokines measured over control while CpG was a strong inducer of both the cytokines (**Figure A.5**). This indicates that the Ni-NCs are potentially a safe delivery vehicle and may result in fewer adverse events upon administration. However, this also indicates that additional (safe) adjuvant(s) may be needed in certain cases to potentiate the immune response by Ni-NCs.

Group/Treatment	Dose His-Gag p41 equivalent (μg)	Dose (mg of NCs)
Naive	0	0
Gag p41-His-Ni-NCs (NC02)	1	0.48
Gag p41-His-Ni-NCs (NC02)	0.5	0.24
Gag p41-His-Ni-NCs (NC02)	0.1	0.048
AH + His-Gag p41	1	0.48
Gag p41-His-Ni-NPs	1	0.1

Table A.4 Mouse immunization study design.
Female BALB/c mice were s.c. administered treatments on day 0 (prime) and 14 (boost). Sera were collected on day 28 and analyzed by ELISA.

Fig. A.4A

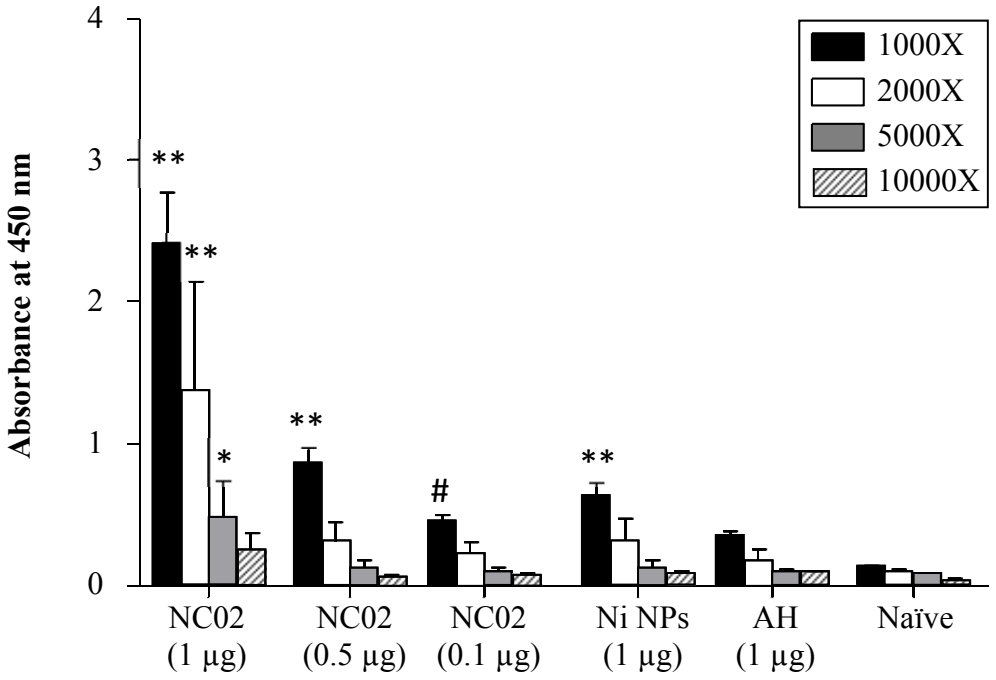
Absorbance at 450 nm
4
3
2
1
0
1000X
2000X
5000X
10000X
**
**
*
**
#
**
NC02 (1 µg)
NC02 (0.5 µg)
NC02 (0.1 µg)
Ni NPs (1 µg)
AH (1 µg)
Naïve

Fig. A.4B

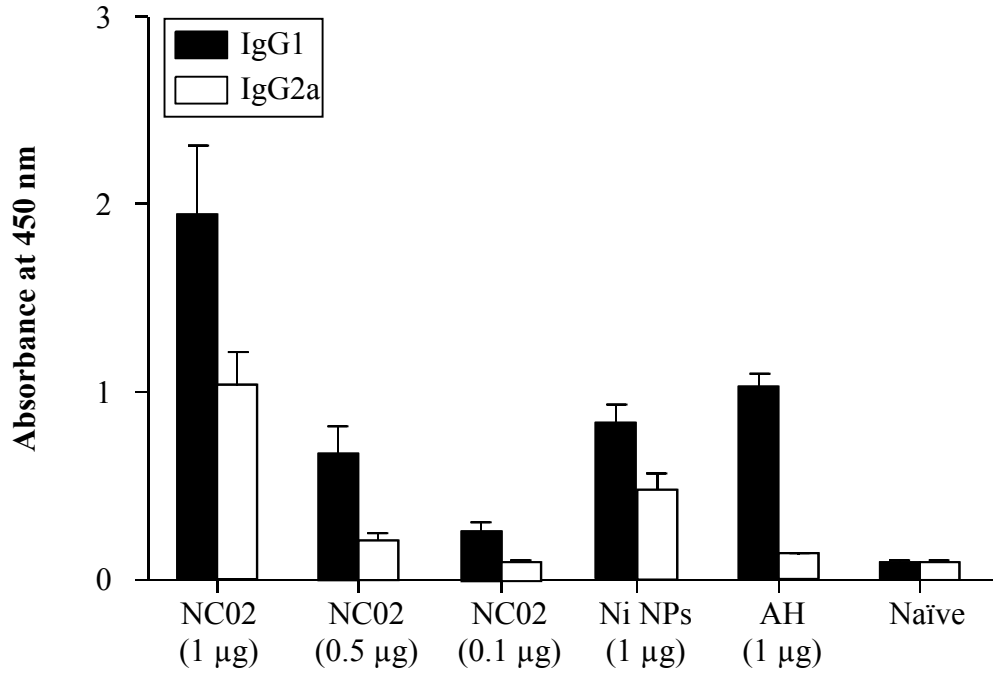

Figure A.4 Antibody responses in BALB/c mice.
A. Female BALB/c mice were immunized on days 0 and 14 with 100 µL of Gag p41-His-Ni-NPs, Gag p41-His-Ni-NC02 or His-Gag p41 adjuvanted with Aluminum Hydroxide (AH).
B. Serum samples were also analyzed for IgG1 and IgG2a levels.
His-Gag p41-equivalent dose is indicated in parentheses on X-axis. Serum was analyzed on day 28 by ELISA. Data represents mean ± SEM (n = 6–7). # $p<0.05$, * $p<0.01$, **$p<0.001$ compared to naïve (untreated) group.

Fig. A.5A

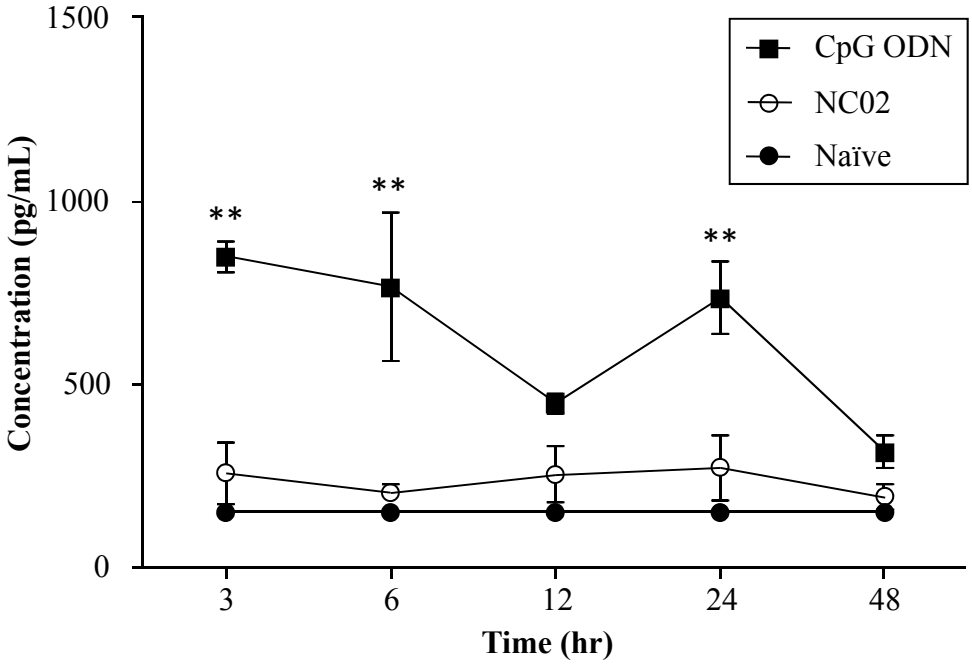
1500
1000
500
0
Concentration (pg/mL)
**
**
**
3
6
12
24
48
Time (hr)
CpG ODN
NC02
Naïve

Fig. A.5B

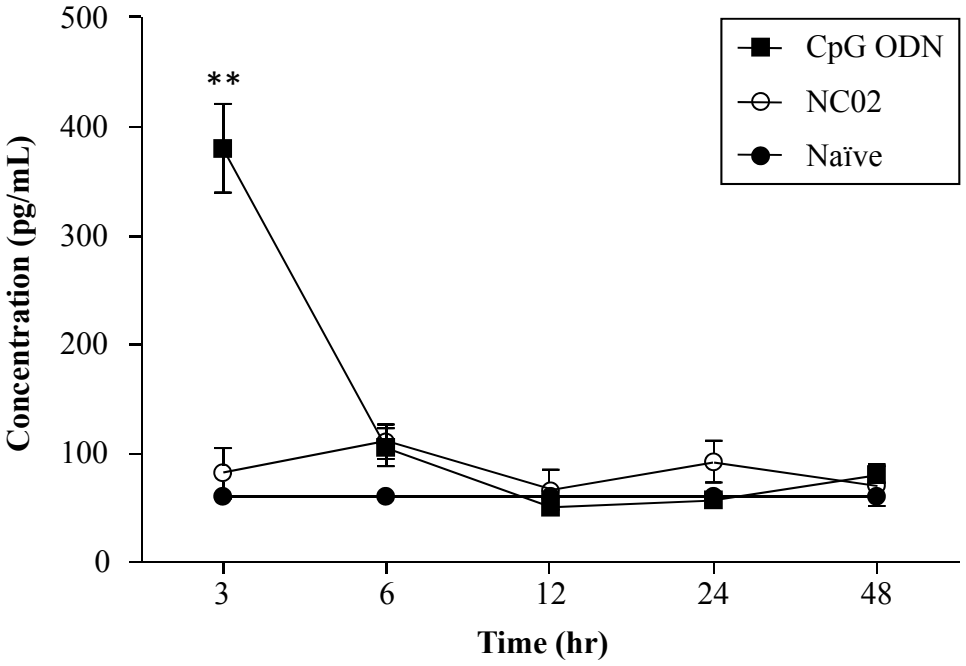

Figure A.5 Serum cytokine analysis.
Serum levels of A) IL-12/p40 and B) CCL5/RANTES were measured at predetermined time points following s.c. administration of formulation NC02 (0.48 mg) in female BALB/c mice. CpG ODN (10 μg) was administered as positive control. Analysis was performed by cytometric bead array flex assay. Data represents mean ± SEM (n = 3), ** $p<0.001$.

A.5. Discussion

This study aimed at developing NCs with chelated Ni on the surface thus providing binding sites for His-tagged antigens. The Ni-NCs of the present study are composed of completely metabolizable or biocompatible components and have the ability to carry multiple antigens as well as an adjuvant. Therefore, using them as a vehicle for the delivery of vaccines is a promising approach.

Delivery of antigen by particulate systems requires their association or entrapment. The effect of the type of association on the resulting immune response has been a matter of debate over the past two decades and several contradicting reports have been published (Shahum and Therien, 1988; Watson et al., 2011). In our previous studies, we observed that increasing the association of the antigen to the surface of the NPs increased the associated antibody responses (Patel et al., 2007b). Continuing on the previously obtained results, we investigated non-covalent attachment of the antigen to the NPs exploiting the Ni-His interaction. NTA has been used as a popular ligand for Ni in delivery systems (Huang et al., 2006). The effect of spacer group and the valency show that while the length of the spacer may have some effect on the accessibility, the valency does not affect the antibody responses (Huang et al., 2009; Watson et al., 2011). The Ni-NCs exhibited specific binding ability for His-tagged model protein although the extent of binding can be increased by improving the binding affinity of surface nickel. This may be done by modifying the length and amphiphilicity of the spacer group to reduce steric effects on the surface of the NPs although some steric hindrance is desired to reduce the exchange of the bound protein with other His-tagged proteins or serum proteins.

The overall safety and absence of hypersensitivity are desirable features of a vaccine formulation. The presence of Ni in the formulations of the present study may be of concern in view of studies implicating adverse events like immunosuppression (Smialowicz et al., 1984) and carcinogenicity (Buzard and Kasprzak, 2000) upon parenteral administration of Ni compounds and Ni containing products. However, the highest dose of the Ni administered in the form of Ni-NCs in the present study was 70 ng. This is approximately 10,000-fold less than the doses shown to cause immunosuppression or carcinogenicity and is expected to be well tolerated. Additionally, the average dietary intake of Ni in humans is estimated to be 69-162 μg/day (Safe Use of Nickel, 2008). Chikh et al. reported no toxicity upon acute s.c. dosing (three weekly injections) of liposomes containing 5% and 10% DGS-NTA-Ni in mice for 30 days (Chikh et al., 2002). To further address this, we examined the serum levels of IL-12/p40 and CCL5/RANTES in mice treated with Ni-NCs. We observed no significant induction of systemic pro-inflammatory cytokines by s.c. administered Ni-NCs. Nevertheless, further investigation of immune response to DGS-NTA-Ni may be needed and antigen delivery systems using components containing Ni must be evaluated for their safety in individuals where adverse events may be expected.

The type of desired immune response, humoral or cellular, is affected by many factors including the nature of the pathogen or the antigen, its mode of entry, types of cells infected and cellular localization, the purpose of immune induction (therapeutic or prophylactic) and host features among others. In most cases, both humoral and cellular responses are desired. Interestingly, particulate antigen delivery systems have shown enhanced cross-MHCI presentation due to their endocytic uptake and thus may lead to both humoral and long-lasting cellular responses making them ideal adjuvants (Chen et al., 2011;

Shen et al., 2006). Interestingly, we have previously shown a strong cytotoxic T-cell and antibody response with the Ni-NPs similar to those used for comparison in the present study (Cui et al., 2004).

We are currently evaluating T-cell responses to further investigate the type of immune responses. To further improve the immune response with the Ni-NCs, we are also investigating the addition of an immunostimulant adjuvant in the Ni-NCs by either surface conjugation or incorporation in the core.

A.6. Conclusions

We have successfully formulated novel NCs with surface accessible Ni and investigated binding of two His-tagged proteins, GFP and Gag p41, respectively, to the surface of Ni-NCs. The Ni-NCs are taken up by the APCs (DC2.4 dendritic cells) but are non-toxic upto 24 hr at high concentrations. Enhanced antibody responses were observed compared to AH at much lower doses of the antigen. Treatment with Ni-NCs resulted in a higher IgG2a/IgG1 ratio compared to AH. The Ni-NCs did not stimulate the production of systemic proinflammatory cytokines, IL-12/p40 and CCL5/RANTES after s.c. injection. Future efforts involve conjugation of different adjuvants on the surface of the Ni-NCs in addition to the surface decoration with a protein antigen to create a system that has both immune-potentiation and efficient antigen delivery characteristics. We also plan to investigate the retention and migration of Ni-NCs from the site of administration.

A.7. References

Aline, F., D. Brand, J. Pierre, P. Roingeard, M. Severine, B. Verrier, and I. Dimier-Poisson. 2009. Dendritic cells loaded with HIV-1 p24 proteins adsorbed on surfactant-free anionic PLA nanoparticles induce enhanced cellular immune responses against HIV-1 after vaccination. Vaccine. 27:5284-5291.

Alving, C.R. 1995. Liposomal vaccines: clinical status and immunological presentation for humoral and cellular immunity. Ann N Y Acad Sci. 754:143-152.

Audran, R., K. Peter, J. Dannull, Y. Men, E. Scandella, M. Groettrup, B. Gander, and G. Corradin. 2003. Encapsulation of peptides in biodegradable microspheres prolongs their MHC class-I presentation by dendritic cells and macrophages in vitro. Vaccine. 21:1250-1255.

Baylor, N.W., W. Egan, and P. Richman. 2002. Aluminum salts in vaccines--US perspective. Vaccine. 20 Suppl 3:S18-23.

Buzard, G.S., and K.S. Kasprzak. 2000. Possible roles of nitric oxide and redox cell signaling in metal-induced toxicity and carcinogenesis: a review. J Environ Pathol Toxicol Oncol. 19:179-199.

Chen, J., Z. Li, H. Huang, Y. Yang, Q. Ding, J. Mai, W. Guo, and Y. Xu. 2011. Improved antigen cross-presentation by polyethyleneimine-based nanoparticles. Int J Nanomedicine. 6:77-84.

Chikh, G.G., W.M. Li, M.P. Schutze-Redelmeier, J.C. Meunier, and M.B. Bally. 2002. Attaching histidine-tagged peptides and proteins to lipid-based carriers through use of metal-ion-chelating lipids. Biochim Biophys Acta. 1567:204-212.

Cooper, H.M., R. Jemmerson, D.F. Hunt, P.R. Griffin, J.R. Yates, 3rd, J. Shabanowitz, N.Z. Zhu, and Y. Paterson. 1987. Site-directed chemical modification of horse cytochrome c results in changes in antigenicity due to local and long-range conformational perturbations. J Biol Chem. 262:11591-11597.

Cui, Z., J. Patel, M. Tuzova, P. Ray, R. Phillips, J.G. Woodward, A. Nath, and R.J. Mumper. 2004. Strong T cell type-1 immune responses to HIV-1 Tat (1-72) protein-coated nanoparticles. Vaccine. 22:2631-2640.

Dong, X., C.A. Mattingly, M. Tseng, M. Cho, V.R. Adams, and R.J. Mumper. 2009a. Development of new lipid-based paclitaxel nanoparticles using sequential simplex optimization. Eur J Pharm Biopharm. 72:9-17.

Dong, X., C.A. Mattingly, M.T. Tseng, M.J. Cho, Y. Liu, V.R. Adams, and R.J. Mumper. 2009b. Doxorubicin and paclitaxel-loaded lipid-based nanoparticles overcome multidrug resistance by inhibiting P-glycoprotein and depleting ATP. Cancer Res. 69:3918-3926.

Duncan, G., T.J. Jess, F. Mohamed, N.C. Price, S.M. Kelly, and C.F. van der Walle. 2005. The influence of protein solubilisation, conformation and size on the burst release from poly(lactide-co-glycolide) microspheres. J Control Release. 110:34-48.

Fuchs, S.M., and R.T. Raines. 2007. Arginine grafting to endow cell permeability. ACS Chem Biol. 2:167-170.

Hochuli, E., H. Dobeli, and A. Schacher. 1987. New metal chelate adsorbent selective for proteins and peptides containing neighbouring histidine residues. J Chromatogr. 411:177-184.

Huang, Z., P. Hwang, D.S. Watson, L. Cao, and F.C. Szoka, Jr. 2009. Tris-nitrilotriacetic acids of subnanomolar affinity toward hexahistidine tagged molecules. Bioconjug Chem. 20:1667-1672.

Huang, Z., J.I. Park, D.S. Watson, P. Hwang, and F.C. Szoka, Jr. 2006. Facile synthesis of multivalent nitrilotriacetic acid (NTA) and NTA conjugates for analytical and drug delivery applications. Bioconjug Chem. 17:1592-1600.

Kim, J.S., C.A. Valencia, R. Liu, and W. Lin. 2007. Highly-efficient purification of native polyhistidine-tagged proteins by multivalent NTA-modified magnetic nanoparticles. Bioconjug Chem. 18:333-341.

Klippstein, R., and D. Pozo. 2010. Nanotechnology-based manipulation of dendritic cells for enhanced immunotherapy strategies. Nanomedicine. 6:523-529.

Knecht, S., D. Ricklin, A.N. Eberle, and B. Ernst. 2009. Oligohis-tags: mechanisms of binding to Ni2+-NTA surfaces. J Mol Recognit. 22:270-279.

Lauer, S.A., and J.P. Nolan. 2002. Development and characterization of Ni-NTA-bearing microspheres. Cytometry. 48:136-145.

Maassen, C.B., W.J. Boersma, C. van Holten-Neelen, E. Claassen, and J.D. Laman. 2003. Growth phase of orally administered Lactobacillus strains differentially affects IgG1/IgG2a ratio for soluble antigens: implications for vaccine development. Vaccine. 21:2751-2757.

Marrack, P., A.S. McKee, and M.W. Munks. 2009. Towards an understanding of the adjuvant action of aluminium. Nat Rev Immunol. 9:287-293.

McKee, A.S., M.W. Munks, M.K. MacLeod, C.J. Fleenor, N. Van Rooijen, J.W. Kappler, and P. Marrack. 2009. Alum induces innate immune responses through macrophage and mast cell sensors, but these sensors are not required for alum to act as an adjuvant for specific immunity. J Immunol. 183:4403-4414.

Ott, G., G.L. Barchfeld, and G. Van Nest. 1995. Enhancement of humoral response against human influenza vaccine with the simple submicron oil/water emulsion adjuvant MF59. Vaccine. 13:1557-1562.

Oyewumi, M.O., S. Liu, J.A. Moscow, and R.J. Mumper. 2003. Specific association of thiamine-coated gadolinium nanoparticles with human breast cancer cells expressing thiamine transporters. Bioconjug Chem. 14:404-411.

Panyam, J., and V. Labhasetwar. 2003. Biodegradable nanoparticles for drug and gene delivery to cells and tissue. Adv Drug Deliv Rev. 55:329-347.

Patel, J.D., S. Gandhapudi, J. Jones, R. O'Carra, J.G. Woodward, and R.J. Mumper. 2007a. Cationic nanoparticles for delivery of CpG oligodeoxynucleotide and ovalbumin: In vitro and in vivo assessment. J Biomed Nanotechnol. 3:97-106.

Patel, J.D., R. O'Carra, J. Jones, J.G. Woodward, and R.J. Mumper. 2007b. Preparation and characterization of nickel nanoparticles for binding to his-tag proteins and antigens. Pharm Res. 24:343-352.

Peek, L.J., C.R. Middaugh, and C. Berkland. 2008. Nanotechnology in vaccine delivery. Adv Drug Deliv Rev. 60:915-928.

Platt, V., Z. Huang, L. Cao, M. Tiffany, K. Riviere, and F.C. Szoka, Jr. 2010. Influence of multivalent nitrilotriacetic acid lipid-ligand affinity on the circulation half-life in mice of a liposome-attached His6-protein. Bioconjug Chem. 21:892-902.

Porath, J., J. Carlsson, I. Olsson, and G. Belfrage. 1975. Metal chelate affinity chromatography, a new approach to protein fractionation. Nature. 258:598-599.

Rabinovich, N.R., P. McInnes, D.L. Klein, and B.F. Hall. 1994. Vaccine technologies: view to the future. Science. 265:1401-1404.

Romagnani, S. 2000. T-cell subsets (Th1 versus Th2). Ann Allergy Asthma Immunol. 85:9-18; quiz 18, 21.

Safe use of nickel in the workplace. Nickel Institute and Nickel Producers Environmental Research Association.2008

Shahum, E., and H.M. Therien. 1988. Immunopotentiation of the humoral response by liposomes: encapsulation versus covalent linkage. Immunology. 65:315-317.

Shen, H., A.L. Ackerman, V. Cody, A. Giodini, E.R. Hinson, P. Cresswell, R.L. Edelson, W.M. Saltzman, and D.J. Hanlon. 2006. Enhanced and prolonged cross-presentation following endosomal escape of exogenous antigens encapsulated in biodegradable nanoparticles. Immunology. 117:78-88.

Sloat, B.R., M.A. Sandoval, A.M. Hau, Y. He, and Z. Cui. 2010. Strong antibody responses induced by protein antigens conjugated onto the surface of lecithin-based nanoparticles. J Control Release. 141:93-100.

Smialowicz, R.J., R.R. Rogers, M.M. Riddle, and G.A. Stott. 1984. Immunologic effects of nickel: I. Suppression of cellular and humoral immunity. Environ Res. 33:413-427.

Wang, X., T. Uto, T. Akagi, M. Akashi, and M. Baba. 2008. Poly(gamma-glutamic acid) nanoparticles as an efficient antigen delivery and adjuvant system: potential for an AIDS vaccine. J Med Virol. 80:11-19.

Watson, D.S., V.M. Platt, L. Cao, V.J. Venditto, and F.C. Szoka, Jr. 2011. Antibody response to polyhistidine-tagged peptide and protein antigens attached to liposomes via lipid-linked nitrilotriacetic acid in mice. Clin Vaccine Immunol. 18:289-297.

Yan, W., A. Jain, R. O'Carra, J.G. Woodward, W. Li, G. Li, A. Nath, and R.J. Mumper. 2009. Lipid nanoparticles with accessible nickel as a vaccine delivery system for single and multiple his-tagged HIV antigens. HIV/AIDS Res Palliat Care. 1:1-11.

APPENDIX B

Spectral Characterization of Synthesized Compounds

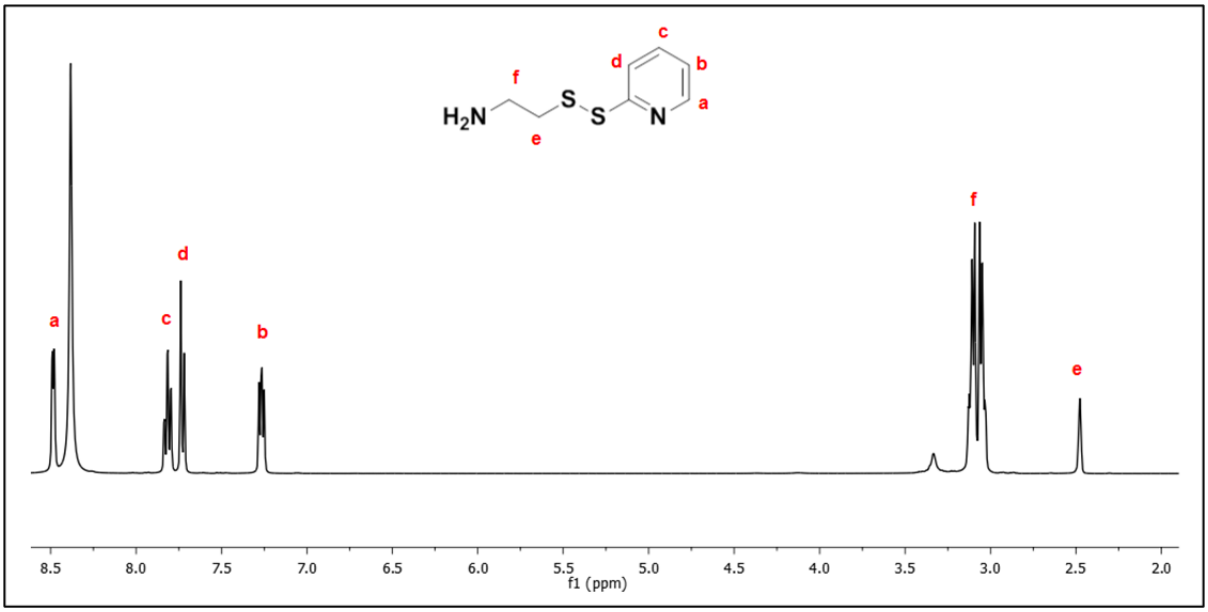

Figure B.1 ^{1}H NMR spectra for 2-(2-Pyridyldithio) ethylamine hydrochloride.

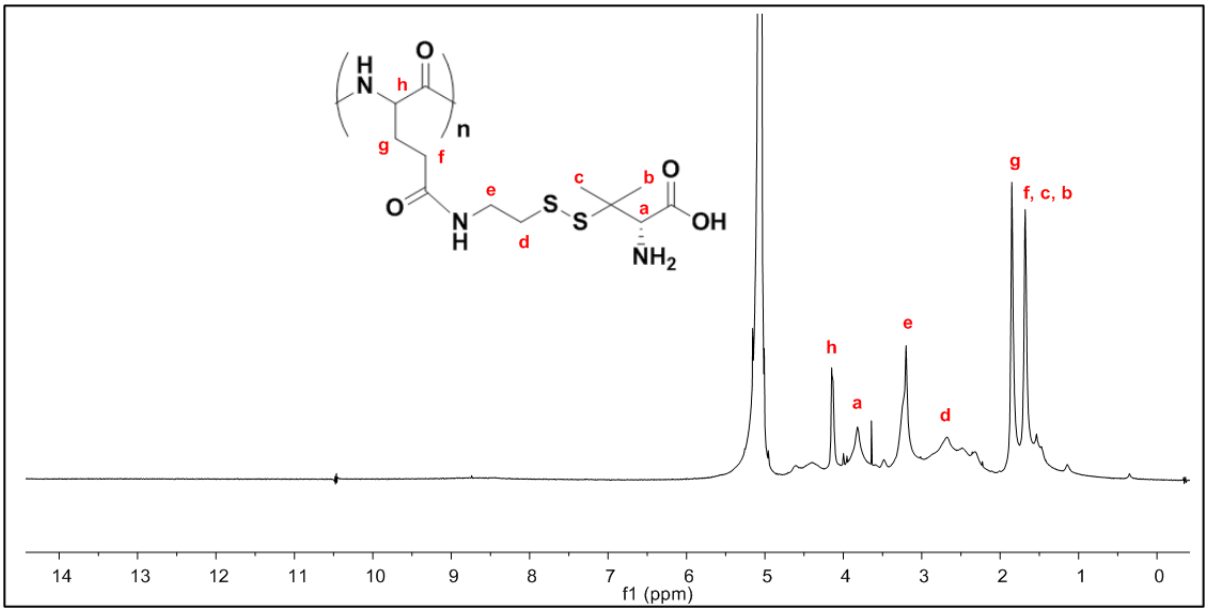

Figure B.2 ^{1}H NMR spectra for PGA-D-pen conjugate.

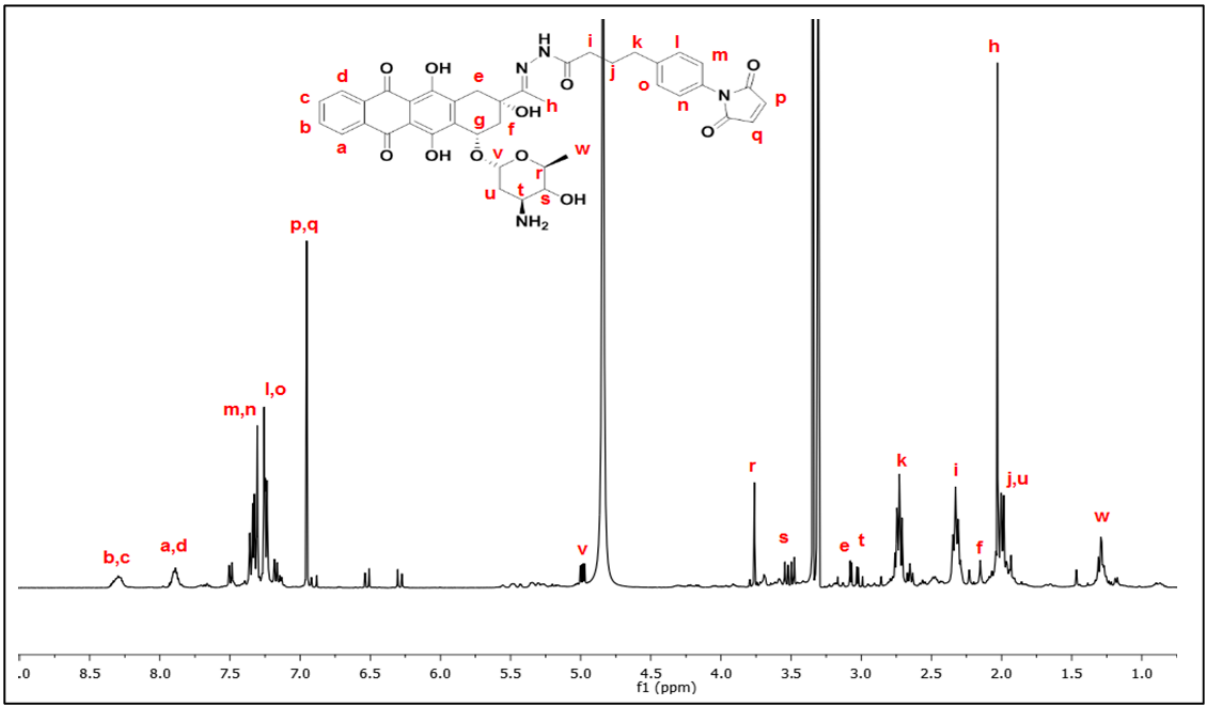

Figure B.3 ^{1}H NMR spectra for idarubicin-4-maleimidophenylbutyric acid hydrazide hydrochloride conjugate (Ida-MPBH).

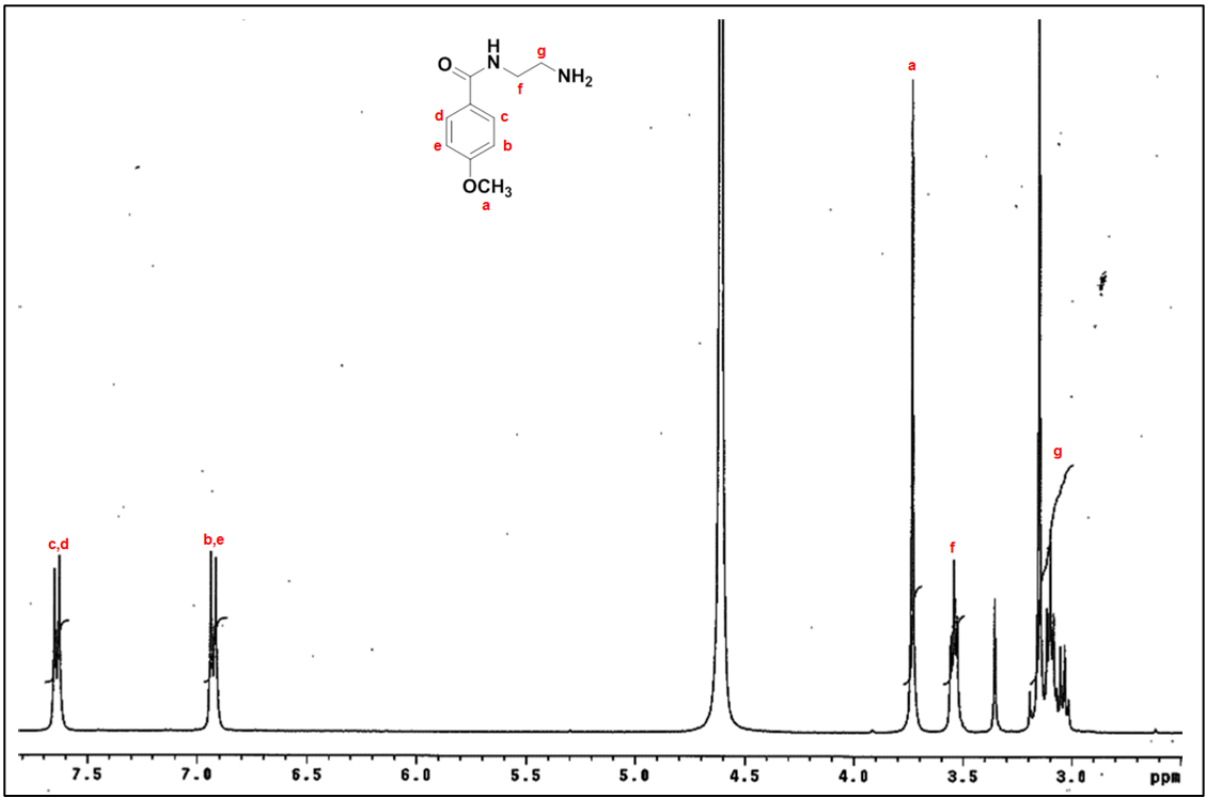
O
H
N
g
NH2
f
d
c
e
b
OCH3
a
a
g
f
c,d
b,e
7.5
7.0
6.5
6.0
5.5
5.0
4.5
4.0
3.5
3.0
ppm

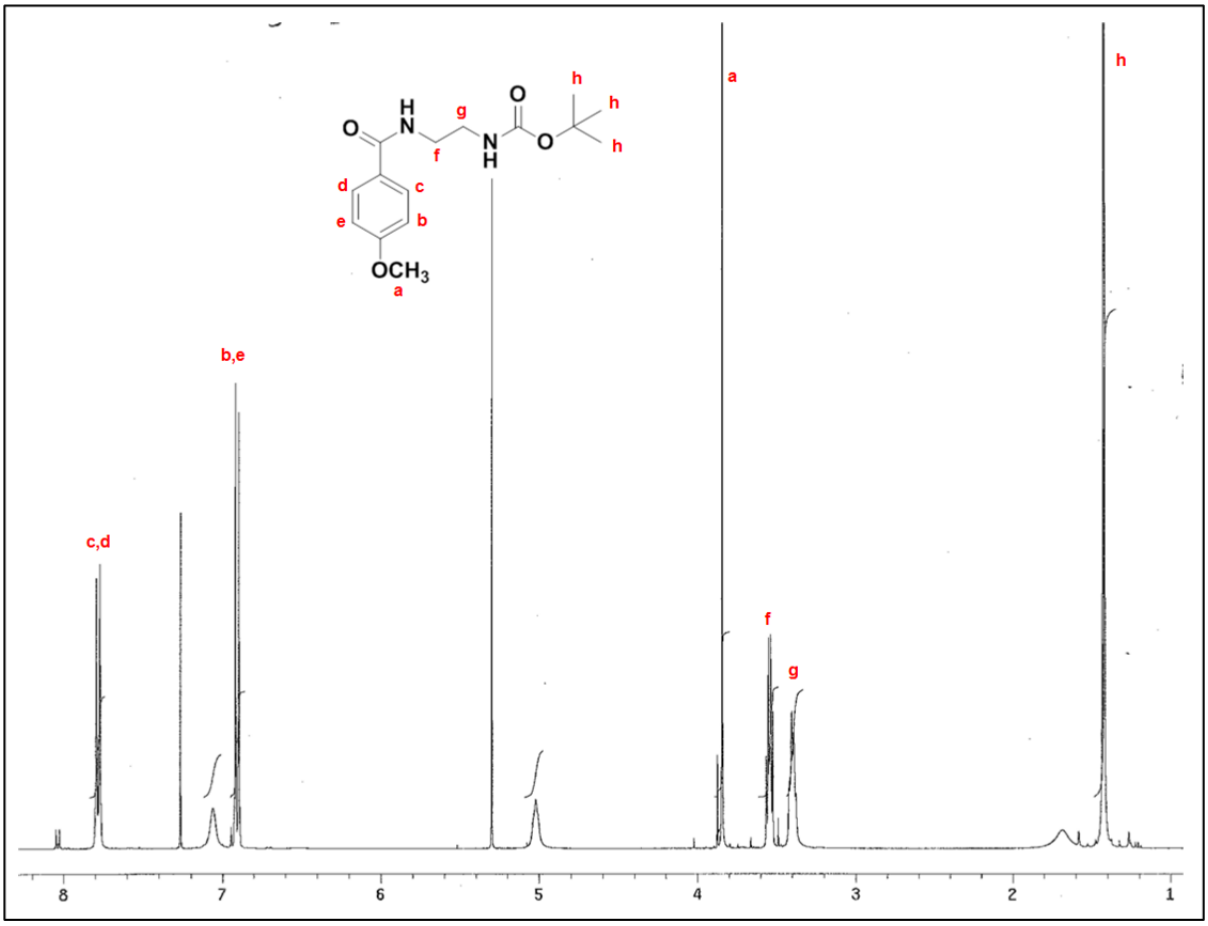
h
a
h
g
h
h
O
H
N
f
N
H
O
O
d
c
e
b
OCH3
a
b,e
c,d
f
g
8
7
6
5
4
3
2
1

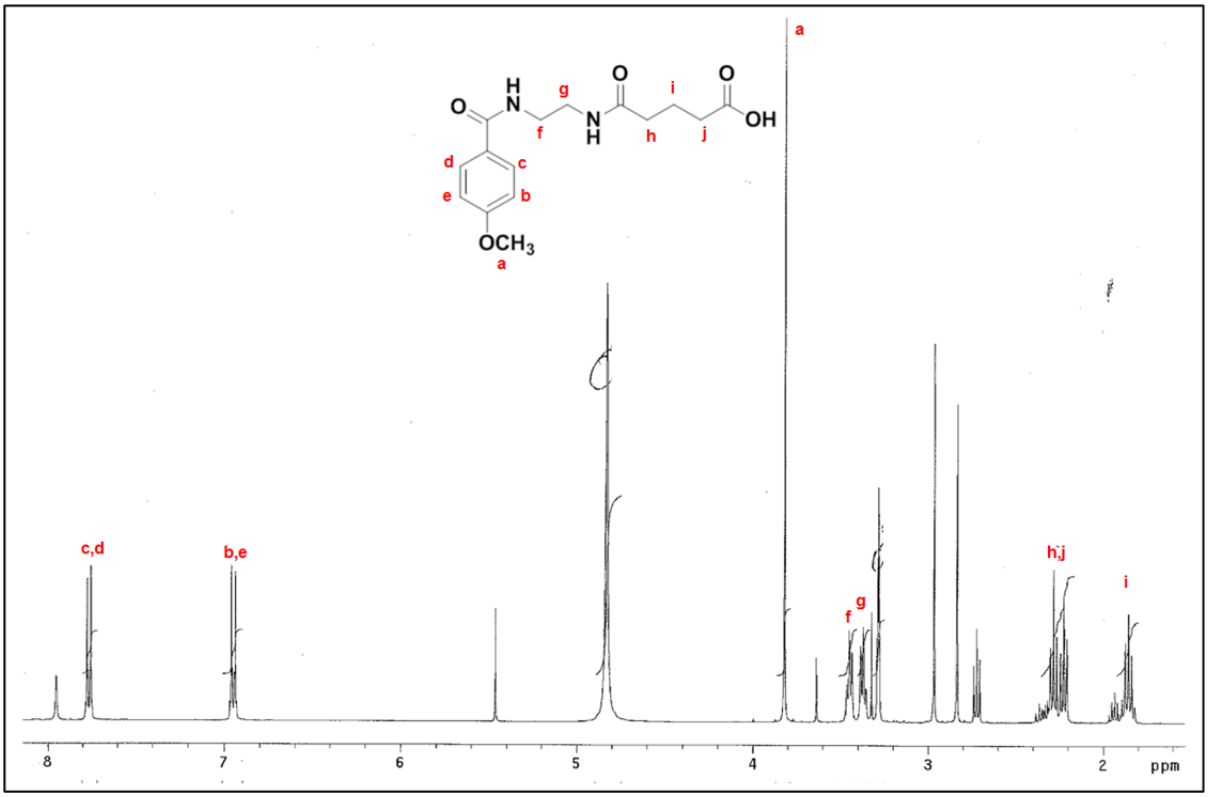
a
c,d
b,e
f
g
h,j
i
8
7
6
5
4
3
2
ppm

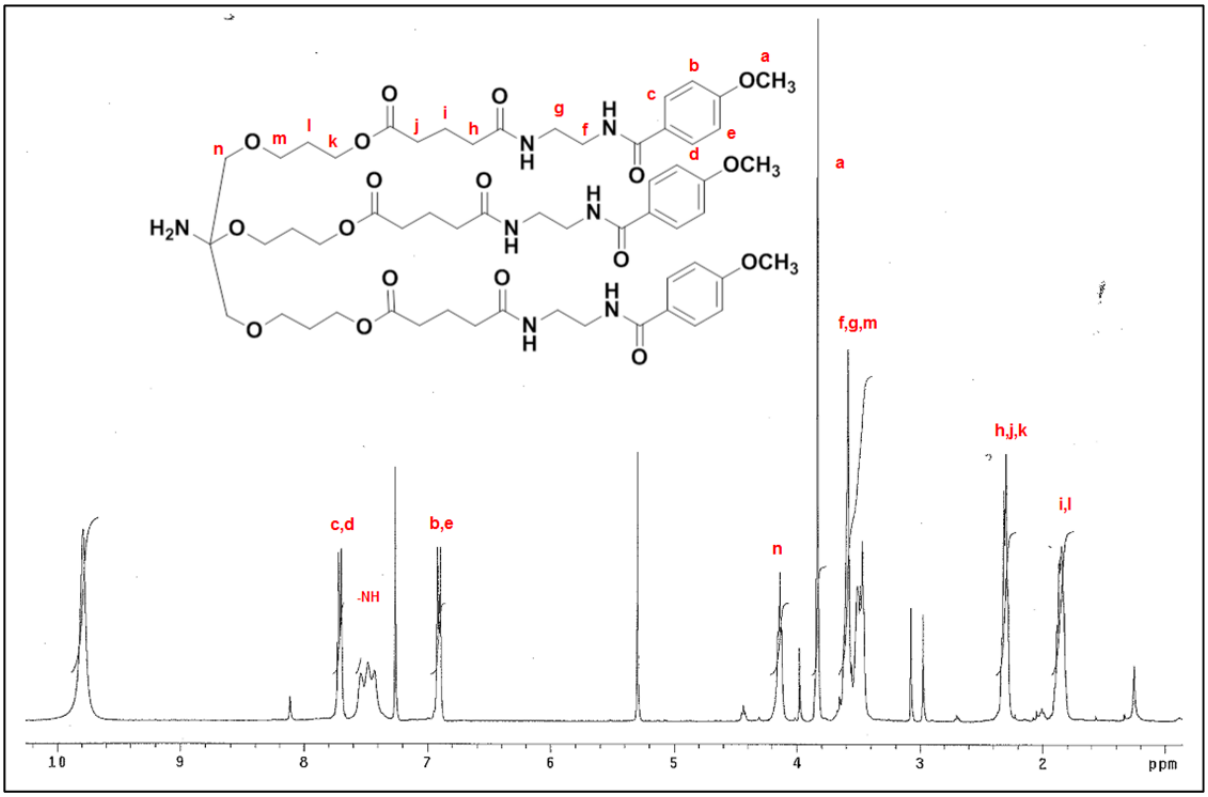

Figure B.4 ^{1}H NMR spectra for trivalent anisamide and intermediates.
The spectra refer to compounds 1-4 in Figure 4.1.